Reactive Oxygen Species and Redox-relevant Enzymes as Regulators of the Osteogenic Differentiation of Human Bone Marrow Mesenchymal Stem Cells

Inaugural-Dissertation

zur Erlangung des Doktorgrades
der Mathematisch-Naturwissenschaftlichen Fakultät
der Heinrich-Heine-Universität Düsseldorf

vorgelegt von

Dana-Chantal Strangmann
aus Stade

Düsseldorf, Mai 2018

aus dem Institut für Unfall- und Handchirurgie

der Heinrich-Heine-Universität Düsseldorf

Gedruckt mit der Genehmigung der
Mathematisch-Naturwissenschaftlichen Fakultät der

Heinrich-Heine-Universität Düsseldorf

Berichterstatter:

1. Prof. Dr. rer. nat. Christoph V. Suschek

2. Prof. Dr. rer. nat. Henrike Heise

Tag der mündlichen Prüfung: 09.07.2018

Table of Contents

Summary

Bone defects are one of the most serious pathologies. Any disturbances during the maturation and differentiation processes of MSCs lead to deteriorations of the bone healing processes. Due to the wide-ranging differentiation potential of MSCs, these promising types of cells are the source of bone healing processes. Therefore, MSCs became relevant for diverse therapeutical approaches within the regenerative medicine to treat bone healing disorders such as osteogenesis imperfecta, hypophosphatasia, osteoporosis and osteoarthritis. Cell aging processes are responsible for alterations of ROS levels, cell proliferation and differentiation capacities, cell morphology, telomerase activity, energy metabolism and levels of Runx2, FOXOs and p53. Interestingly, oxygen can form reactive oxygen species which constitute important regulatory second messenger during cell signaling processes. As low levels of ROS are required to regulate cell signaling pathways during proliferation or osteogenic differentiation processes, elevated levels can result in adipogenic differentiation proceedings which lead to obesity and consequently to impaired bone remodeling and thus bone defects. Higher ROS concentrations are harmful and can also cause cell death and apoptosis which also result in bone healing disorders. For that reason, approaches to regulate a balance between the formation and degradation of ROS and thus healthy bone healing processes, pro- and antioxidant enzymatic pathways are gaining in importance.

In previous osteogenic differentiation investigations, regular as well as osteogenically dysfunctional hBMSCs were observed. Remarkably, the addition of the antioxidative enzyme catalase could restore the impaired osteogenic differentiation potential of osteogenically dysfunctional – so called low responder – human adipogenic stromal cells. Therefore, the effects of catalase were also tested on hBMSCs. We observed that the catalase treatment also resulted in a restoration of osteogenically dysfunctional hBMSCs. Since catalase is known for the chemical degradation of hydrogen peroxide to water and oxygen, we focused on investigations of its antioxidative effects during the osteogenic differentiation. For that reason, the osteogenic differentiation dimension was assessed by the determination of the extent of matrix calcification, the alkaline phosphatase activity and the gene expression of matrix proteins, such as SPARC and type 1 collagen, depending on the addition of diverse antioxidative additives and compared to the restoration potential of catalase. Only MnSOD, hemoglobin and thymol showed a slight increase of the osteogenic differentiation potential. Nonetheless, no additive showed a comparable osteogenic restoration potential as catalase. In this case, it is important to note that all used additives cannot degrade hydrogen peroxide but reduce ROS levels via diverse chemical reactions. The impact of catalase addition on the protein expression of antioxidative relevant proteins such as NOX4, SOD1/2, FOXO1, Nrf2, GPX and catalase were also assessed. Furthermore, the expression of apoptosis regulating proteins such as p53 and Akt were determined. GPX, catalase, Akt, Nrf2 and NOX 4 showed similar expression patterns. The addition of catalase during the osteogenic differentiation of responder and low responder cells resulted in reduced expressions of the previously mentioned proteins. Differences between the expressions of responder and low responder cells could not be observed which emphasizes that the restoration potential of catalase is not regulated via the investigated proteins.

In the following, the test results highlighted that catalase but also inactivated catalase can restore the impaired osteogenic differentiation potential of low responder cells. These outcomes suggest that the antioxidative reaction mechanism is not the key pathway for the restoration mechanism. Since investigations of the cell viability and apoptosis rates showed no further indications, the additions of iron compounds were analyzed. Iron is the central ion of the active center of catalase and might be the reason for the restoration potential of catalase and inactivated catalase since the inactivation process does not destroys the iron ion. Remarkably, iron sulfate and iron chloride restore the impaired osteogenic differentiation to an equal extent as catalase does. Furthermore, the addition of iron sulfate can decrease the osteogenic differentiation potential of responder cells which might be caused by the cytotoxic effect of elevated iron concentrations. Interestingly, iron as well as catalase are discussed as potential producers of hydroxyl radicals. Hydroxyl radicals are known for their rigidly reactivity. The measurement of the hydroxyl radical amount indicates that this hypothesis might be a reasonable explanation for the restoration potential of catalase and inactive catalase because the inactive catalase might also produce hydroxyl radicals. Since the impacts on the expression of the investigated proteins by adding iron sulfate or chloride are differing to the results after a catalase treatment, further comparing investigations are obligatory.

Due to the restoration potential of iron ions on the osteogenic differentiation, the effects of the treatment with catalase or rather iron compounds on the protein expression of aconitase 1 and 2 were analyzed. Via the two isoforms of aconitase, iron is a relevant regulator of the citrate cycle which in turn regulates the citrate concentration, a relevant compound of the bone matrix, and also the energy generation in form of ATP. As these investigations and further tests of the energy metabolism showed no indications in one direction or the other, the regulation of the osteogenic restoration potential by the hydroxyl radical generation seems reasonable. To verify these hypotheses, further investigations are required. Nonetheless, the catalase treatment of osteogenically dysfunctional MSCs might be a promising therapeutical approach in regenerative therapies of bone healing disorders.

Zusammenfassung

Pathologische Veränderungen der Knochenheilung führen zu schwerwiegenden Knochendefekten. Jegliche Störungen während der Reifungs- und Differenzierungsabläufe von MSCs führen zu Mängeln im Rahmen der Knochenhomöostase. Aufgrund des breiten Differenzierungspotentials von MSCs sind diese vielversprechenden Zellen die Quelle der Knochenbildung. Um krankhafte Knochenheilungsstörungen wie Osteogenesis imperfecta, Hypophosphatasie, Osteoporose und Osteoarthritis zu behandeln, wurden MSCs zunehmend für verschiedene therapeutische Ansätze in der regenerativen Medizin relevant. Zellalterungsprozesse sind verantwortlich für Veränderungen der ROS Konzentrationen, der Zellproliferations- und -differenzierungskapazitäten, der Zellmorphologie, der Telomeraseaktivität, des Energiestoffwechsels und der Konzentrationen von Runx2, FOXOs und p53. Reaktive Sauerstoffspezies werden aus Sauerstoff gebildet und stellen wichtige regulatorische Second Messenger bei zellulären Signalprozessen dar. Während geringe Mengen an ROS erforderlich sind, um Signalwege der Zelle während der Proliferation oder der osteogenen Differenzierungsprozesse zu regulieren, können erhöhte Spiegel zur Adipogenese führen. Diese verstärkte adipogene Differenzierung hat eine Verfettung der Knochen und damit eine beeinträchtigte Knochenhomöostase zur Folge. Weiterhin können stark erhöhte ROS-Konzentrationen apoptotische Signalwege einleiten und damit über den ausgelösten Zelltod ebenfalls zu Knochenheilungsstörungen führen. Aus diesem Grund gewinnen Ansätze zur Regulation des ROS Gleichgewichts und den damit in Verbindung stehenden gesunden Knochenheilungsprozessen, pro- und antioxidative Enzymsysteme an Bedeutung.

In früheren Versuchen der osteogenen Differenzierung wurden sowohl reguläre als auch osteogen dysfunktionale hBMSCs beobachtet – sogenannte Responder oder Low Responder hBMSCs. Bemerkenswerterweise konnte durch die Zugabe des antioxidativen Enzyms Katalase das osteogene Differenzierungspotential der Low Responder humaner adipogener Stromazellen wiederhergestellt werden. Aufgrund dieser Erkenntnis wurden die Auswirkungen von Katalase ebenfalls im Rahmen der osteogenen Differenzierung der hBMSCs getestet. Wir beobachteten, dass die antioxidative Behandlung mit Katalase auch hier zu einer Wiederherstellung des osteogenen Differenzierungspotentials von Low Responder Zellen führt. Da Katalase für den chemischen Abbau von Wasserstoffperoxid zu Wasser und Sauerstoff bekannt ist, wurde der Fokus auf die Untersuchungen der Katalase spezifischen antioxidativen Effekte während der osteogenen Differenzierung gelegt. Aus diesem Grund wurde das Ausmaß der osteogenen Differenzierung durch die Bestimmung der Matrixbildung, der Aktivität der alkalischen Phosphatase und der Genexpression von Matrixproteinen, wie SPARC und Typ 1 Kollagen, in Abhängigkeit von der Zugabe verschiedener antioxidativer Zusatzstoffe untersucht. Diese Ergebnisse wurden zusätzlich mit dem Wiederherstellungspotential der Katalase verglichen. Lediglich MnSOD, Hämoglobin und Thymol zeigten eine leichte Optimierung des osteogenen Differenzierungspotentials. Keines der Zusätze zeigte jedoch ein vergleichbares osteogenes Wiederherstellungspotential wie die Katalase. Hierbei ist es wichtig anzumerken, dass ROS über verschiedene chemische Reaktionen reduziert wird, allerdings die verwendeten antioxidativen Zusätze nicht in der Lage sind Wasserstoffperoxid abzubauen.

Die Auswirkungen des Zusatzes von Katalase auf die Expression von antioxidativ relevanten Proteinen wie NOX4, SOD1 / 2, FOXO1, Nrf2, GPX und Katalase wurden ebenfalls untersucht.

Weiterhin wurde die Expression von Apoptose-regulierenden Proteinen wie p53 und Akt bestimmt. Interessanterweise zeigten GPX, Katalase, Akt, Nrf2 und NOX 4 ähnliche Expressionsmuster. Die Zugabe von Katalase während der osteogenen Differenzierung von Responder und Low Responder hBMSCs führte bei den oben erwähnten Proteinen zu reduzierten Expressionsraten. Unterschiede zwischen den Responder und Low Responder Donoren konnten nicht beobachtet werden. Diese fehlenden Unterschiede unterstreicht, dass das Wiederherstellungspotential der Katalase wahrscheinlich nicht über die untersuchten Proteine reguliert wird. Im Folgenden konnte zusätzlich gezeigt werden, dass Katalase, aber auch inaktivierte Katalase in der Lage sind, das beeinträchtigte osteogene Differenzierungspotential von Low Responder Donoren wiederherzustellen. Diese Ergebnisse legen nahe, dass der antioxidative Reaktionsmechanismus nicht der Schlüsselweg für den Wiederherstellungsmechanismus ist. Untersuchungen der Viabilität und der Apoptoserate der Zellen ergaben keine weiterführenden Erkenntnisse, sodass die Bedeutung des Eisens als Zentralion des aktiven Zentrums der Katalase genauer untersucht wurde. Da auch beim Inaktivierungsprozess der Katalase keine Zerstörung des Eisenions erfolgt, würde es auch die positive Wirkung der inaktivierten Katalase auf die osteogene Differenzierung erklären. Bemerkenswerterweise stellen Eisensulfat und Eisenchlorid die beeinträchtigte osteogene Differenzierung in gleichem Maße wieder her wie Katalase. Darüber hinaus ist die Zugabe von Eisensulfat in der Lage das osteogene Differenzierungspotential von Responder hBMSCs zu verringern, was der mutmaßlichen zytotoxischen Wirkung von erhöhten Eisenkonzentrationen zugeschrieben werden könnte. Interessanterweise wird sowohl Eisen als auch Katalase als potenzieller Produzent von Hydroxylradikalen diskutiert. Hydroxylradikale sind für ihre ausgeprägte Reaktivität bekannt. Die Ergebnisse der Messung der Hydroxylradikalmenge zeigen, dass diese Hypothese eine sinnvolle Erklärung für das Wiederherstellungspotential von Katalase und inaktiver Katalase sein könnte, da die inaktive Katalase auch Hydroxylradikale erzeugen könnte. Da sich die Auswirkungen auf die Expression der untersuchten Proteine durch Zugabe von Eisensulfat oder -chlorid von den Ergebnissen nach einer Katalase-Behandlung unterscheiden, sind weitere vergleichende Untersuchungen nötig. Aufgrund des Wiederherstellungspotentials von Eisenionen bei der osteogenen Differenzierung wurde die Wirkung der Behandlung mit Katalase bzw. Eisenverbindungen auf die Proteinexpression von Aconitase 1 und 2 untersucht. Im Rahmen der beiden Isoformen der Aconitase ist Eisen ein relevanter Regulator des Citratzyklus, der wiederum einerseits die Citratkonzentration, eine relevante Verbindung der Knochenmatrix, und andererseits die Energiegewinnung in Form von ATP reguliert. Da diese und auch weitere Untersuchungen des Energiestoffwechsels keine Hinweise in die eine oder andere Richtung ergaben, erscheint die Regulation des osteogenen Wiederherstellungspotentials durch die Hydroxylradikalgenerierung weiterhin sinnvoll. Um diese Hypothese weiter zu untermauern, sind allerdings weitere Untersuchungen erforderlich. Die Katalase-Behandlung von osteogen dysfunktionalen MSCs könnte schließlich ein vielversprechender therapeutischer Ansatz im Rahmen der regenerativen Therapien von Knochenheilungsstörungen werden.

List of Figures

List of Equations

List of Tables

List of Abbreviations

°C	Degree Celsius
µg	Microgram
µl	Microliter
µm	Micrometer
µM	Micromolar
hASCs	Human adipogenic stromal cells
ALP	Alkaline phosphatase
ATP	Adenosine triphosphate
Bax	Bcl-2 associated X protein
BCA	Bioinonic-Assay
BMP	Bone Morphogenetic Protein
BrdU	Bromdesoxyuridine
BSA	Bovine serum albumin
Cbfa1	Core-binding factor alpha 1
cDNA	Complementary DNA
C/EBP	CCAAT/Enhancer-Binding Proteins
CFU	Colony Forming Units
cm	Centimeter
COL1A1	Type 1 collagen
Da	Dalton
Dlx5	Distal-less homeobox 5
DMEM	Dulbecco's Modified Eagle's Medium
DMSO	Dimethyl sulfoxide
DNA	Deoxyribonucleic acid
DPBS	Dulbecco's phosphate-buffered saline, with calcium and magnesium
DUO	Dual oxidase
EDTA	Ethylenediaminetetraacetate
ECM	Extracellular matrix
FACS	Fluorescence-activated cell sorting
FAD	Flavin adenine dinucleotide
FCS	Fetal calf serum

FGF-2	Fibroblast growth factor 2
FOXO	Forkhead box protein
FSC	Forward scatter
GAPDH	Glyceraldehyde 3-phosphate dehydrogenase
Groucho/TLE	Groucho/transducin-like enhancer
GSH	Glutathione
GSSG	Glutathione disulfide
hBMSCs	Human bone marrow mesenchymal stem cells
HEPES	4-(2-hydroxyethyl)-1-piperazineethanesulfonic acid
HLA	Human leukocyte antigen
HPR	Horseradish peroxidase
IGF	Insulin like growth factor
IL-6	Interleukin 6
In vitro	Studies of biological materials outside their normal biological context
In vivo	Studies of biological materials in living organism
JNK	c-Jun N-terminal kinase
LFA-3	Lymphocyte function-associated antigen 3
MAPK Mitogen-Activated Protein Kinase	Mitogen-activated protein kinase
M-CSF	Macrophage colony-stimulating factor
MHC	Major histocompatibility complex
ml	Milliliter
mM	Millimolar
mm	Millimeter
mRNA	Messenger ribonucleic acid
miRNA	MicroRNA
Msx2	Msh homeobox protein 2
NADP	Nicotinamide adenine dinucleotide phosphate
Nell-1	Neural EGFL Like 1

nm	Nanometer
NOX	NADPH oxidase
OC	Osteocalcin
OP	Osteopontin
OSX	Osterix
PAGE	Polyacrylamide gel electrophoresis
PAX1	Paired box protein 1
PBS2-	Phosphate-buffered saline, without calcium and magnesium
PCL	Polycaprolactone
PEEK	Polyether ether ketone
PFA	Paraformaldehyde
PGA	Polyglycolic acid
pH	Potentia Hydrogenii
Pi	Local phosphate source
PLA	Polylactic acid
PKC	Protein-Kinase-C
PPARγ	Peroxisome proliferator-activated receptor
PTH	Parathyroid hormone
RANK	Receptor activator of nuclear factor kappa-B
RANKL	Receptor activator of nuclear factor kappa-B ligand
RIPA	Radio-Immunoprecipitation Assay (lysis buffer for Western blot analysis)
ROS	Reactive oxygen species
RT-PCR	Real-Time PCR
Runx2	Runt-related transcription factor 2
SMAD	Combination of “Small Body Size” = SMA (gene of caenorhabditis elegans) and Mothers Against Decapentaplegic = MAD (gene of drosophila)
SOD	Superoxide dismutase
SPARC	Secreted protein acidic and rich in cysteine

SSC	Side scatter
TAZ	Transcriptional coactivator with PDZ-binding motif
TBS	Tris buffered salt solution
TBS-T	Tris buffered salt solution with Tween 20
TEMED	N,N,N´,N´- Tetramethylethylenediamine
TGF-β	Transforming growth factor-β
TIPS	Thermally induced phase separation
UV	Ultra-Violette
VCAM-1	Vascular cell adhesion protein 1
VEGF	Vascular endothelial growth factor
WNT	Wingless und Int-1

1 Introduction

1.1 Bone – Structure and Function

Bone is an obligatory rigid organ of the human skeleton. This organ supports and protects the locomotor system and other organs. Furthermore, it is known for its capability of mineral storage such as calcium and phosphate [1]. The bone tissue is dynamic which is exhibited by an active bone homeostasis, also known as a permanently bone remolding. This metabolically active tissue consists of diverse cell types which maintain the dynamic bone formation and resorption. A balance between these two processes is necessary for undisturbed bone remodeling processes. Bone formation and the related mineralization of the bone tissue are performed by osteoblasts. On the contrary, osteoclasts are responsible for bone resorption and for the release of stored minerals. The third type of the bone tissue denotes inactive osteocytes which derive from mature osteoblasts and are imbedded in the mineralized matrix. The matrix mineralization is attributed to the osteocyte differentiation. Thereby, the osteocyte differentiation is supported by diverse factors such as vitamin K [2, 3]. To achieve the described metabolic and mechanical functions, the mineralized bone tissue is composited of two distinct types of bone – cortical bone and trabecular bone. The extracellular matrix consists of collagen type 1 [4] osteocalcin [5], secreted protein acidic and rich in cysteine (SPARC) [6-8].

The vertebrae skeleton consists of five diverse types of bones. The long, short, flat, irregular and sesamoid bones have distinct functions in the human skeleton but nonetheless show all equal processes of the bone formation**.** *Figure 1* shows the diverse bone types more detailed.

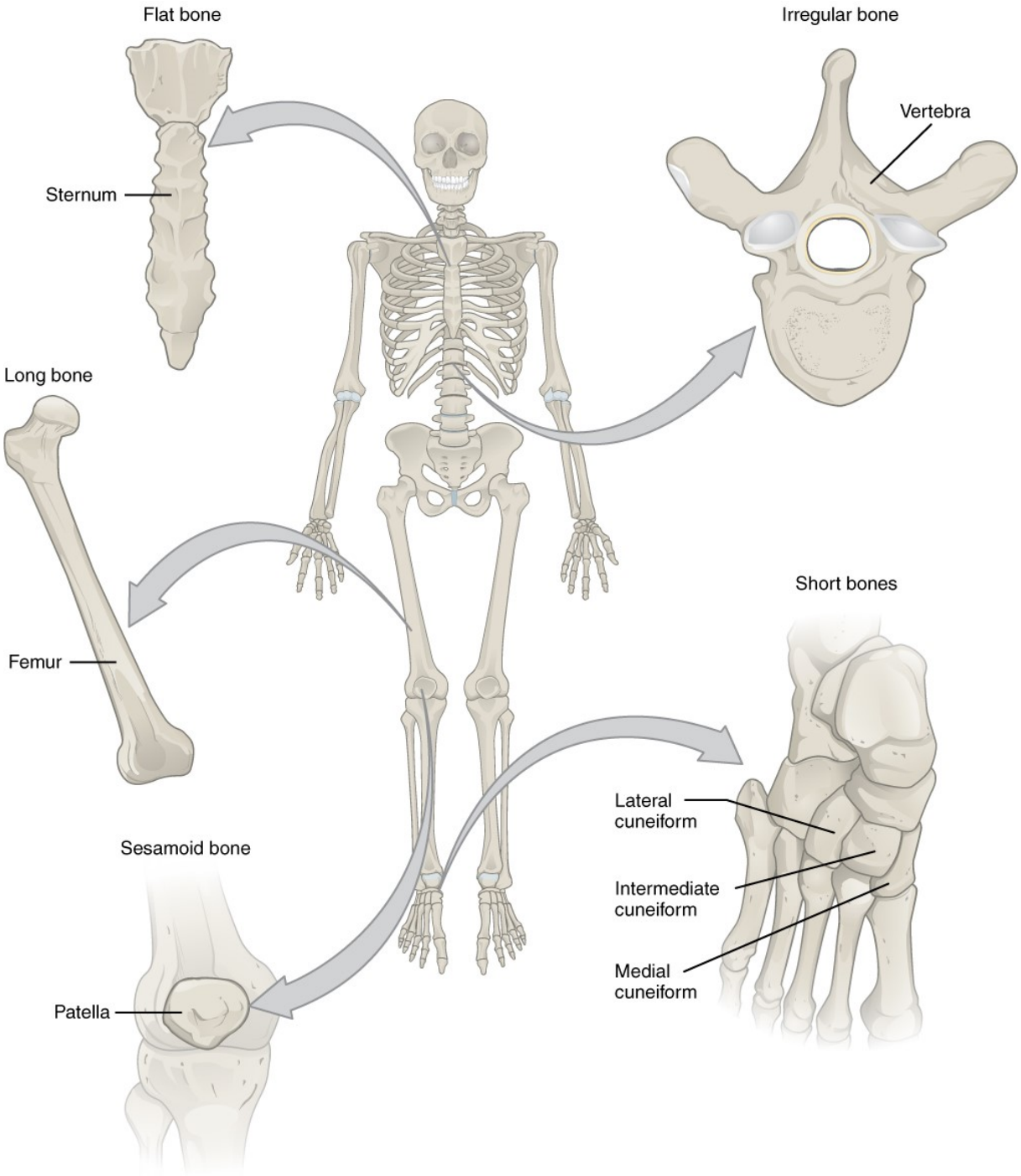

Figure 1: Classification of bones [9]

1.2 Bone Formation and Healing: A Balance between Formation and Resorption

Within bone modeling, two different processes can be differentiated: endochondral ossification (indirect ossification) and intramembranous ossification (direct ossification). For both types, the differentiation of the originally existing mesenchymal tissue into bone tissue is obligatory [10].

1.2.1 Intramembranous Ossification (Direct Ossification)

Flat bones are formed by the direct ossification. First, mesenchymal stem cells derive from the neural crest and in the following proliferate to be able to condense to form nodules. These mesenchymal stem cells can *inter alia* differentiate into cells of the capillaries or osteoblasts (see chapter *1.3* for a more detailed description of mesenchymal stem cells). Osteoblasts are bone precursor cells which deposit osteoid matrix, also called prebone matrix. This calcified matrix consists of a secreted calcium binding collagen-proteoglycan matrix. Through binding calcium and phosphate ions, the prebone matrix becomes calcified. Even though osteoblasts are separated from the formed matrix, occasionally, osteoblasts get trapped in the matrix and consequently differentiate into mature bone cells – osteocytes. Interestingly, the entire matrix forming area is surrounded by mesenchymal cells which form a bone surrounding membrane – the periosteum. As the inner layer of the periosteum is also converted in osteoblasts which further form more osteoid matrix, several layers of bone are formed [10]. *Figure 2* shows the procedure of matrix formation.

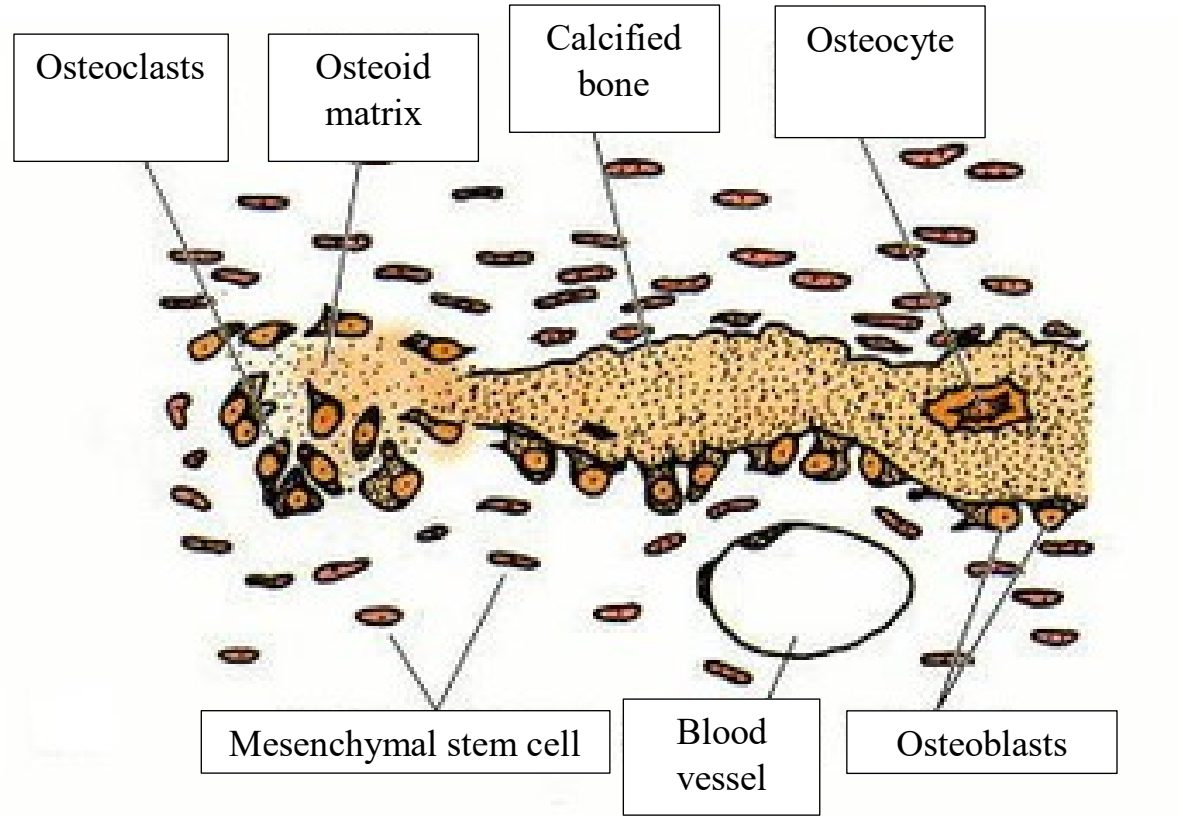

Figure 2: Schematic description of bone formation by intramembranous ossification (modified presentation based on [10]).

Bone morphogenetic proteins (BMP) initiate osteogenic differentiation of mesenchymal stem cells by activating Cbfa1 (core-binding factor alpha (1) [10].

1.2.2 Endochondral Ossification (Indirect Ossification)

Within endochondral ossification, cartilage tissue is formed by mesenchymal stem cells which subsequently turn into bone tissue [11]. To form bone out of cartilage tissue, five stages are necessary which are highlighted in *figure 3*. At first, the mesenchymal cells form a condensed mass which is caused by paracrine factors which in turn induce nearby mesodermal cells to express the transcription factors Pax1 (paired box protein 1) and Scleraxis. Cserjesi as well as Sosic and coworkers proved that these transcription factors are specialized to initiate cartilage formation [10, 12-14]. In image C of *figure 3*, it is shown that formed chondrocytes of the center exhibit hypertrophy and apoptosis and consequently form mineralized matrix. Caused by the cell death, blood vessels can enter the formation and in consequence lead to an accumulation of osteoblast [15, 16]. The osteoblasts, which were transported via the blood vessels, bind at the cartilaginous matrix and deposit bone matrix. The hypertrophic chondrocytes, their metabolism and mitochondrial membranes alter and eventual die by apoptosis [16, 17].

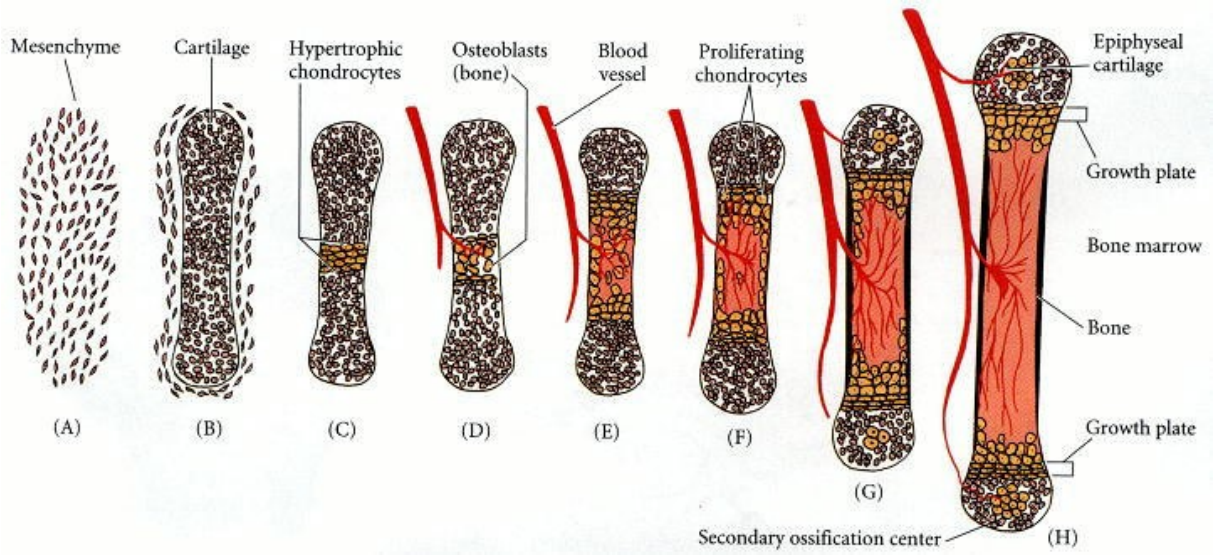

Figure 3: Schematic description of bone formation by the five steps of endochondral ossification [10]

1.2.3 Osteogenic Differentiation Cascade

Bone remodeling, a lifelong process, and bone formation processes, which occur during the growth period, are characterized by bone turnover. Both processes are controlled by various key factors such as vitamin D, steroids and parathyroid hormone (PTH). Furthermore, growth factors such as macrophage colony-stimulating factor (M-CSF), vascular endothelial growth factor (VEGF), transforming growth factor-β (TGF-β1/2), insulin-like growth factor (IGF), fibroblast growth factor 2 (FGF-2), receptor activator of nuclear factor kappa-B ligand (RANKL), cytokine modulators (prostaglandins), MAPK (mitogen-activated protein kinases)

signaling and the Interleukin-6 family are crucial regulators of the bone turnover processes during the osteogenic differentiation [18].

1.2.3.1 Osteoblastogenesis - Regulation on the Molecular Level

During the osteogenic differentiation, the BMP and WNT (Wingless und Int-1) pathways are crucial for a trouble free osteogenic process [19, 20]. Proteins of the SMAD family are activated by the BMP pathway and SMAD in turn is a crucial regulator of the expression of Runt-related transcription factor 2 (Runx2). Runx2 is one of the relevant osteogenic transcription factors such as osterix (OSX), SPARC, osteopontin (OP) and type 1 collagen (COL1A1). Runx2 initiates mesenchymal stem cells to differentiate into osteoblasts. Thereby, Runx2 is an osteoblast-specific transcription factor which regulates osteogenic processes upstream of the other mentioned proteins [21, 22] The SMAD activation by BMP and the following activation of Runx2, which results in a regulation of osteogenic-specific transcription factors, is demonstrated in *figure 4*.

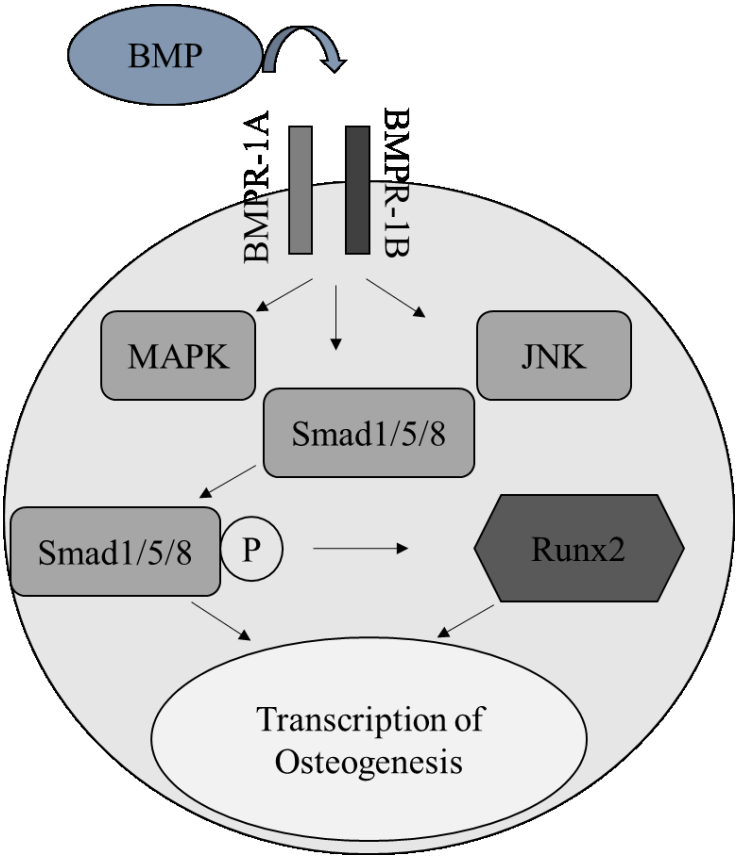

Figure 4: Signaling pathway of BMP, SMAD, RUNX2 and downstream osteogenic transcription factors. By binding of BMP to the BMP receptor SMAD, MAPK and JNK are activated. Due to the activation by phosphorylation, SMAD initiates Runx2 to also translocate into the cell nucleus. Thus, both proteins induce the transcriptional expression of osteogenesis related genes (own presentation based on [21].

Moreover, Runx2 is also regulated by the osteogenic relevant WNT pathway. It is important to note that the WNT pathway is a relevant pathway of the regulation of many processes such as tissue regeneration, tumorigenesis and organogenesis [23-25]. It can be distinguished between the canonical and non-canonical WNT pathway. Whereas the canonical WNT pathway regulates, depending on the osteoprotegerin-RANKL ratio, promotion or inhibition of osteoblast differentiation [26], the non-canonical WNT pathway positively affects the osteoblast differentiation by an inhibition of the peroxisome proliferator-activated receptor (PPARγ) expression [27]. RANKL promotes the osteoclastogenesis which results in bone resorption. To promote bone formation, an inhibition of RANKL is obligatory. Furthermore, to positively affect the osteoblastogenesis, it is necessary to inhibit the expression of PPARγ which is an adipogenesis promoting protein. To promote osteogenesis, adipogenic-specific proteins need to be downregulated and vice versa [28-30]. For healthy conditions, a balance between adipogenesis and osteogenesis is required [31].

Runx2 can form complexes with transcription factors such as C/EBPs, Dlx5 or Msx2 and regulates via the expression of osteocalcin via this formation [18]. Runx2 is also able to inhibit the osteogenic process at later stages via an interaction with the transcription factors Twist or Groucho/TLE [32, 33]. The promoting and inhibiting effects of Runx2 regarding the osteoblastogenesis are highlighted in *figure 5*.

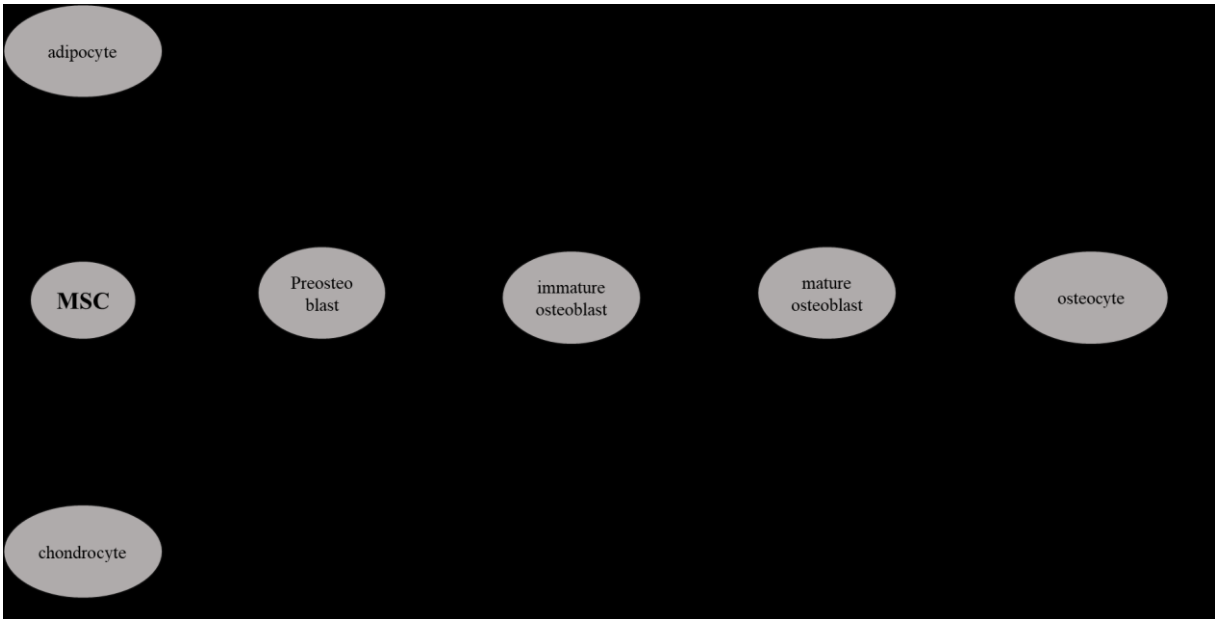

Figure 5: The osteoblast differentiation is regulated by the crosstalk of diverse transcription factors. In case of inhibiting or promoting effects of Msx1 and 2, not every detail has yet been settled. Physiological function or the stage at which the factor mainly works remain to be proven which is highlighted by the dotted lines (modified presentation based on [33].

Besides the mentioned regulatory processes and factors, DNA methylation, short, non-coding RNAs, so called microRNA (miRNA) [34], as well as chromatin structure modification which all are epigenetic factors, influence osteogenic differentiation processes. For instance, OSX might be regulated by *inter alia* miR-31, miR-93, miR-143, miR-145, miR-637 and miR-214, whereas the expression of Runx2 might be affected by *inter alia* miR-34c, miR-133a, miR-135a, miR-137, miR-205, miR-217, miR-338, miR-23a, miR-30c, miR-204/211 and miR-103a. Additionally, it is assumed that the expression of COL1A1 is influenced by miRNAs such as miR-29, miR-Let7 [18].

1.2.3.1.1 Formation of Calcified Matrix - Regulation on the Molecular Level

Differentiated osteoblasts produce enzymes which are obligatory for the matrix formation. Alkaline phosphatase (ALP) is the most relevant enzyme to promote matrix calcification. ALP is crucial for the catalytic process of the hydrolysis of monoesters in phosphoric acid. This chemical reaction results in increased phosphor levels which are necessary for the formation of calcified matrix [35]. Hydroxyapatite is the main component of the extracellular matrix. $Ca_5(PO_4)_3(OH)$ or $Ca_{10}(PO_4)_6(OH)_2$ are the main hydroxyapatite formations [36]. At later stages, structure proteins such as osteocalcin (OC), OP [37, 38], SPARC and COL1A1 are expressed. These proteins are relevant for the matrix stability and are expressed at the beginning of the mineralization process [39, 40]. A schematic demonstration of the protein expressions during the osteogenic matrix formation is shown in *figure 6*. The used donors for this work showed varying time periods of protein expressions or mineralization processes.

Therefore, the given information of the times of expressions and mineralization just show a general trend and small deviations are possible.

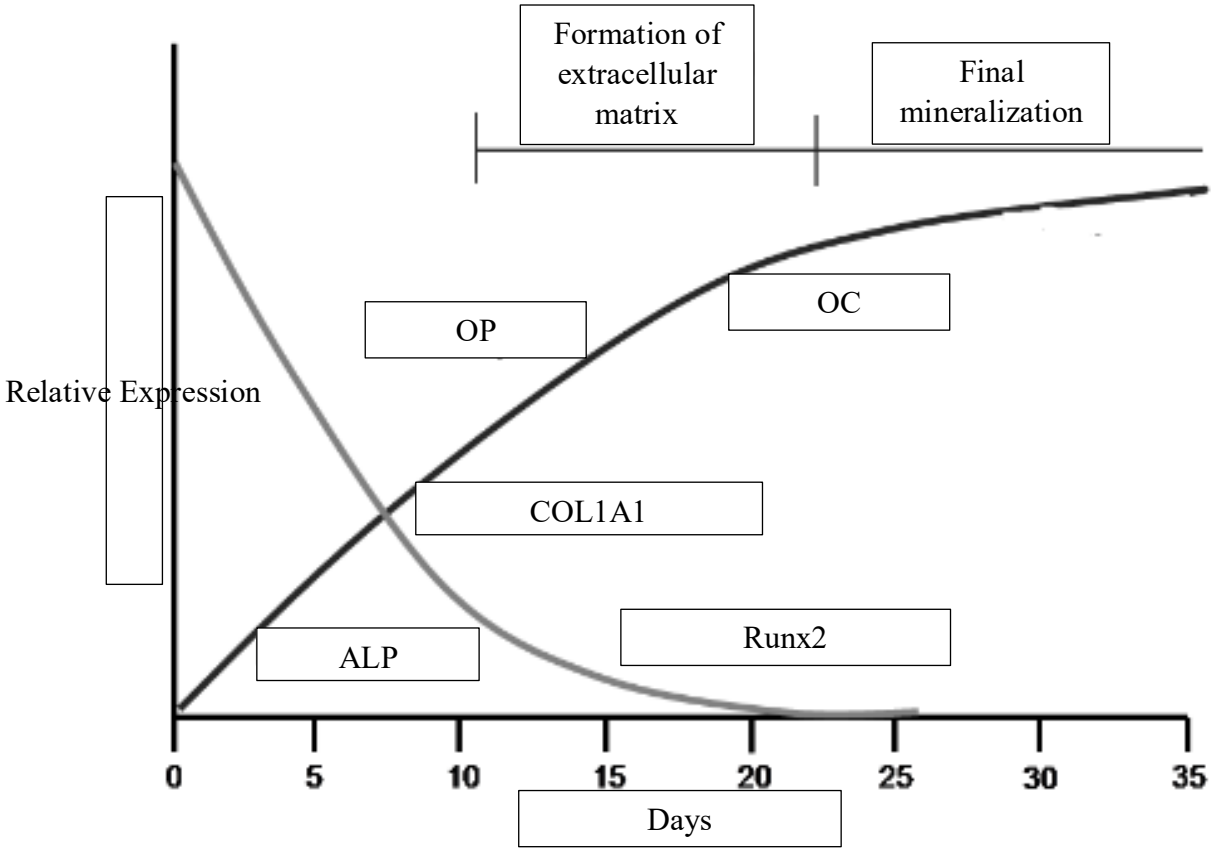

Figure 6: *In vitro* formation of calcified matrix on molecular levels. Schematic demonstration of the crosstalk of the diverse osteogenic proteins during matrix calcification (own representation based on [40]).

1.2.4 Pathological Conditions of Bone Healing

As described in the previous sections, adult mesenchymal stem cells (MSCs) are the source of the bone healing processes. Any disturbances *inter alia* during the maturation or differentiation of MSCs result in an impaired bone healing proceeding which reason manifest bone defects. Since bone defects are one of the most serious pathologies, tissue engineering, which is an important field of the regenerative medicine, is an important therapy aspect. Thereby, MSCs became relevant therapeutic agents within treatments of osteogenesis imperfecta, hypophosphatasia, osteoporosis, osteoarthritis, rheumatoid arthritis and osteonecrosis of the femoral head [41]. Alteration of bone healing processes are mostly attributed to aging processes which in turn result in deviations of levels of reactive oxygen species, capacities of cell proliferation [42, 43] and differentiation, cell morphology, telomerase activity [15, 44], energy metabolism [45], Wnt signaling [46] and levels of Runx2 [47], FOXOs (Forkhead box proteins) [48] and p53 [49, 50].

1.3 Human Bone Marrow Stem Cells (hBMSCs)

Stem cells are unique cells which exhibit the ability of self-renewal. Furthermore, these types of cells can differentiate into various cell types. Two main groups of stem cells are known. The first category is represented by embryonic stem cells (ESC) which are totipotent and can differentiate into every cell of the mesoderm, endoderm or ectoderm [51]. Adult stem cells are the second group which are pluripotent and can differentiate to tissue-specialized cells of the mesoderm, ectoderm or rather the endoderm and therefore exhibit limited range of differentiation lineage possibilities. Due to many risks (e.g. tumorigenicity), which are attributed to the implantation of ESCs, adult stem cells are safer for implantation purposes [52]. To use adult MSCs for these implantation purposes, they need to be isolated from a tissue of the donor before the cells can be expanded and later implanted into the donor's body.

MSCs can be isolated from various tissues. The isolation of MSCs from the bone marrow represents a common process. After harvesting these cells, they can be expanded in cell culture and can be differentiated into cells of diverse tissues [53-56]. HBMSCs are able to differentiate into chondrogenic [57-60], myogenic, adipogenic [57, 59] and osteogenic cells [57, 59, 61] which depend on the presence of lineage-specific induction factors [59, 62]. Since mesenchymal cells also promote hematopoiesis, defects of these cells adversely affect osteogenesis as well as hematopoiesis [63, 64].

1.3.1 Characterization and Isolation of HBMSCs

By plating MSCs on plastic dishes in fetal calf serum (FCS), Friedenstein isolated and expanded these types of cell *in vitro* in 1982 for the first time [65, 66]. Due to the adherence to plastic, MSCs can easily be separated from the other cells of the bone marrow such as hematopoietic cells. Furthermore, using selected FCS, which selectively enhance the adherence, the isolation is made more successful [67]. The bone marrow isolated hBMSCS show a typical immunophenotype and are uniformly positive for CD29, CD44, CD71, CD90, CD106, CD120a, CD124, SH2 and SH3. Moreover, it is demonstrated that these cells are negative for CD14, CD34 and the leukocyte common antigen CD45 [12]. Flow cytometry analysis further proved that MSCs are also positive for VCAM-1, LFA-3 and HLA MHC Class I. These surface markers suggest that MSCs can interact with T-cells [57, 68]. Systemically transplanted MSCs show multi-potential differentiation and long-term engraftment which suggests that MSCs can acquire the phenotype of the tissues in which they engraft [59, 69, 70].

1.4 Reactive Oxygen Species (ROS)

Even though oxygen is an obligate requirement for living beings, it is also attributed to cell toxicity. Since oxygen can form reactive oxygen species, it is able to damage cells. Reactive oxygen species are a group of highly active molecules which contain free radicals or pro-oxidative substances such as hydrogen peroxide. Due to their high reactivity, they react readily *inter alia* with lipids, nucleic acids or proteins [71, 72]. As low levels of ROS are required to regulate cell signaling processes during proliferation or differentiation processes, elevated levels result in cell death and apoptosis [73-75]. Via pro- and antioxidant enzymatic pathways, a balance between formation and degradation of ROS is maintained which in turn is obligatory for healthy conditions during cell signaling process such as cell proliferation, differentiation, autophagy, apoptosis and senescence [76].

1.4.1 Sources of Reactive Oxygen Species (ROS)

ROS are chemical molecules which derive from oxygen and are, caused by their initiation of oxidative stress, harmful chemicals. Oxygen derived radicals show a higher reactivity than for instance hydrogen peroxide. Both are ROS. Radicals are characterized by a single unpaired electron which causes the high reactivity [77, 78]. The most relevant ROS are hydrogen peroxide (H_2O_2), superoxide anions ($O_2\cdot^-$) and hydroxyl radicals ($HO\cdot$) [79]. Whereas hydrogen peroxide and superoxide anions are formed during the respiratory chain in mitochondria and both are dependent on one another and additionally are necessary for cell signaling process under healthy conditions, hydroxyl radicals are invariably harmful [76]. In *table 1*, the relevant ROS and the relating chemical reactions are demonstrated in detail.

Table 1: Examples of the most important reactive oxygen species and their chemical reaction.

Radical	Reaction
Superoxide anion $O_2^{\cdot-}$	$O_2 + e^- \rightarrow O_2^{\cdot-}$
Hydrogen peroxide H_2O_2	$O_2^{\cdot-} + 2H^+ \rightarrow H_2O_2 + O_2$
Hypochlorous acid HOCl	$H^+ + Cl^- + H_2O_2 \rightarrow HOCl + H_2O$
Hydroxyl radical $HO^{\cdot}$	$H_2O_2 + e^- \rightarrow 2HO^{\cdot}$

The main sources of intracellular ROS are the endoplasmic reticulum and the respiratory chain within the mitochondria. During the process of the respiratory chain, the NADPH oxidase (NOX) is the main source of ROS [79-81]. NOX is the only enzyme which primary functions by ROS formation (see: *figure 7*). NOX are multi-subunit enzyme complexes and the family consists of seven members: NOX1-5, Dual Oxidase 1 and 2 (DUOX1 and DOUX2) [82-85]. The regulatory enzymes p22phox, p47phox, p67phox, p40phox and Rac

GTPase of the NOX1-4 complexes are necessary for the activation, stability and the localization of the enzyme [86]. After NOX activation, an electron is transferred to FAD and via two hemes to molecular oxygen. Because of the electron transfer to the oxygen, superoxide anions are formed [86-88]. Xanthine oxidase is another example of a ROS generating enzyme which highlights that NOX is not the only ROS producing enzyme. But nonetheless, NOX is the main ROS producer [89, 90].

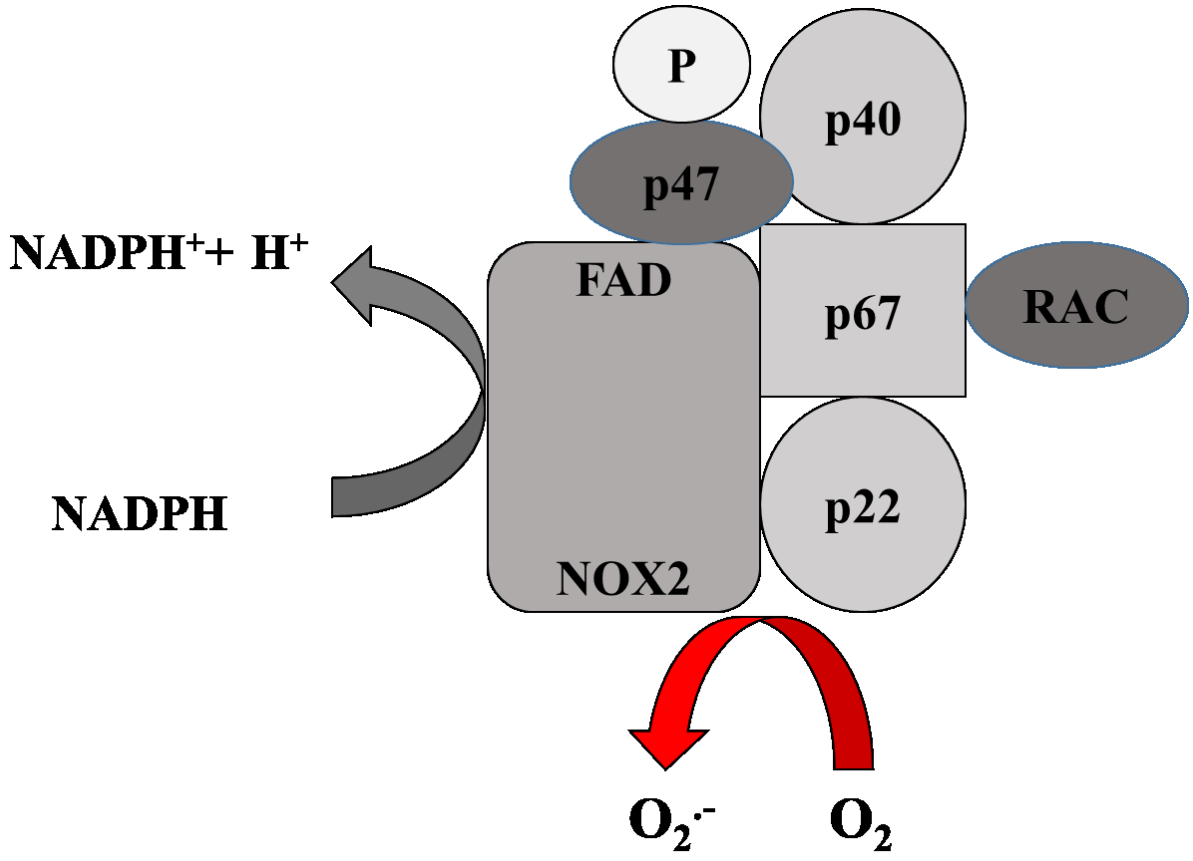

Figure 7: NADPH oxidase-derived reactive oxygen species. This image highlights the interaction of the complex of NOX with the regulatory enzymes p22phox, p47phox, p67phox, p40phox and Rac GTPase and presents the superoxide anion generation (own representation based on [85]).

As previously mentioned in this section, a balance of ROS is required for healthy cell signaling processes. Elevated levels of ROS result in bone obesity. This disorder correlates with dysregulations of lipid and glucose metabolism, downregulation of osteogenic processes and subsequently with bone defects and metabolic diseases which in turn rise the rates of morbidity and mortality. Thus, abnormalities in ROS levels cause imbalance between adipogenesis and osteogenesis. The required balance is further regulated by diverse other adipogenic or osteogenic factors which are highlighted in *figure 8*.

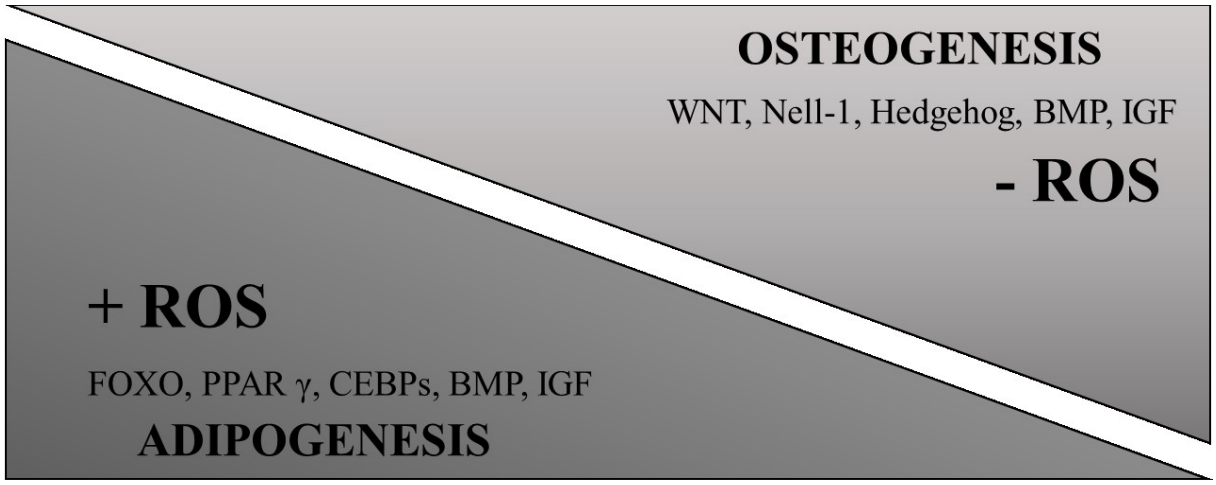

Figure 8: Signaling cascades of osteogenesis and adipogenesis. *Inter alia*, Wnt/β-catenin and Nell-1 signaling induce osteogenesis, whereas PPARγ and C/EBPs signaling promote adipogenic differentiation. BMP and IGF signaling induce both differentiation processes. At lower ROS levels, osteogenesis is improved while adipogenesis is promoted by the presence of higher ROS levels. Own representation based on [91].

1.4.2 Antioxidant Systems of Cells

As described in the previous paragraph, an imbalance of ROS can cause cellular damages and consequently serious pathological disorders. To regulate the balance of ROS, pro-oxidative and antioxidative regulatory processes are required [86, 92, 93]. The antioxidative system contains enzymatic and non-enzymatic approaches. *Inter alia*, vitamin C and E or carotenoids represent non-enzymatic antioxidative substances, whereas superoxide dismutase, catalase, peroxiredoxin, glutathione peroxidase and glutathione S-transferase are cellular antioxidative enzymes [76].

Superoxide dismutase, which catalyzes the dismutation of superoxide anions to hydrogen peroxide, exists in three isoforms with different metals. Copper-zinc SOD (SOD1) can be found in the cytoplasm, the manganese SOD (SOD2) is located in the nucleus and plasma membrane and the third superoxide dismutase is also a copper-zinc SOD (SOD3) and can be found in the extracellular matrix [94, 95]. The reaction of superoxide dismutase is correlated with catalase reaction. Superoxide dismutase degrades superoxide anions to hydrogen peroxide which in turn is degraded to water and oxygen by catalase [96-98]. In mammals, the reactions of catalase and superoxide dismutase are co-existing [90, 99-101]. Hydrogen peroxide is also degraded in mammals by glutathione peroxidase and peroxiredoxin. The depending reactions of NOX, SOD, catalase and glutathione peroxidase are demonstrated in *figure 9*.

[redacted]

Figure 9: Chemical reactions of the ROS generation and degradation. (Own representation based on [102].)

1.4.2.1 Catalase

1900, Loew developed catalase as a hydrogen peroxide degrading enzyme [103]. Later, it was found out that catalase consists of a protoporphyrin ring which is the active part of the enzyme. The active center is formed by an iron ion [97]. In *figure 10*, the structure of catalase is presented. The central iron ion in the subunit is visible.

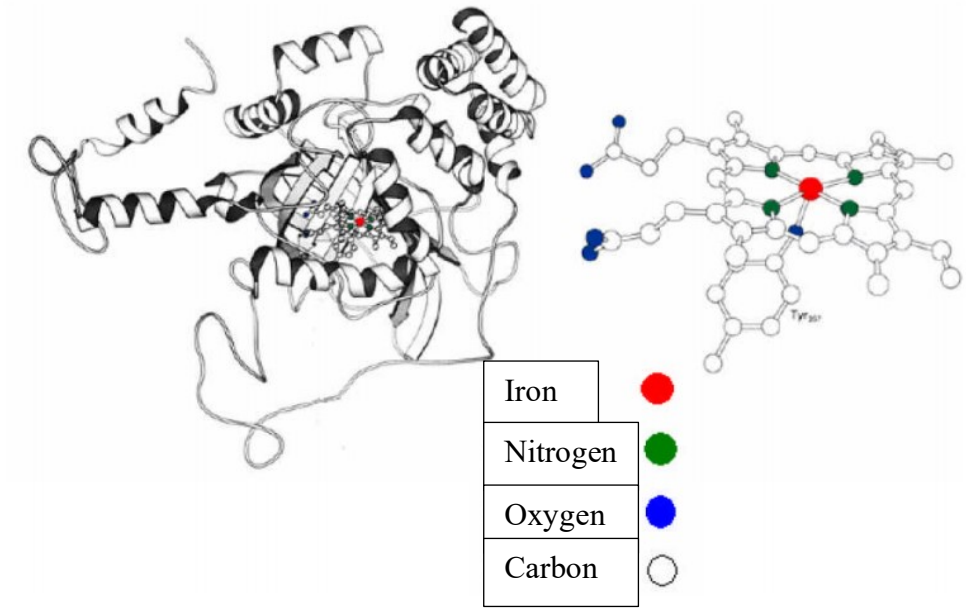

Figure 10: Structure of one subunit of catalase. Four subunits form the catalase. Bovine liver catalase is shown (modified presentation based on [104]).

Catalases are classified after Goldberg and Hochmann in three groups: typical catalases, atypical catalases and catalase-peroxidases [97]. Catalase degrades hydrogen peroxide via two states – the ferricatalase and compound I – to oxygen and water which is shown in *figure 11*.

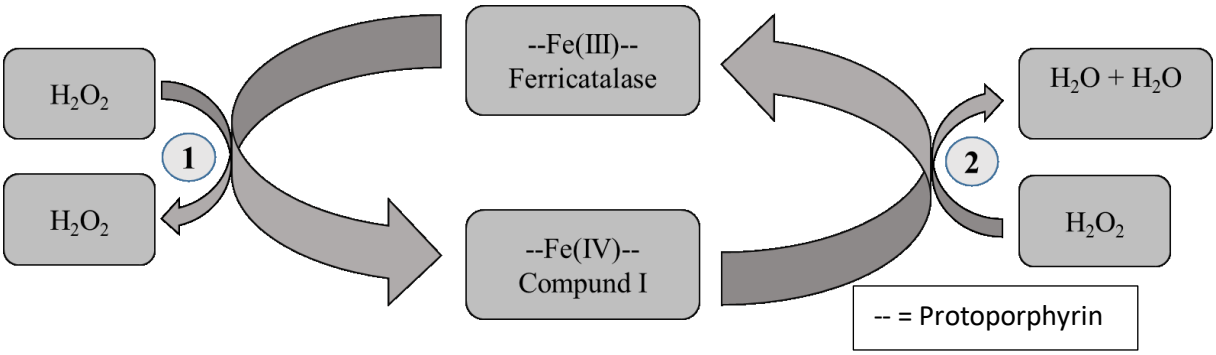

Figure 11: Degradation of hydrogen peroxide via two stages of catalase. (Own presentation based on [104].)

It is also important to note that a hydroxyl generation is hypothesized which might depend on hydrogen peroxide concentrations. This theory emphasizes that catalase might react as an antioxidant as well as a pro-oxidant substance [105, 106]. Further details are described in *6.1.1*. Due to the high reactivity of hydroxyl radicals, they are relevant regulators during damaging processes such as lipid peroxidation [107, 108]. Furthermore, regulative effects during cell signaling processes of osteogenesis might be reasonable.

1.5 Aging of Cells

Since the microenvironment of MSCs and cellular signaling processes are relevant for MSC differentiation, any deviations such as aging can lead to adverse effects.

Aging correlates with a distinct decrease of the number of adult BMSCs and with the ability of proliferation and differentiation of these cells [109-111]. Interestingly, the total number of nucleated cells decreases, whereas the number of osteoblastic progenitors did not significantly decrease for men but did for women [112]. It is suggested that aging processes impair the availability and growth potential of MSCs for osteogenic differentiation which furthermore varies between the sex of the host [113]. Zhou and coworkers investigated that aged MSCs present increased numbers of senescence-associated apoptotic cells, a decreased proliferation rate and β-galactosidase positive cells. Moreover, genes, which are involved in apoptotic regulatory pathways such as p53, its target p21 and BAX, are overexpressed in aged hosts [49, 114, 115]. Additionally, less CFU-ALP^{+} cells and shortened telomeres were observed which indicates a loss of differentiation and proliferation function [113, 116]. Since an inflammatory phase with an increased survival of anti-inflammatory M2 macrophages and a reduced pro-inflammatory factor secretion is obligatory for bone healing, ageing impairs timely bone regeneration processes [117].

1.6 Tissue Engineering

The increasing need for tissue replacements and organs motivated scientists to investigate various possibilities in the field of regenerative medicine. By tissue engineering concepts, biocompatible, laboratory-made tissues are generated. These tissues should be able to replace damaged tissues without leading to complications such as rejections. To prevent these types of complications, approaches are performed in which individual hBMSCs of each donor are used. These cells are expanded *in vitro*. Furthermore, the cells are cultivated under influences of different growth factors and further substances which initiate the differentiation processes of the desired tissue. Depending on the tissue, special combinations of differentiation inducing factors and three-dimensional scaffolds are used. After the generation of the desired

cell construct, the damaged tissue was replaced with the new cells [118]. The combination of cells and biomaterials represent the foundation to generate tissue replacements of patient specific cells [119, 120]. *Figure 12* illustrates the cycle of harvest of individual cells, the cell preparation – such as isolation, cultivation, proliferation and differentiation in combination with a scaffold – and the implantation of the tissue replacement into the donor's body.

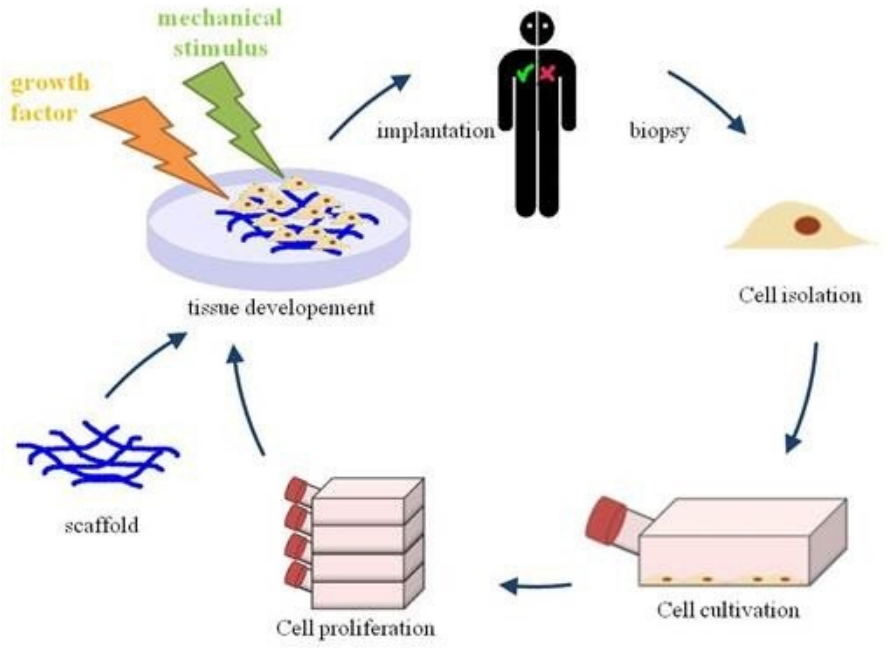

Figure 12: Tissue engineering of individual donor cells and optimal scaffolds. The image shows the cycle of the cell harvest, cell preparations and lastly, the implantation of the designed tissue replacement [121].

The demands on modern biomaterials for tissue replacement are high. The stimulated healing processes of bones should be positively affected. The new tissue should grow fast and exhibit high resistance and stability [122, 123]. To achieve these aims, engineering approaches were orientated at original signaling pathways of growth factors and the natural structure of bone cells and their matrix. To obtain an optimal replacement tissue, the replacement should exhibit osteogenic (*inter alia* mediated by osteoblasts), osteoconductive (*inter alia* mediated by trabecular structures) and osteoinductive characteristics (*inter alia* mediated by diverse osteogenic growth factors) [124-128]. Furthermore, a formation of a three-dimensional structure is obligatory to mediate the cell signaling process and a strong engraftment [120, 129-131]. The use of scaffolds, matrices, cell culture techniques and three-dimensional printing are in the focus of tissue engineering [123, 131, 132].

1.6.1 Used Scaffolds for Bone Replacements

To bridge the gap between research and clinical application of tissue replacements, ideal scaffolds should improve homing, cell viability, proliferation, osteogenic differentiation, vascularization and host integration [133]. Furthermore, the scaffolds should be serializable by industrial techniques and reproducible on a large scale with cost effective processes. *Figure 13* highlights the required characteristics of bone replacements.

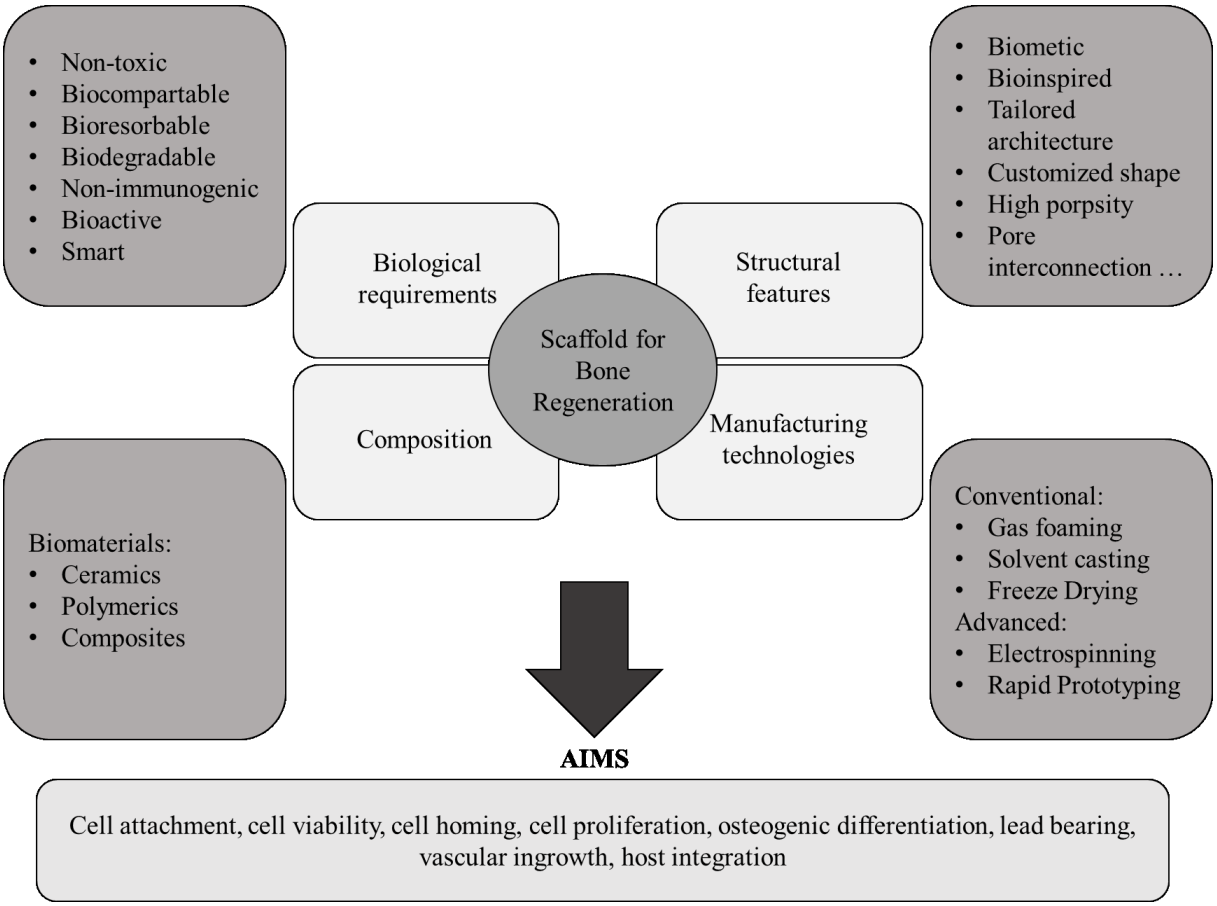

Figure 13: Characteristics of an ideal scaffold. Bone tissue engineering is orientated towards the described features. (Own presentation based on [131])

The key features of scaffolds for bone tissue engineering are shown in the upper part of the figure and can be described as follows:

- Manufacturing technologies: conventional and advanced technologies to generate three-dimensional scaffolds are listed.
- Structural features: scaffolds should mimic the anatomical three-dimensional structure of native bone extracellular matrix (ECM) [128].

- Biological requirements: the scaffold should be biodegradable, able to integrate and interact with the surrounding environment, be non-toxic and also minimize the risk of rejection [133-136].
- Composition: most used scaffolds are synthetic polymers, naturally derived polymers or a combination of both.

To achieve a restoration of the physiological structures and functions and also cell engraftment, application purposes, which are listed in the lower part of the scheme, are required [137, 138]. Hyaluronic acid, fibrin, collagen and chitosan are examples of used naturally derived polymers. These polymers show good osteoconductivity, biocompatibility and low immunogenicity. On the contrary, a difficult control of the degradation rate and a low mechanical stability represent the main disadvantages. Polyether ether ketone (PEEK), polyglycolic acid (PGA), polyanhydride, polycaprolactone (PCL), polypropylene fumarate (PPF), polyphosphazene and polylactic acid (PLA) are used as synthetic polymers. These substances exhibit a controlled degradation rate, an improved cell engraftment, the possibility to design bone mechanical properties and can fabricate complex structures [139, 140]. Synthetic and natural hydrogels are another important class of polymers which are used to form scaffolds for bone replacements. These polymers can mimic extracellular matrix structures and thus are capable of the delivery of cell signaling molecules [138].

To fabricate scaffolds, diverse manufacturing technologies, which are grouped in conventional technologies and rapid prototyping, are used. Typically used conventional technologies are: lyophilization, thermally induced phase separation (TIPS), gas foaming, powder-forming process, sol–gel technique and electrospinning [141]. Rapid prototyping processes are: stereolithography, fused deposition modeling, selective laser sintering, three-dimensional printing and bioprinting [142-145].

Even though the research of bone tissue engineering is developing rapidly, several challenges need to be bridged to progress approaches of clinical applications [131].

2 Objectives of the Study

Within this study, positive and adverse consequences of pro- and antioxidative influences on the osteogenic differentiation of mesenchymal stem cells of the human bone marrow (hBMSCs) should be thoroughly investigated.

In this context, the following issues should be analyzed:

1. The deviating behavior of responder and low responder hBMSC donors during the cultivation in osteogenesis promoting osteogenic differentiation medium by the evaluation of osteogenic differentiation indicating parameters such as the extent of matrix calcification and the activity of alkaline phosphatase.
2. Differences between the two donor types and impacts of the treatment with catalase on the expression of ROS related proteins such as NOX4, SOD1/2, FOX1, Nrf2, catalase and glutathione peroxidase.
3. Differences between the two donor types and impacts of the treatment with catalase on the expression of proteins referring the apoptosis pathway such as AKT and p53 and further on the apoptosis rate.
4. Differences between the two donor types and impacts of the treatment with catalase on the gene expression of osteogenic structure proteins such as SPARC, collagen type 1 and osterix.
5. Deviations of the energy metabolism of low responder and responder cells by the determination of the ATP generation and the glucose homeostasis during the osteogenic differentiation of both donor types in connection with potential consequences by pro- and antioxidative treatments.
6. Positive and adverse effects on the cell viability of hBMSCs and hypothetical interferences to the osteogenic differentiation potentials of responder and low responder donors.
7. Evaluation of impacts on the FGF-2 homeostasis of responder and low responder cells.
8. Clarification of the chemical reaction process of catalase and the potentially related pro- and antioxidative effects by a determination of the amount of hydroxyl radicals, further test runs with inactivated catalase, visualization of impacts on the adipogenic accumulation of lipids and, since catalase contains an iron ion in the active center, test runs with iron (II) and (III) compounds.

Obtained data of these investigations intend to clarify on one hand the molecular signaling pathway of the impaired osteogenic differentiation potential of low responder hBMSCs and

on the other hand the molecular mechanism of the observed restoration of a significantly impaired osteogenic differentiation potential by a catalase treatment. The identification of the involved factors can be used as a foundation of development of new clinical application approaches within the treatment of bone healing disorders.

3 Materials

3.1 Consumables

Table 2: List of used consumables and materials

Consumables and Materials	Company
Medical gloves for single use (Micro-Touch® Nitra-Tex®)	Ansell GmbH; München; Germany
2,0 ml Reaction vessesl (Safe-Lock Tubes™ 2,0 ml)	Eppendorf AG; Hamburg; Germany
1,5 ml Reaction vessesl (Safe-Lock Tubes™ 1,5 ml)	Eppendorf AG; Hamburg; Germany
0,5 ml Reaction vessesl (Safe-Lock Tubes™ 0,5 ml)	Eppendorf AG; Hamburg; Germany
Cryo Vessel (Cryo.s™ 2 ml)	Greiner Bio-One GmbH; Kremsmünster; Austria
6 well plate (6-well CELLSTAR® Tissue Culture Plates)	Greiner Bio-One GmbH; Kremsmünster; Austria
12 well plate (12-well CELLSTAR® Tissue Culture Plates)	Greiner Bio-One GmbH; Kremsmünster; Austria
24 well plate (24-well CELLSTAR® Tissue Culture Plates)	Greiner Bio-One GmbH; Kremsmünster; Austria
48 well plate (48-well CELLSTAR® Tissue Culture Plates)	Greiner Bio-One GmbH; Kremsmünster; Austria
96 well plate (96-well CELLSTAR® Tissue Culture Plates)	Greiner Bio-One GmbH; Kremsmünster; Austria
Nunc™ F96 MicroWell™ Plate (white)	Fisher Scientific GmbH; Schwerte; Germany
15 ml falcon tubes	Greiner Bio-One GmbH; Kremsmünster; Austria
50 ml falcon tubes	Greiner Bio-One GmbH; Kremsmünster; Austria
FACS reaction vessel (FALCON® 5 ml)	BD Bioscience; Heidelberg; Germany
T75 flask, CELLSTAR® Cell Culture Flasks 75 cm^2 red filter cap	Greiner Bio-One GmbH; Kremsmünster; Austria

Petri dish, CELLSTAR® dish diam. × H 145 mm × 20 mm, vented	Greiner Bio-One GmbH; Kremsmünster; Austria
Bottles (1000 / 500 / 250 ml)	Schott AG; Mainz; Germany
Measuring cylinder (500 / 100 / 50 ml)	VWR®; Darmstadt; Germany
Measuring cylinder (plastic, 1000 ml)	VITLAB GmbH; Grossostheim, Germany
Glass cuvette (10,00 mm)	Hellma® Analytics GmbH & Co. KG; Muellheim; Germany
Beakers (250 / 100 / 50 ml)	Schott AG; Mainz; Germany
Combs (for 15 gel pockets)	Bio-Rad Laboratories GmbH; München; Germany
Casting frames	Bio-Rad Laboratories GmbH; München; Germany
Casting stands	Bio-Rad Laboratories GmbH; München; Germany
Glass plate (1 mm) with spacer	Bio-Rad Laboratories GmbH; München; Germany
Nitrocellulose membrane, pore size: 0,2 µm	Biotechnologie GmbH; Erlangen; Germany
4–20% Mini-PROTEAN® TGX Stain-Free™ Protein Gels, 15 well, 15 µl #4568096	Bio-Rad Laboratories GmbH; München; Germany
Neubauer counting chamber	LO Laboroptik; Friedrichsdorf; Germany
Stripetten (5 ml Corning® Costar® Shorty Stripette® Serological Pipets)	Sigma-Aldrich-Chemie GmbH; München; Germany
Stripetten (10 ml Corning® Costar® Shorty Stripette® Serological Pipets)	Sigma-Aldrich-Chemie GmbH; München; Germany
Stripetten (25 ml Corning® Costar® Shorty Stripette® Serological Pipets)	Sigma-Aldrich-Chemie GmbH; München; Germany
Combitips advanced® 10 ml #0030089464	Eppendorf AG; Hamburg; Germany
Combitips advanced® 5 ml #0030089456	Eppendorf AG; Hamburg; Germany
10/20 µl XL Graduated, Filter Tip #S1120-3810	STARLAB INTERNATIONAL GmbH; Hamburg; Germany

200 µl Graduated, Filter Tip #S1120-8810	STARLAB INTERNATIONAL GmbH; Hamburg; Germany
1000 µl XL Graduated, Filter Tip #S1122-1830	STARLAB INTERNATIONAL GmbH; Hamburg; Germany
Pasteur pipettes (ISO 7712) (glass)	BRAND GmbH + CO KG; Wertheim; Germany
Cell scrapers (28 cm)	Greiner Bio-One GmbH; Kremsmünster; Austria
Sterile filter (Millex®-GS 0,22 µm)	MERCK Millipore; Darmstadt; Germany
Whatman paper	Bio-Rad Laboratories GmbH; München; Germany
Stripetten (5 ml Corning® Costar® Shorty Stripette® Serological Pipets)	Sigma-Aldrich-Chemie GmbH; München; Germany
Stripetten (10 ml Corning® Costar® Shorty Stripette® Serological Pipets)	Sigma-Aldrich-Chemie GmbH; München; Germany
Stripetten (25 ml Corning® Costar® Shorty Stripette® Serological Pipets)	Sigma-Aldrich-Chemie GmbH; München; Germany
Pasteur pipettes (ISO 7712) (glass)	BRAND GmbH + CO KG; Wertheim; Germany
Whatman paper	Bio-Rad Laboratories GmbH; München; Germany

3.2 Equipment

Table 3: List of used equipment

Equipement	Company
Bench HERAsafe®	Thermo Fisher Scientific GmbH; Dreieich; Germany
Incubator	Thermo Fisher Scientific GmbH; Dreieich; Germany
Refrigerator	Nalge Nunc International; Rochester (NY); United States

Icebox Revco Ultima	Thermo Fisher Scientific GmbH; Dreieich; Germany
Heated bath	Thermo Fisher Scientific GmbH; Dreieich; Germany
Heating block	Thermo Fisher Scientific GmbH; Dreieich; Germany
Water bath	Thermo Fisher Scientific GmbH; Dreieich; Germany
Magnetic stirrer (IKA® RET control/t IKAMAG® safety control)	IKA®-Werke GmbH & Co. KG; Staufen; Germany
Scales (Kern 440; ABJ-N)	Kern & Sohn GmbH; Balingen; Germany
Suction pump	KNF Neuberger GmbH; Freiburg; Germany
Cryo freezer	Schmidt Laborgeräte GJM Handel und Service GmbH; Wien; Austria
Fume cupboard	Waldner Laboreinrichtungen GmbH & Co. KG; Wangen; Germany
Centrifuge Heraeus Megafuge 16 R	Thermo Fisher Scientific GmbH; Dreieich; Germany
Centrifuge Heraeus Pico 17 Microcentrifuge	Thermo Fisher Scientific GmbH; Dreieich; Germany
Vortex Mixer Art. No 444-1372	VWR®; Darmstadt; Germany
Roll mixer RM5-V 1750; RM5-V80 1752	Labortechnik Fröbel GmbH; Lindau; Germany
Eppendorf Research® fix 0,5 - 10 µl	Eppendorf AG; Hamburg; Germany
Eppendorf Research® fix 10 - 100 µl	Eppendorf AG; Hamburg; Germany
Eppendorf Research® fix 10 - 200 µl	Eppendorf AG; Hamburg; Germany
Eppendorf Research® fix 100 - 1000 µl	Eppendorf AG; Hamburg; Germany
Pipettboy accu-jet® pro	BRAND GmbH & Co. KG; Wertheim; Germany
Multipette® plus	Eppendorf AG; Hamburg; Germany
Microscope Zeiss Axiovert 40	Carl Zeiss AG; Oberkochen; Germany
Mikroskop Zeiss Axiovert 200	Carl Zeiss AG; Oberkochen; Germany

Multilabel Counter VICTOR™ V Multilabel counter model 1420	Perkin Elmer; Waltham; United States
Flow cytometer FACS Calibur	BD Bioscience; Heidelberg; Germany
NanoDrop spectrophotometer ND-1000	Thermo Fisher Scientific GmbH; Dreieich; Germany
PowerPac™ Basic Power Supply	Bio-Rad Laboratories GmbH; München; Germany
Blotting apparatus	Thermo Fisher Scientific GmbH; Dreieich; Germany
MyCycler™ Thermal Cycler System #1709703	Bio-Rad Laboratories GmbH; München; Germany
Sonification apparatus	Hielscher Ultrasonics GmbH; Berlin; Germany
ChemiDoc™ MP Imaging System	Bio-Rad Laboratories GmbH; München; Germany
Real Time PCR System (7300)	Applied Biosystems GmbH; Darmstadt; Germany
Spectrophotometer Specord 205	Analytik Jena AG; Jena, Deutschland

3.3 Substances and Solutions

Table 4: List of used substances and solutions

Substances / Solutions	Company
FCS (Fetal Bovine Serum Gold)	PAA Laboratories GmbH; Cölbe; Germany
Hepes H3375 ≥99,5 %	Sigma-Aldrich-Chemie GmbH; München; Germany
Penicillin/Streptomycin	PAN-Biotech GmbH; Aidenbach; Germany
Bovine serum albumin (BSA)	PAA Laboratories GmbH; Cölbe; Germany
Bromphenol blue	Carl Roth GmbH + Co. KG; Karlsruhe; Germany
4 % Paraformaldehyde	Sigma-Aldrich-Chemie GmbH; München; Germany
p-Nitrophenyl phosphate solution	Sigma-Aldrich-Chemie GmbH; München; Germany

Alizarin Red S	Sigma-Aldrich-Chemie GmbH; München; Germany
Neutral red #553-24-2	Sigma-Aldrich-Chemie GmbH; München; Germany
Cetylpyridinium chloride	Sigma-Aldrich-Chemie GmbH; München; Germany
2-Mercaptoethanol	Sigma-Aldrich-Chemie GmbH; München; Germany
RIPA buffer	Abcam plc; Cambridge; United Kingdom
Milk powder	Carl Roth GmbH + Co. KG; Karlsruhe; Germany
Ponceau S	SERVA Electrophoresis GmbH; Heidelberg; Germany
DPBS (Dulbecco`s phosphate buffered saline w: Calcium w: Magnesium)	PAN-Biotech GmbH; Aidenbach; Germany
RPMI 1640 #P04-17500	PAN-Biotech GmbH; Aidenbach; Germany
PBS	Biochrom GmbH; Berlin; Germany
Developing solution 1 (Clarity™ Western ECL Substrate #170-5060) Luminata™ Forte Western HRP Substrate #WBLUF0100)	Bio-Rad Laboratories GmbH; München; Germany
Developing solution 2 (Luminata™ Forte Western HRP Substrate #WBLUF0100)	MERCK Millipore; Darmstadt; Germany
FACS clean #340345	BD Bioscience; Heidelberg; Germany
FACS buffer FACS Flow™ BD Bioscience #342003	BD Bioscience; Heidelberg; Germany
FACS Rinse #340346	BD Bioscience; Heidelberg; Germany
Trypan blue 0,4 %	Sigma-Aldrich-Chemie GmbH; München; Germany
Trypsin/EDTA solutions (0,05 % / 0,02 %) in PBS, without Ca^{2+}, Mg^{2+}	Biochrom GmbH; Berlin; Germany
Tween 20	Sigma-Aldrich-Chemie GmbH; München; Germany

Triton™ X-100	Sigma-Aldrich-Chemie GmbH; München; Germany
PBS, without Ca^{2+}, Mg^{2+}	Biochrom GmbH; Berlin; Germany
Carl Roth® TRIS PUFFERAN®, ≥ 99,3 %, Buffer Grade, Tris-(hydroxymethyl) aminomethan #648310	Carl Roth GmbH + Co. KG; Karlsruhe; Germany
Tris Base, Molecular Biology Grade Calbiochem® #648310	MERCK Millipore; Darmstadt; Germany
Tris-HCl #648310648313	MERCK Millipore; Darmstadt; Germany
Tris, Hydrochloride	ULTROL® Grade Calbiochem®
Triton™ X-100	Sigma-Aldrich-Chemie GmbH; München; Germany
Purified water	Otto Fischer GmbH & Co. KG; Waldkirch; Germany
Roti-Mark Western Set	Carl Roth GmbH + Co. KG; Karlsruhe; Germany
N,N,N´,N´-Tetramethylethylenediamine (TEMED)	Carl Roth GmbH + Co. KG; Karlsruhe; Germany
Sodium dodecylsulfate (SDS)	VWR®; Darmstadt; Germany
RNase Inhibitor 2500 U (Ambion®)	Thermo Fisher Scientific GmbH; Dreieich; Germany
Random primer (octamers)	Jena Bioscience GmbH; Jena; Germany
Power SYBR Green	Applied Biosystems GmbH; Darmstadt; Germany
Oligo dT15	Sigma-Aldrich-Chemie GmbH; München; Germany
Microbiologically pure water	5PRIME
Methanol (Methanol for analysis EMSURE® ACS, ISO, Reag. Ph Eur)	MERCK Millipore; Darmstadt; Germany
Fibroblast Growth Factor-basic / FGF-2	PeproTech; Hamburg; Germany
Dexamethasone	Sigma-Aldrich-Chemie GmbH; München; Germany
Isopropanol (2-Propanol EMPLURA®)	MERCK Millipore; Darmstadt; Germany

Hydrogen peroxide (H_2O_2)	VWR®; Darmstadt; Germany
DMSO Dimethyl sulfoxide D2650 - HybriMax™, sterile-filtered, BioReagent, suitable for hybridoma, ≥99.7 %	Sigma-Aldrich-Chemie GmbH; München; Germany
Adenosine 5'-triphosphate (ATP) disodium salt hydrate	Sigma-Aldrich-Chemie GmbH; München; Germany
D-Mannitol	Sigma-Aldrich-Chemie GmbH; München; Germany
Trolox	Sigma-Aldrich-Chemie GmbH; München; Germany
EUK134	Sigma-Aldrich-Chemie GmbH; München; Germany
MnTBAP - Calbiochem	Sigma-Aldrich-Chemie GmbH; München; Germany
SOD2 / MnSOD	Sigma-Aldrich-Chemie GmbH; München; Germany
Catalase from bovine liver	Sigma-Aldrich-Chemie GmbH; München; Germany
Iron (II) sulfate heptahydrate	Sigma-Aldrich-Chemie GmbH; München; Germany
Iron (III) chloride	Merck KGaA; Darmstadt, Germany
Hemoglobin human	Sigma-Aldrich-Chemie GmbH; München; Germany
3-Amino-1,2,4-triazole (ATA)	Sigma-Aldrich-Chemie GmbH; München; Germany
β-Glycerophosphate disodium salt hydrate	Sigma-Aldrich-Chemie GmbH; München; Germany
L-Ascorbic acid 2-phosphate	Sigma-Aldrich-Chemie GmbH; München; Germany
Hoechst 33342	Pierce Biotechnology; Rockford; United States
Propidium iodide	Sigma-Aldrich-Chemie GmbH; München; Germany

Fluorescence Mounting Medium #S3023	Agilent Technologies; Santa Clara; United States

3.4 Kit Systems

Table 5: List of used kit systems

Kit System	Company
Pierce™ BCA Protein Assay Kit #23225	Thermo Fisher Scientific GmbH; Dreieich; Germany
RT-PCR Kit #210210 Oligo dT- Primermix (20 µM) dNTP-Mix (5 mM) Omniscript Reverse Transcriptase (4 U/µl) RNase-Inhibitor (40 U/µl)	Qiagen N.V.; Hilden; Germany
RNA Isolation: RNeasy Mini Kit #74106	Qiagen N.V.; Hilden; Germany
DNA-free Kit #AM1906 Puffer DNase I DNase-Inhibitor	Ambion, Thermo Fisher Scientific GmbH; Dreieich; Germany
ATP Kit #LBR-T010	Biaffin GmbH & Co KG; Kassel; Germany
Cell Meter™ Mitochondrial Hydroxyl Radical Detection Kit *Red Fluorescence* #16055	AAT Bioquest, Inc.; Sunnyvale; United States
Glucose-Glo™ Assay #J6021	Promega GmbH; Mannheim; Germany
Human FGF basic Quantikine ELISA Kit #DFB50	R&D Systems, Inc.; Minneapolis; United States
CellTiter-Blue® Cell Viability Assay #G8081	Promega GmbH; Mannheim; Germany
Cell Proliferation ELISA, BrdU (colorimetric) #11 647 229 001	Roche Diagnostics GmbH; Roche Applied Science; Mannheim; Germany
Catalase Assay Kit # Cay707002-96	Biomol GmbH; Hamburg; Germany

3.5 Antibodies

Table 6: List of used antibodies

Type of Antibody	Company
Mouse anti-Human Catalase monoclonal antibody #TA502564	OriGene EU; Acris Antibodies GmbH; Herford; Germany
Anti-GAPDH hFAB™ Rhodamine Antibody #12004167	Bio-Rad Laboratories GmbH; München; Germany
Rabbit Anti-Human SOD (Mn) polyclonal #SPC-118	StressMarq Biosciences Inc.; Victoria; British Columbia
Rabbit Anti-SOD1 polyclonal #2770	Cell Signaling Technology®; Leiden; Netherlands
Rabbit Anti-NADPH oxidase 4 monoclonal antibody #ab109225	Abcam plc; Cambridge; Great Britain
Rabbit Anti-Human p53 polyclonal antibody #9282	Cell Signaling Technology®; Leiden; Netherlands
Mouse Anti- Alkaline Phosphatase monoclonal antibody #sc-271431	Santa Cruz Biotechnology; Texas; United States
Mouse Anti-IRP1 monoclonal antibody #sc-166022	Santa Cruz Biotechnology; Texas; United States
ACO2 (D6D9) XP® Rabbit mAb #6571	Cell Signaling Technology®; Leiden; Netherlands
Rabbit Anti-Human RUNX2 polyclonal antibody #sc-10758	Santa Cruz Biotechnology; Texas; United States
Rabbit Anti-Human FOXO1 monoclonal antibody #2880	Cell Signaling Technology®; Leiden; Netherlands
Anti-rabbit IgG (H+L), F(ab')2 Fragment (Alexa Fluor® 488 Conjugate) #4412	Cell Signaling Technology®; Leiden; Netherlands
FITC conjugated Goat anti-Mouse IgG (H+L) #DAB-87640	Dianova GmbH; Hamburg; Germany
Fluorescein (FITC) AffiniPure Donkey Anti-Rabbit IgG (H+L) # 711-095-152	Jackson ImmunoResearch Laboratories, Inc.; West Grove; Germany
Mouse Anti- SPARC monoclonal #sc-398419	Santa Cruz Biotechnology; Texas; United States

Mouse Anti-Osterix monoclonal #sc-393325	Santa Cruz Biotechnology; Texas; United States
Mouse Anti-COL1A monoclonal #sc-59772	Santa Cruz Biotechnology; Texas; United States
Goat Anti-Mouse Immunoglobulin #P0447	Agilent Technologies; Santa Clara; United States
Goat Anti-Rabbit Immunoglobulin #D0487	Agilent Technologies; Santa Clara; United States

3.6 Primer

Table 7: List of used primer

Primer sequence	Company
SPARC Forward 5' GCTGGATGAGAACAACAC 3'	Eurofins Genomics; Ebersberg; Germany
SPARC Reverse 5' AAGAAGTGGCAGGAAGAG 3'	
Collagen Type 1 Forward 5' ACATGTTCAGCTTTGTGGACC 3'	
Collagen Type 1 Reverse 5' TGTACGCAGGTGATTGGTGG 3'	

3.7 Buffer, Solutions, Media

Table 8: List of used media

Buffer / Solutions / Media	Ingrediens
Freezing medium	10 % FCS
	Dimethylsulfoxid (DMSO)
Proliferation cell culture medium	500 ml Dubleccos MEM (Gibco™)
	10 % FCS
	1 % Penicillin / Streptomycin
	1 % Hepes H3375 ≥99,5 %
	0.2 % FGF-2
Osteogenic cell culture medium	500 ml Dubleccos MEM (Gibco™)
	10 % FCS
	1 % Penicillin / Streptomycin

	0.02 % Dexamthasone
	10 mM/L beta-glycerophosphate
	0.05 mMl/L L-ascorbic acid-2-phosphate
Abcam: For protein lysates: RIPA buffer storage at -20 °C, dissolved in Aqua dest.	50 mM Tris pH=8
	1 % NP-40
	0.1 % SDS
	150 mM NaCl
	0.5 % Na-deoxycholate
	Before use: phosphatase inhibitor and proteinase inhibitor need to be added
Laemmli buffer storage bei 4 °C, dissolved in Aqua dest.	250 mM Tris-HCI, pH 6.8
	0.1 % Bromophenol blue
	8 % SDS
	40 % Glycerol
	Before use: 20 % 2- mercaptoethanol need to be added
Resolving gel buffer Storage at RT, dissolved in Aqua dest.	0.4 % SDS
	1.5 M Tris
Stacking gel buffer Storage at RT, dissolved in Aqua dest.	0.4 % SDS
	0.5 M Tris
Transfer buffer Storage at RT, dissolved in Aqua dest.	192 mM Glycine
	25 mM Tris-Base, pH 8.0 – 10.5
Electrophoresis buffer Storage at RT, dissolved in Aqua dest.	192 mM Glycine
	0.1 % SDS
	25 mM Tris, pH 8.3 – 8.8
Blotting buffer Storage at RT, dissolved in Aqua dest.	150 ml 10x Transfer buffer
	150 ml Methanol
	1200 ml H_20
Blocking solution	150 mM NaCl

(immunohistochemically staining)	7.7 mM Tris, pH 7.5
	3 % Triton X-100
TBS	150 mM NaCl
	7.7 mM Tris, pH 7.5

3.8 Software

Table 9: List of used software

Software	Function
MS Office 2010	Drawing up documents
GraphPad Prism 5.0	Data and statistical analysis
EndNote X7, Thomson Reuters	Bibliography
Workout 2.0	Photometric measurement
Wallac 1420 Workstation	Photometric measurement
WinAspect 2.5.0.0	Photometric measurement by means of a spectrophotometer
Quantity One 4.6.5 Basic	Western blot analysis
Image Lab™ Software	Western blot analysis
BD CellQuest™ Pro	Flow cytometric measurement
ABI Prism 7300 System SDS v 1.4	qRT-PCR analysis, Applied Bioscience

4 Methods

4.1 Cell Culture

Within this work, exclusively hBMSCs were used for all investigative approaches. The cells were received from our cooperation partner of the department for trauma surgery at the Hannover Medical School. HBMSCs were obtained by patients which were admitted to hospital due to a traumatic injury. According to the guidelines of the ethic committee of the Hannover Medical School (study number: 2562), the patients or their legal guardians gave their consent to use the cell preparations for research purposes. 35 donors were available to conduct the investigations. Within the sample collection, our cooperation partner also prepared anamnesis datasheets of every donor (see appendix). Among others, these datasheets include information about blood counts, physical activity, body mass index, alcohol consumption, surface marker analysis of the hBMSCs and certain pre-existing conditions. Furthermore, pretests regarding the ability of osteogenic, adipogenic and chondrogenic differentiation potential were conducted. Thus, a system and listing of R-hBMSCs and LR-hBMSCs existed on delivery. The hBMSCs were delivered in cell passage one. Before using these cells for any tests, the hBMSCs were subcultivated to obtain a bigger number of cells in the same cell passage to make them more comparable within one test approach. In general, tests were run with cells in passages between three and eight. During these tests, constant attention was paid to use cell cultures of different donors with the same or nearby cell passage. HBMSCs were cultured in proliferation medium which consists of Dulbecco's modified eagle (DMEM, 4.5 g glucose) supplemented with 10 % FCS, 1 % Penicillin/Streptomycin, 1 % HEPES and 0.2 % FGF-2 to reach confluence. At a confluence of approximately 85 %, osteogenic differentiation was initiated by adding an osteogenic medium (DMEM with 4.5 g glucose supplemented with 10 % FCS, 1 % Penicillin/Streptomycin, 0.02 dexamethasone, 10 mM/L beta-glycerophosphate and 0.05 mM /L L-ascorbic acid-2-phosphate) instead of the proliferation medium. The cell cultivation occurred in an incubator at 37 °C and 5 % CO_2. The medium was changed every two to three days.

4.1.1 Sub Cultivation

At first, the medium supernatant was removed from the cultivated cells to subsequently wash the cells with PBS to remove remains of the medium. After aspirating the PBS again, 7 ml trypsin/EDTA solution was added to the cell culture in a T75 flask to detach the cells from the bottom of the culture flask. The cells were incubated with the trypsin/EDTA solution for three

to five minutes in an incubator at 37 °C and 5 % CO_2. In the following, the cells were detached by a so called *"shake off"* procedure. Within this process, the flask was taped lightly so that the cells were detached. An incubation at 37° C is necessary to reach an effective temperature range of the serine protease trypsin. Additionally, for an optimal result, it is important to have a pH range close to 7.5. In case the trypsin treatment is not resulting in a complete detachment of the cells, a cell scraper should be used to complete the cell detachment. The enzyme activity was stopped by the addition of an equivalent or 1.5-fold amount of culture medium which contained FCS. The cells were resuspended several times to make sure to transfer the whole number of cells. The cell suspension was transferred in a 50 ml falcon tube and centrifuged at 1200 rpm for 5 minutes. Afterwards, the supernatant was decanted and the cells were resuspended with a defined volume of culture medium or freezing medium depending on following procedure. If a defined cell number had been needed for a test or freezing the cells, the cell number would have been determined with trypan blue and a hemocytometer (Neubauer counting chamber) which is described in paragraph *4.1.2.* If the knowledge about the defined cell number is not needed, the cells and a defined volume of medium can be transferred for instance in a new culture flask. For an optimal cellular nutrition, a change of media was required every two to three days.

4.1.2 Determination of the Cell Number with a Hemocytometer (Neubauer Counting Chamber)

The cell number determination is necessary for freezing and thawing processes. For this purpose, a cover glass was moistened and placed on the hemocytometer. The formation of Newton's rings under the microscope point to a correct position of the cover glass. *Figure 14* shows the apparatus of a hemocytometer. 10 µl of the cell suspension and 10 µl of trypan blue were mixed. 10 µl of this compound in turn was filled with an Eppendorf Research® fix 0.5 - 10 µl in the room between the hemocytometer and the cover glass which was supported by capillary forces. Trypan blue is an anionic diazo dye which can stain dead cells because of the broken membrane whereas living cells do not absorb the dye. All this leads to blue colored dead cells and undyed / white living cells which can be observed under the microscope. *Figure 15* shows a microscopic image of cells after the use of trypan blue. During the work with trypan blue, it is imperative to work fast to get representative results of the cell viability and number because of the cytotoxic effect of this dye. To determine the cell number per milliliter, all four counter boxes were counted and the mean value was calculated. The mean value in turn was multiplied with 10^4 because of a chamber volume of 0.1 µl.

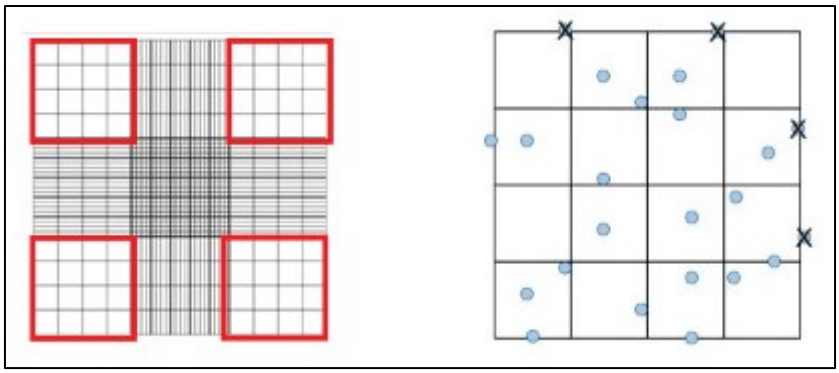

Figure 14: Principle of a hemocytometer [146]

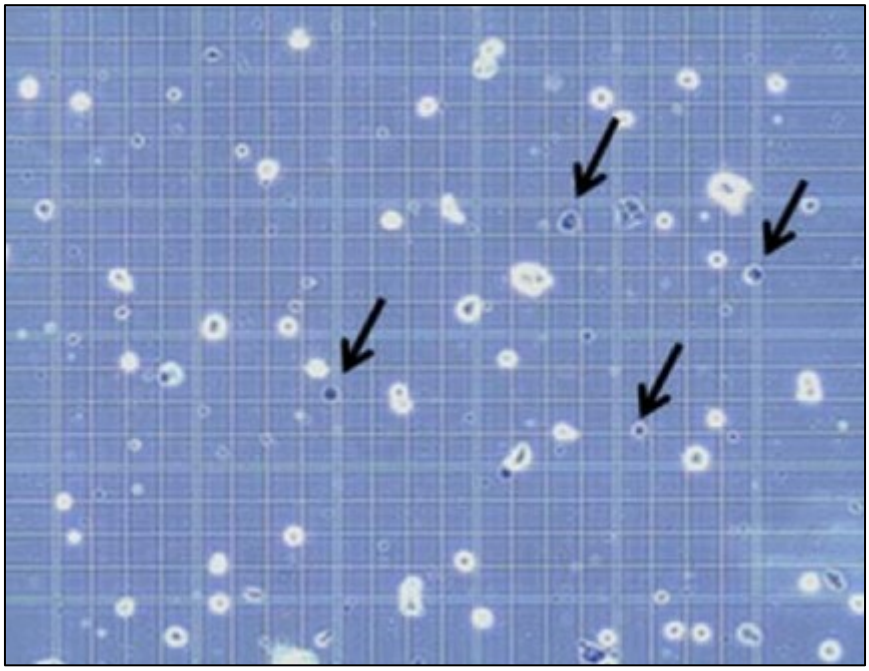

Figure 15: Difference between living and dead cells (dead cells are shown by the arrows) [147]

4.1.3 Cryopreservation of HBMSCs

As already mentioned in chapter *4.1.1*, cells were detached by an incubation with a trypsin solution and, when necessary, with a cell scraper and afterwards washed with PBS to remove all medium remains. To freeze cells, it was required to count the cells before putting them into the freezing medium and the cryo vessels, which is described in section *4.1.2*. One milliliter of freezing medium was frozen with a total amount of 1 to 1.5 million cells. After counting the cells, the needed volume of freezing medium was calculated. After the centrifugation, the remaining cell pellet was resuspended in the refrigerated freezing medium. One milliliter of this cell suspension was transferred per cryo vessel. For a gentle freezing process, the cryo vessels with the cell suspensions were positioned in a controlled cryo freezer at -80 °C for 24 hours. The content of the controlled cryo freezer is 100 % isopropyl which helps to cool down

the cells 1 °C per minute. *Figure 16* shows the used freezing vessel which is filled up with isopropyl. The freezing medium is a compound of FCS and 10 % of DMSO. At temperatures above 0 °C, DMSO shows cytotoxic effects which leads to the necessity to work fast and keep the cells and the freezing medium refrigerated during the entire procedure by using an ice box. Additionally, the freezing medium should always be freshly prepared.

Figure 16: "Thermo Scientific™ Mr. Frosty™" [148]

4.1.4 Thawing Process of HBMSCs

As mentioned in paragraph *4.1.3*, the cells were frozen in freezing medium with the cytotoxic DMSO which also required fast work. The cell suspensions were gently thawed in a water bath and afterwards resuspended in culture medium in a new 50 ml falcon. These cell suspensions were centrifuged at 1200 rpm. The media supernatants were decanted and the cells resuspended in fresh medium. Lastly, the cell suspensions were sown in new cell culture flasks or microtiter plates. After sowing, the cells were incubated in an incubator at 37 °C and 5 % CO_2 until they were used for tests.

4.2 Osteogenic Differentiation

HBMSCs were differentiated in an osteogenic medium which is a compound of 500 ml Dulbecco's modified eagle (DMEM, 4.5 g glucose), 10 % FCS, 1 % Penicillin / Streptomycin, 0.02 % dexamethasone, 10 mM/L beta-glycerophosphate and 0,05mMl/L L-ascorbic acid-2-phosphate. First, the cells were cultured in a proliferation medium until reaching a confluence of 85% as described in paragraph *4.1*. After confluence, hBMSCs were treated with the osteogenic differentiation medium. A differentiation test period was set to 28 days for the first test runs and to 21 days for later tests. An osteogenic differentiation is defined by the formation of calcified matrix. The first signs of the matrix calcification were seen at day 14. For the comparison of the diverse types of donors (low responder / responder hBMSCs), it

was necessary to pick a test duration of at least 21 days. The osteogenic differentiation of hBMSCs reached a peak at day 21. Therefore, for comparison purposes, day 21 was set as the date of evaluation. The extent of matrix calcification and the activity of alkaline phosphatase were measured to determine the dimension of osteogenic differentiation. Analogous to paragraph *4.1*, the media was changed every two to three days.

4.2.1 Incubation with Diverse Antioxidative and Oxidative Approaches during Osteogenic Differentiation

Analogous to paragraph *4.2*, after reaching confluence, the cells were cultured in osteogenic medium which was supplemented with various additives which are listed in *table 10*. The test duration was also set to 21 days. To evaluate the dimensions of the osteogenic differentiation approaches, the extent of matrix calcification and the activity of alkaline phosphatase were measured at day 21. To determine the best concentration of the additives for an optimal osteogenic differentiation, the concentrations of catalase, hydrogen peroxide, iron (III) chloride and iron (II) sulfate heptahydrate were titrated. For each substance, the most effective concentration was used for continuing test runs. In case of iron (III) chloride and iron (II) sulfate heptahydrate, no ideal concentration could be determined. This aspect is described more detailed in paragraph *5.2.1.8*. Due to the chemical instability of the most used additives, all solutions were always prepared freshly except for heat inactivated catalase. The preparation of heat inactivated catalase is described in paragraph *4.2.3*. The change of media was also performed every two to three days.

Table 10: List of used additives and used concentrations

Additive	Concentration	Source of the concentration
Catalase from bovine liver	62,5 U/ml, 125 U/ml, 250 U/ml, 500 U/ml, 1000 U/ml	Self-determined
Heat inactivated catalase from bovine liver	125 U/ml	Self-determined
MnTBAP	25 µM	[149]
EUK134	25 µM	[150]
Hemoglobin human	10 nM	Self-determined

3-Amino-1,2,4-triazole (ATA) in combination with catalase	500 µM / 1 mM (ATA) + 125 U/ml (catalase)	Usually used concentration in our laboratory
Hydrogen peroxide (H_2O_2)	10 µM, 20 µM, 40 µM, 100 µM	[151]
SOD2 / MnSOD	300 U/ml	[152]
D-Mannitol	10 µM, 1 M	[153]
Trolox	500 µM	[154]
Ethylenediaminetetraacetic acid disodium salt dehydrate (EDTA)	10 µM	[155]
Iron(III) chloride ($FeCl_3$)	5 µM, 10 µM, 20 µM, 50 µM	Self-determined and usually used concentration in our laboratory
Iron(II) sulfate heptahydrate (Fe_2SO_4)	5 µM, 10 µM, 20 µM, 50 µM	Determined regarding to iron 3
Thymol	100 µg/ml	Self-determined and usually used concentration in our laboratory
IL-33	50 ng/ml	[156]

4.2.2 Incubation of HBMSCs with Catalase for Different Time Durations

After reaching confluence in proliferation medium, the osteogenic differentiation tests were started as described in paragraph *4.2.1*. To analyze which part of the osteogenic differentiation process is influenced by the addition of catalase, hBMSCs were treated for different durations with osteogenic differentiation medium supplemented with 125 U/ml catalase. The evaluation of the dimension of osteogenic differentiation was performed at day 21 as described in chapter *4.3*. *Table 11* explains the used types of media and additives at different test periods.

Table 11: Catalase incubation for different test periods

Type of medium	Test period
Osteogenic differentiation medium	21 days

Osteogenic differentiation supplemented with 125 U catalase	5 days use of a catalase supplemented medium and use of catalase free medium for subsequent days
	7 days use of a catalase supplemented medium and use of catalase free medium for subsequent days
	14 days use of a catalase supplemented medium and use of catalase free medium for subsequent days
	Use of a catalase supplemented medium for the entire period (21 days)

4.2.3 Heat Inactivation of Catalase

10 µl of catalase were heated in a 2 ml reaction vessel at 95 °C with a heating block for 24 hours. The dried suspension was convicted in a sterile 50 ml falcon and mixed with 46 ml osteogenic differentiation medium to obtain a concentration of 125 U/ml of heat inactivated catalase. Before use, this solution was cooled off for another period of 24 hours in the refrigerator.

4.2.3.1 Proof of the Inactivation by OxiSelect™ Catalase Activity Assay Kit

The activity of the used catalase was proofed by this assay. Furthermore, the performance of this kit was necessary to demonstrate the inactivation of the heat inactivated catalase.

4.2.3.1.1 Principle of OxiSelect™ Catalase Activity Assay Kit

To detect the catalase activity, this sensitive quantitative fluorometric assay was performed. For this assay, cell lysates were prepared. 1-2 x 10^4 cells were resuspended in assay buffer and sonicated afterwards. In the end, the solution was centrifuged. The samples had to be tested immediately or stored at -80 °C. Catalase is known for degradation of hydrogen peroxide to water and oxygen. Catalase is one of the most popular antioxidative enzymes in living organisms. In this assay, horseradish peroxidase triggers the reaction of 10-Acetyl-3, 7-dihydroxyphenoxazine with the remaining hydrogen peroxide in a ratio of 1:1. Within this chemical reaction, the highly fluorescent resorufin is formed. *Equation 1* and *Equation 2* show the relevant chemical reactions of this assay. The fluorescence signal of resorufin was measured with a microplate reader with an excitation filter of 530 - 560 nm and an emission

filter of ~ 590 nm. The catalase activity is inversely proportional to the measured fluorescence intensity of Resorufin.

$$Reaction\ 1: H_2O_2 \xrightarrow{Catalase} 2H_2O + O_2$$

Equation 1: First chemical reaction of the determination of the activity of catalase

$$Reaction\ 2: H_2O_2(Remaining) + ADHP \xrightarrow{Horsradish\ peroxidase} Resorufin\ (fluorescence)$$

Equation 2: Second chemical reaction of the determination of the activity of catalase

All working solutions as well as the standard were prepared freshly and mixed thoroughly before use to obtain representative results. The standard was performed according to manufacturer specifications. The samples, controls and the standard were assayed in duplicate. 25 µl of a sample was added to each well of a 96 well microtiter plate. In the following, 25 µl of a 40 µM hydrogen working solution was added to each sample and mixed thoroughly. After an incubation of 30 minutes, 50 µl of the ADHP/HRP working solution was added to each well, mixed, incubated for another 30 minutes at 37 °C and protected from light. In the end, the microtiter plate was read out with a microplate reader and the activity of catalase was calculated by comparing to standard values.

4.3 Evaluation of the Dimension of the Osteogenic Differentiation

First signs of the beginning differentiation could be seen under the microscope already after five to seven days of culturing in osteogenic differentiation medium. The cells showed a changed cell morphology. However, at this point it was not possible to make a statement about the type of differentiation (adipogenic, chondrogenic or osteogenic differentiation). The formation of calcified matrix and an increased activity of alkaline phosphatase in the beginning of osteogenic differentiation were evidences for an osteogenic differentiation. Initial indications for an osteogenic differentiation were seen at day 14. At this time, a few nodules of calcified matrix were already formed which were verified with alizarin red staining. For the most donors, it could be analyzed, that at day 21, the extent of matrix calcification has reached its maximum. HBMSCs were cultured in 24 well plates until reaching confluence and afterwards treated with different additives in osteogenic differentiation medium which is listed in *table 10*.

The added additives showed different antioxidative mechanism. Trolox is a radical catcher [157]. As the used catalase was a 0.1 % thymol aqueous suspension, thymol, due to its hydroxyl group, as a hydroxyl radical scavenger, was tested. Mannitol is also known as a

hydroxyl radical scavenger [158] and was tested for that reason. EUK134 as mimetic of catalase and MnSOD [159] and MnTBAP as a mimetic of catalase [160, 161] were used to assess the antioxidative reaction of catalase on the optimization of the osteogenic differentiation. MnSOD was used to investigate the influence of the degradation of the superoxide anion. Compared to catalase, hemoglobin also has a porphyrin ring as the enzymatic center [162] and was tested for that reason. The antioxidative effects of catalase are attributed to the porphyrin ring structure with the bound iron complex (see *1.4.2.1*). Due to the strong chelating effects of EDTA, it also was tested.

4.3.1 Alizarin Red Staining

The dimension of the osteogenic differentiation was evaluated by staining the calcified matrix with alizarin red. Alizarin red is an anthraquinone dye which is used to stain calcium deposits. As the first step of the staining process, the medium was removed gently from each well by using Pasteur pipettes and a suction pump to avoid damaging the matrix. The cells were washed three times with PBS. After thorough aspirating the PBS, the cells were fixed with 4 % paraformaldehyde for 15 minutes at room temperature. Subsequently, the fixing solution was removed and the cells were washed three times with purified water to remove remains of the fixing solution. The cells were incubated with 1 ml of a 0.05 % alizarin red solution per well of a 24 well plate for 20 minutes at 37 °C. The bound dye was dissolved out of the matrix with 10 % cetylpyridinium chloride. Afterwards, the dye was removed and the cells were washed three times with purified water. Due to the very instable matrix, the washing procedure had to be performed very gently. After removing the water completely, 1 ml of cetylpyridinium chloride was added per well and the cells were incubated for two to four hours to dissolve out the dye of the matrix. The colored cetylpyridinium chloride solution can be read out with spectrophotometer at wavelength of 600 nm. Based on the values of the optical density at 600 nm, a statement of the extent of matrix calcification and thereby in turn of the dimension of osteogenic differentiation could be made. The 10 % cetylpyridinium chloride solution was used as a blank and the colored cetylpyridinium chloride solution had to be diluted when the solution concentration exceeded the measurement range of the device to determine the values.

4.3.2 Measurement of Alkaline Phosphatase Activity

The hydrolysis of phosphate esters is catalyzed by alkaline phosphatase. This reaction is run in an alkaline buffer. p-Nitrophenyl phosphate solution was used as a phosphatase substrate which turned yellow when the active alkaline phosphatase could dephosphorylate the

phosphate. The measurement of the activity of alkaline phosphatase was used as an indicator for the beginning of osteogenic differentiation. The medium was aspirated completely from the cells. After washing the cells thoroughly with PBS, it was necessary to remove the PBS completely. PBS itself could form a yellow colored solution with the p-nitrophenyl solution. Thus, a PBS and p-nitrophenyl solution were used both as blanks. 300 µl of the p-nitrophenyl solution was added to each well of a 24 well plate for 15 minutes and protected from light. After incubation, 10 µl of the yellow colored solution of each well was transferred to a well of a 96 well plate and mixed with 90 µl purified water. A double determination was performed. The dilution was necessary due to a strong coloring and the resulting inaccurate values. Because of the quickly changing color, fast work was required. The 96 well plate was read out by a multilabel counter at a wavelength of 405 nm.

4.3.3 Taking Microscopic Images

To document the matrix calcification, images were taken with a microscope camera of the microscope Zeiss Axiovert 40. An example image is shown in *figure 17*. The pictures were taken after every alizarin red staining and before dissolving the dye with cetylpyridinium chloride. A 10-fold magnification was used.

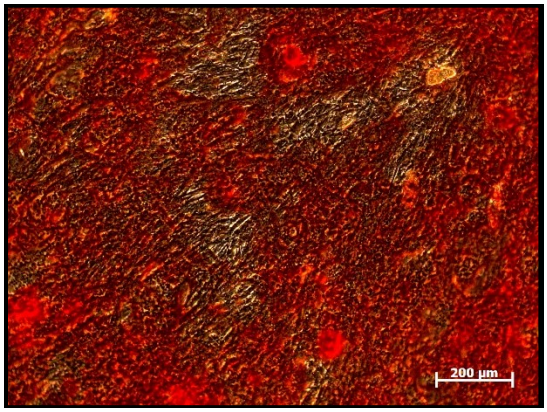

Figure 17: Cell culture which shows after alizarin red staining a red colored calcified matrix (own presentation).

4.4 Evaluation of Cell Viability and Cell Proliferation

To assess metabolic processes of hBMSCs, it was necessary to analyze information about their cell viability and the proliferation activity. In case of an impaired proliferation rate or cell viability, other metabolic processes were consequently affected. Therefore, a normalization of other tests was required. Due to the impact of the chemical reaction of resazurin to resorufin on the respiratory chain and the use of additives during the osteogenic differentiation tests which were also interfering with the respiratory chain, three different types of assays were used. CellTiter-Blue® Cell Viability Assay, Cell Proliferation

(colorimetric) ELISA (bromdesoxyuridine (BrdU)) and neutral red uptake test were performed. The mitochondrial energy metabolism was assessed with CellTiter Blue assay, the damages of the DNA were determined with the DNA intercalating dye bromdesoxyuridine and the activity of lysosomes (only living cells have active lysosomes) was evaluated by the neutral red test.

4.4.1 Determination of the Cell Viability with the CellTiter-Blue® Cell Viability Assay

The principle of this test is based on a fluorometric method for assessing the number of viable cells. As an indicator for the cell viability, the dye resazurin is used. The reduction of resazurin to resorufin is performed by viable cells. In *figure 18*, the chemical reduction is shown. The reaction is highly fluorescent. Nonviable cells have no metabolic activity left and are consequently not able to reduce resazurin. Therefore, no fluorescence can be detected by multilabel counter at a wavelength of 590 nm. $3x10^4$ hBMSCs were counted and cultured as described above in a 96 well microtiter plate. The CellTiter-Blue® Reagent was diluted in a ratio of 1:200 and after aspirating the media of the wells, 100 µl of the CellTiter solution was added to each well. The cells were incubated with CellTiter-Blue® Reagent solution for 60 minutes in an incubator at 37 °C with 5 % CO_2. During the incubation process, it was important to avoid interruptions to achieve reliable results. The procedure of the test is shown in *figure 19*, *table 13* and *table 14* the different test approaches are explained.

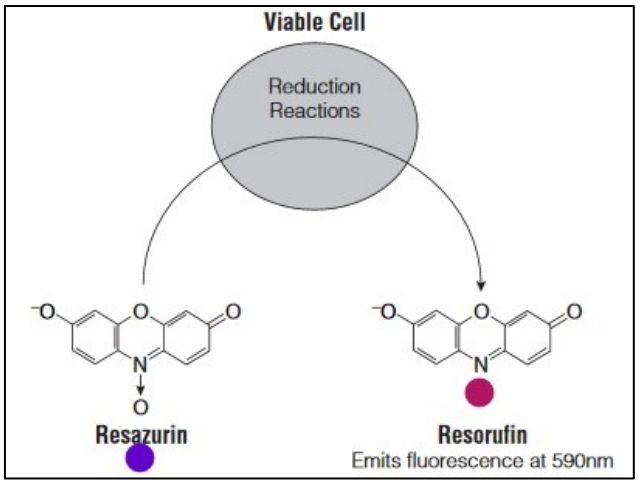

Figure 18: Chemical reaction of resazurin to resorufin. The fluorescence intensity of resorufin at a wavelength of 590 nm can be determined. The fluorescence intensity is proportional to the cell viability [163].

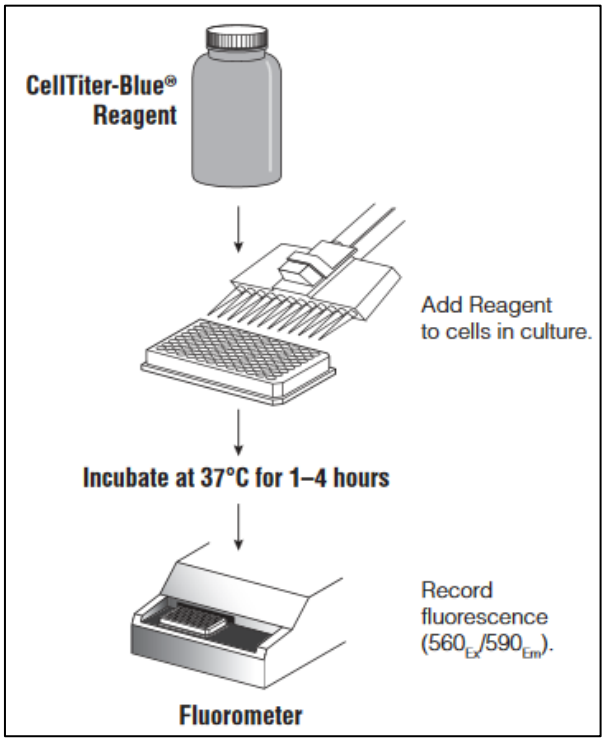

Figure 19: Principle of the CellTiter-Blue® Cell Viability Assay. This figure describes in a short way how the test is performed [163].

Table 12: CellTiter Blue Assay to test the impact of the addition of FGF-2. Cell cultures were cultured for different time periods in proliferation medium which unsupplemented or supplemented with FGF-2

Days	Ingredients
1 2	Proliferation medium + FGF-2
3 4 5	Proliferation medium - FGF-2

Table 13: Performance of the CellTiter Blue Assay to test the impacts of the different types of media with different additives. Cell cultures were cultured for three days in proliferation and osteogenic differentiation medium which were supplemented with diverse additives.

Additives	Type of medium
No addition Catalase 125 U/ml Heat inactivated catalase 125 U/ml EUK134 25 µM	Proliferation medium
	Osteogenic differentiation medium

Table 14: Performance of the CellTiter Blue Assay to analyze differences between responder and low responder donors. Responder and low responder hBMSCs were treated with different types of media; times of measurement: Day 0, 3, 5, 7

Type of hBMSCs	Additives
Responder hBMSCs	Osteogenic differentiation medium
	Osteogenic differentiation medium + catalase 125 U/ml
Low responder hBMSCs	Osteogenic differentiation medium
	Osteogenic differentiation medium + catalase 125 U/ml

4.4.2 Determination of the Cell Proliferation Rate with Cell Proliferation ELISA, Bromdesoxyuridine (BrdU) (colorimetric)

This assay uses the principle of DNA intercalation. Just special molecules, so-called nucleosides, can bind at the DNA double helix. The DNA must be replicated before the division starts and, consequently, the proliferation of cells can take place. Bromdesoxyuridine is an analog of the nucleoside thymidine which allows bromdesoxyuridine to incorporate into the DNA like a normal nucleoside. *Figure 20* shows the similarity of the nucleosides. The proliferation rate of the cells can be determined by measuring the amount of bromdesoxyuridine with an anti-BrdU fluorescent antibody with an ELISA assay. $3x10^4$ hBMSCs were counted and cultured as described above in a 96 well plate with proliferation and osteogenic differentiation medium which were supplemented with two different additives (catalase and EUK134). After culturing, the cells were incubated for two hours with bromdesoxyuridine. During this incubation, bromdesoxyuridine was incorporated in the DNA in place of thymidine of the cells during their proliferation process. After incubation and washing, FixDen was added to fix the cells on the one hand and denature DNA on the other hand. The denaturing process was important to improve the accessibility of the bound bromdesoxyuridine for the determination by the antibody. The bromdesoxyuridine in the DNA was bound by anti-BrdU-POD. An immune complex of anti-BrdU-POD and bromdesoxyuridine was formed and was detected by the subsequent substrate reaction. The resulting absorbance was measured by a multilabel counter. The absorbance values were proportional to the number of proliferating cells. *Table 20* explains the test approaches.

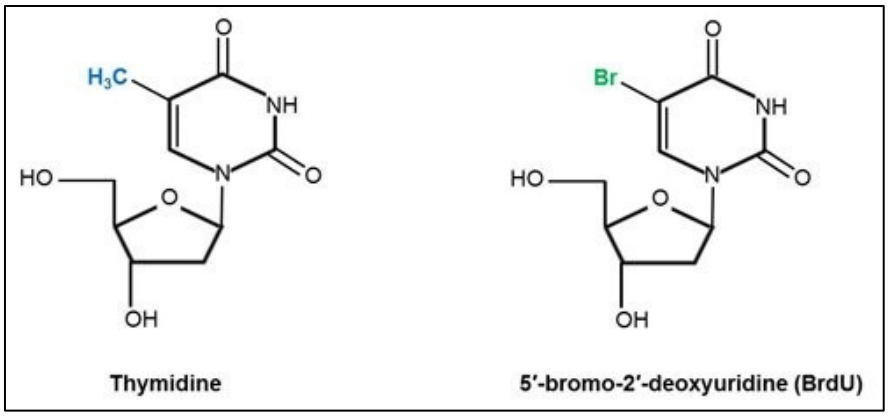

Figure 20: Molecules of DNA intercalation. The comparison of the nucleoside thymidine and bromdesoxyuridine [164].

Table 15: Performance of the Cell Proliferation ELISA, bromdesoxyuridine (BrdU) Assay to assess the influences on hBMSCs of the cultivation in different types of media with diverse additions. Day three with proliferation and osteogenic differentiation medium and diverse additives was assessed.

Additives	Type of medium
No addition Catalase 125 U/ml Heat inactivated catalase 125 U/ml EUK134 25 µM	Proliferation medium
	Osteogenic differentiation medium

4.4.3 Assessment of the Cell Viability by the Neutral Red Test

Fixed cells were stained with neutral red which is a weak cationic azine dye. Neutral red solution was taken up in the lysosomes of living cells. Dead cells do not have any lysosomes left and, therefore, dead cells are not stained. Due to the acidic environment inside the lysosomes, neutral red colors the lysosomes red. Neutral red intensity is proportional to the cell viability.

4.4.3.1 Performance of the Neutral Red Test

3 x 10^4 hBMSCs were plated in a 24 well plate and treated with different media and additives for diverse times of measurement. Cells were fixed with 4 % paraformaldehyde and afterwards incubated with 1 ml / well neutral red staining solution (0.5 ml of a 0.4 % neutral red solution mixed with 50 ml used medium) for one hour. At last, the dye was released with 1 % 1 N HCL isopropyl solution and the optical density was measured with a multilable reader at a wavelength of 540 nm. *Table 16* explains the experimental approaches.

Table 16: Types of media, additives and times of measurement which were set to assess the cell viability.

Medium	Additives	Duration [days]
Proliferation medium	No addition	3,7 and 14
Osteogenic differentiation	No addition	
	Catalase 125 U/ml	

4.5 Principle of the Pierce™ BCA Protein Assay Kit

The determination of the protein concentration explained in paragraph *4.6* is necessary for the Western blot analysis. HMBSCs were not seeded with a defined number of cells. The start of the test procedure was dependent on reaching 85 % of confluence. The principle of this assay is based on the detection of a cuprous cation (Cu^{+}) by bicinchoninic acid (BCA). In an alkaline medium, Cu^{2+} was reduced to Cu^{+} by proteins, which is known as the biuret reaction where chopper forms a light blue chelate complex with proteins. The existence of sodium potassium tartrate in the alkaline medium was necessary to form the colored chelate complex. The main step was the reaction of the bicinchoninic acid with the reduced cuprous cation. Two molecules of bicinchoninic acid and one cuprous ion formed the purple-colored reaction product which exhibited a linear absorbance at 562 nm with increasing protein concentrations.

4.5.1 Procedure of the Pierce™ BCA Protein Assay Kit

HBMSCs were cultured in 6 well plates. The osteogenic differentiation tests were started after the cell cultures reached a confluence of 85 %. To harvest proteins at different times, the medium of each well was decanted and 1 ml of PBS was added. The cells were harvested through cell scrapers. In the following, the cell suspension was centrifuged and the supernatant was aspirated. 30 – 50 µl (depending on the size of the cell pellet) of RIPA buffer was added to the cell pellet and sonicated. These sample solutions were diluted with PBS in a ratio of one to six. 10 µl of each sample and standard solution was pipetted on a 96 well plate in a double determination. 200 µl working reagent was added to each well. The working reagent was prepared freshly of compound A (bicinchoninic acid) and compound B (4 % copper sulfate solution) in a ratio of 50 to one. The samples were incubated for 30 minutes at 37 °C and protected from light for the entire incubation process. The number of proteins in the samples was determined by measuring the absorbance at the wavelength of 562 nm based on the protein standard samples. *Table 17*explains the preparation of standard samples. The arrow diagram of *figure 21* describes the process of the test.

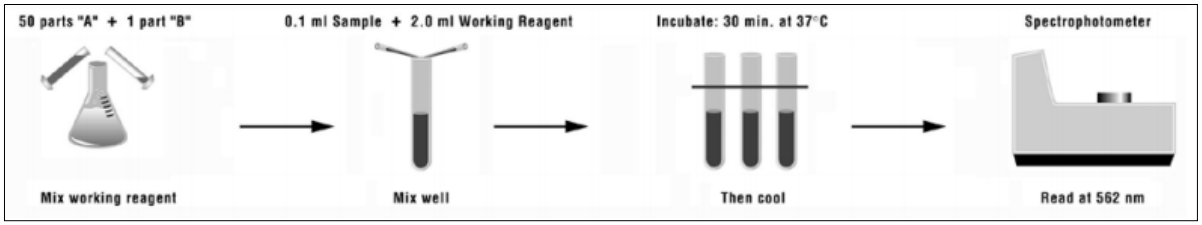

Figure 21: Procedure of the Pierce™ BCA Protein Assay Kit [164]

Table 17: Preparation of the BSA standard for the protein determination

Concentration (µg/µl)	Sample	BSA-Standard (µl)	PBS (µl)
2	A	300	0
1.5	B	375	125
1	C	325	325
0.75	D	175 of B	172
0.5	E	325 of C	325
0.25	F	325 of E	325
0.125	G	325 of F	325
0.025	H	100 of G	400
0 = BLANK	I	0	400

4.6 Western Blot Analysis

The key proteins of osteogenic differentiation were analyzed by a semi quantitative measurement of expressed proteins via western blot analysis. Analyses were performed at day zero, seven and 21. HMBSCs were treated with diverse additives during the test period which are mentioned in *table 18*.

Table 18: Used types of antibodies

Type of Antibody
Mouse anti-Human Catalase monoclonal antibody
Anti-GAPDH hFAB™ Rhodamine Antibody
Rabbit Anti-Human SOD (Mn) polyclonal
Rabbit Anti-SOD1 polyclonal
Rabbit Anti-NADPH oxidase 4 monoclonal antibody

Rabbit Anti-Human p53 polyclonal antibody
Mouse Anti- Alkaline Phosphatase monoclonal antibody
Mouse Anti-IRP1 monoclonal antibody
ACO2 (D6D9) XP® Rabbit mAb
Rabbit Anti-Human RUNX2 polyclonal antibody
Rabbit Anti-Human FOXO1 monoclonal antibody

4.6.1 Glycerinaldehyd-3-phosphat-Dehydrogenase (GAPDH) as the Housekeeping Protein

Due to the catalytic reaction during the glycolysis (catalyzes the conversion of glyceraldehyde 3-phosphate to D-glycerate 1,3-bisphosphate) within the energy metabolism, GAPDH is essential for all living organisms. As a rule, all protein expressions are normalized to the expression of the housekeeping protein GAPDH. GAPDH was influenced by several additives which were added to the osteogenic differentiation medium and resulted in an inconsistent protein band. *Figure 22* the difference between a consistent and inconsistent band. Thus, a normalization of the investigated protein expressions to the expression of GAPDH was not appropriate. The protein expressions were normalized to their control (day zero / untreated cells).

Figure 22: Protein bands of GAPDH. Left: not a consistent band and not usable for normalization; Right: a consistent protein band, useable for normalization.

4.6.2 Principles of Western Blot

By western blot, which is a transfer (blotting) of proteins on a membrane, many proteins of interest can be detected by different reactions. Diffusion, capillary action or electrophoresis are the diverse ways the transfer can be performed. To investigate the key proteins of the osteogenic differentiation and other metabolic processes, the western blot method was used to determine their expression profiles at various times and diverse conditions. In our laboratory, electrophoresis is used to transfer the proteins. After blotting, a Ponceau S staining was made to control the blotting process.

4.6.3 Preparation of Gels

In the beginning, self-poured gels were used. Two different types of gels were required for the protein separation. The composition of the gels is described in *table 19*.

Table 19: Ingredients of used SDS gels

Size of the protein	%	30 % Acrylamid (ml)	H2O (ml)	Other additives
250-120 kDa	7	1.875	3.75	1.875 ml 4-fold resolving gel buffer 10 µl TEMED 25 µl APS
40-15 kDa	12	3	2.625	

A speedy work during the entire procedure was required. Before mixing the respective components, the glass plates needed to be thoroughly cleaned and put in the casting equipment. After adding APS, which speeded the polymerization, the resolving gel solution was poured in the space between the two glass plates. For a symmetrical form, the gel was covered with ethanol. 20 minutes of reaction time was needed to form a stable gel. The ethanol was removed and the stacking gel was poured immediately and the comb with 15 wells inserted carefully. To form a stable gel, 20 minutes of reaction time were needed. The formed wells held a volume of 16 µl. The gels were always prepared freshly. Storage of these gels was possible at 4 °C for a maximum of three days. To prevent the gels from drying out, they were kept moistened. At a later time, stain free gels of the company BioRad were used.

4.6.4 Preparation of the Samples

The volume of water and protein was determined for the calculation of the protein concentration. The volumes of water and protein were mixed before running the gel electrophoresis. 4 µl of Laemmli buffer was added to the mixture which was done under the fume hood. The Laemmli buffer is a Tris-Glycin buffer which is mixed with 20 % β-mercaptoethanol. The composition of 4 x Laemmli buffer is shown in *table 20*. Due to health hazard aspects of β-mercaptoethanol, it is obligatory to work carefully and under a ventilated fume hood. After the addition of Laemmli buffer, the samples were centrifuged and in the following heated for 5 minutes at 95 °C. 16 µl of each sample was filled in the wells of the gel. The first well was filled with a protein marker for later differentiation of the proteins by their sizes.

Table 20: Composition of 4 x Laemmli buffer: storage at 4° C; heat before use; add 20 % β -mercaptoethanol

Ingredients	Amount
250 mM Tris-HCL, pH 6.8	0.3 g
40 % Glycerol	4 ml
8 % SDS	0.8 g
0.1 % Bromophenol blue	0.01 g
Ad 10 ml H_2O	

4.6.5 Procedure of the SDS Polyacrylamide Gel Electrophoresis (SDS-PAGE)

Complex protein mixtures were separated according to their molecular weight by the process of SDS polyacrylamide gel electrophoresis. The proteins were denatured by the addition of Laemmli buffer and the heating process (95 °C). Due to the denaturing process, sodium dodecylsulfate was bound to the polypeptide chains. To charge the proteins equally, the negatively charged sodium dodecylsulfate covered the charge of the proteins which is proportional to the molecular weight of the proteins. To reach linearity of the proteins, β-mercaptoethanol was added which splits the disulfide bridges. The discontinuous SDS polyacrylamide gel electrophoresis used a combination of two different types of gels, the resolving and the stacking gel. The stacking gel is large-pored and was run with a low voltage to stack the protein mixture at the resolving gel. The stacking is based on the diverse ions in the gel and the electrophoresis buffer which in turn is the reason for forming the characteristic band at the border of the resolving gel. After filling the first well with a protein marker and the other wells with the samples, a voltage of 60 V was applied for the first 20 minutes. In the following, a voltage of 120 V was applied to pass the resolving gel. Another key function of the blue colored Laemmli buffer was to control the progress of the gel electrophoresis. *Figure 23* shows the single elements of the used apparatus to perform the splitting of the proteins.

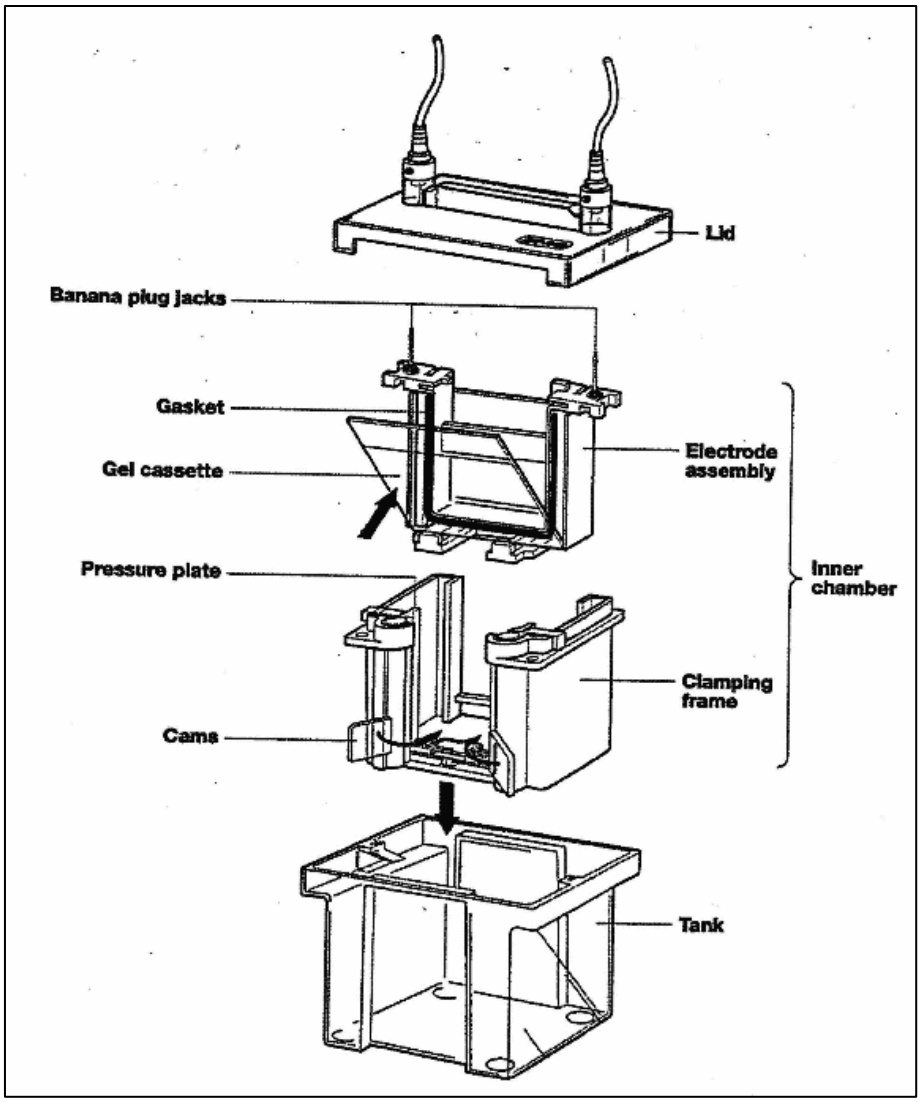

Figure 23: SDS gel electrophoresis apparatus [165]

4.6.6 Imaging of the Gels after SDS Polyacrylamide Gel Electrophoresis

To control the blotting process in addition to the Ponceau S staining (see: chapter *4.6.8*), it was required to take images of the gels before and after blotting. To take these images, stain free gels were imaged with the "stain free" program function of the imaging system. *Figure 24* shows an image of a stain free gel after running the electrophoresis.

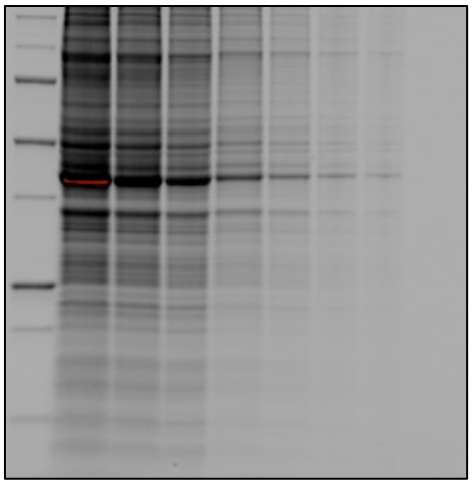

Figure 24: Example a of stain free gel after running SDS gel electrophoresis [166]

4.6.7 Blotting

The blotting process is the transfer of proteins on the nitrocellulose membrane. The individual components were moistened with blotting buffer. The membrane and the gel were placed between two whatman papers. For a successful blotting process, it was important to make sure that the gel was on top of the membrane. With application of voltage, the proteins were transferred from the gel to the membrane. The blotting system ran for 30 minutes with a voltage of 25 V and an electricity of 2.5 A. *Figure 25* shows the arrangement of the blotting equipment.

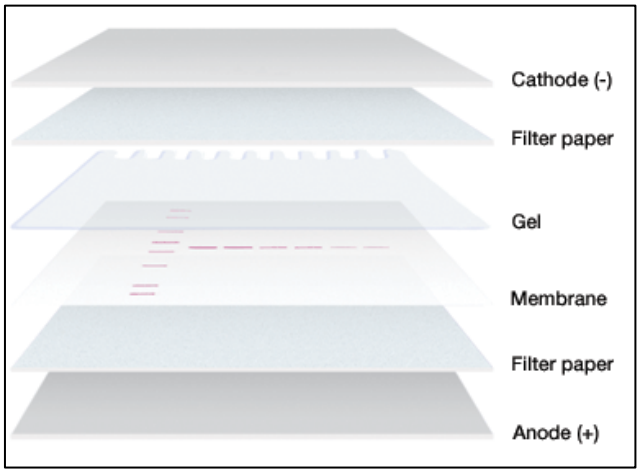

Figure 25: Protein blotting method. Gel and membrane setup for electrophoretic transfer [167]

4.6.8 Ponceau S Staining

After blotting, the membrane was incubated with the Ponceau S staining solution for three to five minutes. *Table 21* shows the ingredients of the composition. Purified water was used to clean the membrane from remains of the dye and to make the protein bands visible. Due to

positive charged amino groups of the proteins, the dye could bind and color the protein bands. In the following, PBS was used to decolorize the membrane. *Figure 26* shows a stained gel.

Table 21: Composition of Ponceau S staining solution

Ponceau S Dye
(storage at room temperature protected from light)
0,1 % Ponceau
3 % Acetic acid

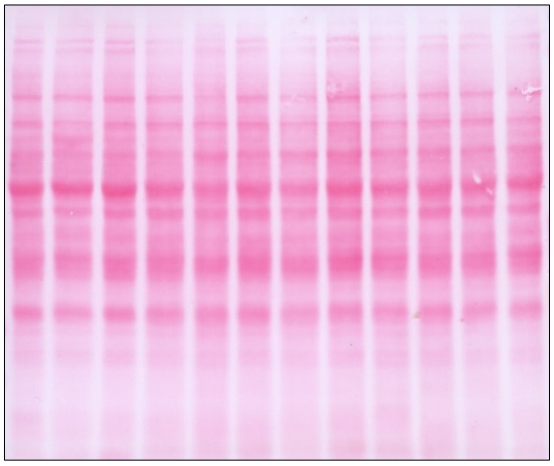

Figure 26: Example of Ponceau S stained gel.

4.6.9 Immunolabeling and Detection

To identify the investigated proteins by immune markers, the membrane was blocked with a BSA blocking solution for one hour at room temperature. The blocking solution was used to prevent unspecific bindings which can be the reason for an unclear background and significantly limit the scope of the results. In general, a 5 % BSA blocking solution was used. After blocking, the membrane was incubated with the diverse antibody solutions (see: *table 6*) at 4 °C over night. Antibodies of one species were used at the same time. In case of two or more different species, one after another was used. However, GAPDH constituted an exception. The incubation of the GAPDH antibody lasted one hour at room temperature. Additionally, GAPDH was detected differently. The used antibody to detect GAPDH is a rhodamine coupled antibody. The detection of GAPDH occurred because of the fluorescence signal, and therefore, no further secondary antibody was needed. In all other cases, a following incubation with a secondary antibody was obligatory to determine the proteins. After incubation with the primary antibody, the membranes were washed three times for five minutes each with TBS-T to facilitate the evaluation. The washed membranes were incubated with the secondary antibody for one hour at room temperature protected from light and

afterwards washed again three times with TBS-T to remove remains of the antibody solutions. While the concentrations and the buffer solutions (3 / 5 % BSA solution or 5% dry milk blocking buffer (prepared in Tris-buffered saline with 1% Tween 20)) of the primary antibodies were defined by the manufacturer, the secondary antibody was always used in a concentration of 1:1000 in TBS-T. The secondary antibody is coupled with horseradish peroxidase which catalyzes the reaction of the chemiluminescence which in turn led to the visualizing of the proteins by oxidizing the luminol of the developing solution. The membrane blots were coated evenly with the developing solution and put in the imaging system to irradiate the blot with UV light and to detect the proteins. For the densitometric evaluation with the Image Lab software, images were taken at several times after incubation with the developing solution. For further tests, the blots were stored protected from light at 4 °C in TBS.

4.7 Principle of the RT-PCR

The real-time RT- PCR is a duplication method to quantify mRNA expressions which uses DNA intercalating fluorescence dyes to detect the resulting products. SYBR Green I was used as the fluorescence dye and is an asymmetric cyanine dye. The dye absorbs blue light at a wavelength at 494 nm and emits green light at a wavelength at 521 nm. The fluorescence intensity is proportional to the amount of the expressed mRNA product which was determined in the second phase (exponential phase). Due to a small quantity, the DNA was amplified in the first and third phase.

4.7.1 Sample Preparation

Collagen type 1 and SPARC, also known as osteonectin, are the key proteins of the calcified matrix which is formed during the final osteogenic differentiation process [168, 169]. Due to the formation of calcified matrix, SPARC as well Collagen type 1 could not be isolated from the matrix cells which made it impossible to detect these two matrix proteins by western blot analysis. For the sample collection, hBMSCs were cultured and treated in 6 well plates for 21 days. At day zero, seven and 21 samples were prepared for testing the gene expression which is explained in *table 22*. Similar to the protein extraction, which is described in chapter *4.5.1,* the medium was aspirated and 1 ml of PBS was added to each well. With a cell scraper cells were detached from the well bottom and collected in a tube. To avoid contamination, it is obligatory to use a new cell scraper for each well. The cell suspension was centrifuged for three minutes and the supernatant was decanted. The resulting cell pellet was frozen without

further addition of any substance at -80 °C to store the sample before starting the RT-PCR testing with the RNA isolation which is mentioned in paragraph *4.7.2*.

Table 22: Cell culturing for RT-PCR. The cells were treated differently and the samples were collected at different time periods.

Days	Ingredients
0	Proliferation medium
7 and 21	Osteogenic differentiation medium
	Osteogenic differentiation medium + catalase 125 U/ml
	Osteogenic differentiation medium + heat inactivated catalase 125 U/ml

4.7.2 RNA Isolation of HBMSCs

The RNeasy Kit of Quiagen was used to isolate the RNA from the hBMSC samples. During the isolation process, all steps were carried out at room temperature. According to the manufacturer specifications, all needed solutions were prepared freshly. The isolation procedure of this kit is based on the method after Chomczynski and Sacchi [170]. 350 µl of β-mercaptoethanol supplemented RLT buffer was added to each collected cell pellet, thoroughly mixed and vortexed for one minute. Afterwards, the lysate was pipetted into a QIAshredder spin column placed in a 2 ml collection tube and centrifuged. For further homogenization, 350 µl of ethanol was added and centrifuged. The flow-through was discarded. After adding 700 µl of RW1, the sample was centrifuged and flow-through discarded again. This procedure was repeated with 500 µl RPE buffer. After adding a new collection tube and centrifuging again, the RNeasy spin column was placed in a new 1.5 ml collection tube and 30-50 µl RNase free water (amount of water was dependent on the size of the original cell pellet) was added and centrifuged for one time. The isolated RNA remained in the 1.5 ml collection tube.

4.7.3 Spectrophotometrically Determination of the Isolated RNA Amount

By a photometer (nanodrop), the concentration and purity of the isolated RNA was spectrophotometrically determined. The absorption at a wavelength of 260 nm showed the concentration and the absorption of a wavelength at 280 nm showed the purity of the sample. To ensure a linear dependency, it was important to ensure that the range of the concentration and the purity was between 1.8 and 2.0. *Figure 27* shows an optimal absorbance curve and an

also optimal ratio A_{260}/A_{280} which is measured with the software of the nanodrop (see: *table 9*).

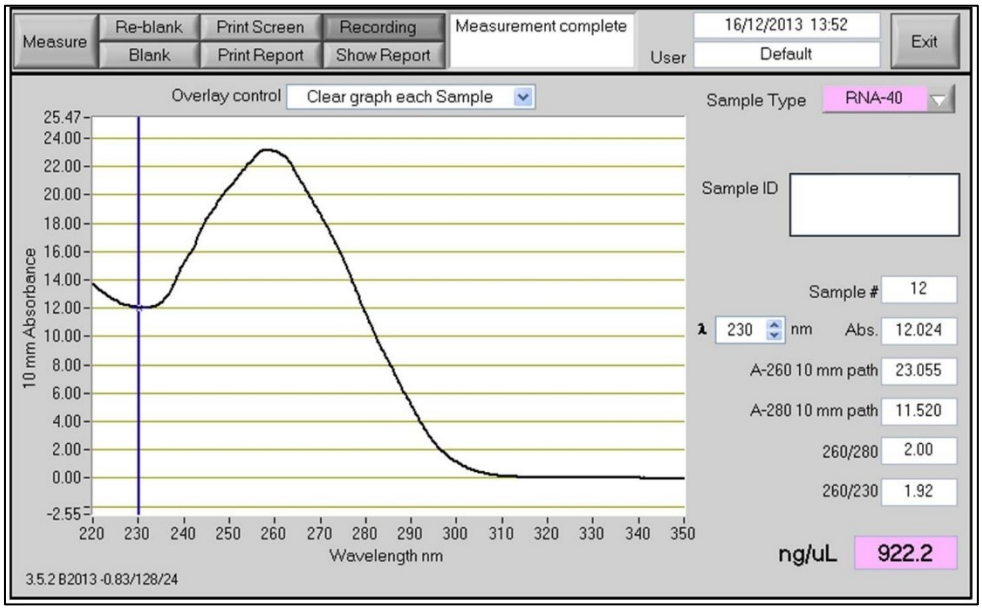

Figure 27: Determination of RNA concentration and purity with the nanodrop [171]

4.7.4 Reverse Transcription of the Total Amount of RNA into cDNA

In general, 500 ng of RNA were transcribed to 500 ng of cDNA. First, the samples were diluted to 500 ng/10 µl and the concentration of cDNA was 25 ng/µl at a volume of 20 µl per well. Within this test, a cDNA amount of 0.5 ng/µl (2 ng in 10 µl water) was used. To transcribe the mRNA to cDNA, a master mix (see: *table 23*) was added. 10 µl of the RNA sample was mixed with 10 µl of the master mix and transcribed in the thermocycler (BioRad) for 60 minutes at 37 °C to cDNA. The samples were stored at -20 °C in case they were not used immediately for the following test.

Table 23: Composition of the master mix for one approach

Ingredient	Volume [µl]
RNase free water	4.5
10- fold RT-Puffer	2
dNTP-Mix (je 5 mM)	2
Oligo dT Primermix (20 µM)	1
RNase-Inhibitor (40 U/µl)	0.25
Reverse Transcriptase (4 U/µl)	0.25
Volume of the master mix	10

500 ng of total RNA	10
Total volume	20

4.7.5 Determination of the Gene Expression of SPARC and Collagen Type 1

For the determination of the gene expressions of SPARC and collagen type 1, 4 µl of the transcribed sample was mixed with 21 µl of another master mix whose composition is described in *table 24* and *table 25.* A total volume of 25 µl of every sample was pipetted onto a PCR 96 multiwell plate. Additionally, three non-template controls (NTC), which were a mixture of 21 µl master mix and 4 µl water, were also pipetted into each well to control a thorough working process. In case of contaminated water, the NTCs would also have shown similar measured values as the samples. If that had been the case, the test would have been run again. 18s was used as a housekeeping gene. Therefore, the samples were tested with primers for SPARC, type 1 collagen and 18s to normalize the investigated genes during the calculation process to the 18s gene. GAPDH was also used in the first trials to assess which housekeeping gene was the most appropriate solution. As described in paragraph *4.6.1,* GAPDH was influenced by the used additives during the osteogenic differentiation process. Therefore, a use of GAPDH as housekeeping gene was not used for further tests. The samples were processed by a real-time thermocycler.

Table 24: Composition of the master mix for the gene of interest. Ingredients and amount for one approach are listed.

Ingredients	Volume [µl]
SYBR Green master mix	12.5
DNase free water	7
Primer (gene of interest) forward and reverse	0.75 (each)

Table 25: Composition of the master mix for the housekeeping gene 18s. Ingredients and amount for one approach are listed.

Ingredients	Volume [µl]
SYBR Green master mix	12.5
DNase free water	8
Primer (18s) forward and reverse	0.25 (each)

4.7.6 Evaluation of the Data

The software calculated the so-called Ct value from the exponential part of the graph. By quantifying the data with the ΔΔCT method, the treated samples were normalized to day zero. The ratio of treated and untreated samples is the relative expression difference which is normalized to the housekeeping gene and is calculated by the formula: $2^{-\Delta\Delta CT}$. *Table 26* shows the structure of this formula to calculate the gene expressions.

Table 26: Used formula for data analysis

Formula
ΔCT = CT gene of interest – CT housekeeping gene
ΔΔCT = ΔCT gene of interest - ΔCT housekeeping gene (control)
Ratio = $2^{-\Delta\Delta CT}$

4.8 Determination of SPARC, Collagen Type 1 and Osterix by an Immunohistochemically Staining

SPARC and collagen type 1 are obligatory proteins to form a calcified matrix. Osterix is known as an important transcription factor during the osteogenic differentiation which is necessary to form a mature osteoblast. Osterix deficiency is related with impaired osteoblast differentiation and bone formation. Osterix is regulating processes before SPARC and collagen type 1 are involved [172]. Due to the binding to the calcified matrix, SPARC and collagen type 1 could not be detected via western blot analysis. To investigate the impact of the osteogenic differentiation processes in combination with the respective additives, cell cultures were immunohistochemically stained.

4.8.1 Procedure of the Immunohistochemically Staining in Conformity with a Protocol of Abcam

HBMSCs were cultured on cover glasses in 12 well plates. Cover glasses were first autoclaved and afterwards placed with a sterilized tweezer in each well. After reaching confluence, cells were treated with osteogenic differentiation medium and different additives (catalase and inactivated catalase). Day 14 and day 21 represented times of evaluation. Low responder and responder hBMSCs were treated equally and compared in the end. At day zero, 14 and 21 samples were collected. The media were aspirated and after washing with PBS, the cells were fixed with 4 % paraformaldehyde for 15 minutes and subsequently washed with PBS to remove any remains. If not used immediately for the further steps of the test, the

samples were stored at 4 °C covered with PBS. The samples could be stored for a maximum of two weeks. Longer storage times led to a detachment of the cell layer / matrix. To perform the test, the cover glasses were each washed twice in TBS supplemented with 0.03 % Triton X-100 for 15 minutes. Triton X-100 is a nonionic surfactant and was used as a detergent to lyse cells to extract the proteins of living cells. The compound of Triton X-100 and TBS was used to reduce surface tensions. TBS instead of PBS was used to get a cleaner background. In the following, the cells were blocked with a blocking solution which contained TBS and 0.3% Triton for one hour at room temperature to prevent unspecific bindings. After a washing process, the primary antibody which was diluted in TBS with 1 % BSA (concentration was used according to the manufacturer specifications) was added on the cover glasses. The primary antibody incubated over night at 4 °C. Before adding the secondary antibody, the cover glasses were washed thoroughly. The secondary antibodies, coupled with fluorescence dyes, were added to the cells for two hours at room temperature. The cells were cleaned after the incubation from remains of the antibodies with 0.1 M PBS. For the last 10 minutes of the secondary antibody incubation, Hoechst 33342 was also added to the cells (50 µl / well). Hoechst 33342 is a cell-permeable DNA dye which emits blue fluorescence at a wavelength of 460-490 nm. It was used to stain the cell nuclei to see the conditions of the cells (living or dead cells). The cover glasses were then bonded on a microscope slide with a fluorescence mounting medium and afterwards dried out to microscope the cells on the following day. During the incubation with the secondary antibody the samples were protected from light. On the following day, images were taken with the microscope Zeiss Axiovert 200 with a 100-fold magnification.

4.9 Determination of the Amount of ATP in Low Responder and Responder hBMSCs

To analyze the potential difference of the ATP amount in low responder and responder hBMSCs, an ATP assay by Biaffin GmbH & Co KG was performed. The assay is based on bioluminescence in which luciferin in combination with ATP was oxidized by luciferase which resulted in a luminescence at a wavelength of 560 nm. *Equation 3* shows the chemical reaction.

$$luciferin + ATP + O_2 \xrightarrow{Mg^{2+},\ luciferase} oxyluciferin + AMP + pyrophosphate + CO_2 + light$$

Equation 3: Chemical reaction of the ATP determination assay

4.9.1 Principle and Performance of the ATP measurement

50 x 10^4 hBMSCs per well were cultured in 12 well plates in proliferation medium for one day for showing adherence and were subsequently tested at day three, seven and 14 after a treatment with proliferation medium and osteogenic differentiation medium for the entire test period. The cells were detached from the well bottom and centrifuged at 17000 rpm. The supernatant was decanted and the cell pellet was resuspended with 1 ml of boiling purified water to break the cell membrane. In the following, the suspension was centrifuged again at 17000 rpm. The supernatant was transferred in a new 1.5 ml reaction vessel whereas the rest was discarded. The aqueous solution was stored at -80 °C or used directly for the following steps. To normalize the ATP amount, the DNA amount of the samples was photometrically measured. 2 µl of each sample was used for the photometric DNA measurement by the spectrophotometer. *Figure 28* shows the evaluation of the measurement of DNA amount. The stock solutions as well the standard solution were freshly prepared as recommended by the manufacturer specifications. Due to the light-sensitive reaction, a white 96 well microtiter plate was used. 50 µl of the sample and 50 µl the reaction mix were pipetted on the plate and measured after 10 minutes of incubation. For the first test runs, the plate was read out after 10, 20 and 30 minutes of incubation to ascertain the optimal incubation duration. The plates were read out with a multilabel counter and calculated by the workout software. At last, the calculated ATP amount was normalized to the DNA amount.

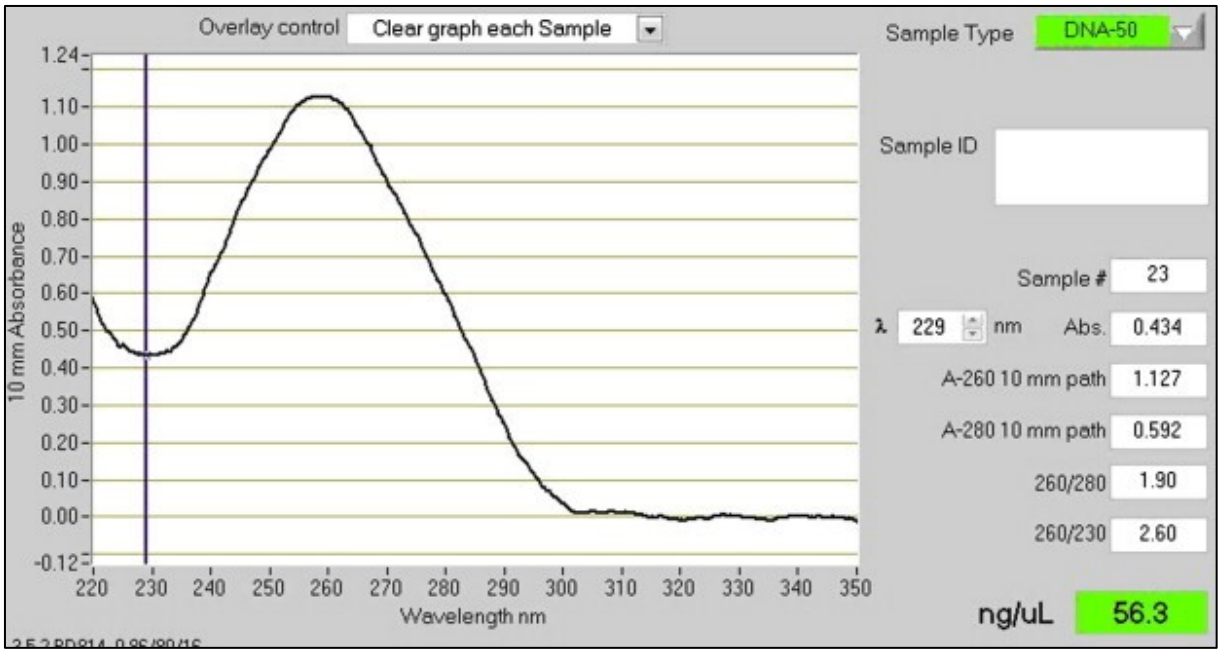

Figure 28: Measurement of DNA by a photometer (nanodrop) [171]

4.10 Determination of Cellular Glucose Amount of hBMSCs

To analyze the energy metabolism more detailed and to identify differences of low responder and responder hBMSCs, the glucose amount of the media of the cells was determined with a bioluminescent assay (Glucose-Glo™ Assay).

4.10.1 Principle and Performance of the Glucose-Glo™ Assay

The assay is based on a glucose oxidation and NADH production with a bioluminescent NADH detection system. The details of the chemical reaction are described in the *figure 29*. 30 x 10^4 hBMSCs per well of one responder and one low responder were cultured in 96 well plates in proliferation medium (glucose free RPMI medium) for one day to get adherent and were subsequently tested at day three, five and seven after they were treated with different media compositions which is explained in *table 27*. The stock solutions as well the standard solution were freshly prepared as recommended by the manufacturer specifications. At every time of measurement, 3 µl of the sample medium was mixed with 97 µl PBS. The mixture was frozen at -20 °C. At the end of the test periods, all samples were thawed and diluted to a final dilution of 100-fold. 50 µl of this solution was transferred to a 96 well assay plate and 50 µl glucose detection reagent was added. It was incubated for 60 minutes and occasionally shaken gently. The plates were read out with a multilabel counter at a wavelength of 562 nm and calculated by the workout software.

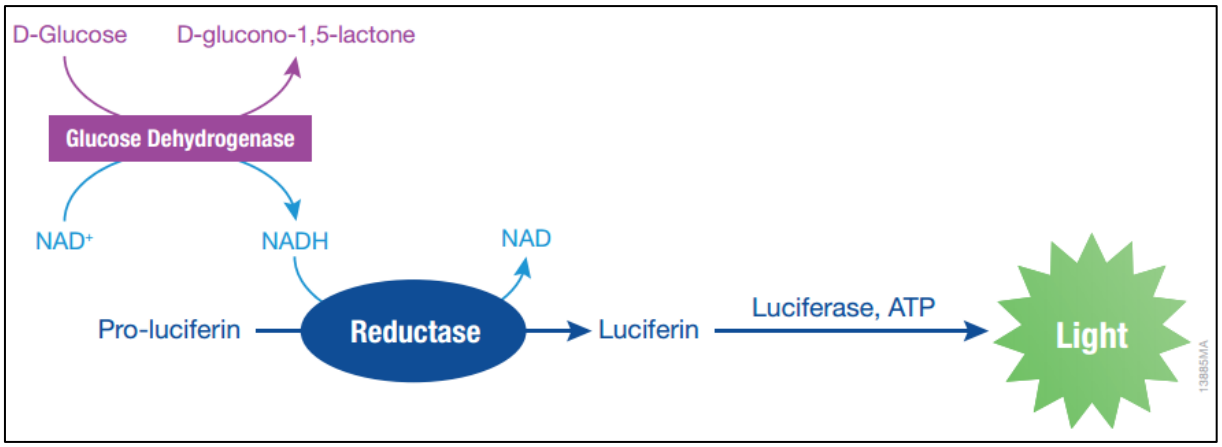

Figure 29: Chemical reaction of the Glucose- Glo Assay™ [173]

Table 27: Type of used medium with different additives (RPMI, a glucose free medium was used as basic medium)

Type of medium	Additives
Proliferation medium	No addition
	Catalase 125 U/ml
	Mannitol 10 µl

Osteogenic differentiation medium	No addition
	Catalase 125 U/ml
	Mannitol 10 µl

4.11 Determination of Fibroblast Growth Factor in HBMSCs in Diverse Media Compositions

FGF-2 is known for influencing the osteogenic differentiation within several pathways [174-176]. Thus, human FGF basic was measured in cell culture supernatants of hBMSCs with the Quantikine Human FGF basic Immunoassay kit which is an ELISA to analyze the impact on the osteogenic differentiation regarding the use of diverse culturing media.

4.11.1 Principle of the Quantikine Human FGF Basic Immunoassay Kit

This kit used the quantitative sandwich enzyme immunoassay technique. Therefore, a monoclonal antibody specific for FGF-2 was already coated on a 96 well plate. The stock solutions as well the standard solution were freshly prepared according to the manufacturer specifications. After adding a FGF-2 containing sample, FGF-2 was bound and a secondary enzyme linked monoclonal antibody for FGF-2 was able to bind the immobilized FGF-2 standards after remaining unbound substances were washed out. The remains of the unbound antibody enzyme reagent were also removed by washing. In the following, a substrate solution was added and incubated under constant control for 30 minutes. After developing the color (approximately 30 minutes), a stop solution was added and the optical density was measured with a multilabel reader at a wavelength of 405 nm and calculated by the workout software.

4.12 Oil Red O Staining

Oil Red O is used to determine triglycerides in fixed cells. Paraffin-fixed protein-bound lipids can also be stained by this dye. 150 mg Oil red powder was diluted in 50 ml 99 % isopropyl. This stock solution was diluted with purified water in a ratio three to two and after an incubation duration of 10 minutes filtrated. Due to the low durability of the solution, it always was prepared freshly. HBMSCs were cultured and treated as described in *4.3.1*. Formation of protein bound lipids was analyzed after different treatments, which is described in *table 28*. After aspirating the media, the cells were incubated with 1 ml each of 60 % isopropyl for two to five minutes. The isopropyl was removed and 1 ml of the oil red solution supplemented with 50 µl per well was transferred to each well. The cells were incubated 5 minutes at room

temperature. At last, images were taken with the microscope Zeiss Axiovert 40 with a 10-fold magnification.

Table 28: Treatments for the oil red staining

Medium	Additive	Concentration
Osteogenic differentiation medium	Catalase	125 U/ml
	MnTBAP	25 µM
	EUK134	25 µM
	Hydrogen peroxide	100 µM

4.13 Analysis of the Impact of Hydroxyl Radicals on the Osteogenic Differentiation

Hydroxyl radicals are short living harmful reactive oxygen species which can damage several processes of the energy metabolism. It is postulated that catalase is not just able to degrade hydrogen peroxide to water and oxygen but is also able to generate hydroxyl radicals at lower hydrogen peroxide concentrations [105]. Since catalase treatment was also performed to test the influence on osteogenic differentiation, the effects of hydroxyl radicals were also tested.

4.13.1 Principle of the Cell Meter™ Mitochondrial Hydroxyl Radical Detection Kit

HBMSCs were counted, as described in *4.2.1,* and 4 x 10^4 cells were plated on a 96 well microtiter plate. HBMSCs were cultured until being adherent and afterwards treated with diverse additives for two-time durations which is explained in *table 29*. Working solutions were prepared freshly according to the manufacturer specifications. The medium was aspirated and the cells were incubated with 100 µl of MitoROS™ OH580 working solution for one hour at 37 °C. After washing with DPBS for three times, 100 µl of assay buffer was added to each well. At last, fluorescence increase was measured by using a fluorescence microplate reader at Ex/Em = 540/590 nm (cut off = 570 nm) with bottom read mode.

Table 29: Additives and incubation duration for hydroxyl radical determination

Incubation [h]	Additives
1.5	No addition Catalase 125 U/ml Heat inactivated catalase 125 U/ml 40 µM H_2O_2 Catalase 125 U/ml + 40 µM H_2O_2 Inact. catalase 125 U/ml + 40 µM H_2O_2
3.5	

4.14 Measurement of Apoptosis of Responder and Low Responder HBMSCs

Due to the fact of an impaired osteogenic differentiation potential of low responder hBMSCs, it was important to analyze apoptosis effects during proliferation and growing processes.

4.14.1 Principle of the Flow Cytometry

Cellular properties, such as cell size and cell granularity, can be determined quantitatively and qualitatively with the flow cytometry method. The photodetectors forward scatter (FSC) and side scatter (SSC) are used to detect cell size and cell granularity. By prior labeling with fluorescence dyes, special cell structures (e.g. surface marker) could be determined. Various fluorescence detectors measured the intensity of fluorescence emission of the fluorescence coupled cells.

4.14.2 Procedure of the Evaluation of the Apoptosis Rate

Prior to the plating on a 24 well plate, the cells were counted as described in paragraph *4.1.2* **Determination of the Cell Number with a Hemocytometer (Neubauer Counting Chamber)**. 4 x 10^4 cells were cultured in each well until reaching confluence. Subsequently, the cells were treated with different additives for zero, four, seven and 14 days which is described in *table 30*. At the times of measurement, the media were decanted and PBS was added to each well. Cells were detached with a cell scraper of the well bottom and centrifuged at 1400 rpm for four minutes. After discarding the supernatant, the cells were resuspended with 500 µl PBS and 4.5 ml cooled 70 % ethanol was added for fixation. The incubation period lasted 15 minutes on ice. In the following, the samples were centrifuged at 1400 rpm for four minutes. The supernatant was discarded and the cell pellet resuspended and incubated for 30 minutes at room temperature with 200-500 µl (depending on the size of the cell pellet) propidium iodide solution (20 µg/ml in PBS). Propidium iodide is a DNA intercalating fluorescence dye which can penetrate perforated cell membranes but cannot penetrate in living cells. *Figure 30* explains the intercalation process. Propidium iodide absorbs light at a wavelength of 488 nm and emits light at 590 nm. In case of intercalation of propidium iodide in the DNA, the absorption and emission values are shifted to 535 nm or 617 nm. The fluorescence intensity, which showed the apoptosis rate, was measured with the flow cytometer FACS Calibur. The evaluation was performed with the software CellQuest Pro (both: Becton Dickinson). *Figure 30* shows the evaluation of the apoptosis rate with CellQuest Pro. The method was performed after the protocol of Carlo Riccardi and Ildo Nicoletti [177].

Table 30: Treatment during the apoptosis determination

Medium	Additive	Day
Proliferation medium	No addition	0
Osteogenic differentiation medium	No addition	4, 7, 14
	Catalase 125 U/ml	
	Heat inactivated catalase 125 U/ml	
	MnTBAP 25 µM	
	EUK134 25 µM	

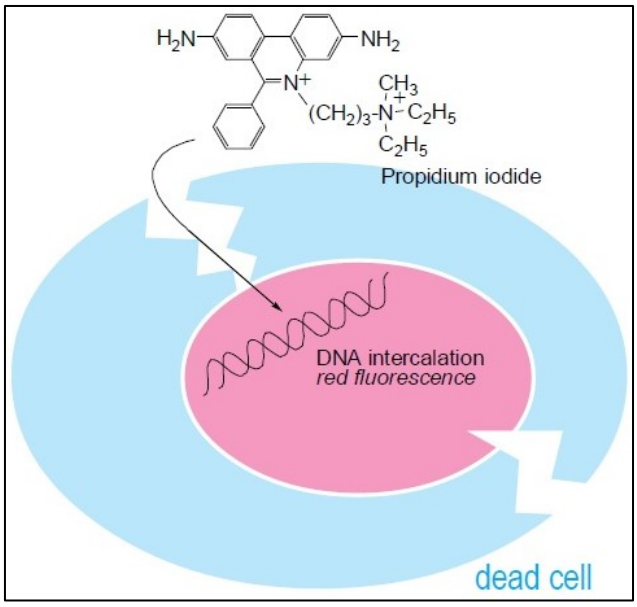

Figure 30: DNA intercalation of propidium iodide [178]

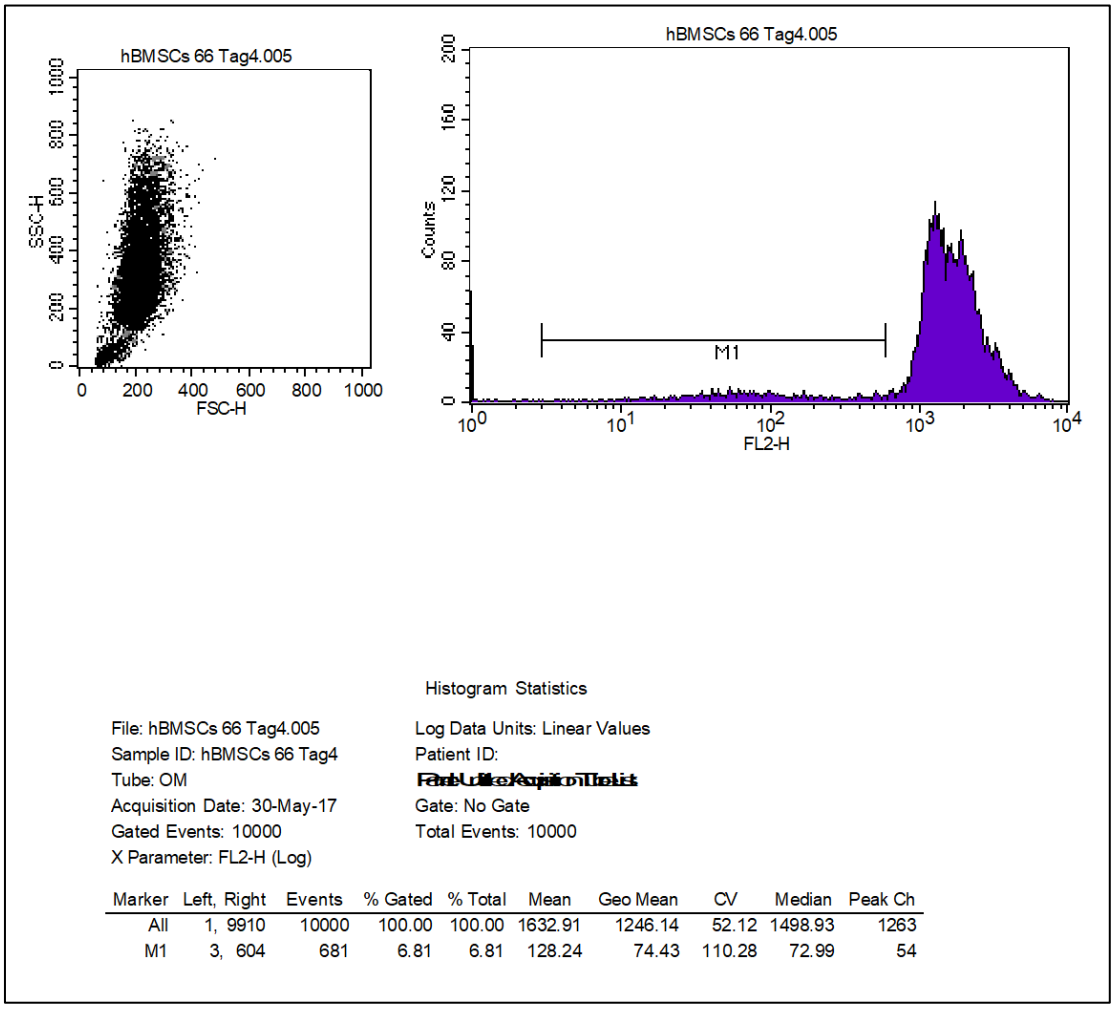

Marker	Left,	Right	Events	% Gated	% Total	Mean	Geo Mean	CV	Median	Peak Ch
All	1,	9910	10000	100.00	100.00	1632.91	1246.14	52.12	1498.93	1263
M1	3,	604	681	6.81	6.81	128.24	74.43	110.28	72.99	54

Figure 31: Evaluation of apoptotic cells with CellQuest Pro (own representation of measurment)

4.15 Statistical Analysis

The statistical evaluation and data archiving was done with GraphPad Prism 5.0. In case of a normal distribution, one-way ANOVA or two-way ANOVA with subsequent Bonferroni posttests were used. To analyze paired data, also a one tailed, a paired t-test was applied. A p-value < 0.05 was considered as significant.

5. Results

5.1 Culturing of hBMSCs in Proliferation Medium

After reaching confluence in proliferation medium, hBMSCs were, as described in paragraph *4.2,* cultured in an osteogenic differentiation medium to induce the formation of calcified matrix. The extent of matrix calcification was used to assess the dimension of the osteogenic differentiation potential of the different donor cells. *Figure 32* shows a cell culture of hBMSCs after culturing in proliferation medium for one week until the cell cultures reached confluence. As soon as the investigated cell cultures reached this confluence, the osteogenic differentiation tests were started. To initiate osteogenic differentiation, the cells were treated with an osteogenic differentiation medium which is described in *table 8*. In *figure 32*, the typical morphology of hBMSCs is shown. Mesenchymal stem cells formed elongated fibroblast-like cells. This morphology is typical for proliferating hBMSCs. Due to the cell morphology, cell conditions were able to be assessed. In case of a different cell morphology, it was assumed that the cells were stressed and potentially would have shown a divergent behavior relating the osteogenic differentiation. A divergent cell morphology, which stressed cells show, is depicted in the right image of *figure 32.* To avoid falsifications, cell cultures, which had a similar or even equal appearance, were not used for further tests.

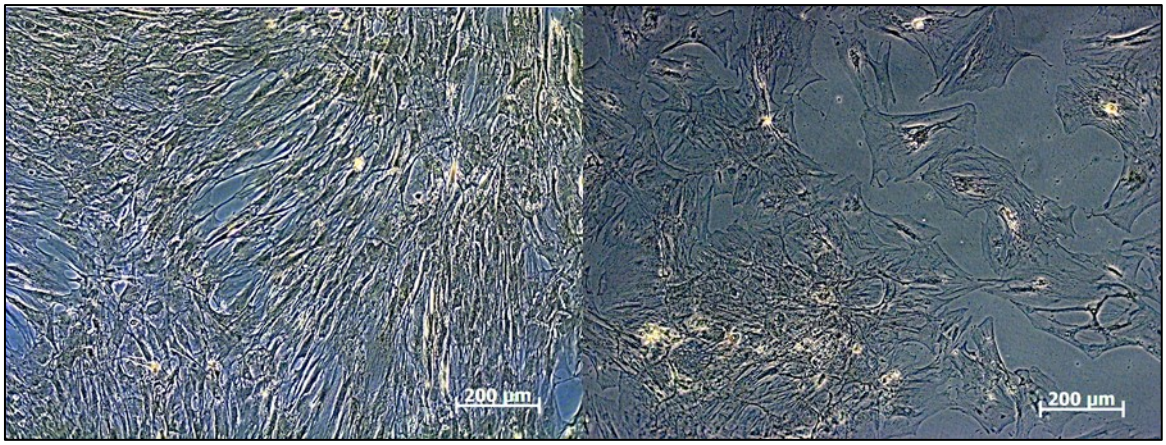

Figure 32: hBMSCs cultured in proliferation medium. The cells reached confluence. The left image shows the optimal conditions to start investigations of the osteogenic differentiation. In the left image, a regular unstressed cell culture of hBMSCs is shown, whereas in the right image, a cell culture with stressed cells is shown. Images were taken with a camera of the microscope Zeiss Axiovert 40 with a 10-fold magnification.

5.2 Osteogenic Differentiation of Regular and Osteogenically Dysfunctional HBMSCs

HBMSCs were treated for a duration of 21 days with an osteogenic differentiation medium. For the first tests, cells were stained with alizarin red at day zero, seven, 14 and 21 to assess the dimension of osteogenic differentiation. In *figure 33*, a cell culture of osteogenically

regular cells is presented. The images show cells at day zero with no matrix calcification and the extent of matrix formation after 21 days of cultivation in osteogenic differentiation medium.

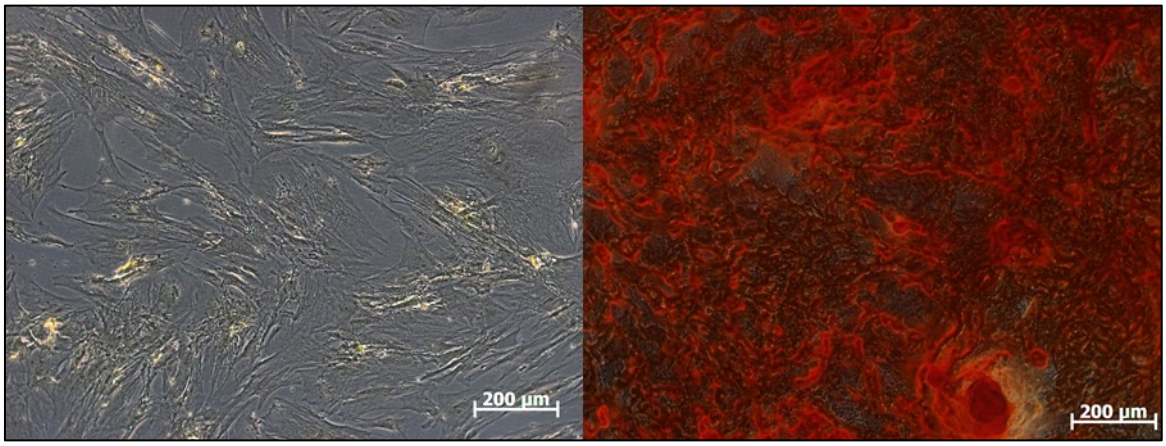

Figure 33: Regular hBMSCs culture treated with osteogenic differentiation medium. Left image: a confluent cell layer at day zero; right image: day 21 with a pronounced calcified matrix; images were taken with a camera of the microscope Zeiss Axiovert 40 with a 10-fold magnification.

During the investigations of osteogenic differentiation processes, hBMSC cultures, which showed no or a significantly impaired osteogenic differentiation potential, were also observed. It is important to note that all cell cultures were treated equally. During the osteogenic differentiation test series, no differences except of the formation of the calcified matrix were observed. The left image of *figure 34* shows a confluent cell culture which was cultured for approximately one week in proliferation medium. The center image was taken after culturing the cells in osteogenic differentiation medium for 21 days and staining with alizarin red to color calcium deposits. As no red coloring could be observed, it was obvious that no matrix calcification took place during the test duration. The right image shows a cell culture with a weak formation of calcified matrix which was significantly weaker compared to regular differentiated hBMSCs. It was evident that a change of the cell morphology happened during the culturing in osteogenic differentiation medium. Changes in cell morphology were obligatory to a formation of calcified matrix. Even longer cultivation periods for 28 days of osteogenically dysfunctional hBMSCs did not lead to a pronounced matrix calcification. Some donors with a weak formation of calcified matrix were also observed as mentioned in *figure 33*. These cell cultures showed some nodules of calcium deposits. An example of a

formation of few nodules is presented in the right image of *figure 34*.

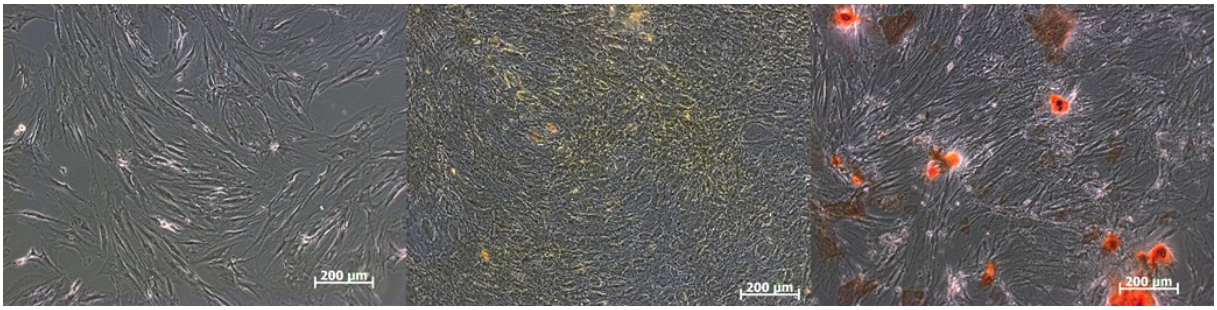

Figure 34: Osteogenic differentiation test of an osteogenically dysfunctional cell culture. Left image: day zero (culturing hBMSCs for one week in proliferation medium); center image: osteogenically dysfunctional cells which were cultured for 21 days in osteogenic differentiation medium and showed no matrix calcification; right image: osteogenically dysfunctional cells which were cultured for 21 days in osteogenic differentiation medium and showed a weak matrix calcification.

Osteogenic differentiation of regular hBMSCs was characterized by a change of the cell morphology in the first two weeks, the formation of nodules of calcified matrix at least at day 14 and a significant formation of calcified matrix (see also: *figure 35*). Interestingly, after culturing in osteogenic differentiation medium, osteogenically regular cells already showed pronounced indications of a calcified matrix at day 14 which is shown in *figure 35*.

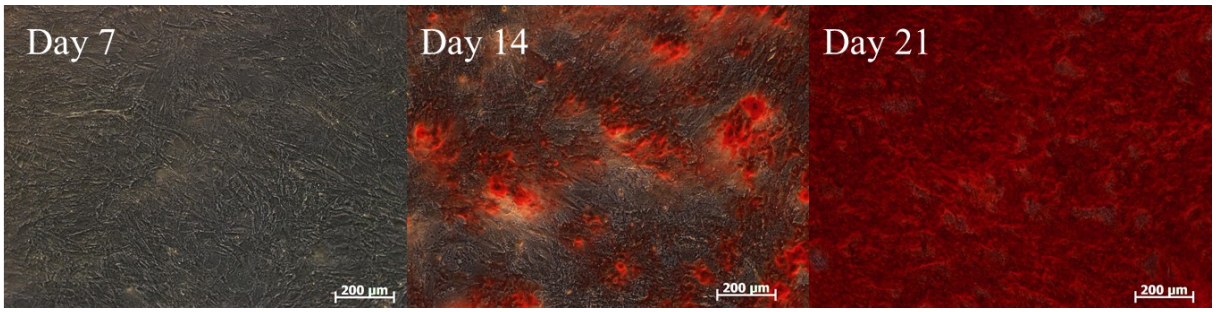

Figure 35: Osteogenic differentiation of an osteogenically regular cell culture. HBMSCs were cultured in osteogenic differentiation medium for different time periods. At day 7, 14 and 21, the cell layer was stained with alizarin red. At least at day seven, the cells showed a changed cell morphology. First nodules of calcified matrix were already formed at day 14. At day 21, the cell layer was fully covered with a calcified matrix.

5.2.1 Assessment of the Osteogenic Differentiation of HBMSCs after Treatments with Diverse Antioxidative Additives

According to investigations of adipogenic stroma cells, it was assumed that hBMSCs would also show an enhanced osteogenic differentiation after a treatment with antioxidative additives during the osteogenic differentiation process. The treatment with antioxidative additives would relate with a reduced amount of damaging reactive oxygen species. Diverse antioxidative additives with different mechanisms of action were used to investigate the

impacts of oxidative stress provoked by different radicals on the osteogenic differentiation potential. All used additives are listed in *table 10*.

5.2.1.1 Influence of a Catalase Treatment on the Osteogenic Differentiation

As an optimal concentration of catalase to treat hBMSCs for optimized osteogenic differentiation has not yet been described in the literature, diverse concentrations were tested for several time periods. *Table 31* shows the details of the performed test.

Table 31: Details of the treatment with catalase

Type of additive	Concentration [U/ml]	Times of measurement [days]
Bovine liver catalase	62,5; 125; 250; 500; 1000	0; 7; 14; 21

The treatment with the diverse catalase concentrations led to different extents of calcified matrix. It is obvious that an osteogenically dysfunctional hBMSC culture showed a significantly improved osteogenic differentiation potential after a cultivation in catalase supplemented osteogenic differentiation medium. After several test runs, a concentration of 125 U/ml was determined to lead to the best outcomes. The osteogenic differentiation was assessed on one hand by evaluation of the images of calcified matrix and on the other hand by the dissolution of the alizarin red dye with a cetylpyridinium chloride solution and the determination of the optical density of the dissolved dye. The measured optical density is proportional to the amount of calcium deposits and therefore to the extent of matrix calcification. The extent of bound alizarin red relating to the used catalase concentrations is shown in the *figure 36*. An optimal catalase approach with a concentration of 125 U/ml for 21 days was determined.

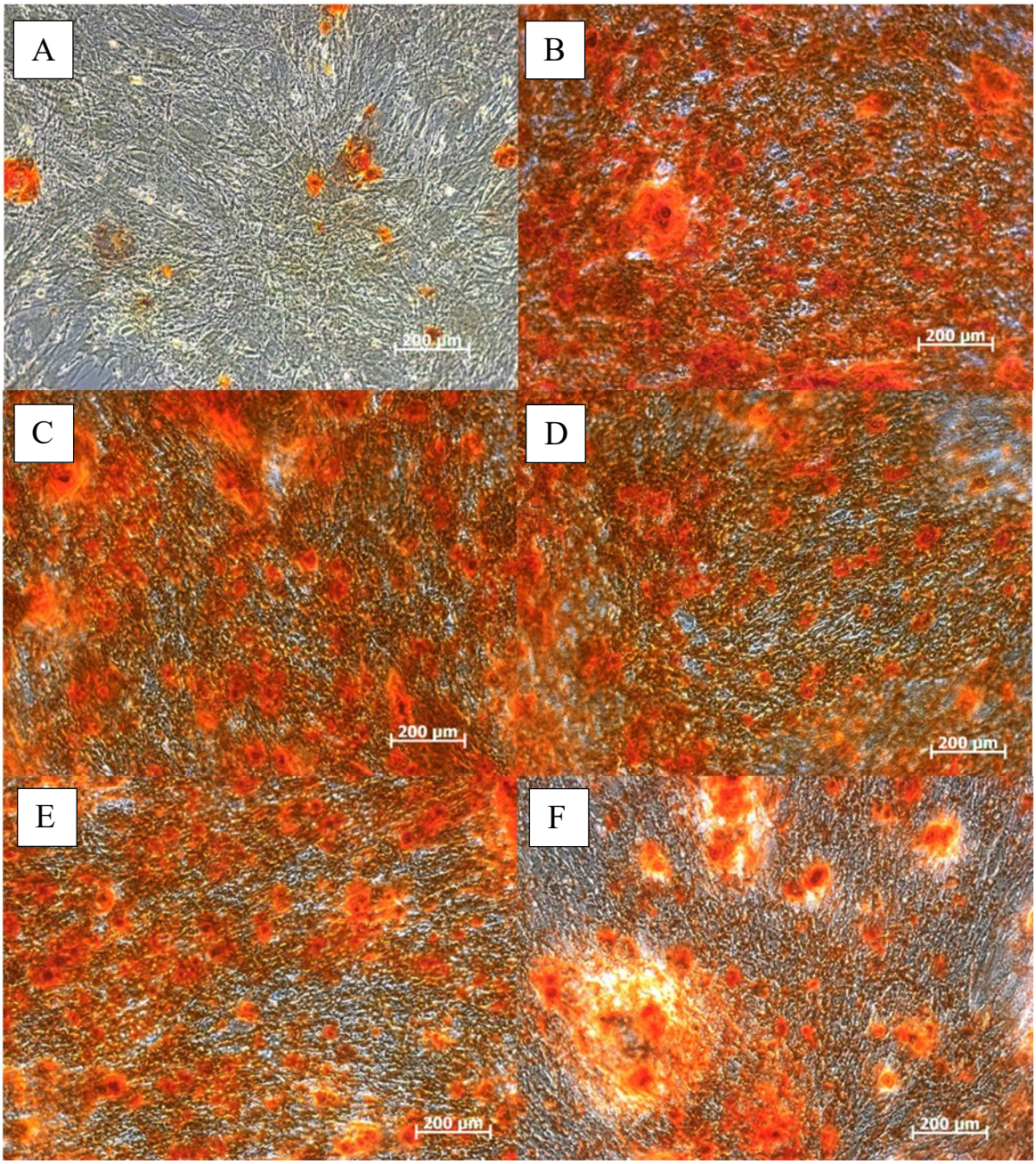

Figure 36: Alizarin red staining at day 21 after treating hBMSCs with diverse catalase concentrations. A: no addition to the osteogenic differentiation medium; B: 62.5 U/ml Catalase; C: 125 U/ml Catalase; D: 250 U/ml; E: 500 U/ml; F: 1000 U/ml

5.2.1.1.1 Impact of a Treatment with Catalase on Regular and Osteogenically Dysfunctional HBMSCs

As mentioned in paragraph *5.2.1.1*, the treatment of osteogenically dysfunctional hBMSCs with catalase resulted in a significantly improved formation of calcified matrix. Catalase was able to lead to an optimal osteogenic differentiation potential. Interestingly, the osteogenic differentiation potential of regular hBMSCs was not affected by the addition of catalase.

figure 37 shows the impact of a catalase treatment on the osteogenic differentiation potential of regular hBMSCs. This type of cells is called responder hBMSCs.

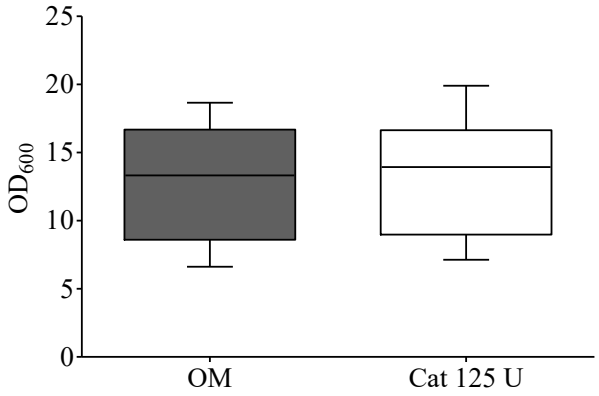

Figure 37: Measurement of the optical density at 600 nm of the dissolved alizarin red dye. HBMSCs were cultured in osteogenic differentiation medium for 21 days. All cell cultures were treated equally except of the treatment with catalase (125 U/ml). Cell cultures were stained at day 21 with alizarin red and the dye was dissolved. The optical density of the obtained solution was determined. The optical density is proportional to the amount of calcified matrix. (OM = osteogenic differentiation medium; Cat = catalase; n = 4)

Figure 38 shows the significantly enhanced formation of calcified matrix by a treatment with catalase for 21 days of osteogenically dysfunctional hBMSCs. These cells are called low responder cells. This type of cells could not differentiate under regular conditions into osteoblasts. The treatment with catalase resulted in a distinct restoration of the impaired osteogenic differentiation potential. These donors are called catalase responders.

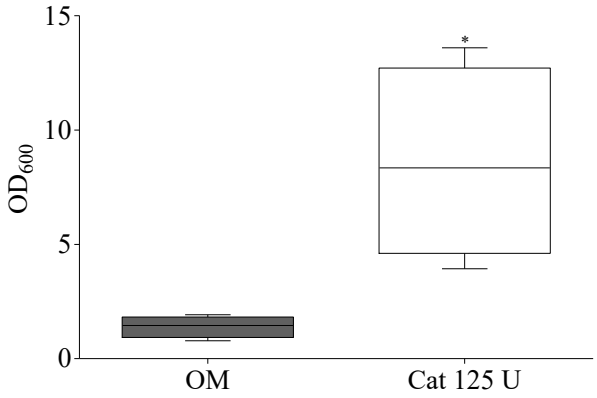

Figure 38: Measurement of the optical density at 600 nm of the dissolved alizarin red dye. Osteogenically dysfunctional hBMSCs were cultured in osteogenic differentiation medium for 21 days. All cell cultures were treated equally except of the treatment with catalase (125 U/ml). Cell cultures were stained at day 21 with alizarin red and the dye was dissolved. The optical density of the obtained solution was determined. The optical density is proportional to the amount of calcified matrix. (* = significant to OM [$p < 0.05$]; OM = osteogenic differentiation medium; Cat = catalase; n = 8)

Additionally, the activity of alkaline phosphatase, which is also an indicator of the osteogenic differentiation [179], was determined. The activity of alkaline phosphatase rose to initiate the differentiation processes. The activity was determined at day 21 of responder as well as low responder hBMSCs which were both cultured in osteogenic differentiation medium and were treated with catalase. As shown in *figure 39*, the addition of catalase leads to insignificant increase of the activity of alkaline phosphatase of responder hBMSCs.

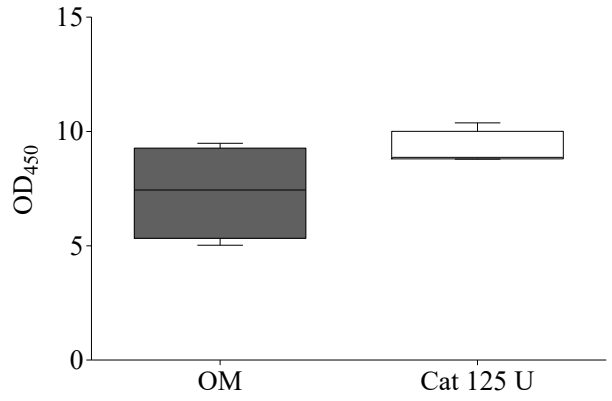

Figure 39: Measurement of the activity of alkaline phosphatase of responder hBMSCs. HBMSCs were cultured in osteogenic differentiation medium for 21 days. All cell cultures were treated equally except of the treatment with catalase (125 U/ml). At day 21, cell cultures were incubated with a nitrophenyl phosphate solution and the optical density of the obtained solution was determined at 450 nm. The values of the optical density are proportional to the activity of alkaline phosphatase. (OM = osteogenic differentiation medium; Cat = catalase; n = 4)

The increase of the activity of alkaline phosphatase of low responder hBMSCs, which were treated with catalase, was significant. *Figure 40* shows the increase of the activity of alkaline phosphatase by a catalase treatment.

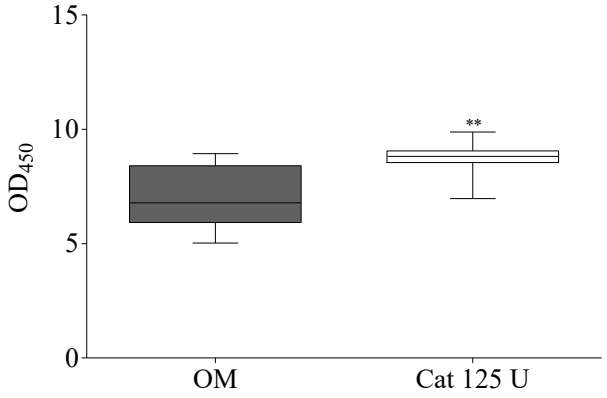

Figure 40: Measurement of the activity of alkaline phosphatase of low responder hBMSCs. HBMSCs were cultured in osteogenic differentiation medium for 21 days. All cell cultures were treated equally except of the treatment with catalase (125 U/ml). At day 21, cell cultures were incubated with a nitrophenyl phosphate solution and the optical density of the

obtained solution was measured at 450 nm. The values of the optical density are proportional to the activity of alkaline phosphatase. (** = significant to OM [$p < 0.033$]; OM = osteogenic differentiation medium; Cat = catalase; n = 8)

Interestingly, the difference of the activity of responder and low responder hBMSCs was not significant. Therefore, catalase led to an enhanced activity of alkaline phosphatase but the difference of responder and low responder hBMSCs, which were both not treated with catalase, was not significant. *Figure 41* shows that the activity of alkaline phosphatase of low responder cells was slightly lower than the activity of responder cells.

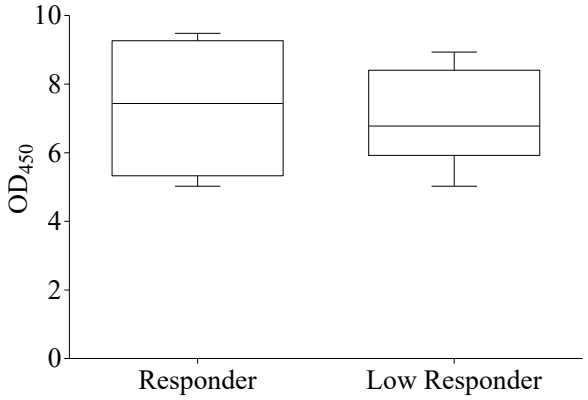

Figure 41: Measurement of the activity of alkaline phosphatase of responder and low responder hBMSCs in comparison. HBMSCs were cultured in osteogenic differentiation medium for 21 days. All cell cultures were treated equally except of the treatment with catalase (125 U/ml). At day 21, cell cultures were incubated with a nitrophenyl phosphate solution and the optical density of the obtained solution was determined at 450 nm. The values of the optical density are proportional to the activity of alkaline phosphatase. The activity of responder and low responder cells were compared (n = 4 - 8).

5.2.1.2 Influence of Antioxidative Additives on the Osteogenic Differentiation Potential of Low Responder Cells

To assess the dimension of the osteogenic differentiation potential of low responder hBMSCs after a treatment with diverse antioxidative approaches, the cell cultures were stained at day 21 with alizarin red. Images were taken and afterwards, the dye was dissolved to measure the optical density of the obtained solution which was proportional to the extent of matrix calcification and therefore to the osteogenic differentiation potential. As described in paragraph *5.2.1.1.1,* catalase led to an optimization of the osteogenic differentiation potential of low responder donors. Due to the known antioxidative chemical reaction of catalase, which is explained in detail in section *1.4.2.1*, further antioxidative additives with different mechanisms of action were tested. In paragraph *4.2.1*, the antioxidative effects of the individual substances are explained. The test duration was set for 21 days. Without any addition to the osteogenic differentiation medium, the low responder hBMSCs could not form

a calcified matrix. The addition of catalase led to a significant enhanced calcified matrix formation. Since no optimization of the formation of calcified matrix was observed, it was obvious that the addition of 25 µM MnTBAP, 25 µM EUK134, 500 µM trolox and 10 µM mannitol did not enhance the osteogenic differentiation potential of low responder cells. The extent of matrix calcification was as weak as of low responder cell cultures which were cultured in unsupplemented osteogenic differentiation medium. The addition of 100 µg/ml thymol, 10 µM EDTA, 300 U MnSOD and 150 nm hemoglobin led to a slightly improved osteogenic differentiation potential which was not as pronounced as the osteogenic differentiation potential after a treatment with catalase. *Figure 42* shows the red colored calcified matrix after staining with alizarin red. The significant improvement by a catalase treatment is visible. The slight optimization is also seen after the treatment with hemoglobin (F). The treatment with EUK134 even led to a deterioration of the osteogenic differentiation potential. Additionally, it is conspicuous that the cells were stressed by the treatment with EUK134. Some donors died during the EUK134 treatment. Remarkably, the treatment with trolox led to a prominent lipid accumulation which is highlighted in *figure 43*.

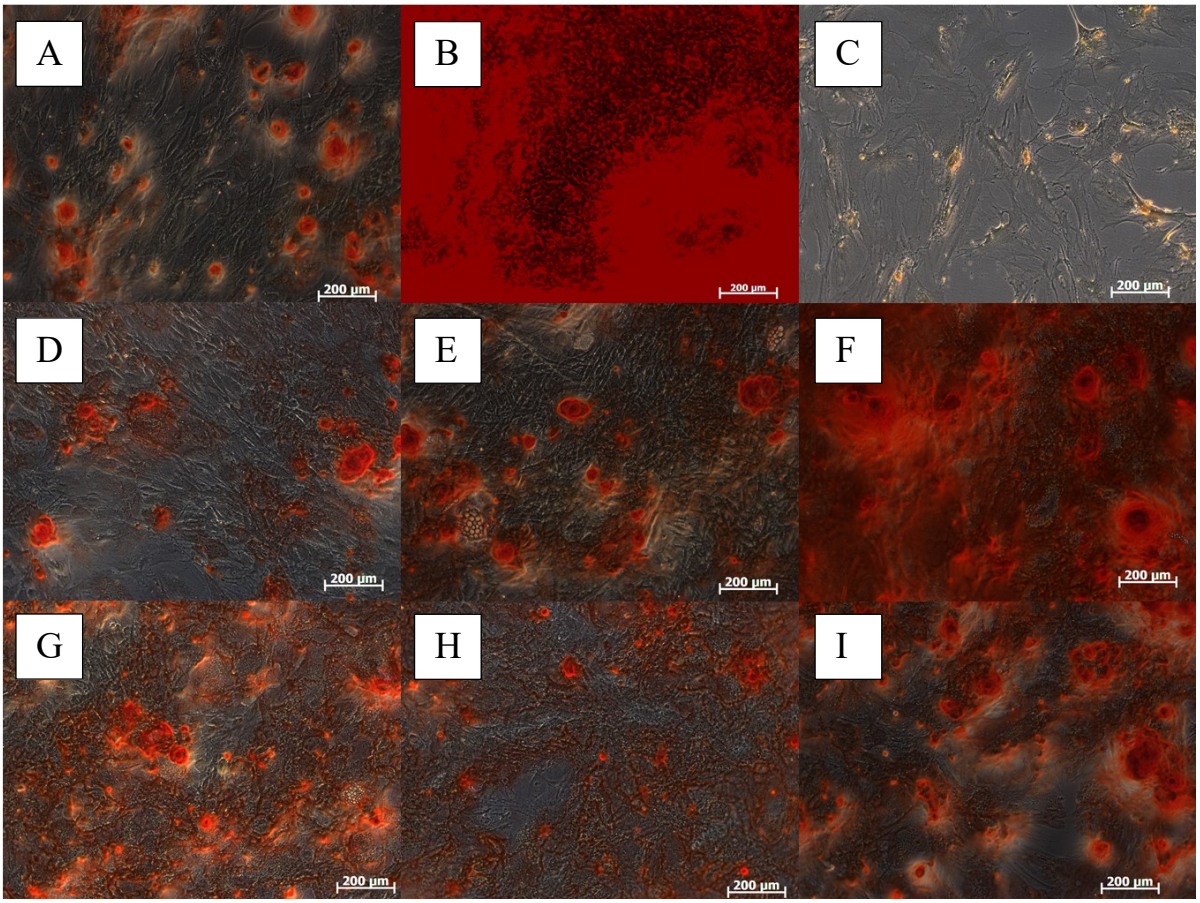

Figure 42: Formation of calcified matrix after culturing in osteogenic differentiation medium with diverse additives. After reaching confluence, low responder hBMSCs were cultured in osteogenic differentiation medium which was supplemented with diverse additives. At day 21, the cell cultures were stained with alizarin red to detect the extent of matrix calcification. A: Cells cultured in osteogenic differentiation medium with no supplements; B: cells treated with 125 U/ml catalase; C: cells treated with 25 µM EUK134; D: cells treated with 25 µM MnTBAP; E: cells treated with 500 µM trolox; F: cells treated with 15 nM hemoglobin; G: cells treated with 300 U/ml MnSOD; H: cells treated with 100 µM thymol; I: cells treated with 10 µM mannitol

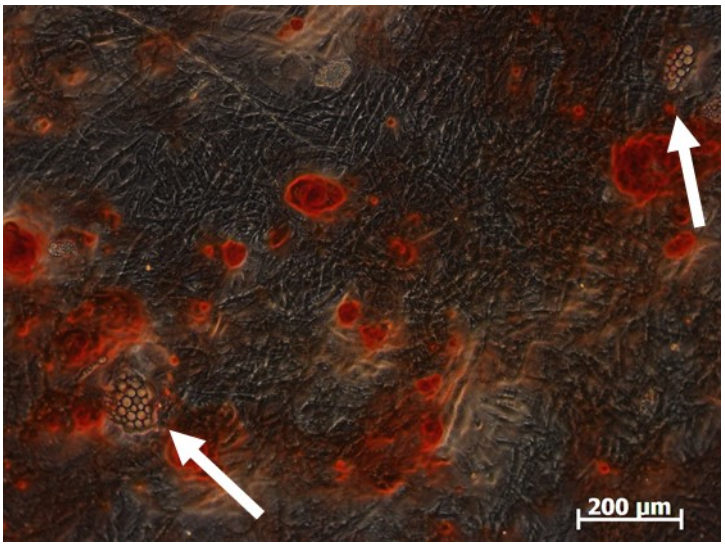

Figure 43: Adipogenic differentiation and fat formation caused by a treatment with trolox. After reaching confluence, low responder hBMSCs were cultured in osteogenic differentiation medium which was supplemented with trolox. At day 21, the cell cultures were stained with alizarin red to detect the extent of matrix calcification. Interestingly, no osteogenic differentiation but a fat formation (indication of an adipogenic differentiation) was observed.

In *figure 44,* the precise extent of matrix calcification and therefore the dimension of osteogenic differentiation potential is shown. The significant enhanced matrix calcification is visible. Also, the positive trend of hemoglobin and MnSOD can be identified. The negative effect of EUK134 on the formation of calcified matrix is also presented. The significant values showed that only 125 U/ml catalase could turn osteogenically dysfunctional hBMSCs from low responder cells to catalase responder cells. Due to the chemical reaction, catalase produces water and oxygen by a degradation of hydrogen peroxide (see: chapter *1.4.2.1*). Since the other additives exhibited different antioxidative mechanisms, they could not degrade hydrogen peroxide. The individual mechanisms are described in section *4.3*.

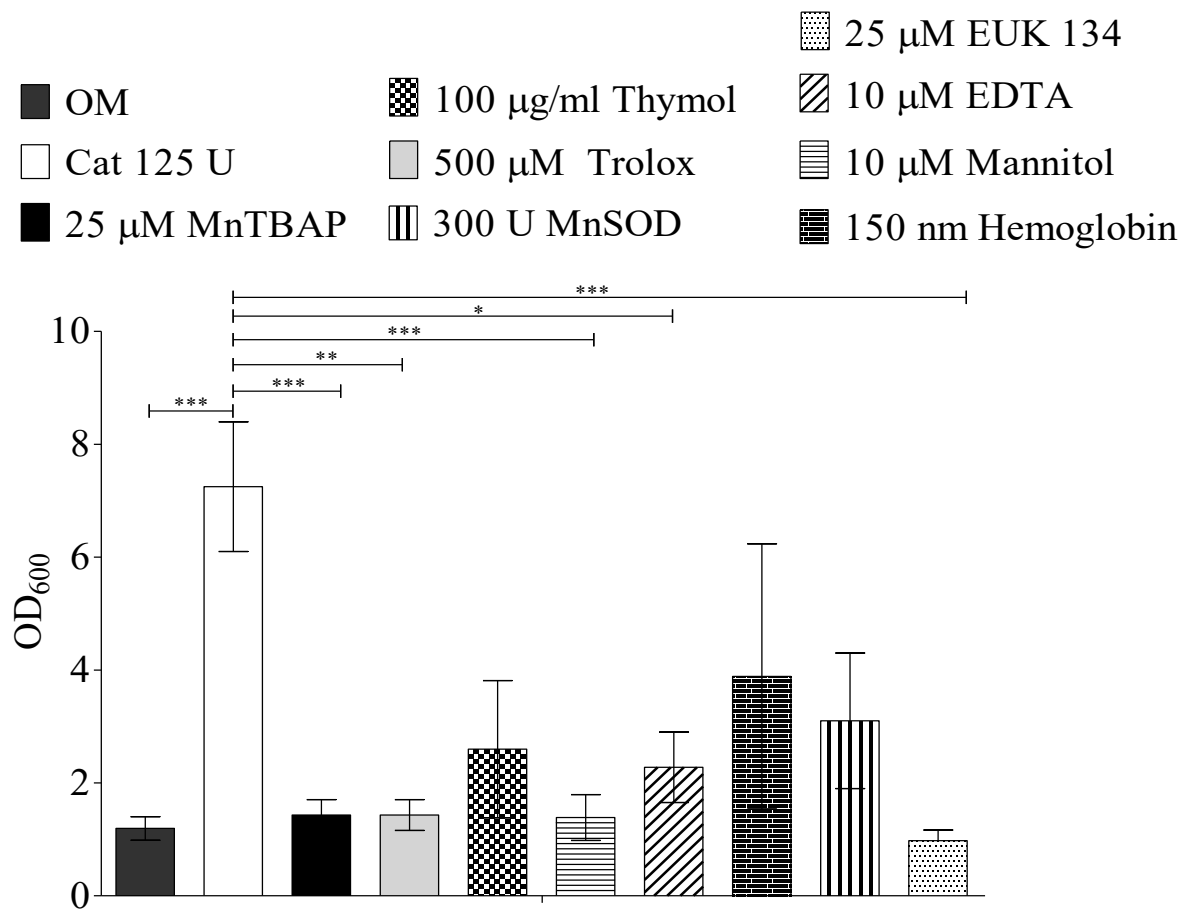

Figure 44: Assessment of calcified matrix after addition of antioxidative additives. Osteogenically dysfunctional hBMSCs were cultured in osteogenic differentiation medium for 21 days. All cell cultures were treated equally except of the different supplements. Cell cultures were stained at day 21 with alizarin red and the dye was dissolved. The optical density of the obtained solution was determined. The optical density is proportional to the amount of calcified matrix (* = significant [$p < 0.05$]; ** = significant [$p < 0.033$]; *** = significant [$p < 0.001$]; OM = osteogenic differentiation medium; Cat = catalase; n = 2 - 12).

In *figure 45*, the activity of alkaline phosphatase is presented. In general, alkaline phosphatase needed to be upregulated in the beginning of the osteogenic differentiation process. The upregulation of alkaline phosphatase is an initial step to activate the following osteogenically relevant transcription factors [179]. Thus, during the osteogenic differentiation progress, a correlation of the extent of matrix calcification was obligatory. Due to the correlation of the results of day seven and 14 to day 21, the representative results of day 21 are shown. Interestingly, the expected correlation of the matrix formation and the activity of alkaline phosphatase was not met in all cases. The alkaline phosphatase activity of cell cultures, which were treated with trolox, was stronger upregulated than with a catalase treatment even though the matrix formation was not enhanced. Conversely, the alkaline phosphatase activity was not elevated after a treatment with MnTBAP, mannitol or EUK134, and also the matrix formation

was not improved. In the described cases, the correlation of these two osteogenic differentiation indicators was fulfilled.

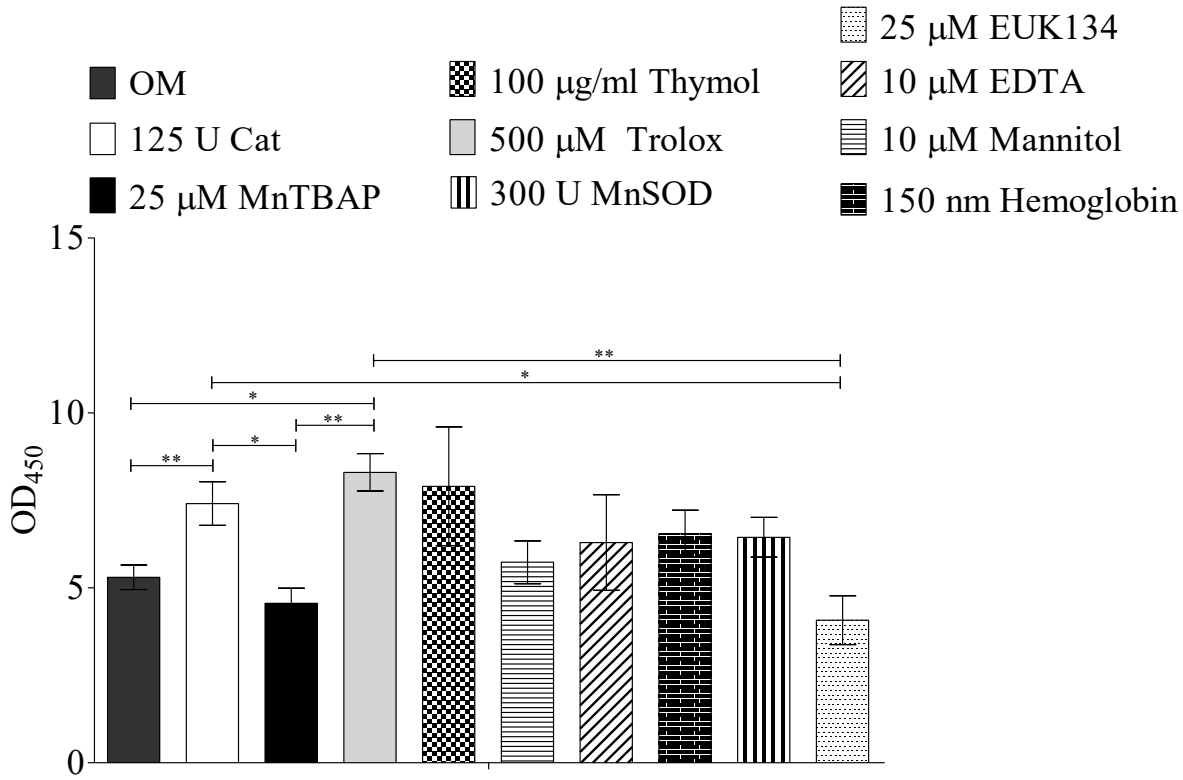

Figure 45: Assessment of the activity of alkaline phosphatase after addition of antioxidative additives. Osteogenically dysfunctional hBMSCs were cultured in osteogenic differentiation medium for 21 days. All cell cultures were treated equally except of the different supplements. At day 21, cell cultures were incubated with a nitrophenyl phosphate solution. Due to the hydrolysis to nitrophenyl, which was catalyzed by alkaline phosphatase, the solution turned yellow. The optical density was determined of the obtained solution at a wavelength of 450 nm. The optical density is proportional to the activity of alkaline phosphatase. (* = significant [$p < 0.05$]; ** = significant [$p < 0.033$]; OM = osteogenic differentiation medium; Cat = catalase; n = 2 - 12).

Furthermore, the used catalase was purified of thymol by centrifugation. The supernatant, which contained the thymol, was decanted and the remaining catalase was resuspended in medium. The improvement of the matrix calcification by catalase without thymol was not significant as demonstrated in *figure 46*. Both preparations resulted in an enhanced osteogenic differentiation potential of low responder hBMSCs. To show the equal potential of both compositions, it was not necessary to also test the activity of alkaline phosphatase.

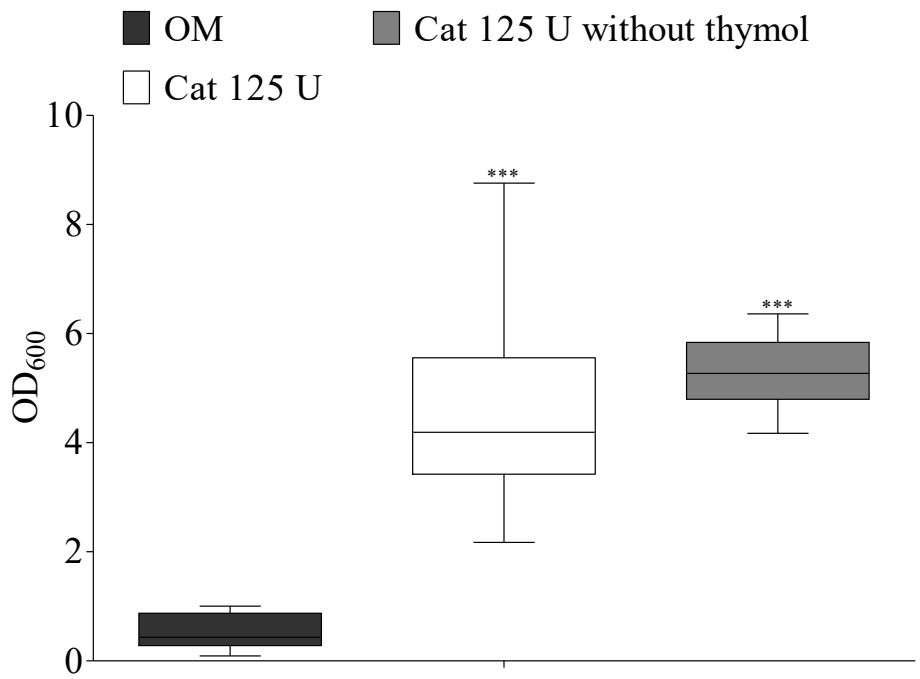

Figure 46: Assessment of the matrix calcification after addition of catalase with and without thymol. Osteogenically dysfunctional hBMSCs were cultured in osteogenic differentiation medium for 21 days. All cell cultures were treated equally except of the different supplements. Cell cultures were stained at day 21 with alizarin red and the dye was dissolved. The optical density of the obtained solution was determined. The optical density is proportional to the amount of calcified matrix (*** = significant to OM [$p < 0.001$]; OM = osteogenic differentiation medium; Cat = catalase; n = 5 - 6).

5.2.1.3 Influence of Antioxidative Additives on the Osteogenic Differentiation Potential of Responder Cells

As already demonstrated in paragraph *5.2*, osteogenically regular responder hBMSCs could form a calcified matrix in unmodified osteogenic differentiation medium. Nevertheless, responder hBMSCs were also treated with the previously described additives (see: chapter *5.2.1.2*) to assess the impact on the osteogenic differentiation potential. *Figure 47* demonstrates the alizarin red stained calcified matrix. Since the addition of MnTBAP, catalase, trolox, EDTA, mannitol, thymol, MnSOD and hemoglobin resulted in an equally extent of matrix calcification, an image of the matrix calcification of responder cells which were treated with MnTBAP is representatively shown in the figure. The osteogenic differentiation potential of responder hBMSCs was neither positively nor adversely affected by a treatment with MnTBAP, catalase, trolox, EDTA, mannitol, thymol, MnSOD or hemoglobin. Remarkably, the treatment with EUK134 led to a significant impaired calcified matrix formation and therefore osteogenically differentiation potential. Also, the cell morphology was conspicuous. Similarly, morphological changes were also exhibited by low

responder cultures after a treatment with EUK134. As visible in *Figure 47,* the cell morphology indicates stressed cells.

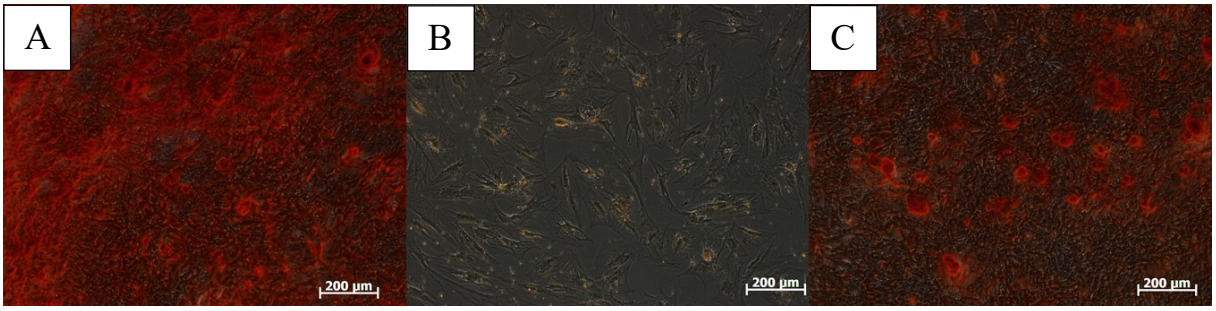

Figure 47: Formation of calcified matrix after culturing in osteogenic differentiation medium supplemented with diverse additives. After reaching confluence, responder hBMSCs were cultured in osteogenic differentiation medium which was supplemented with diverse additives. At day 21, the cell cultures were stained with alizarin red to detect the extent of matrix calcification. Representative images of the stained cell cultures are presented. A: Cells cultured in osteogenic differentiation medium with no supplements; B: treatment with 25 µM EUK134; C: treatment with 25 µM MnTBAP (representative image for the treatment with catalase, trolox, EDTA, mannitol, thymol, MnSOD and hemoglobin)

5.2.1.4 Influence of Hydrogen Peroxide on the Osteogenic Differentiation Potential of Low Responder and Responder Cells

Due to the impairment of the osteogenic differentiation potential of responder and low responder hBMSCs caused by the treatment with EUK134 which can degrade superoxide anions and hydrogen peroxide, hBMSCs were treated with different concentrations of hydrogen peroxide. The impact of hydrogen peroxide was tested at low responder hBMSCs. The times of measurements were set at day 14, 21 and 28. Day 28 was also analyzed to see if hydrogen peroxide had cytotoxic effects at later stages. Within the same approach, the cells were treated with catalase or hydrogen peroxide to assess their osteogenic differentiation potential in comparison to catalase which had a positive effect on the osteogenic differentiation (see: *figure 42* and *figure 44*). The positive effect of a catalase treatment on the osteogenic differentiation is also highlighted in *figure 48.* Additionally, the graph shows clearly that the addition of hydrogen peroxide does not lead to an optimization of the osteogenic differentiation potential of low responder hBMSCs.

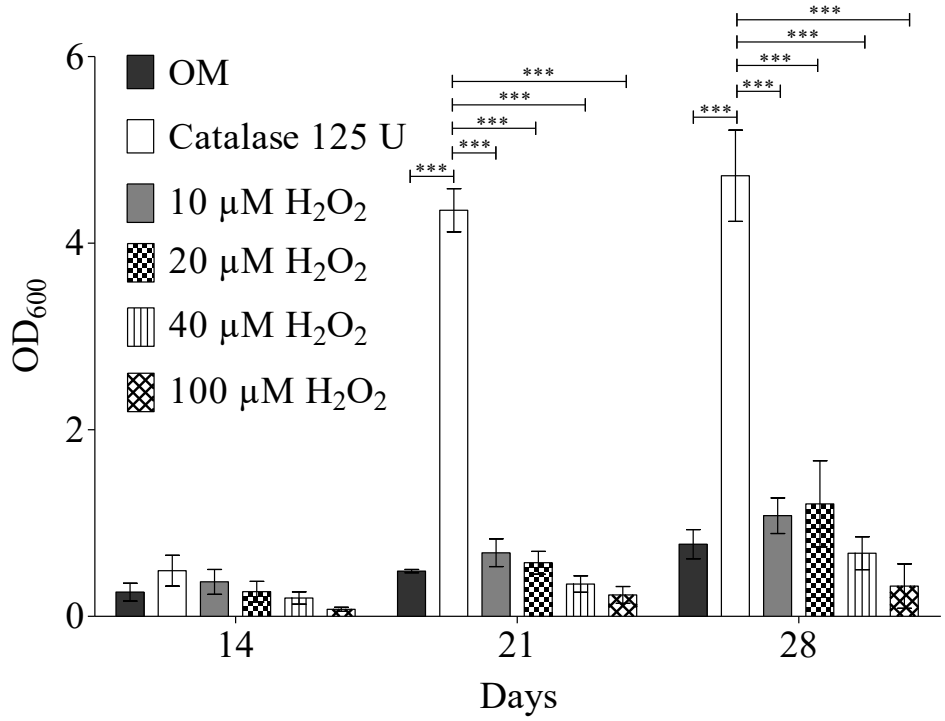

Figure 48: Assessment of calcified matrix after addition of antioxidative additives. Osteogenically dysfunctional hBMSCs were cultured in osteogenic differentiation medium for a total of 28 days. All cell cultures were treated equally except for the addition of catalase and the different concentrations of hydrogen peroxide. Cell cultures were stained at day 14, 21 and 28 with alizarin red. In the following, the dye was dissolved. The optical density was determined of the obtained solution at 600 nm. The optical density is proportional to the amount of calcified matrix (*** = significant [$p < 0.001$]; OM = osteogenic differentiation medium; Cat = catalase; n = 4).

Figure 49 shows the stained calcified matrix after the treatment with unsupplemented osteogenic differentiation medium, catalase and with different concentrations of hydrogen peroxide supplemented osteogenic differentiation medium at day 28. As already pointed out in *figure 49*, catalase led, as expected, to an optimized osteogenic differentiation potential. In general, the addition of hydrogen peroxide did not lead to a distinct increase of the matrix formation. Interestingly, in some cases, as seen in the images C and D of *figure 49*, a weak positive effect could be determined. To conclude, the addition of antioxidative catalase, which diminishes the amount of hydrogen peroxide (see: chapter *1.4.2.1*) as well as the addition of hydrogen peroxide in concentrations between 10 µM and 20 µM, led to an improved osteogenic differentiation of low responders. Nonetheless, the weak improvement by hydrogen peroxide addition was not statistically significant. Furthermore, cell cultures, which were treated with hydrogen peroxide, also showed indications of adipogenic differentiation (demonstrated by the fat formations which are pointed out by the white arrows in *figure 49*).

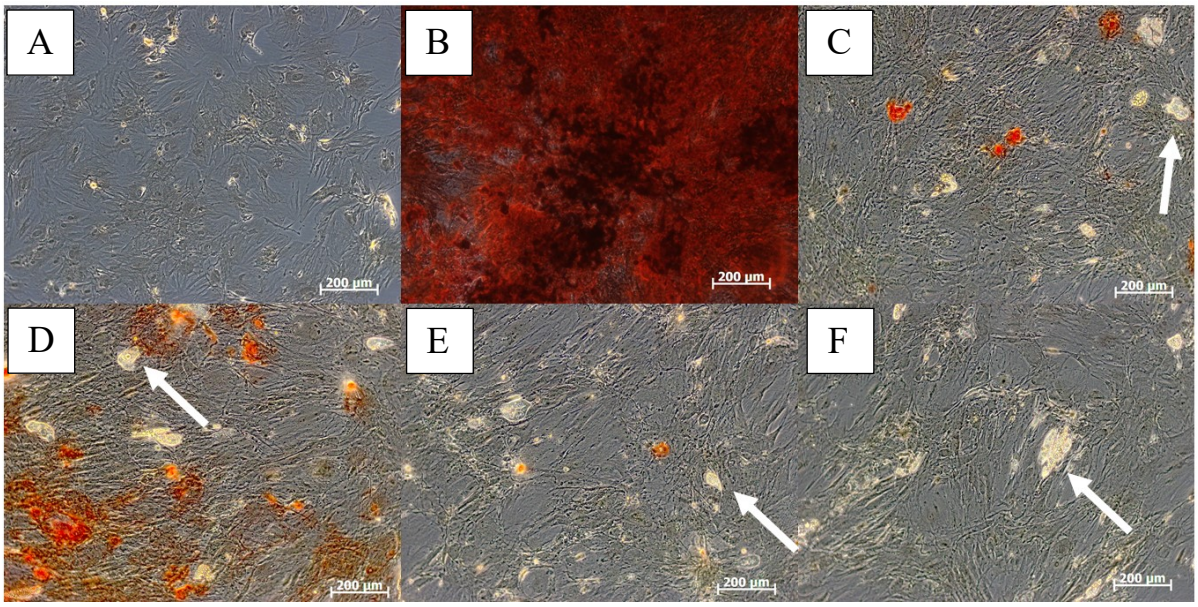

Figure 49: Formation of calcified matrix after a treatment with catalase or different concentrations of hydrogen peroxidase. After reaching confluence, low responder hBMSCs were cultured in unsupplemented, catalase supplemented or hydrogen peroxide supplemented osteogenic differentiation medium. At day 14, 21, 28, the cell cultures were stained with alizarin red to detect the extent of matrix calcification. The images above were taken at day 28. The white arrows show fat formations. A: Cells cultured in osteogenic differentiation medium with no supplements; B: cells treated with 125 U/ml catalase; C: cells treated with 10 µM H_2O_2; D: cells treated with 20 µM H_2O_2; E: cells treated with 40 µM H_2O_2; F: cells treated with 100 µM H_2O_2

It is also important to note that in many cases, the addition of hydrogen peroxide with a concentration of 100 µM led to cytotoxic effects. *Figure 50* shows that the treatment with 100 µM hydrogen peroxide results in cell death.

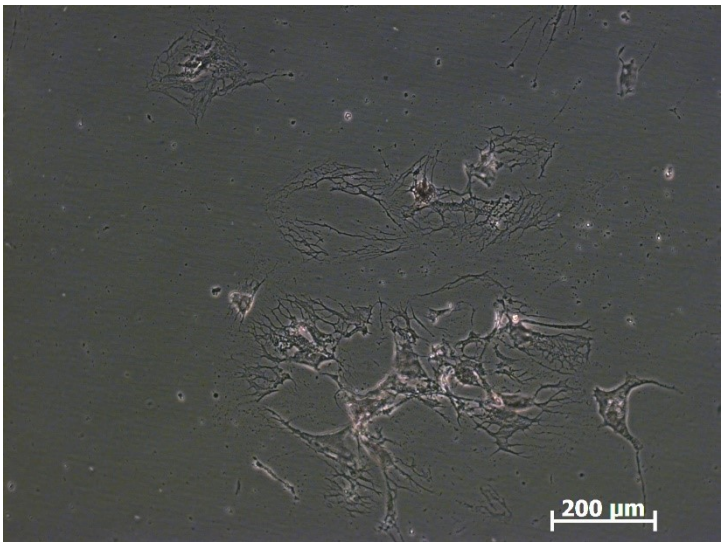

Figure 50: The treatment with 100 µM hydrogen peroxide results in cell death. After reaching confluence, low responder hBMSCs were cultured in osteogenic differentiation medium which was supplemented with 100 µM hydrogen peroxide. At day 14, 21, 28, the cell cultures were stained with alizarin red to detect the extent of matrix calcification. The image above

was taken at day 28. The image shows remains of dead cells which is the strongest indication of the cytotoxic effect of hydrogen peroxide.

Furthermore, the activity of alkaline phosphatase was determined to assess initial indications of the osteogenic differentiation after a treatment with hydrogen peroxide. As shown in *figure 51,* also the activity of alkaline phosphatase was not increased after treating the cells for 14, 21 and 28 days with hydrogen peroxide. The treatment with catalase instead led, as expected, to a significant increase of the activity. With increasing concentrations of hydrogen peroxide, the activity even decreased. In conclusion, the addition of hydrogen peroxide did not improve the formation of calcified matrix as well as the alkaline phosphatase activity of low responder cells.

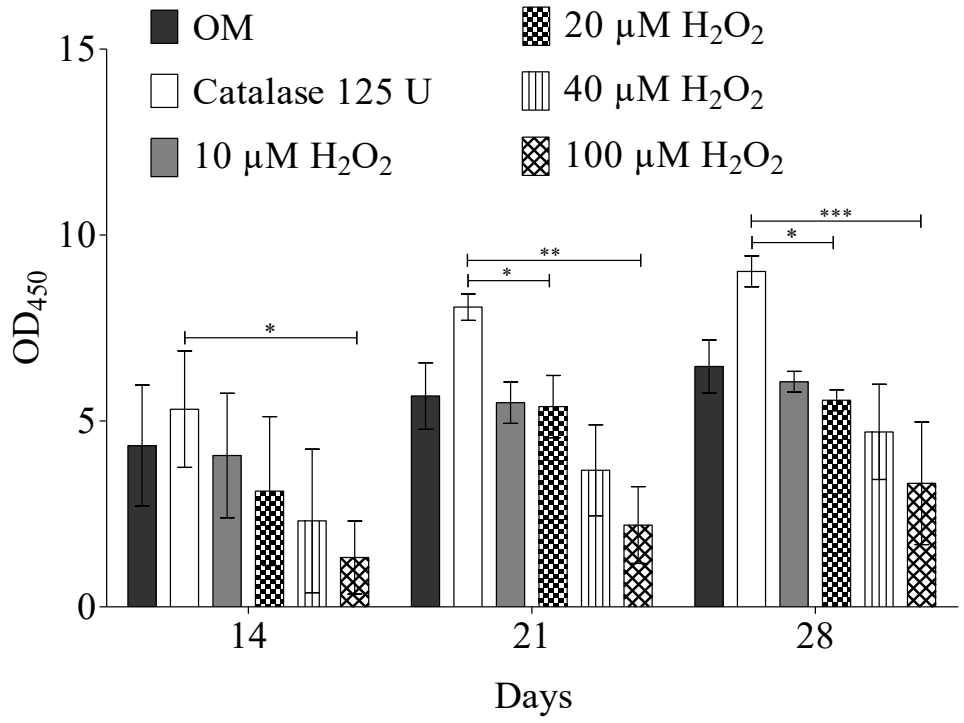

Figure 51: Assessment of the activity of alkaline phosphatase after addition of catalase and hydrogen peroxide in comparison. Osteogenically dysfunctional hBMSCs were cultured in osteogenic differentiation medium for 28 days. All cell cultures were treated equally except of the addition of catalase or different concentrations of hydrogen peroxide. At day 14, 21 and 28, the cell cultures were incubated with a nitrophenyl phosphate solution. Due to the hydrolysis to nitrophenyl, which was catalyzed by alkaline phosphatase, the solution turned yellow. The optical density of the obtained solution was determined at a wavelength of 450 nm. The optical density is proportional to the activity of alkaline phosphatase. (* = significant [$p < 0.05$]; ** = significant [$p < 0.033$]; *** = significant [$p < 0.001$]; OM = osteogenic differentiation medium; Cat = catalase; n = 4).

Responder hBMSCs were also treated with catalase and hydrogen peroxide. 10 µM, 20 µM or 40 µM of hydrogen peroxide did not impair the osteogenic differentiation potential of responder cells. Interestingly, some donors of the responder hBMSCs showed a distinct

matrix calcification during culturing in regular osteogenic differentiation medium (without any further supplements) which was further improved by a treatment with catalase which is shown in *figure 52*. Nonetheless, in most cases, responder hBMSCs showed an equal extent of matrix formation with or without a catalase treatment. The cytotoxic effect of 100 µM hydrogen peroxide applied to responder as well as low responder cells which is highlighted in image F of *figure 52*.

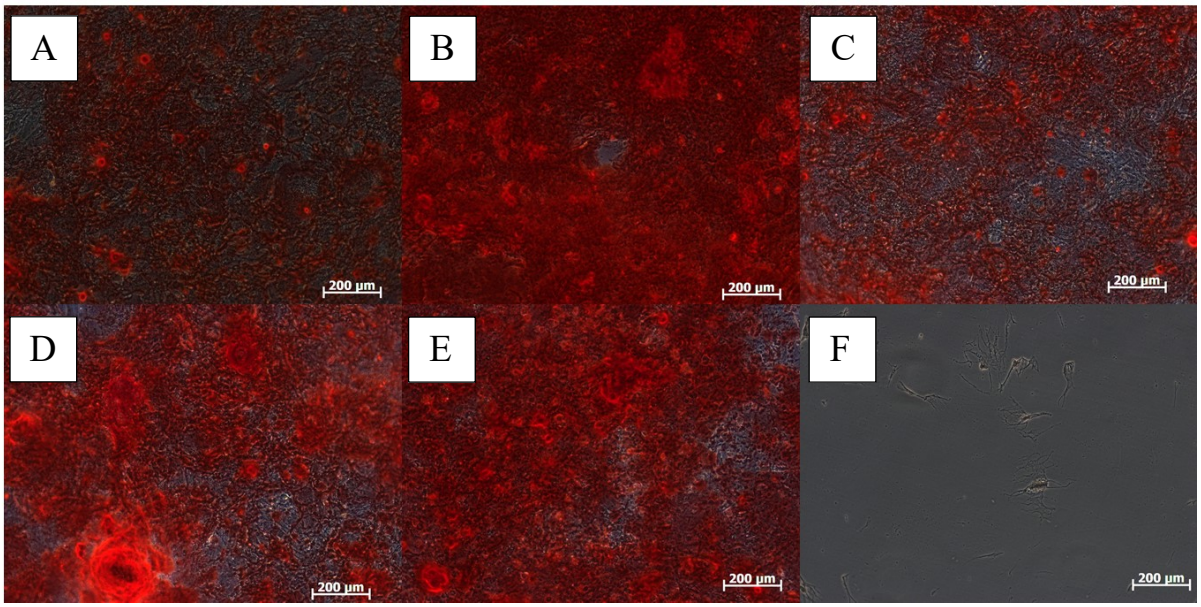

Figure 52: Formation of calcified matrix after a treatment with catalase or rather different concentrations of hydrogen peroxidase. After reaching confluence, responder hBMSCs were cultured in unsupplemented, catalase supplemented or hydrogen peroxide supplemented osteogenic differentiation medium. At day 14, 21, 28, the cell cultures were stained with alizarin red to detect the extent of matrix calcification. The images above were taken at day 21. A: Cells cultured in osteogenic differentiation medium with no supplements; B: cells treated with 125 U/ml catalase; C: cells treated with 10 µM H_2O_2; D: cells treated with 20 µM H_2O_2; E: cells treated with 40 µM H_2O_2; F: cells treated with 100 µM H_2O_2

5.2.1.5 Impact of Catalase and Heat Inactivated Catalase in Comparison to the Osteogenic Differentiation Potential of Low Responder Cells

Low responder hBMSCs were also treated in a new test series with heat inactivated catalase to prove that the antioxidative reaction is the key mechanism to restore the osteogenic differentiation potential of osteogenically dysfunctional hBMSCs.

5.2.1.5.1 Proof of the Successful Inactivation of Heat Inactivated Catalase

The catalase was inactivated as described in paragraph *4.2.3*. To demonstrate the inactivation of the heat inactivated catalase, two tests were performed. The first test was performed to hint at the inactivation and was used as a pretest. 1 ml hydrogen peroxide was added to 10 ml of medium and 2.15 µl of the catalase stock solution was added to initiate the degradation of

hydrogen peroxide which was manifested by a distinct bubbling. The same procedure was performed with heat inactivated catalase. Immediately after adding the active catalase, the solution bubbled heavily as expected. Quite the contrary, the addition of heat inactivated catalase did not result in a bubbling. This simple test already indicated the loss of function to degrade hydrogen peroxide of the heat inactivated catalase. Additionally, a catalase assay was performed to assess the catalase activity. The catalase activity of 12.5 U/ml catalase was measured in medium supplemented with phenol red and FCS as well as in medium without phenol red and FCS and in assay buffer. The same solutions were prepared to test the heat inactivated catalase. As shown in *figure 53*, the heat inactivated catalase showed no activity and the regular catalase showed an activity. Thereby, the success of the inactivation of catalase by heat was proven.

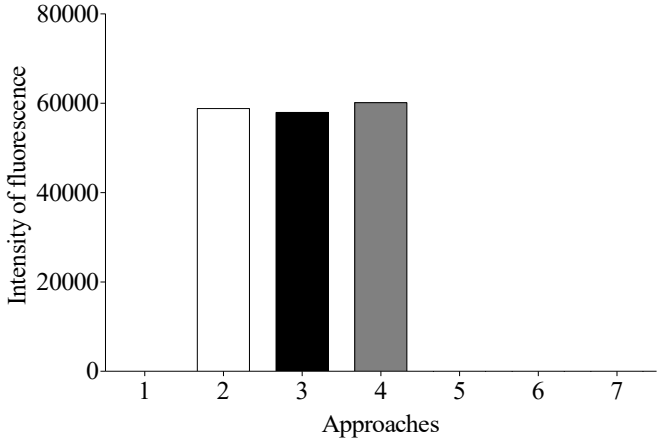

Figure 53: Determination of catalase activity of heat inactivated catalase and active catalase by the OxiSelect™ Catalase Activity Assay Kit.

5.2.1.5.1 Impact of Heat Inactivated Catalase on the Osteogenic Differentiation of Low Responder Cells

Low responder cells were treated after reaching confluence in proliferation medium with unsupplemented osteogenic differentiation medium, osteogenic differentiation medium supplemented with 125 U/ml catalase or 125 U/ml heat inactivated catalase. At day 21, the extent of matrix calcification was determined to assess the osteogenic differentiation potential. The addition of catalase as well as heat inactivated catalase resulted in an equal improvement of matrix calcification**.** *Figure 54* shows the evaluation of the extent of calcium deposits of the tested osteogenically dysfunctional hBMSCs.

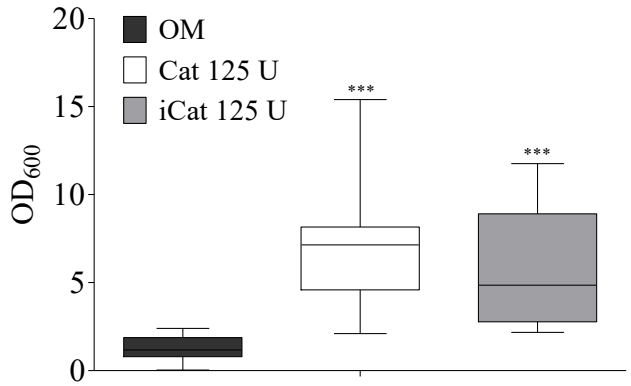

Figure 54: Assessment of calcified matrix after addition of catalase and heat inactivated catalase. Osteogenically dysfunctional hBMSCs were cultured in osteogenic differentiation medium for 21 days. All cell cultures were treated equally except for the addition of catalase or heat inactivated catalase. Cell cultures were stained at day 21 with alizarin red and the dye was dissolved. The optical density of the obtained solution was determined at 600 nm. The optical density is proportional to the amount of calcified matrix (*** = significant to OM [$p < 0.001$]; OM = osteogenic differentiation medium; Cat = catalase; iCat = inactivated catalase; n = 11).

Additionally, images were taken before the alizarin red stain was dissolved to determine the optical density and thereby the precise extent of matrix calcification. *Figure 55* shows the red stained calcium deposits after the incubation with alizarin red. In these images, the positive effect of catalase and heat inactivated catalase can be identified.

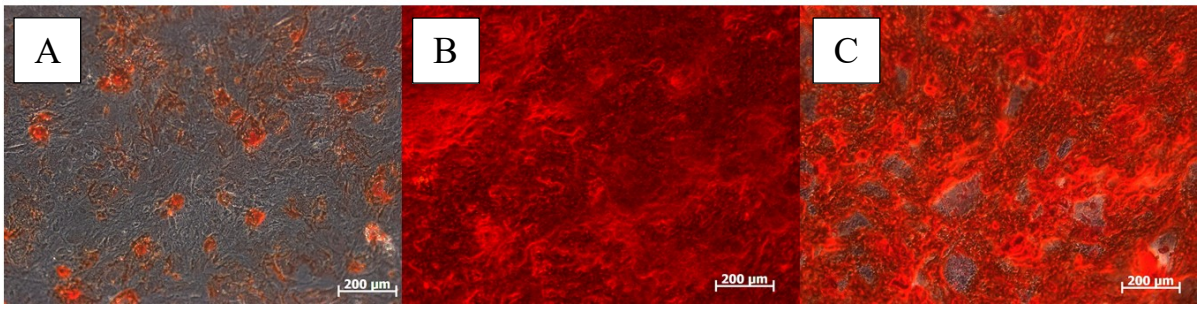

Figure 55: Formation of calcified matrix after a treatment with catalase or heat inactivated catalase. After reaching confluence, low responder hBMSCs were cultured in osteogenic differentiation medium which was not supplemented, supplemented with catalase or with heat inactivated catalase. At day 21, the cell cultures were stained with alizarin red to detect the extent of matrix calcification. A: Cells cultured in osteogenic differentiation medium with no supplements; B: cells treated with 125 U/ml catalase; C: cells treated with 125 U/ml heat inactivated catalase

Furthermore, the activity of alkaline phosphatase as another indicator of osteogenic differentiation was determined. The significant increase of the activity of alkaline phosphatase after the treatment with catalase or heat inactivated catalase correlated to the risen extent of matrix calcification. *Figure 56* demonstrates the elevated activity of alkaline phosphatase.

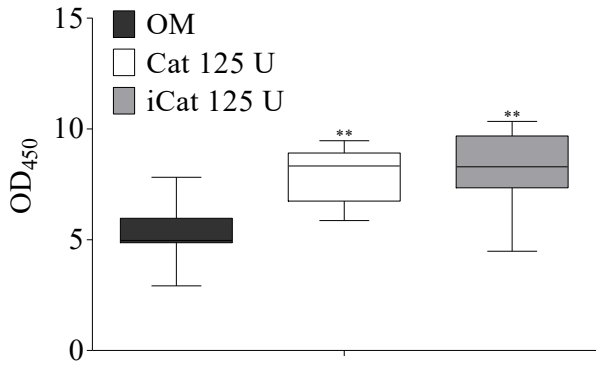

Figure 56: Assessment of the activity of alkaline phosphatase after addition of catalase or heat inactivated catalase. Osteogenically dysfunctional hBMSCs were cultured in osteogenic differentiation medium for 21 days. All cell cultures were treated equally except of the addition of catalase and heat inactivated catalase. At day 21, the cell cultures were incubated with a nitrophenyl phosphate solution. Due to the hydrolysis to nitrophenyl, which was catalyzed by alkaline phosphatase, the solution turned yellow. The optical density of the obtained solution was determined at a wavelength of 450 nm. The optical density is proportional to the activity of alkaline phosphatase. (** = significant to OM [$p < 0.033$]; OM = osteogenic differentiation medium; Cat = catalase; iCat = heat inactivated catalase; n = 11).

5.2.1.5.2 Protein Expression of Alkaline Phosphatase

Since the activity of alkaline phosphatase of low responder hBMSCs was risen by the treatment with catalase and heat inactivated catalase, the influence of the treatment was tested according to the protein expression of alkaline phosphatase of responder and low responder donors. Responder as well as low responder donors exhibited similar outcomes after the treatments. As shown in *figure 57* and *figure 58*, the addition of catalase and heat inactivated catalase resulted in a heightened expression of alkaline phosphatase of both types of donors at day seven whereas the protein expression at day 21 was diminished caused by the treatment. The cultivation of responder as well as low responder cells in unsupplemented osteogenic differentiation medium led to increased protein expression at day 21 compared to day seven. Interestingly, this effect is observed for both types of donors even though it had been proven that a rise during the initial stages and a decline at the later stages of osteogenesis of alkaline phosphatase was necessary for an optimal process [180]. It is important to note that the values of the protein expression of alkaline phosphatase were not normalized to the expression of the housekeeping protein GAPDH. Paragraph *5.2.1.5.2.1* explains this topic more detailed. The expressions of day seven and 21 were normalized to the control (day 0).

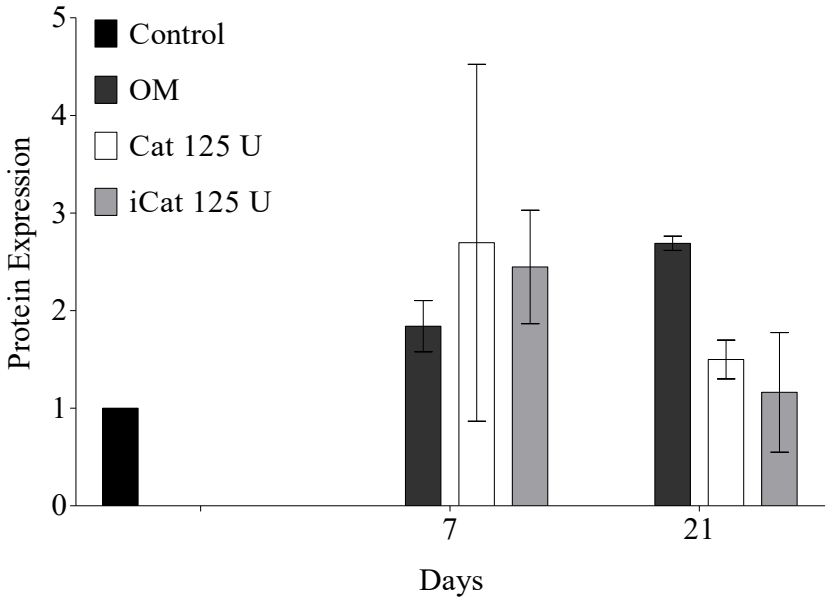

Figure 57: Protein expression of alkaline phosphatase. Cell cultures of responder were treated with unsupplemented, catalase supplemented or heat inactivated catalase supplemented osteogenic differentiation medium for a total of 21 days. At day 7 and 21, proteins were extracted and the protein expression was analyzed (OM = osteogenic differentiation medium; Cat = catalase; iCat = heat inactivated catalase; n = 2).

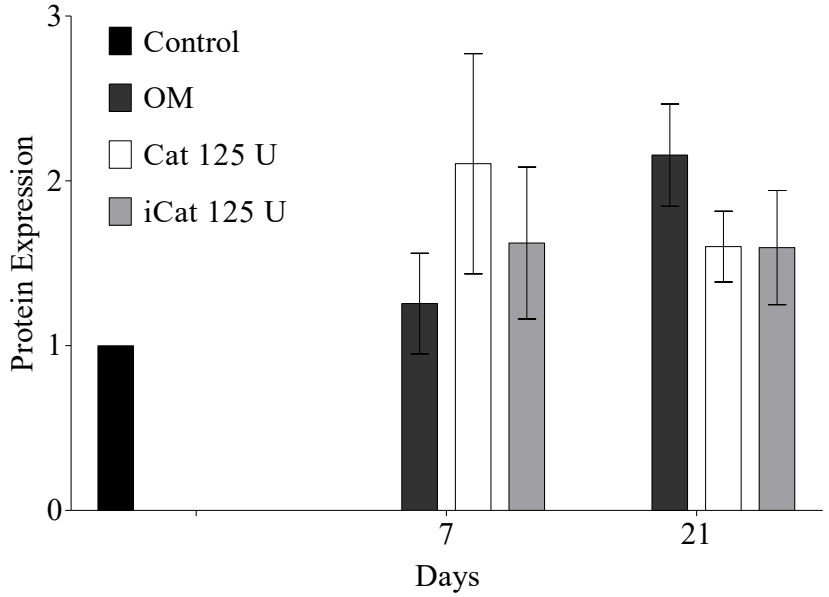

Figure 58: Protein expression of alkaline phosphatase. Cell cultures of low responder were treated with unsupplemented, catalase supplemented or heat inactivated catalase supplemented osteogenic differentiation medium for a total of 21 days. At day 7 and 21, proteins were extracted and the protein expression was analyzed (OM = osteogenic differentiation medium; Cat = catalase; iCat = heat inactivated catalase; n = 3).

The expression pattern is presented in *figure 59*.

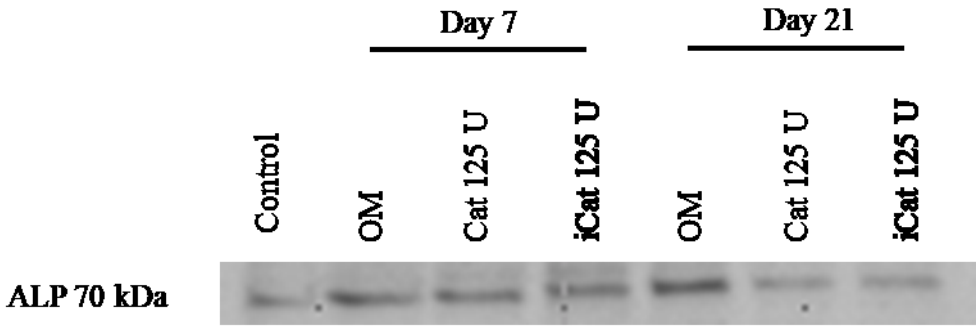

Figure 59: Detail of the alkaline phosphatase expression of a gel of one of the donors (OM = osteogenic differentiation medium; Cat = catalase; iCat = heat inactivated catalase)**.**

5.2.1.5.2.1 Protein Expression of the Housekeeping Protein GAPDH

Since GAPDH is known for being one of the most popular housekeeping genes, the expression was determined simultaneously to the expression of the proteins of interest. In general, the expressions of the proteins of interest were normalized to the expression of GAPDH of the same sample. During the investigations of the osteogenic differentiation of hBMSCs, it became obvious that the different treatments and the osteogenic differentiation process itself did affect the expression of GAPDH. The protein bands of the expressed GAPDH were not consistent as expected which is visible in *figure 60*. Therefore, a normalization to this expression was not reasonable.

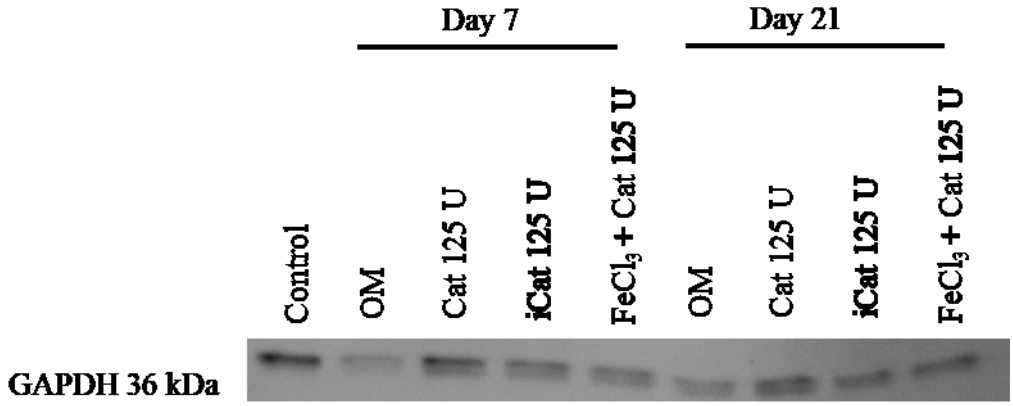

Figure 60: Detail of the GAPDH expression of a gel of one of the donors (OM = osteogenic differentiation medium; Cat = catalase; iCat = heat inactivated catalase).

Figure 61 shows the expression pattern of GAPDH which is representative for responder as well low responder donors. As no differences between responder and low responder donors according to the expression of GAPDH were observed, the condensed results are assessed. The addition of catalase resulted in a significant deviation compared to the other outcomes of differently treated samples. At day seven, the treatment with catalase led to a significant

elevation of the expression of GAPDH whereas the expression was diminished by catalase at day 21. The decrease of the expression was not significant but nonetheless a distinct trend was visible. The expression of GAPDH after a treatment with a combination of catalase and iron chloride was investigated of only one donor. The resulted values might not be representative. To evaluate the expression of GAPDH, the measured values were normalized to day zero (control).

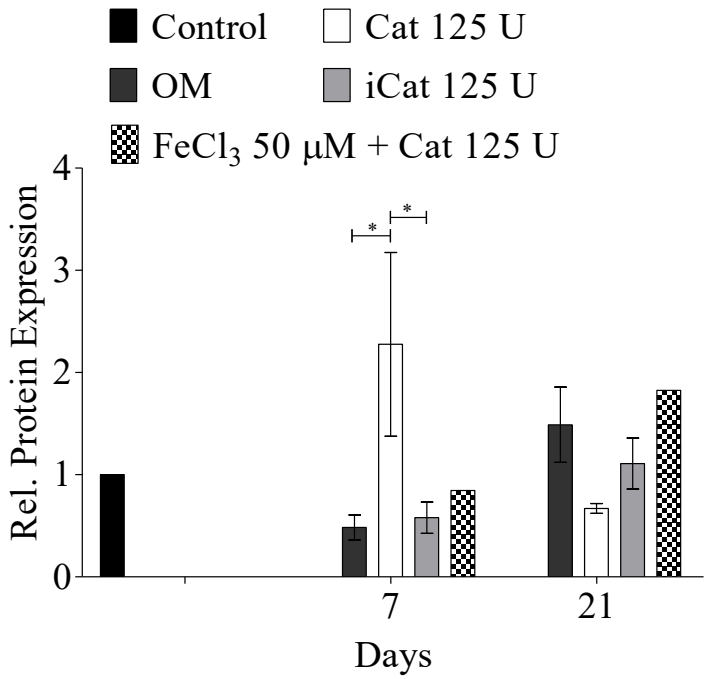

Figure 61: Protein expression of GAPDH. Cell cultures of low responder were treated with unsupplemented, catalase supplemented, heat inactivated catalase supplemented or iron chloride in combination with catalase supplemented osteogenic differentiation for a total of 21 days. At day 7 and 21, proteins were extracted and the protein expression was analyzed (* = significant [$p < 0.05$]; OM = osteogenic differentiation medium; Cat = catalase; iCat = heat inactivated catalase; n = 1 – 5).

5.2.1.6 No Restoration of an Impaired Osteogenic Differentiation Potential of Low Responder HBMSCs – Despite a Treatment with Catalase or Heat Inactivated Catalase

Some cell cultures did not show an optimization of the osteogenic differentiation potential after a treatment with catalase or heat inactivated catalase which is presented in *figure 62*. Nonetheless, the activity of alkaline phosphatase showed the typical increase during a regular osteogenic differentiation. Therefore, the initial steps of osteogenic differentiation were regularly performed but the formation of calcified matrix as the last step was disturbed. The evaluation of the activity of alkaline phosphatase is shown in *figure 63*.

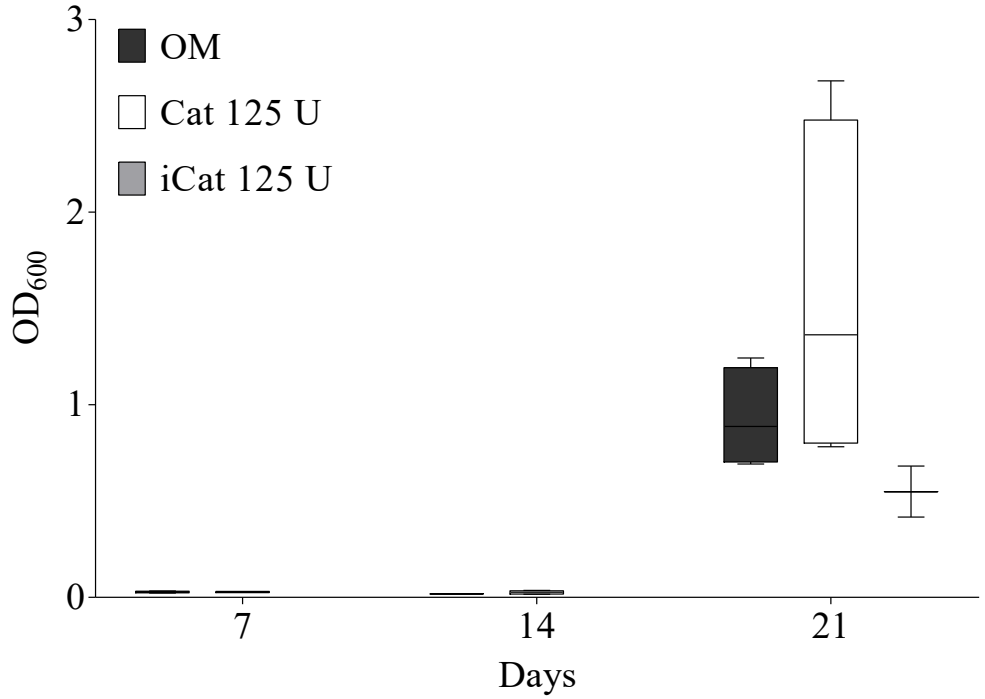

Figure 62: Assessment of calcified matrix of a low responder cell culture after addition of catalase and heat inactivated catalase. A cell culture of an osteogenically dysfunctional donor was cultured in osteogenic differentiation medium for 21 days. All cell cultures were treated equally except for the addition of catalase or heat inactivated catalase. The cell culture was stained at the days seven, 14 and 21 with alizarin red and the dye was dissolved. The optical density of the obtained solution was determined at 600 nm. The optical density is proportional to the amount of calcified matrix (OM = osteogenic differentiation medium; Cat = catalase; iCat = heat inactivated catalase; n = 1; fourfold determination).

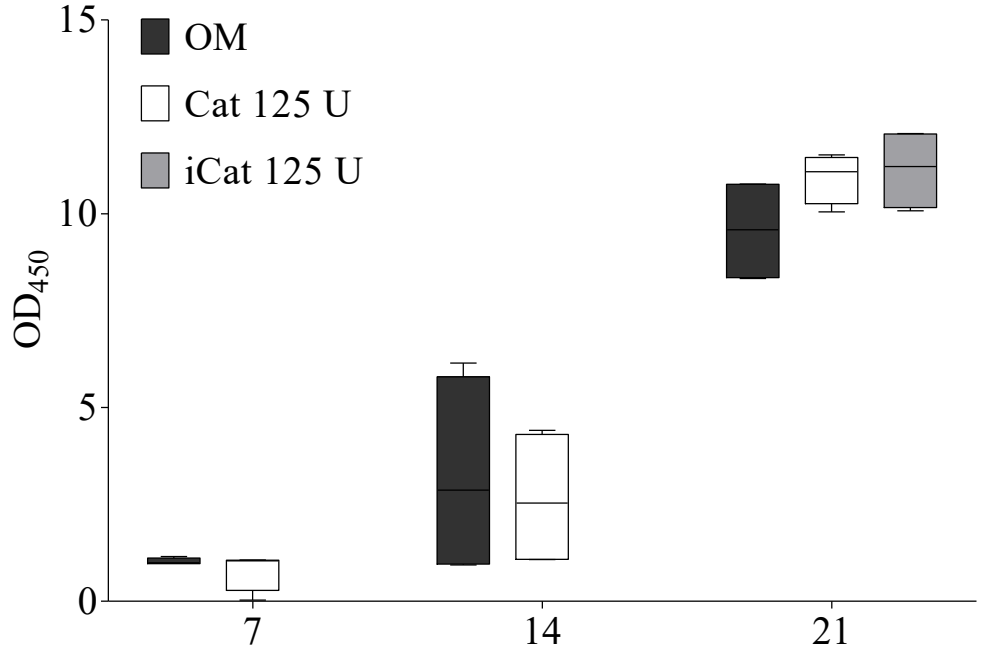

Figure 63: Assessment of the activity of alkaline phosphatase after addition of catalase and heat inactivated catalase. A cell culture of an osteogenically dysfunctional donor was cultured in osteogenic differentiation medium for 21 days. All

cell cultures were treated equally except for the addition of catalase or heat inactivated catalase. At day seven, 14 and 21, the cell culture was incubated with a nitrophenyl phosphate solution. Due to the hydrolysis to nitrophenyl, which was catalyzed by alkaline phosphatase, the solution turned yellow. The optical density of the obtained solution was determined at a wavelength of 450 nm. The optical density is proportional to the activity of alkaline phosphatase. (OM = osteogenic differentiation medium; Cat = catalase; iCat = heat inactivated catalase; n = 1; fourfold determination).

Figure 64 demonstrates the cell culture after staining with alizarin red at day 21. As can be seen, no matrix calcification happened during the osteogenic differentiation process. Even the addition of catalase or heat inactivated catalase did not result in a restoration of the osteogenic differentiation potential. Interestingly, the morphology of the cells did not indicate any stress conditions of the cells. *Figure 62*, *figure 63* and *figure 64* show exceptional results which were observed rarely during the whole project.

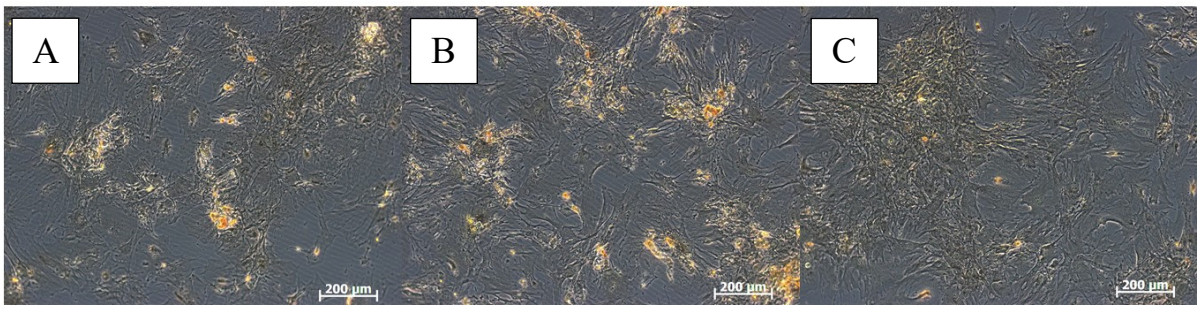

Figure 64: Formation of calcified matrix after a treatment with catalase or heat inactivated catalase. After reaching confluence, low responder hBMSCs were cultured in osteogenic differentiation medium which was not supplemented, supplemented with catalase or with heat inactivated catalase. At day 21, the cell cultures were stained with alizarin red to detect the extent of matrix calcification. A: Cells cultured in osteogenic differentiation medium with no supplements; B: cells treated with 125 U/ml catalase; C: cells treated with 125 U/ml heat inactivated catalase

5.2.1.7 Impact of Inactivated Catalase by Addition of Aminotriazole on Osteogenic Differentiation

As heat inactivated catalase could also restore an impaired osteogenic differentiation potential of low responder cells, the catalase was additionally inactivated irreversibly with aminotriazole which is a specific catalase inhibitor to analyze the mechanism of action more detailed. *Figure 65* shows that the addition of catalase as well as the addition of the combination of catalase and aminotriazole resulted in a restored osteogenic differentiation potential of low responder hBMSCs.

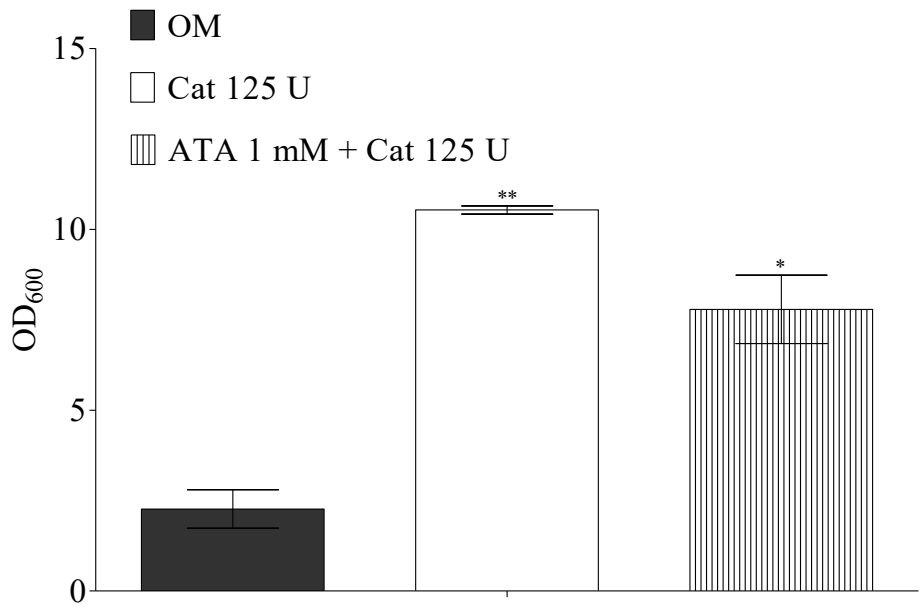

Figure 65: Assessment of calcified matrix of low responder cell cultures after addition of catalase and inactivated catalase with aminotriazole. Cell cultures of osteogenically dysfunctional donors were cultured in osteogenic differentiation medium for 21 days. All cell cultures were treated equally except for the addition of catalase or the combination of catalase and aminotriazole. The cell cultures were stained at day 21 with alizarin red and the dye was dissolved. The optical density of the obtained solution was determined at 600 nm. The optical density is proportional to the amount of calcified matrix (* = significant to OM [$p < 0.05$]; ** = significant to OM [$p < 0.033$]; OM = osteogenic differentiation medium; Cat = catalase; iCat = heat inactivated catalase; n = 5).

Figure 66 shows the red colored calcified matrix after the addition of catalase and inactivated catalase (irreversible inactivation by aminotriazole). The images underline the results of *figure 65*.

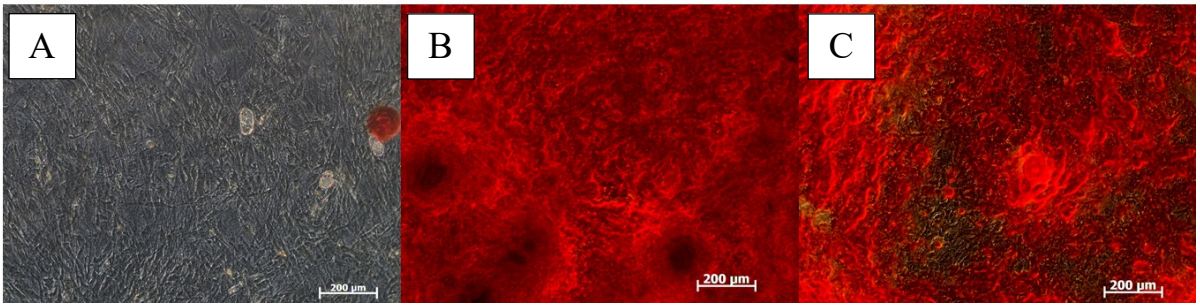

Figure 66: Formation of calcified matrix after a treatment with catalase or the combination of catalase and aminotriazole. After reaching confluence, low responder hBMSCs were cultured in differently supplemented osteogenic differentiation medium. At day 21, the cell cultures were stained with alizarin red to detect the extent of matrix calcification. A: Cells cultured in osteogenic differentiation medium with no supplements; B: cells treated with 125 U/ml catalase; C: cells treated with 125 U/ml catalase and 1 mM aminotriazole

5.2.1.8 Impact of Two Iron Compounds and the Cytokine IL-33 on the Osteogenic Differentiation of hBMSCs

Due to the results of catalase, heat inactivated catalase and aminotriazole inactivated catalase, the single components of catalase were tested individually to assess the impact of the antioxidative effect on the restoration of osteogenic differentiation potential. The active center of catalase contains complexed iron (II) ions. For that reason, iron sulfate and iron chloride were tested. Low responder hBMSCs were treated with catalase, heat inactivated catalase and iron chloride in combination with catalase or heat inactivated catalase. *Figure 67* shows the extent of matrix calcification after a treatment with catalase, inactivated catalase and both in combination with iron chloride. Interestingly, the addition of catalase with iron chloride and heat inactivated catalase with iron chloride also led to an improvement of the impaired osteogenic differentiation potential even though the improvement was not as distinct as the impact of sole applied catalase or inactivated catalase.

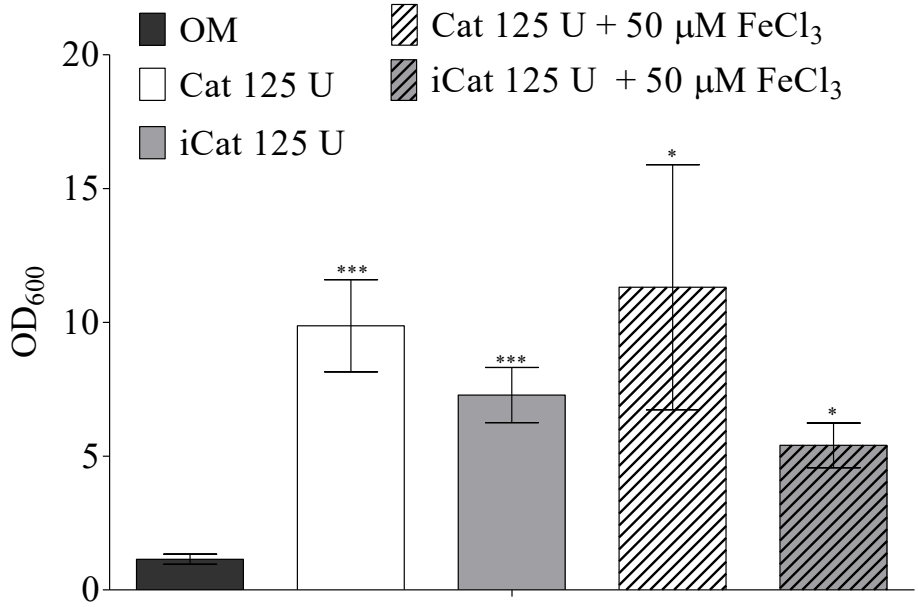

Figure 67: Assessment of calcified matrix of low responder cell cultures after addition of iron chloride in combination of catalase and inactive catalase in comparison to the sole use of catalase and heat inactivated catalase. Cell cultures of osteogenically dysfunctional donors were cultured in osteogenic differentiation medium for 21 days. All cell cultures were treated equally except of the addition of catalase, heat inactivated catalase and catalase with iron chloride or heat inactivated catalase in combination with iron chloride. The cell cultures were stained at day 21 with alizarin red and the dye was dissolved. The optical density of the obtained solution was determined at 600 nm. The optical density is proportional to the amount of calcified matrix (* = significant to OM [$p < 0.05$]; *** = significant to OM [$p < 0.001$]; OM = osteogenic differentiation medium; Cat = catalase; iCat = heat inactivated catalase; n = 3 - 15).

Figure 68 shows the impact of the additives (see above in this section) on the activity of alkaline phosphatase. Even though the activity of alkaline phosphatase was more increased by catalase or heat inactivated catalase, the combination of catalase or heat inactivated catalase with iron chloride also led to a significant elevation of activity of alkaline phosphatase.

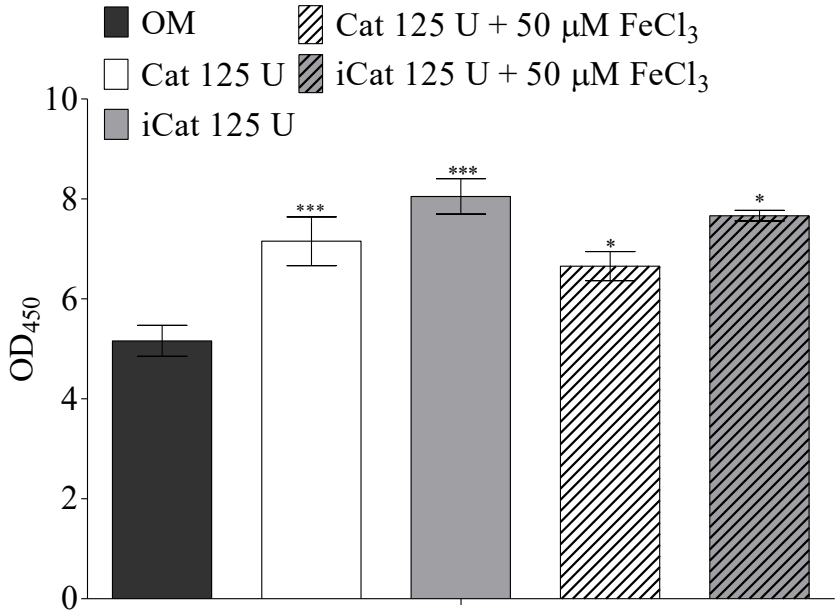

Figure 68: Assessment of the activity of alkaline phosphatase after addition of iron chloride in combination of catalase and inactive catalase in comparison to the addition of catalase and heat inactivated catalase. Cell cultures of osteogenically dysfunctional donors were cultured in osteogenic differentiation medium for 21 days. All cell cultures were treated equally except of the addition of catalase, catalase with iron chloride or heat inactivated catalase in combination iron chloride. At day 21, the cell cultures were incubated with a nitrophenyl phosphate solution. Due to the hydrolysis to nitrophenyl, which was catalyzed by alkaline phosphatase, the solution turned yellow. The optical density of the obtained solution was determined at a wavelength of 450 nm. The optical density is proportional to the activity of alkaline phosphatase (* = significant to OM [$p < 0.05$]; *** = significant to OM [$p < 0.001$]; OM = osteogenic differentiation medium; Cat = catalase; iCat = heat inactivated catalase; n = 3 - 15).

Iron sulfate was also added to the osteogenic medium to assess the influence of iron (II) ions on the osteogenic differentiation of low responder cells. Interestingly, the addition resulted in a significant improvement of the matrix formation and a significant increase of the activity of alkaline phosphatase. The elevated activity of alkaline phosphatase and the enhanced matrix calcification correlated. *Figure 69, figure 70* and *figure 71* present the described results of the treatment with iron sulfate. Furthermore, the cytokine IL-33 was added to show the effects on the osteoblastogenesis. IL-33 is known for an elevated expression in differentiated osteoblasts and the inhibitory effects on osteoclastogenesis [181]. Remarkably, the addition of IL-33 showed no increase of the activity of the alkaline phosphatase and no enhancement of the matrix calcification. Furthermore, the addition of IL-33 indicated a slight decrease of matrix

formation compared to the cultures which were treated with unsupplemented osteogenic differentiation medium (see: *figure 69*).

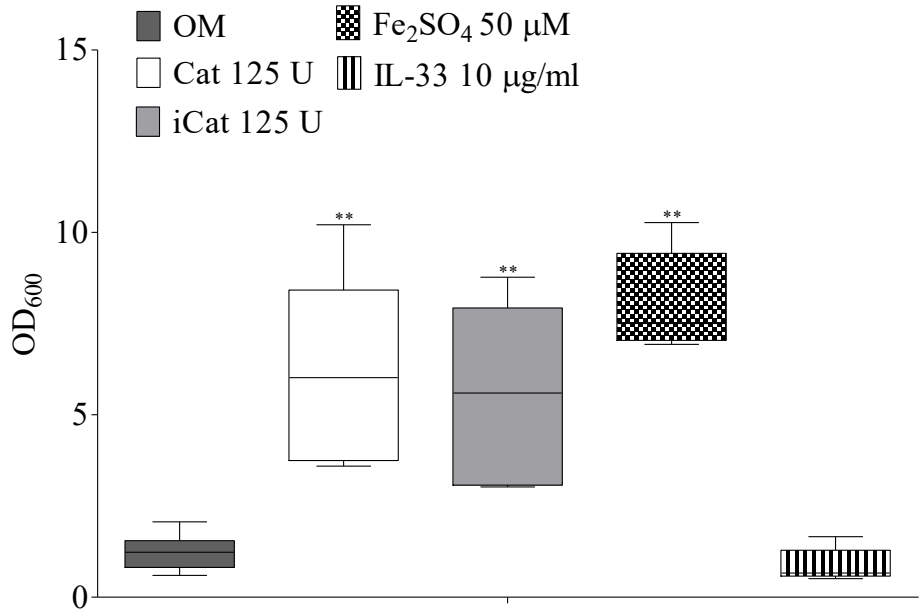

Figure 69: Assessment of calcified matrix of low responder cell cultures after addition of catalase, heat inactivated catalase, iron sulfate and IL-33. Cell cultures of osteogenically dysfunctional donors were cultured in osteogenic differentiation medium for 21 days. All cell cultures were treated equally except of the different additions to the osteogenic differentiation medium. The cell cultures were stained at day 21 with alizarin red and the dye was dissolved. The optical density of the obtained solution was determined at 600 nm. The optical density is proportional to the amount of calcified matrix (** = significant to OM [$p < 0.033$]; OM = osteogenic differentiation medium; Cat = catalase; iCat = heat inactivated catalase; n = 4 – 6).

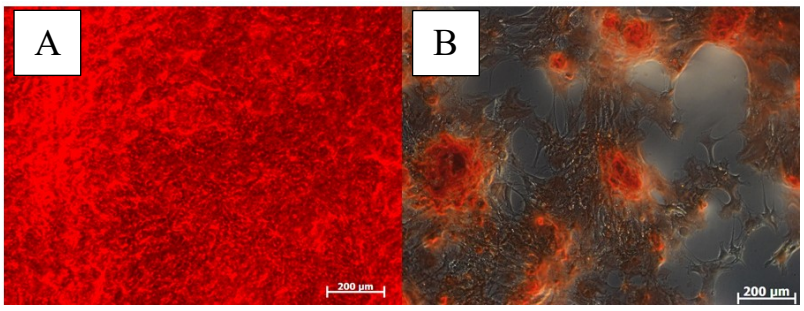

Figure 70: Formation of calcified matrix of low responder hBMSCs after a treatment with iron sulfate and IL-33. After reaching confluence, low responder hBMSCs were cultured in osteogenic differentiation medium which was supplemented differently. At day 21, the cell cultures were stained with alizarin red to detect the extent of matrix calcification. A: cells treated with 50 µM Fe_2SO_4; B: cells treated with 10 µg/ml IL-33

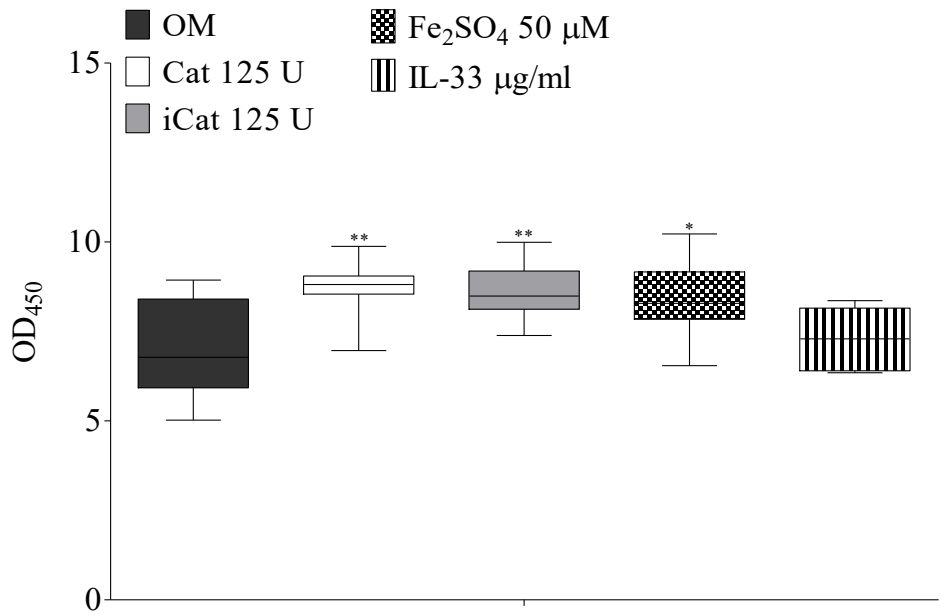

Figure 71: Assessment of the activity of alkaline phosphatase after addition of catalase, heat inactivated catalase, iron sulfate and IL-33. Cell cultures of osteogenically dysfunctional donors were cultured in osteogenic differentiation medium for 21 days. All cell cultures were treated equally except of the different additives to the osteogenic differentiation medium. At day 21, the cell cultures were incubated with a nitrophenyl phosphate solution. Due to the hydrolysis to nitrophenyl, which was catalyzed by alkaline phosphatase, the solution turned yellow. The optical density of the obtained solution was determined at a wavelength of 450 nm. The optical density is proportional to the activity of alkaline phosphatase (* = significant to OM [$p < 0.05$]; ** = significant to OM [$p < 0.033$]; OM = osteogenic differentiation medium; Cat = catalase; iCat = heat inactivated catalase; n = 3 - 15).

Due to the indication of the decrease after an IL-33 addition, effects of iron sulfate and IL-33 on responder hBMSCs were also evaluated. As shown in *figure 72*, the addition of iron sulfate and of IL-33 both led to a distinct impairment of the osteogenic differentiation potential. The decrease of matrix calcification by IL-33 was even more significant.

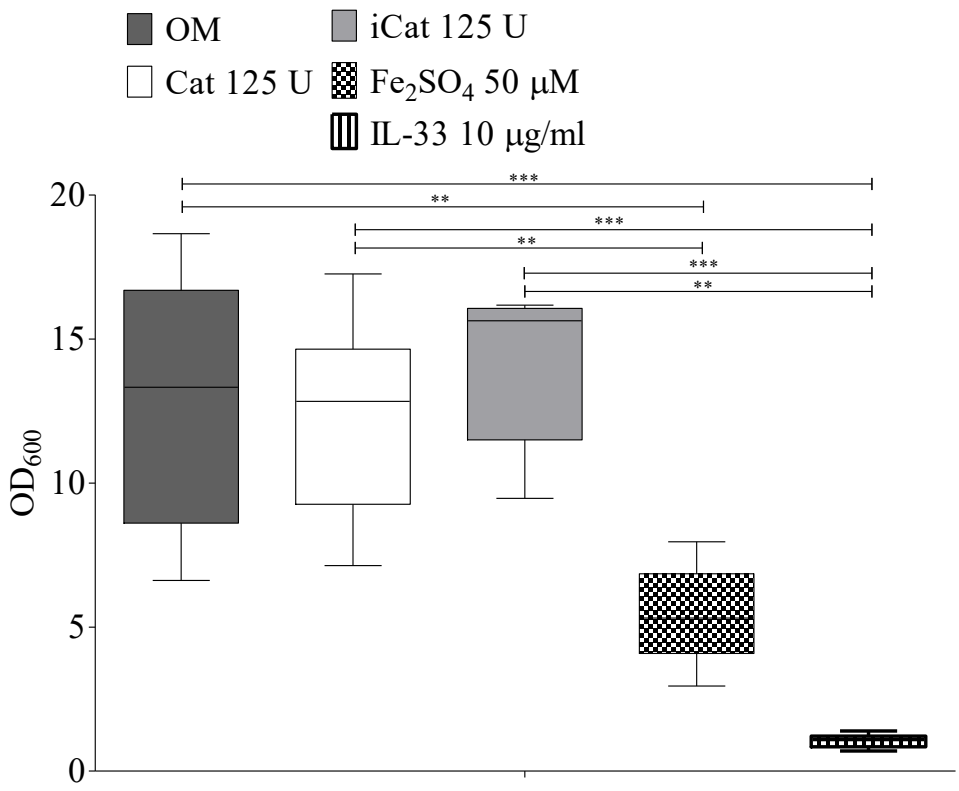

Figure 72: Assessment of calcified matrix of responder cell cultures after addition of catalase, heat inactivated catalase, iron sulfate and IL-33. Cell cultures of osteogenically regular donors were cultured in osteogenic differentiation medium for 21 days. All cell cultures were treated equally except of the different additives to the osteogenic differentiation medium. The cell cultures were stained at day 21 with alizarin red and the dye was dissolved. The optical density of the obtained solution was determined at 600 nm. The optical density is proportional to the amount of calcified matrix (** = significant [$p < 0.033$]; *** = significant [$p < 0.001$]; OM = osteogenic differentiation medium; Cat = catalase; iCat = heat inactivated catalase; n = 5 – 6).

Figure 73 demonstrates the activity of alkaline phosphatase after the treatment with catalase, inactivated catalase, iron sulfate and IL-33 in comparison to untreated samples. The addition of IL-33 led to a slight decrease of the activity but interestingly, the addition of iron sulfate did not result in an impaired activity although the matrix calcification was inhibited by the addition. The usual correlation between the activity of alkaline phosphatase and matrix formation was not fulfilled in this case. To conclude, iron sulfate could restore the osteogenic differentiation potential of low responders but also led to a distinct decrease of the osteogenic differentiation potential of responder hBMSCs whereas the addition of IL-33 led to an inhibition of matrix calcification of both types of donors. The inhibition of the osteogenic differentiation by IL-33 of responder hBMSCs is also highlighted in *figure 74*. This figure illustrates that the cells did not show any indications of stress conditions. The initial change of the cell morphology during the osteogenic differentiation is also visible.

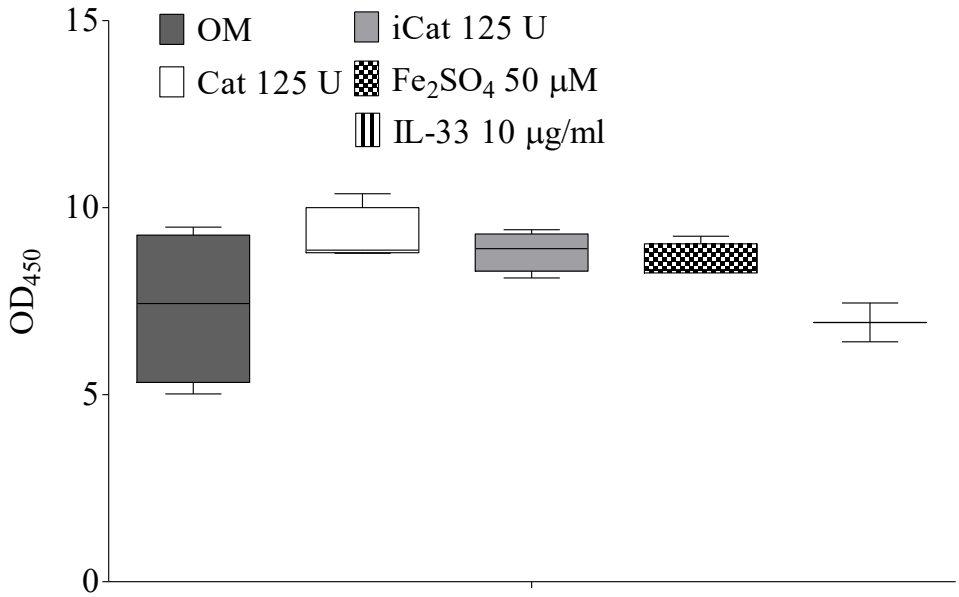

Figure 73: Assessment of the activity of alkaline phosphatase after addition of catalase, heat inactivated catalase, iron sulfate and IL-33. Cell cultures of osteogenically regular donors were cultured in osteogenic differentiation medium for 21 days. All cell cultures were treated equally except of the different additions to the osteogenic differentiation medium. At day 21, the cell cultures were incubated with a nitrophenyl phosphate solution. Due to the hydrolysis to nitrophenyl, which was catalyzed by alkaline phosphatase, the solution turned yellow. The optical density of the obtained solution was determined at a wavelength of 450 nm. The optical density is proportional to the activity of alkaline phosphatase (OM = osteogenic differentiation medium; Cat = catalase; iCat = heat inactivated catalase; n = 2 – 4).

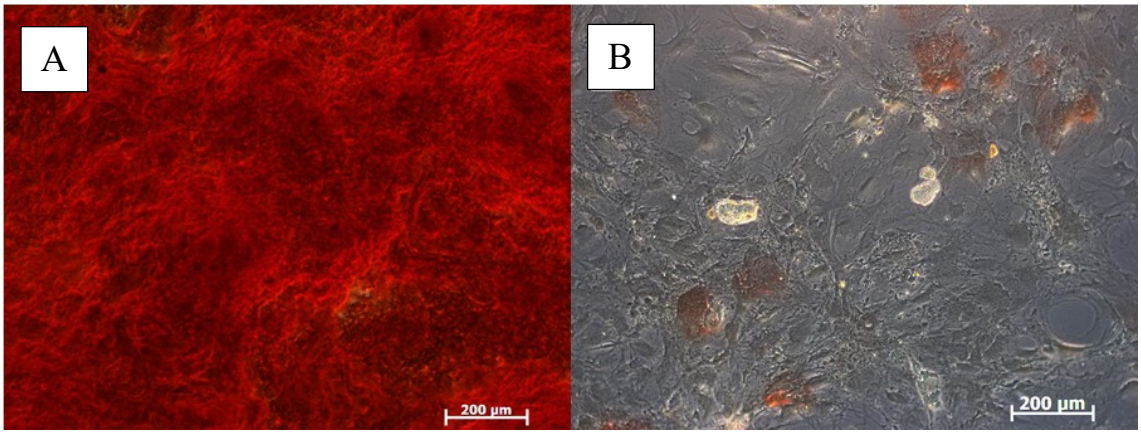

Figure 74: Formation of calcified matrix of responder hBMSCs after a treatment with IL-33. After reaching confluence, responder hBMSCs were cultured in osteogenic differentiation medium which was supplemented differently. At day 21, the cell cultures were stained with alizarin red to detect the extent of matrix calcification. A: cells treated unsupplemented osteogenic differentiation medium; B: cells treated with 10 µg/ml IL-33

5.2.1.8.1 Testing of Diverse Concentrations of Iron Chloride and Iron Sulfate on the Matrix Calcification of Low Responder Cells

Iron chloride and iron sulfate were added to the osteogenic differentiation medium in diverse concentrations. Concentrations of 50 µM, 20 µM, 10 µM and 5 µM were used to determine an optimal concentration and the best substance to optimize the osteogenic differentiation potential of four osteogenically dysfunctional hBMSCs. Interestingly, all four donors showed different reactions to the various additions. *Figure 75* and *figure 76* show the extent of matrix calcification after the different treatments. Remarkably, the activity of alkaline phosphatase, which is shown in *figure 77*, demonstrated that also in this case the activity of alkaline phosphatase did not correlate with the extent of matrix calcification. The evaluated activity of donor 1 is shown in *figure 77* and the dimension of matrix formation of this donor is shown in image A of *figure 75*.

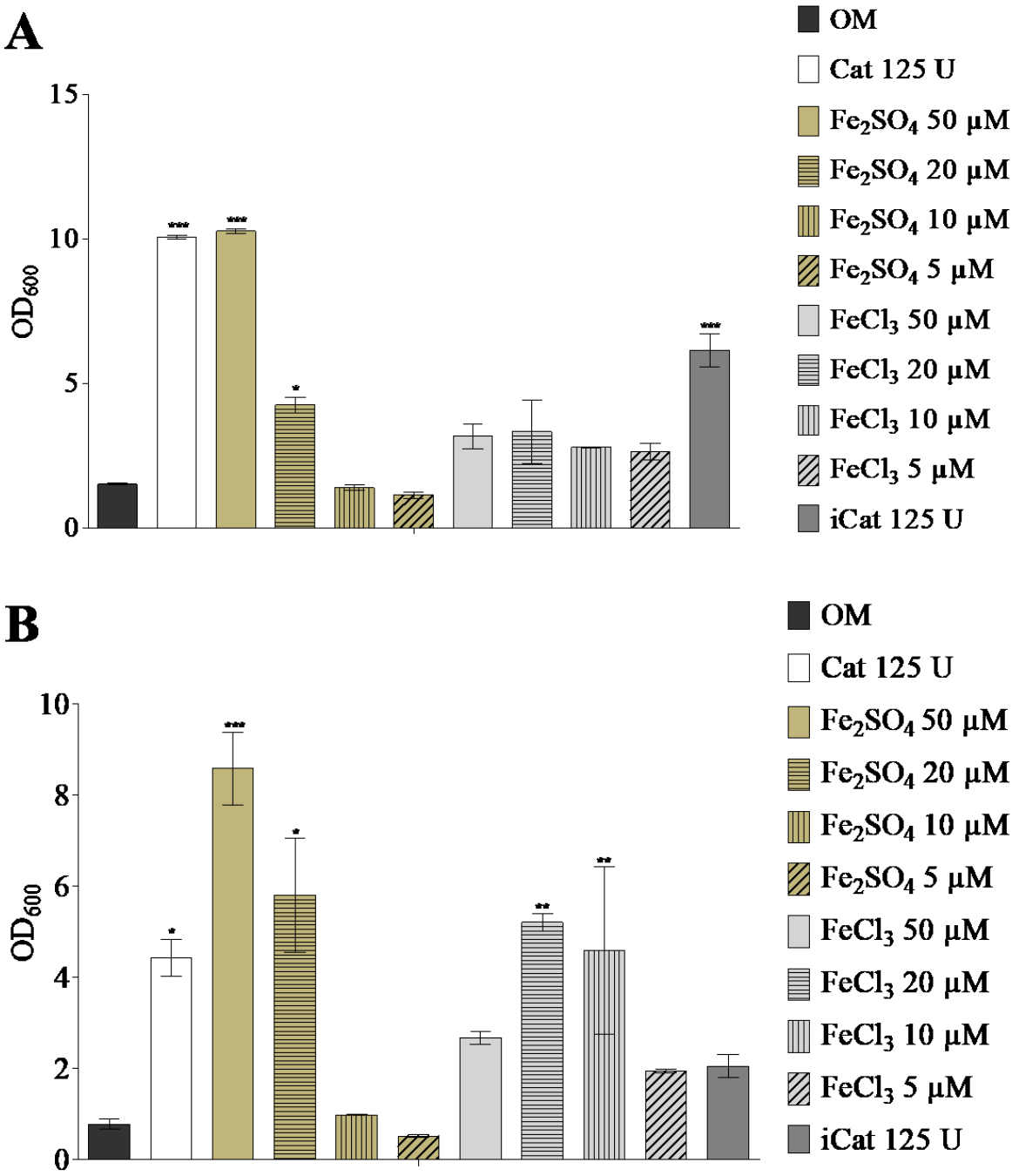

Figure 75: Assessment of calcified matrix of responder cell cultures after addition of catalase, heat inactivated catalase and diverse concentrations of iron chloride and sulfate. Cell cultures of osteogenically dysfunctional donors were cultured in osteogenic differentiation medium for 21 days. All cell cultures were treated equally except of the different additives to the osteogenic differentiation medium. The cell cultures were stained at day 21 with alizarin red and the dye was dissolved. The optical density of the obtained solution was determined at 600 nm. The optical density is proportional to the amount of calcified matrix (* = significant to OM [$p < 0.05$]; * = significant to OM [$p < 0.033$]; *** = significant to OM [$p < 0.001$]; OM = osteogenic differentiation medium; Cat = catalase; iCat = heat inactivated catalase; n = each graph shows one donor with fourfold determination). A: Donor 1; B: Donor 2

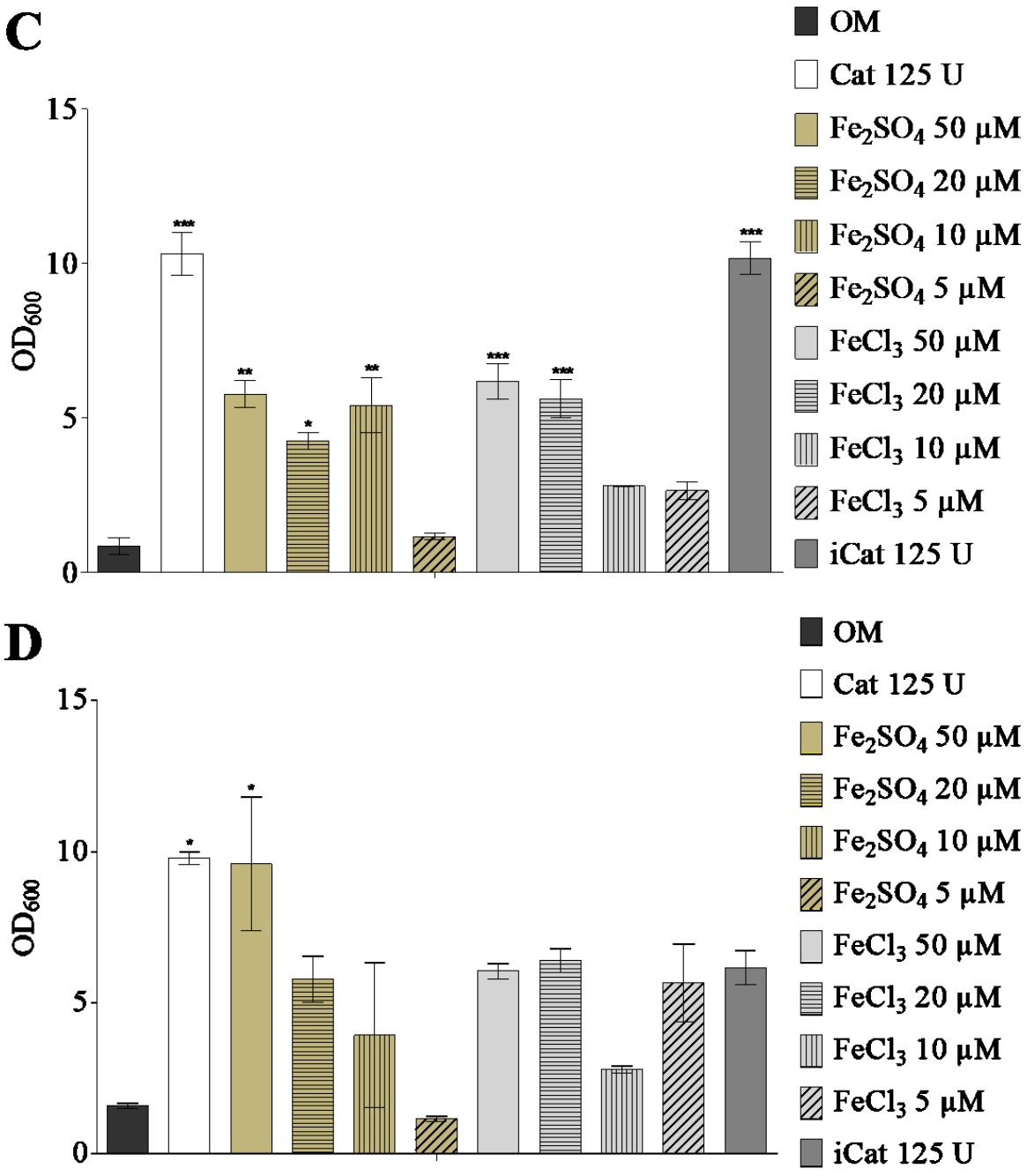

Figure 76: Assessment of calcified matrix of responder cell cultures after addition of catalase, heat inactivated catalase and diverse concentrations of iron chloride and sulfate. Cell cultures of low responder donors were cultured in osteogenic differentiation medium for 21 days. All cell cultures were treated equally except of the different additives to the osteogenic differentiation medium. The cell cultures were stained at day 21 with alizarin red and the dye was dissolved. The optical density of the obtained solution was determined at 600 nm. The optical density is proportional to the amount of calcified matrix (* = significant to OM [$p < 0.05$]; * = significant to OM [$p < 0.033$]; *** = significant to OM [$p < 0.001$]; OM = osteogenic differentiation medium; Cat = catalase; iCat = heat inactivated catalase; n = each graph shows one donor with fourfold determination). C: Donor 3; D: Donor 4

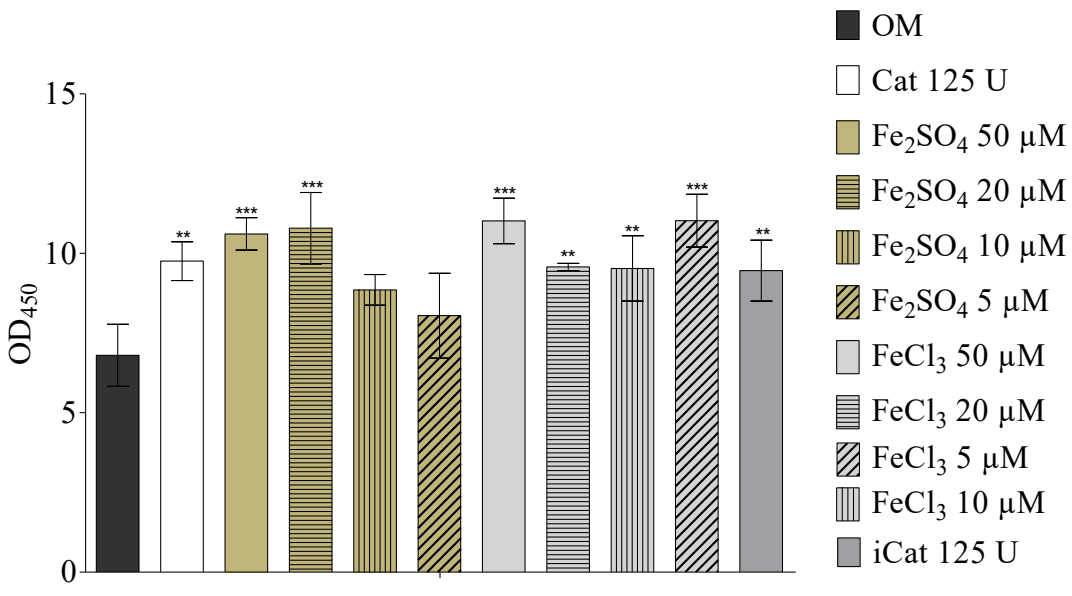

Figure 77: Assessment of the activity of alkaline after addition of catalase, heat inactivated catalase and diverse concentrations of iron chloride and sulfate. Cell cultures of low responder donors were cultured in osteogenic differentiation medium for 21 days. All cell cultures were treated equally except of the different additives to the osteogenic differentiation medium. At day 21, the cell cultures were incubated with a nitrophenyl phosphate solution. Due to the hydrolysis to nitrophenyl which was catalyzed by alkaline phosphatase, the solution turned yellow. The optical density of the obtained solution was determined at a wavelength of 450 nm. The optical density is proportional to the activity of alkaline phosphatase (** = significant to OM [$p < 0.033$]; *** = significant to OM [$p < 0.001$]; OM = osteogenic differentiation medium; Cat = catalase; iCat = heat inactivated catalase; n = 1; fourfold determination of donor 1).

5.2.1.9 Impact of Catalase and Heat Inactivated Catalase Solutions after Centrifugation through 10 kDa Centrifugal Filters on the Osteogenic Differentiation Potential of Low Responder hBMSCs

Due to the results of catalase, heat inactivated catalase, inactivated catalase by aminotriazole and the iron salts regarding the restoration potential of the impaired osteogenic differentiation of osteogenically dysfunctional hBMSCs, catalase and heat inactivated catalase solutions were centrifuged through a 10 kDa centrifugal filter to separate the protein amount of the working solution. The working solutions were protein-free and contained only the potentially existing ions. *Figure 78* presents the influence of the working solutions on the formation of calcified matrix. Obviously, the working solution, which only consisted of diluted ions and no remaining proteins, also led to a restoration of impaired osteogenic differentiation potentials. Nevertheless, the graph also points out that the improvement of the calcified matrix formation is not as distinct as of unmodified catalase or heat inactivated catalase additions.

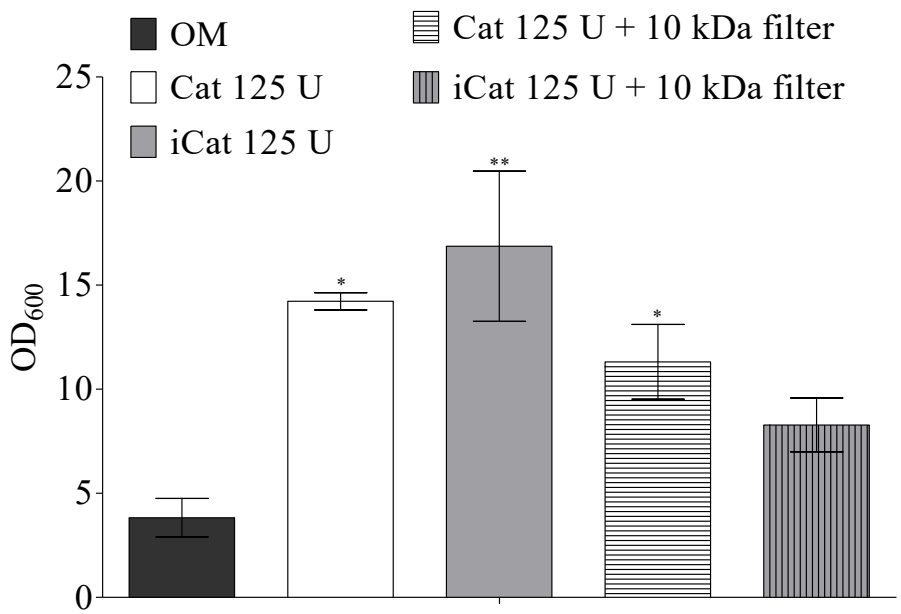

Figure 78: Assessment of calcified matrix of responder cell cultures after addition of catalase, heat inactivated catalase, catalase centrifuged through a 10 kDa centrifugal filter and heat inactivated catalase centrifuged through a 10 kDa centrifugal filter. Cell cultures of osteogenically dysfunctional donors were cultured in osteogenic differentiation medium for 21 days. All cell cultures were treated equally except of the different additions to the osteogenic differentiation medium. The cell cultures were stained at day 21 with alizarin red and the dye was dissolved. The optical density of the obtained solution was determined at 600 nm. The optical density is proportional to the amount of calcified matrix (* = significant to OM [$p < 0.05$]; ** = significant to OM [$p < 0.033$]; OM = osteogenic differentiation medium; Cat = catalase; iCat = heat inactivated catalase; n = 3).

Figure 79 shows the evaluation of the activity of alkaline phosphatase after the treatment of low responder cells with catalase-free ion solutions. The activity was heightened by the addition of catalase, heat inactivated catalase and as well as by the addition of the two protein-free ion solutions. Although the elevation by the ion solution was not significant in every case, a distinct trend is exhibited.

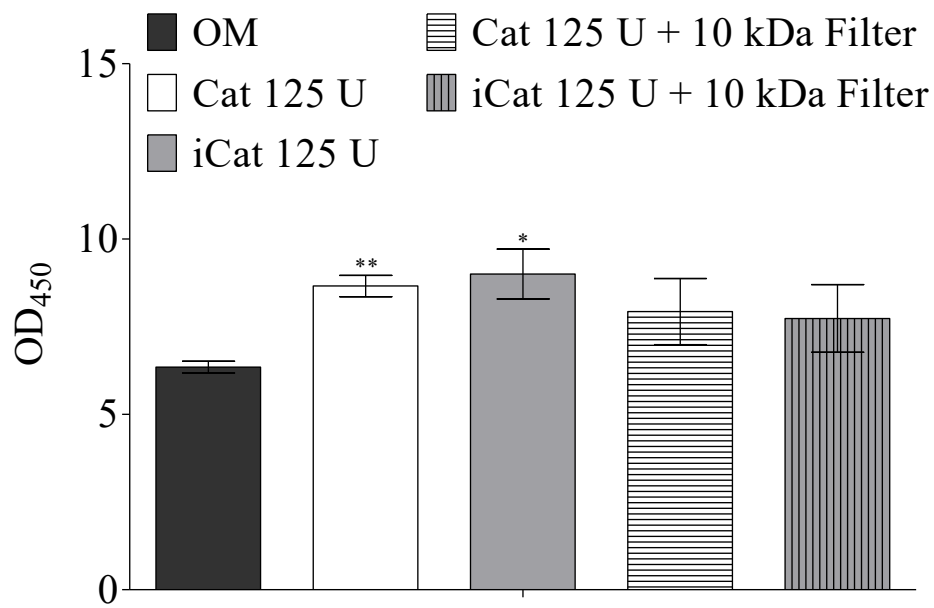

Figure 79: Assessment of the activity of alkaline phosphatase after addition of catalase, heat inactivated catalase, catalase centrifuged through a 10 kDa centrifugal filter and heat inactivated catalase centrifuged through a 10 kDa centrifugal filter. Cell cultures of osteogenically dysfunctional donors were cultured in osteogenic differentiation medium for 21 days. All cell cultures were treated equally except of the different additions to the osteogenic differentiation medium. At day 21, the cell cultures were incubated with a nitrophenyl phosphate solution. Due to the hydrolysis to nitrophenyl which was catalyzed by alkaline phosphatase, the solution turned yellow. The optical density of the obtained solution was determined at a wavelength of 450 nm. The optical density is proportional to the activity of alkaline phosphatase (* = significant to OM [$p < 0.05$]; ** = significant to OM [$p < 0.033$]; OM = osteogenic differentiation medium; Cat = catalase; iCat = heat inactivated catalase; n = 3).

5.2.1.10 Treatment of Low Responder Cells with 125 U/ml Catalase for Different Time Durations

Since catalase led through a yet unknown mechanism to a restoration of the osteogenic differentiation potential of osteogenically dysfunctional hBMSCs, cell cultures of low responders were treated for different time periods with a catalase supplemented osteogenic differentiation medium. The cell cultures were treated for five, seven and 14 days with the catalase supplemented osteogenic differentiation medium and were cultured after the mentioned periods in unsupplemented osteogenic differentiation medium until day 21. At day 21, the extent of matrix calcification was assessed. The results were compared to the results of cell cultures which were cultured for 21 days in unsupplemented osteogenic differentiation medium. As presented in *figure 80*, the treatment with catalase for five, seven or 14 days did not result in a significant restoration of an impaired osteogenic differentiation potential.

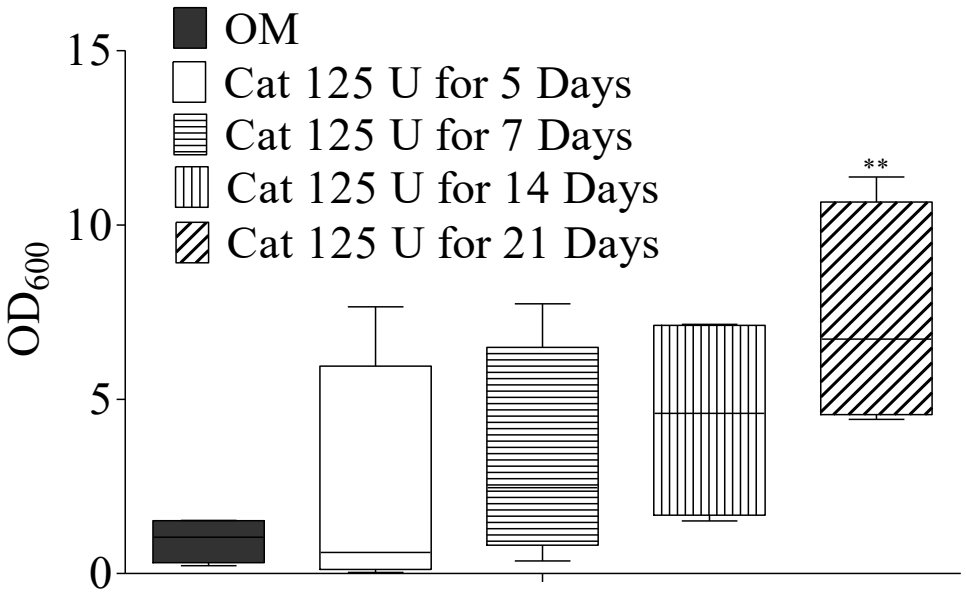

Figure 80: Assessment of calcified matrix of low responder cell cultures after addition of catalase for different time durations. Cell cultures of osteogenically dysfunctional donors were cultured in osteogenic differentiation medium for 21 days. All cell cultures were treated equally except of the catalase treatment for different time durations. The cell cultures were stained at day 21 with alizarin red and the dye was dissolved. The optical density of the obtained solution was determined at a wavelength of 600 nm. The optical density is proportional to the amount of calcified matrix (** = significant to OM [$p < 0.033$]; OM = osteogenic differentiation medium; Cat = catalase; iCat = heat inactivated catalase; n = 4).

5.2.1.11 Influences of the Diverse Treatments during the Osteogenic Differentiation on Expressions of ROS affecting Proteins

Since catalase is known for its antioxidative effects, which is explained more detailed in paragraph *1.4.2.1*, the protein expressions of prooxidative and antioxidative proteins such as of NOX4, catalase, Nrf2, FOXO1, GPX, SOD1 and SOD2 were analyzed by Western blot evaluation.

5.2.1.11.1 Influences on the Expression of NOX4

NOX4 is the most important producer of reactive oxygen species within the respiratory chain of living beings [91]. *Figure 81* shows the effect of different treatments on the protein expression of NOX4. Except for the addition of the combination of iron chloride and catalase, no significant or slight difference could be observed between the various approaches at day seven. The treatment with iron chloride combined with catalase led to a clear decrease of the NOX4 expression. On the contrary, the cultivation in catalase supplemented, heat inactivated catalase supplemented or with a combination of iron chloride and catalase supplemented osteogenic differentiation medium resulted in a distinct decrease of the expression of NOX4

at day 21. It is important to note that only one donor was treated with heat inactivated catalase or a combination of iron chloride and catalase supplemented osteogenic differentiation. For that reason, the results might not be representative. Even though the osteogenic differentiation potential of responder donors was not affected by the addition of catalase, the expression of NOX4 was influenced.

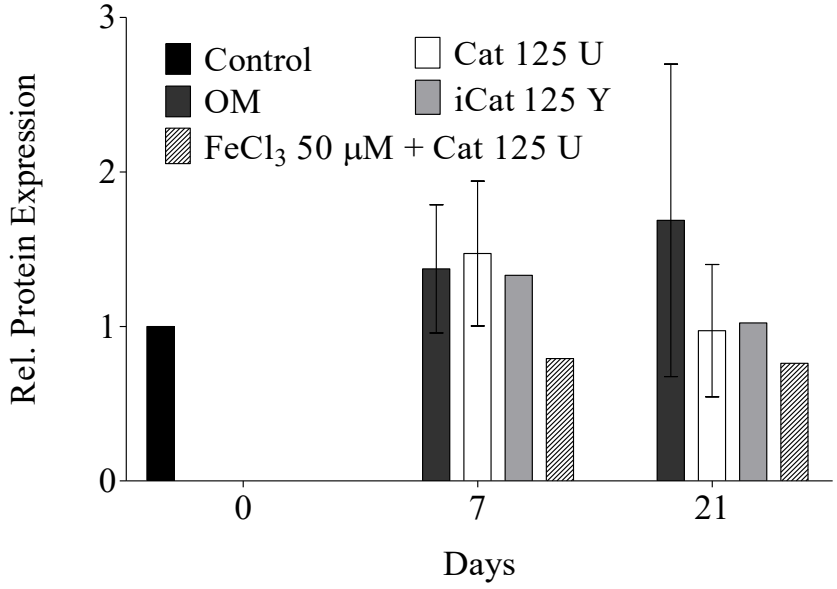

Figure 81: Protein expression of NOX4. Cell cultures of responder were treated with unsupplemented, catalase supplemented, heat inactivated catalase supplemented or with a combination of iron chloride and catalase supplemented osteogenic differentiation medium for a total of 21 days. At day zero, seven and 21, proteins were extracted and the protein expressions were analyzed (OM = osteogenic differentiation medium; Cat = catalase; iCat = heat inactivated catalase; n = 1 - 3).

Figure 82 highlights the results of low responder hBMSCs. The outcomes of responder and low responder cells showed no distinct difference. The addition of catalase supplemented or with a combination of iron chloride and catalase supplemented osteogenic differentiation medium led to a significant decrease of the NOX4 expression compared to the cells which were cultured in unsupplemented osteogenic differentiation medium. To conclude, a trend after the special treatments is visible but which is not significant in all cases and additionally does not differ between responder and low responder cell cultures.

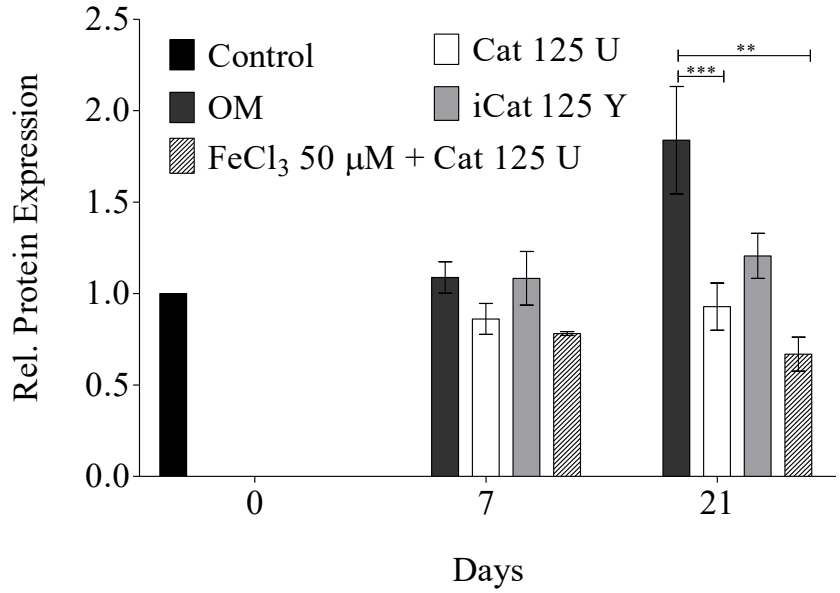

Figure 82: Protein expression of NOX4. Cell cultures of low responder were treated with unsupplemented, catalase supplemented, heat inactivated catalase supplemented or with a combination of iron chloride and catalase supplemented osteogenic differentiation medium for total of 21 days. At day zero, seven and 21, proteins were extracted and the protein expressions were analyzed (** = significant [$p < 0.033$]; (*** = significant [$p < 0.001$]; OM = osteogenic differentiation medium; Cat = catalase; iCat = heat inactivated catalase; n = 2 - 7).

Figure 83 demonstrates the expression pattern of NOX4 on a gel. The results of *figure 84* match with this pattern.

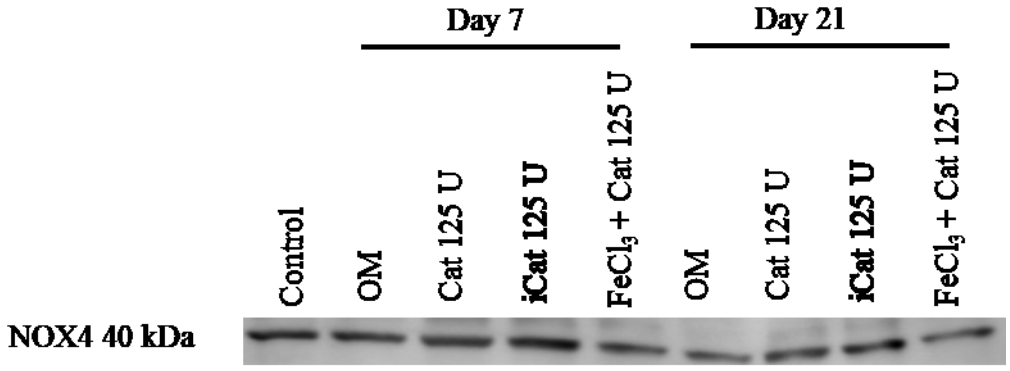

Figure 83: Detail of the NOX4 expression of a gel of one of the donors (OM = osteogenic differentiation medium; Cat = catalase; iCat = heat inactivated catalase).

5.2.1.11.2 Influences on the Expression of catalase

The results of day seven and 21 differed. Whereas the different treatments rose the expression of catalase at day seven, the addition of all substances led to a distinct decrease of the expression at day 21. Only one responder donor was treated with heat inactivated catalase and

with the combination of iron chloride and catalase. For that reason, these results might not be representative.

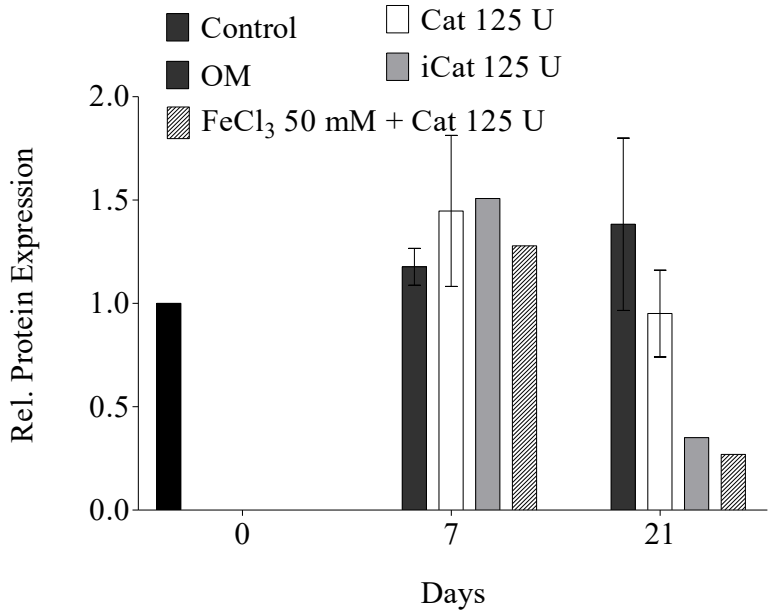

Figure 84: Protein expression of catalase. Cell cultures of responder were treated with unsupplemented, catalase supplemented, heat inactivated catalase supplemented or with a combination of iron chloride and catalase supplemented osteogenic differentiation medium for a total of 21 days. At day zero, seven and 21, proteins were extracted and the protein expressions were analyzed (OM = osteogenic differentiation medium; Cat = catalase; iCat = heat inactivated catalase; n = 1 - 3).

The low responder cell cultures showed similar outcomes caused by the diverse treatments. At day seven, elevated expressions could be observed caused by the treatment with catalase, heat inactivated catalase and the combination of iron chloride and catalase. At day 21, the mentioned treatments led to a diminished expression of catalase.

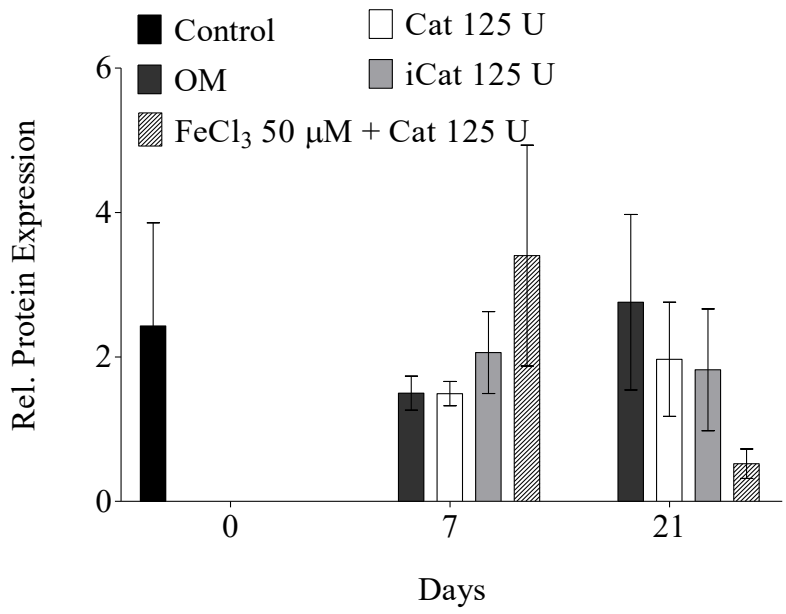

Figure 85: Protein expression of catalase. Cell cultures of low responder were treated with unsupplemented, catalase supplemented, heat inactivated catalase supplemented or with a combination of iron chloride and catalase supplemented osteogenic differentiation medium for a total of 21 days. At day zero, seven and 21, proteins were extracted and the protein expressions were analyzed (OM = osteogenic differentiation medium; Cat = catalase; iCat = heat inactivated catalase; n = 2 - 7).

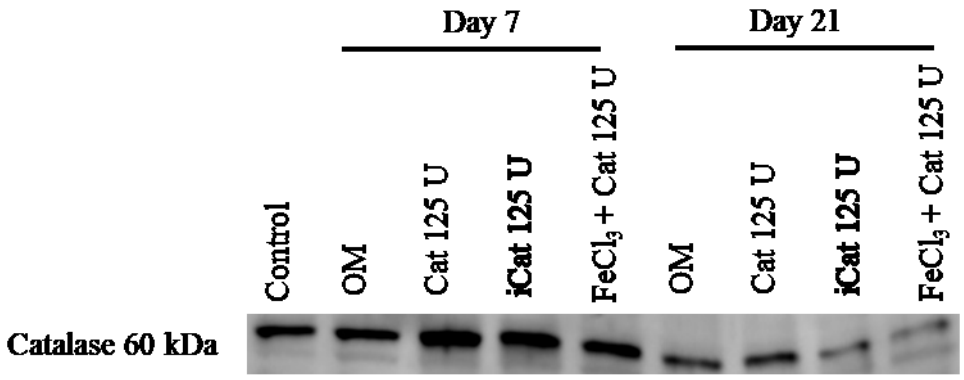

Figure 86: Detail of the catalase expression of a gel of one of the donors (OM = osteogenic differentiation medium; Cat = catalase; iCat = heat inactivated catalase).

Figure 86 demonstrates the changing expression pattern depending on the additives of catalase on a gel. The results of *Figure 84*, *Figure 85* and *Figure 86* match.

5.2.1.11.3 Influences on the Expression of MnSOD (SOD2) and Cu/Zn SOD (SOD1)

The addition of catalase led to a significant improvement of the SOD2 expression at day seven as well as at day 21 of responder cells. The additions of heat inactivated catalase and the combination of catalase and iron chloride also resulted in an elevated expression

compared to the expression pattern of cells which were cultured in unsupplemented osteogenic differentiation medium. At day 21, only the addition of catalase resulted in a heightened expression of SOD2. Since only one donor was treated with heat inactivated catalase and with the combination of catalase and iron chloride, the results might not be representative. Further investigations of more donors are required to make a representative statement. The described outcomes are shown in *figure 87*.

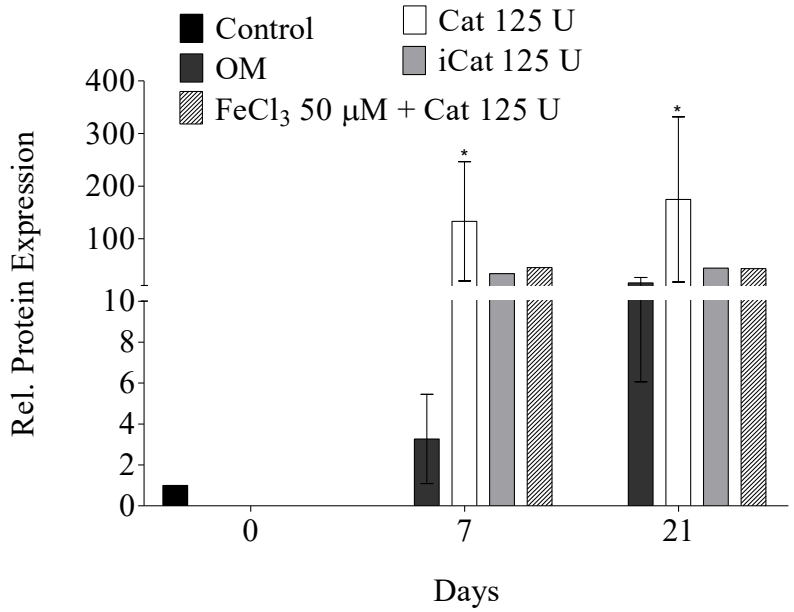

Figure 87: Protein expression of MnSOD. Cell cultures of responder were treated with unsupplemented, catalase supplemented, heat inactivated catalase supplemented or with a combination of iron chloride and catalase supplemented osteogenic differentiation medium for total of 21 days. At day zero, seven and 21, proteins were extracted and the protein expressions were analyzed (* = significant to OM [$p < 0.05$]; OM = osteogenic differentiation medium; Cat = catalase; iCat = heat inactivated catalase; n = 1 - 3).

As shown in *figure 88*, the expression patterns of responder and low responder cells, which were cultured in unsupplemented, catalase or rather heat inactivated catalase supplemented osteogenic differentiation medium, are nearly similar. In case of the low responder cultures which were treated with a combination of catalase and iron chloride, the expression of SOD2 was clearly decreased compared to the expression pattern of equally treated responder hBMSCs. It is important to note that only one low responder donor was investigated after a treatment with a combination of catalase and iron chloride. The deviating results might not be representative.

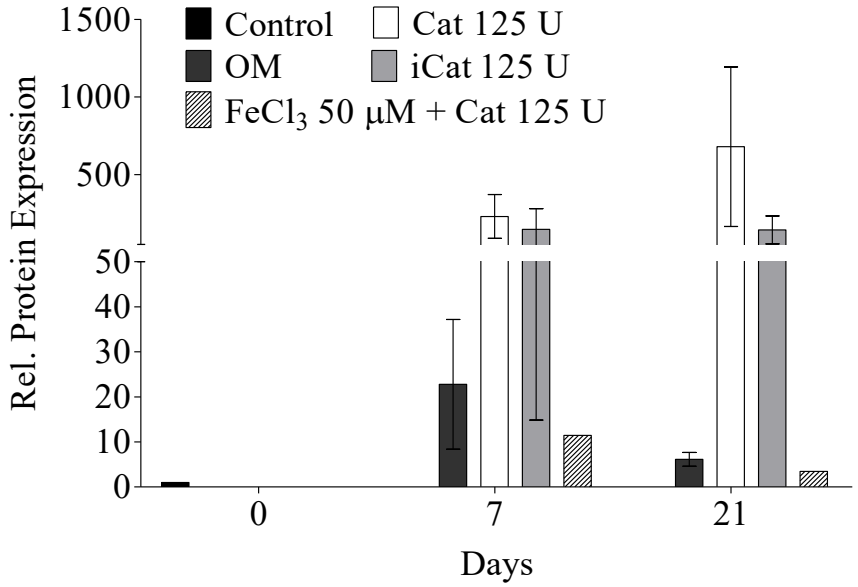

Figure 88: Protein expression of MnSOD. Cell cultures of low responder were treated with unsupplemented, catalase supplemented, heat inactivated catalase supplemented or with a combination of iron chloride and catalase supplemented osteogenic differentiation medium for a total of 21 days. At day zero, seven and 21, proteins were extracted and the protein expressions were analyzed (OM = osteogenic differentiation medium; Cat = catalase; iCat = heat inactivated catalase; n = 2 - 7).

The results presented in *figure 89* and *figure 90* match with the results of the expression pattern of the gel which is shown in *figure 83.* Caused by the fluctuating values, the standard deviations were high which resulted in no significance of the different treatments even though the additives led to distinct increases of the expression of SOD2.

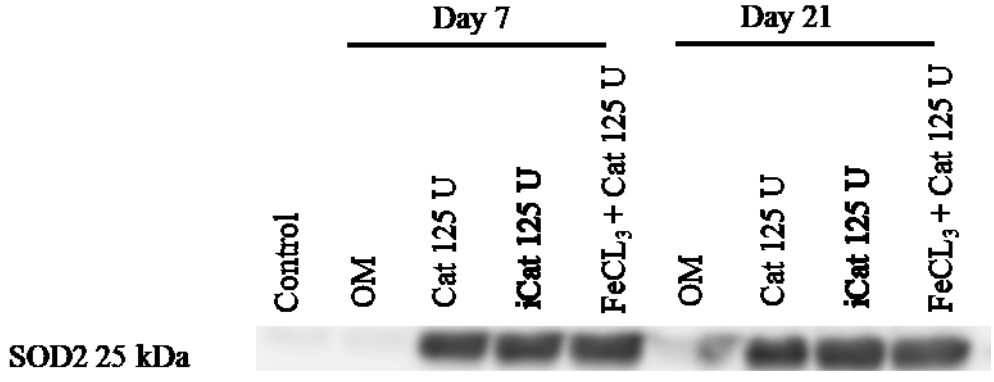

Figure 89: Detail of the SOD2 expression of a gel of one of the responder donors (OM = osteogenic differentiation medium; Cat = catalase; iCat = heat inactivated catalase).

Furthermore, the expression of SOD1 (Cu/Zn SOD) was analyzed and compared to the expression of SOD2. Since the expression of SOD2 was easier to detect, the SOD2 was

mainly investigated. The expression of Cu/Zn SOD was also analyzed for a few donors to prove an equivalent behavior of both SODs towards the diverse treatments. In this case, the investigation of the SOD1 expression of only low responder donors was sufficient. *Figure 90* shows that the differences according to the expressions depending on the different treatments are not as clear as of the expressions of SOD2. Nonetheless, a trend at day 21 is visible. Interestingly, the treatment with heat inactivated catalase resulted in a decrease of the SOD1 expression which differed from the results of the expression of SOD2.

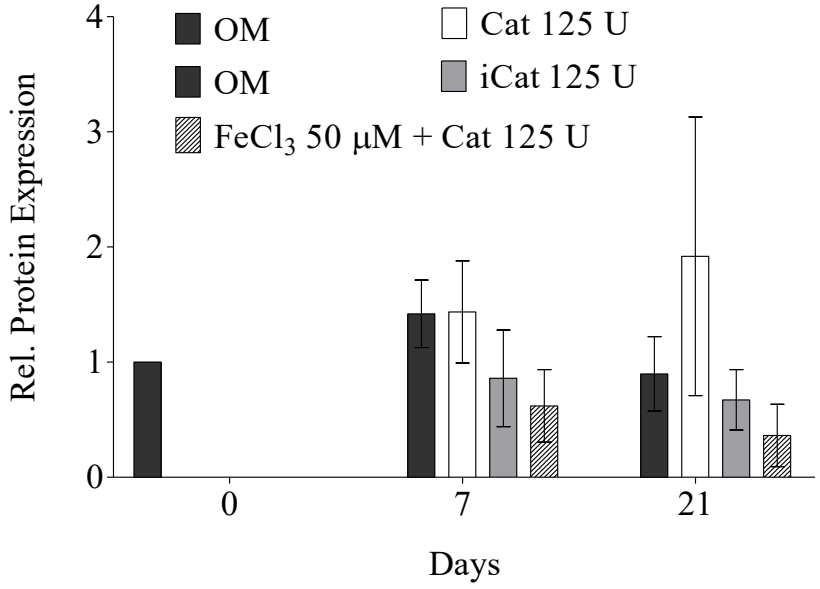

Figure 90: Protein expression of Cu/Zn SOD. Cell cultures of low responder were treated with unsupplemented, catalase supplemented, heat inactivated catalase supplemented or with a combination of iron chloride and catalase supplemented osteogenic differentiation medium for a total of 21 days. At day zero, seven and 21, proteins were extracted and the protein expressions were analyzed (OM = osteogenic differentiation medium; Cat = catalase; iCat = heat inactivated catalase; n = 1 - 4).

Due to the weak expression pattern, which is highlighted in *figure 91*, the evaluation of the expression of SOD1 was difficult to perform which in turn might have resulted in misleading outcomes. *Figure 91* demonstrates a similar trend of the expression patterns compared to *figure 83*. For that reason, the expression pattern of the gel did not completely match the expression pattern which is shown in *figure 90*.

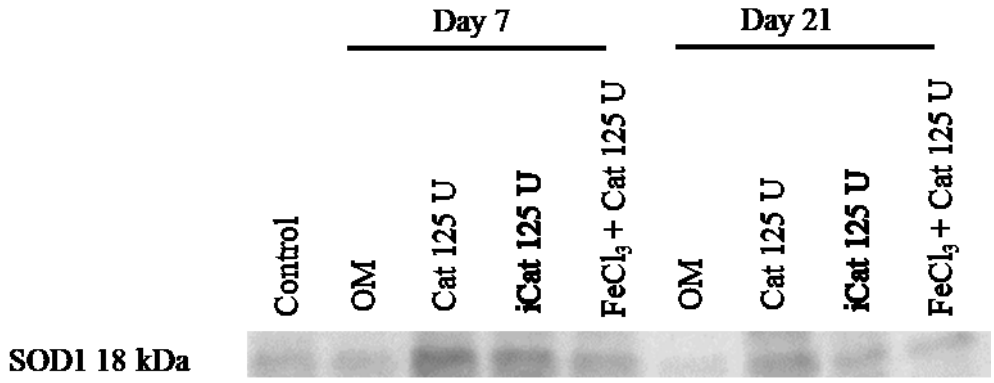

Figure 91: Detail of the SOD1 expression of a gel of one of the responder donors (OM = osteogenic differentiation medium; Cat = catalase; iCat = heat inactivated catalase).

5.2.1.11.4 Influences on the Expression of Nrf2 and FOXO1 of Low Responder Cells

Nrf2 and FOXO1 are both relevant transcription factors to regulate the osteogenic differentiation which are affected by oxidative stress [182]. Therefore, effects on the expression of the different additives were analyzed. As shown in *figure 92*, the addition of catalase, heat inactivated catalase and the combination of iron chloride and catalase resulted in a decreased Nrf2 expression, especially at day 21. The determination of the Nrf2 expression was difficult which is demonstrated in the expression pattern of the gel in *figure 94*. For that reason, the Nrf2 expression could not be evaluated for every donor. Hitherto, the expression of low responder was analyzed.

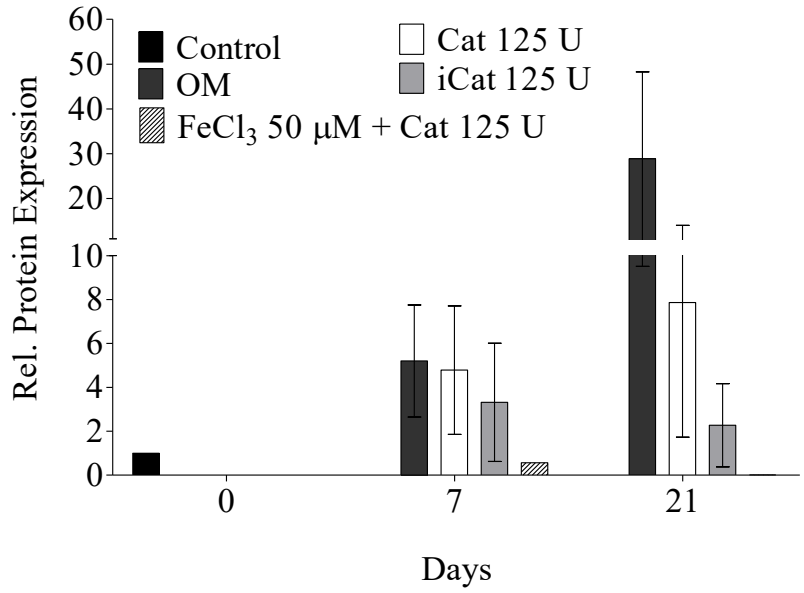

Figure 92: Protein expression of Nrf2. Cell cultures of low responder were treated with unsupplemented, catalase supplemented, heat inactivated catalase supplemented or with a combination of iron chloride and catalase supplemented

osteogenic differentiation medium for a total of 21 days. At day zero, seven and 21, proteins were extracted and the protein expressions were analyzed (OM = osteogenic differentiation medium; Cat = catalase; iCat = heat inactivated catalase; n = 1 - 4).

Also, the evaluation of the FOXO1 expression was difficult which is the reason why, so far, only low responder donors were analyzed. In many cases, the expression pattern was weak and therefore not analyzable which is demonstrated in *figure 94*. *Figure 93* highlights the significant increase of the FOXO1 expression of catalase treated cells. Interestingly, the addition of heat inactivated catalase or the combination of catalase and iron chloride did not result in an elevation. The expression patterns of the gels of *figure 94* match the results of *figure 92* and *figure 93*.

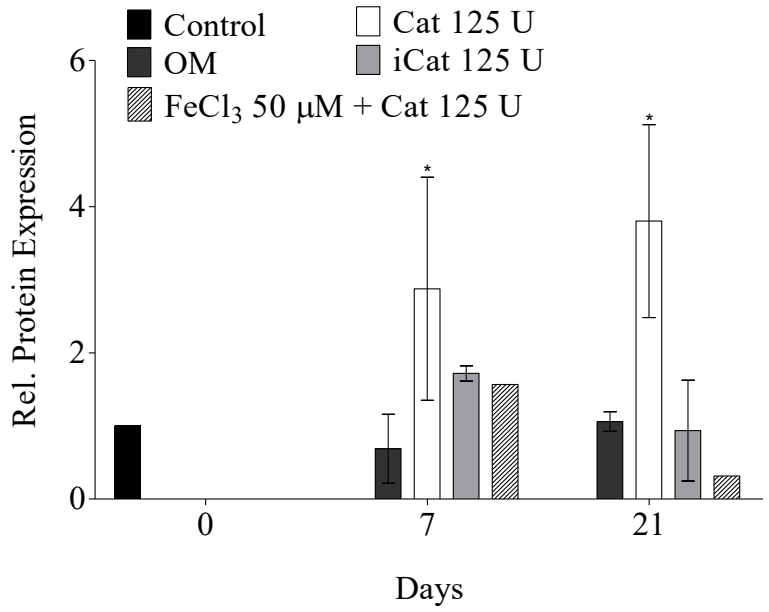

Figure 93: Protein expression of FOXO1. Cell cultures of low responder were treated with unsupplemented, catalase supplemented, heat inactivated catalase supplemented or with a combination of iron chloride and catalase supplemented osteogenic differentiation medium for total of 21 days. At day zero, seven and 21, proteins were extracted and the protein expressions were analyzed (* = significant to OM [$p < 0.05$]; OM = osteogenic differentiation medium; Cat = catalase; iCat = heat inactivated catalase; n = 1 - 4).

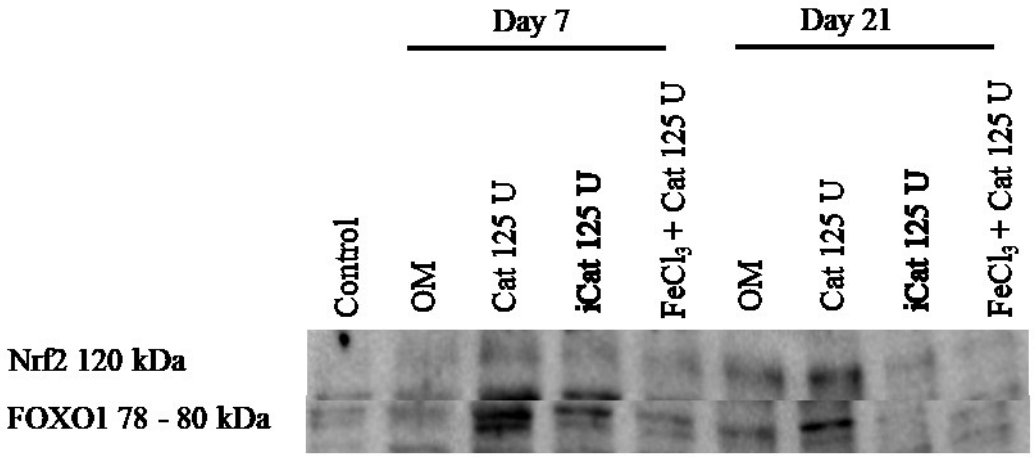

Figure 94: Details of the NRf2 and FOXO1 expression of a gel of one of the low responder donors (OM = osteogenic differentiation medium; Cat = catalase; iCat = heat inactivated catalase).

5.2.1.11.5 Effects on the Expression of Glutathione Peroxidase of Low Responder Cells

At day seven, the addition of catalase as well as the addition of heat inactivated catalase led to a slight increase of the expression compared to expression of cells which were cultured in unsupplemented osteogenic differentiation medium. The addition of the combination of catalase and iron chloride decreased the expression at day seven and day 21 compared to the other expression patterns. At day 21, the cultivation of the cells in catalase and heat inactivated catalase supplemented osteogenic differentiation medium resulted in a distinct decrease of the protein expression. The outcomes are highlighted in *figure 95*. Since the expression patterns were weak, not all donors were analyzable. A good visible expression pattern of glutathione peroxidase on a gel is shown in *figure 96*. Interestingly, the expression pattern of glutathione peroxidase according to the different additions of additives were equal to the expression pattern of catalase under the same conditions which can be seen by comparing *figure 85* and *figure 95*.

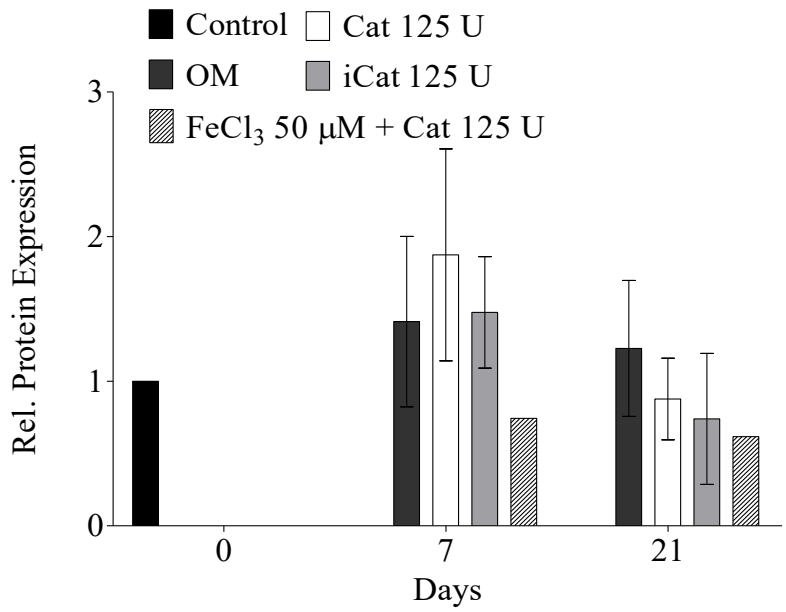

Figure 95: Protein expression of glutathione peroxidase. Cell cultures of low responder were treated with unsupplemented, catalase supplemented, heat inactivated catalase supplemented or with a combination of iron chloride and catalase supplemented osteogenic differentiation medium for a total of 21 days. At day zero, seven and 21, proteins were extracted and the protein expressions were analyzed (OM = osteogenic differentiation medium; Cat = catalase; iCat = heat inactivated catalase; n = 1 - 2).

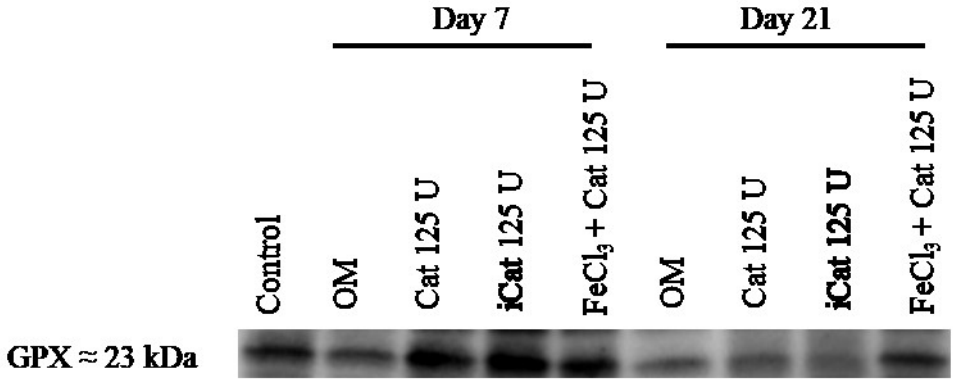

Figure 96: Detail of the GPX expression of a gel of one of the low responder donors (OM = osteogenic differentiation medium; Cat = catalase; iCat = heat inactivated catalase).

5.2.1.12 Impacts on the Expression of p53

Since the apoptosis rate was analyzed, the most effective regulatory protein of the apoptosis pathway - p53 - was also investigated. Similar to the evaluation of FOXO1 and NRf2, the weak expression patterns of p53 were difficult to analyze in many cases. The changing expressions caused by the different treatments were not significant. Nonetheless at day 21, a distinct trend was visible for responder and low responder donors. All described additions led to an increase of the p53 expression compared to the expression of cells which were cultured

in unsupplemented osteogenic differentiation medium. The changes of the expression pattern of responder and low responder hBMSCs are demonstrated in *figure 97* and *figure 98*.

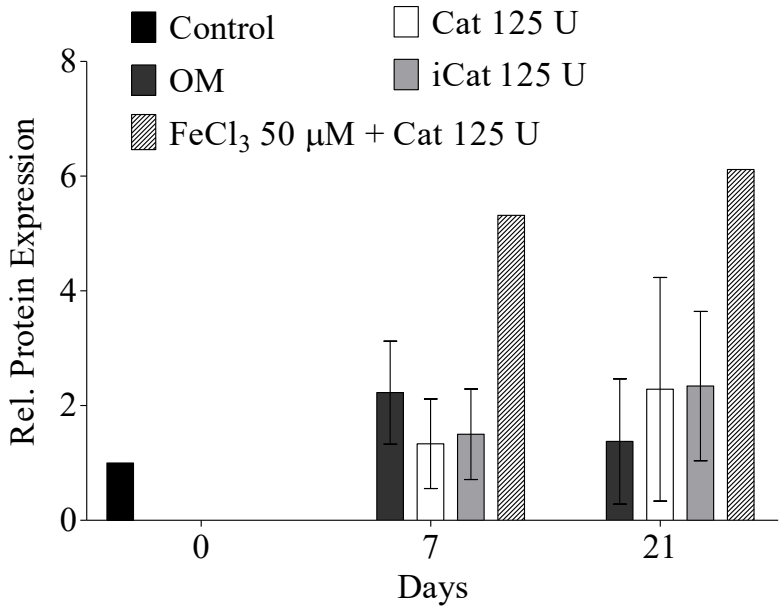

Figure 97: Protein expression of p53. Cell cultures of responder donors were treated with unsupplemented, catalase supplemented, heat inactivated catalase supplemented or with a combination of iron chloride and catalase supplemented osteogenic differentiation medium for a total of 21 days. At day zero, seven and 21, proteins were extracted and the protein expressions were analyzed d (OM = osteogenic differentiation medium; Cat = catalase; iCat = heat inactivated catalase; n = 1 - 4).

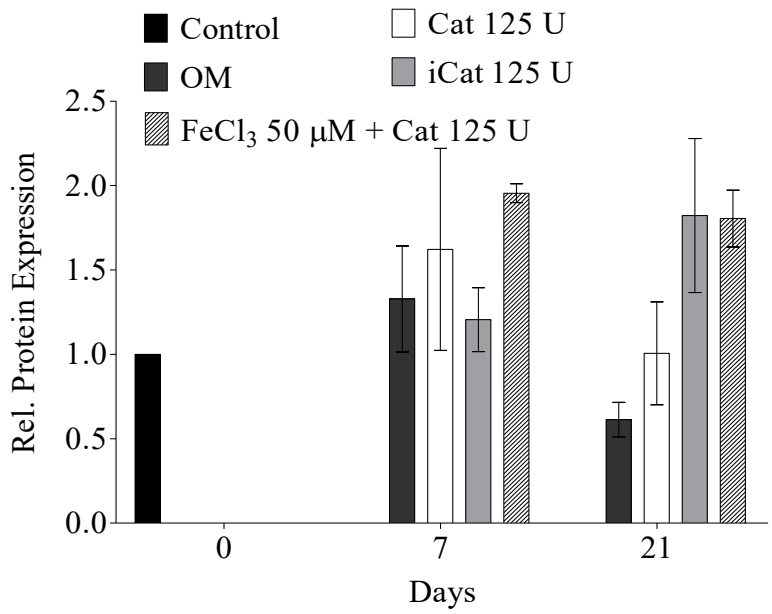

Figure 98: Protein expression of p53. Cell cultures of low responder donors were treated with unsupplemented, catalase supplemented, heat inactivated catalase supplemented or with a combination of iron chloride and catalase supplemented osteogenic differentiation medium for a total of 21 days. At day zero, seven and 21, proteins were extracted and the protein expressions were analyzed (OM = osteogenic differentiation medium; Cat = catalase; iCat = heat inactivated catalase; n = 2 - 4).

Additionally, the expression pattern on the gel is shown in *figure 99*.

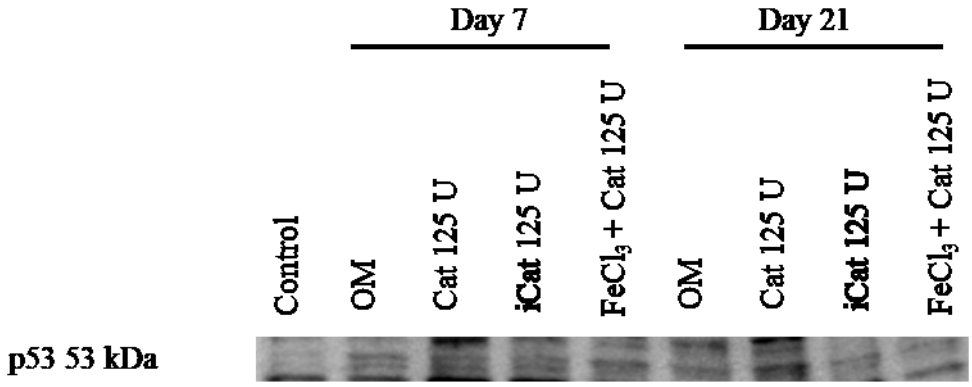

Figure 99: Detail of the p53 expression of a gel of one of the low responder donors (OM = osteogenic differentiation medium; Cat = catalase; iCat = heat inactivated catalase).

5.2.1.13 Impacts on the Expression of AKT

AKT is a crucial protein to regulate multiple cellular processes. For example, cell proliferation, glucose metabolism, apoptosis and glucose metabolism are regulated by AKT [183]. Furthermore, AKT and p53 counteract (see: *figure 139*) which was another reason for analyzing the expression of both proteins. The addition of catalase and heat inactivated

catalase led to an increase of the expression of AKT at day seven compared to the expression of cells which were cultured in unsupplemented osteogenic differentiation medium. The addition of the combination of catalase and iron chloride led to no change of the expression at day seven but resulted in a decrease at day 21. Moreover, the AKT expression was decreased at day 21 by the treatment with catalase and heat inactivated catalase which is demonstrated in *figure 100*.

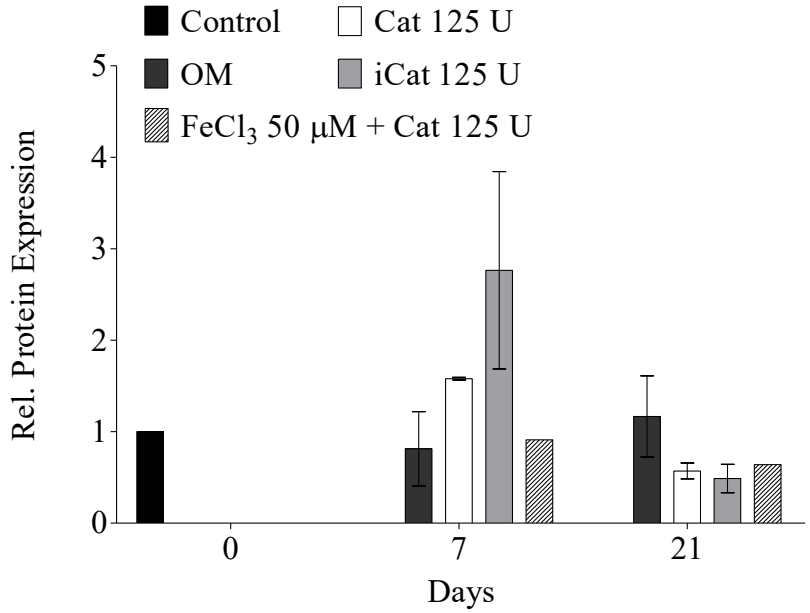

Figure 100: Protein expression of AKT. Cell cultures of low responder donors were cultured in unsupplemented, catalase supplemented, heat inactivated catalase supplemented or with a combination of iron chloride and catalase supplemented osteogenic differentiation medium for total of 21 days. At day zero, seven and 21, proteins were extracted and the protein expressions were analyzed (OM = osteogenic differentiation medium; Cat = catalase; iCat = heat inactivated catalase; n = 1 - 2).

The expression pattern was weak which made it difficult to evaluate the expression of AKT. *figure 101* demonstrates the expression pattern of AKT on a gel.

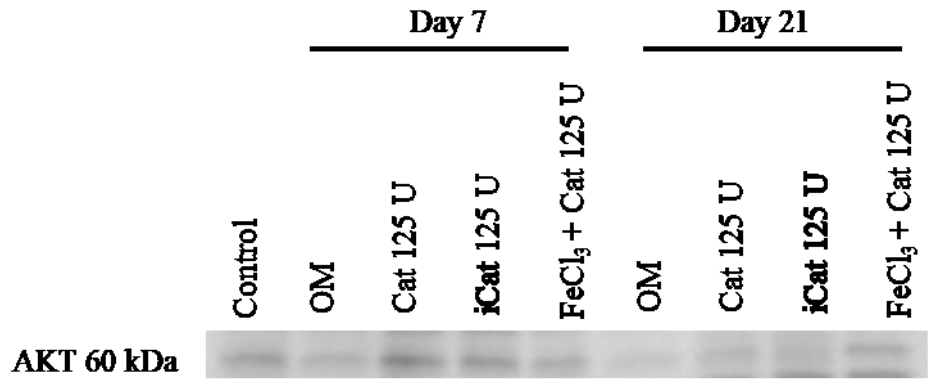

Figure 101: Detail of the AKT expression of a gel of one of the low responder donors (OM = osteogenic differentiation medium; Cat = catalase; iCat = heat inactivated catalase).

5.2.1.14 Impacts on the Expression of Iron Responsive Element and Aconitase 2

The additions of the iron ions resulted in an improvement of the osteogenic differentiation potential of low responder donors and simultaneously in an impairment of the osteogenic differentiation potential of responder hBMSCs which is demonstrated in paragraph *5.2.1.8*. Due to these results, the expressions of aconitase 1 (IRP-1) and 2 (Aco2) depending on the diverse treatments were analyzed. Aconitase 1 and 2 are important enzymes regarding the ATP generation which is explained in paragraph *6.3*. The expression patterns of IRP-1 and Aco2 are shown in *figure 102* and *figure 103*. The expression of both enzymes was evaluated of responder and low responder cells for day seven and day 21 on one gel to compare the different expression patterns. At day 21, the expression pattern of responder and low responder cells were similar. The addition of catalase and heat inactivated catalase resulted in an increased expression of IRP-1 and aconitase 2. It is important to point out that the increase of the expression by catalase addition was more distinct compared to the other additives. The addition of iron chloride and sulfate clearly did not change the expression patterns of aconitase 1 and 2. At day seven, the addition of catalase led to a decrease of the expression of aconitase 1 and 2 of low responder hBMSCs whereas a slight increase of aconitase 1 and 2 expressions of responder cells could be observed. To summarize, the treatment with catalase affected the expression of aconitase 1 as well of aconitase 2 of responder and low responder hBMSCs. However, the expression patterns after a catalase treatment did not equal the patterns after an iron chloride or sulfate treatment which would have indicated an iron depending impact on the osteogenic differentiation. Additionally, the effects of a heat inactivated catalase treatment were equal to the effects of a catalase treatment even though the effects after the addition of heat inactivated catalase were not distinct.

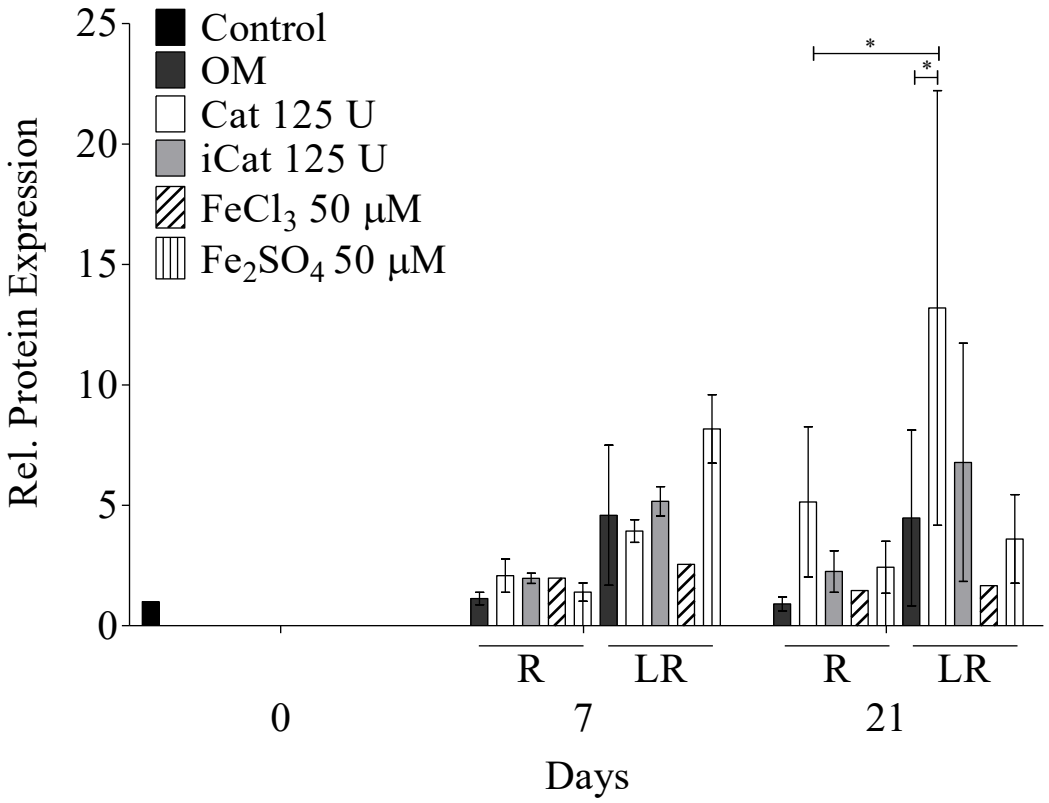

Figure 102: Protein expression of IRP-1. Cell cultures of responder (n = 4) and low responder (n = 2) donors were treated with unsupplemented, catalase supplemented, heat inactivated catalase supplemented iron chloride supplemented or iron sulfate supplemented osteogenic differentiation medium for a total of 21 days. At day zero, seven and 21, proteins were extracted and the protein expressions were analyzed (OM = osteogenic differentiation, Cat = catalase, iCat = heat inactivated catalase; * = significant [$p < 0.05$]).

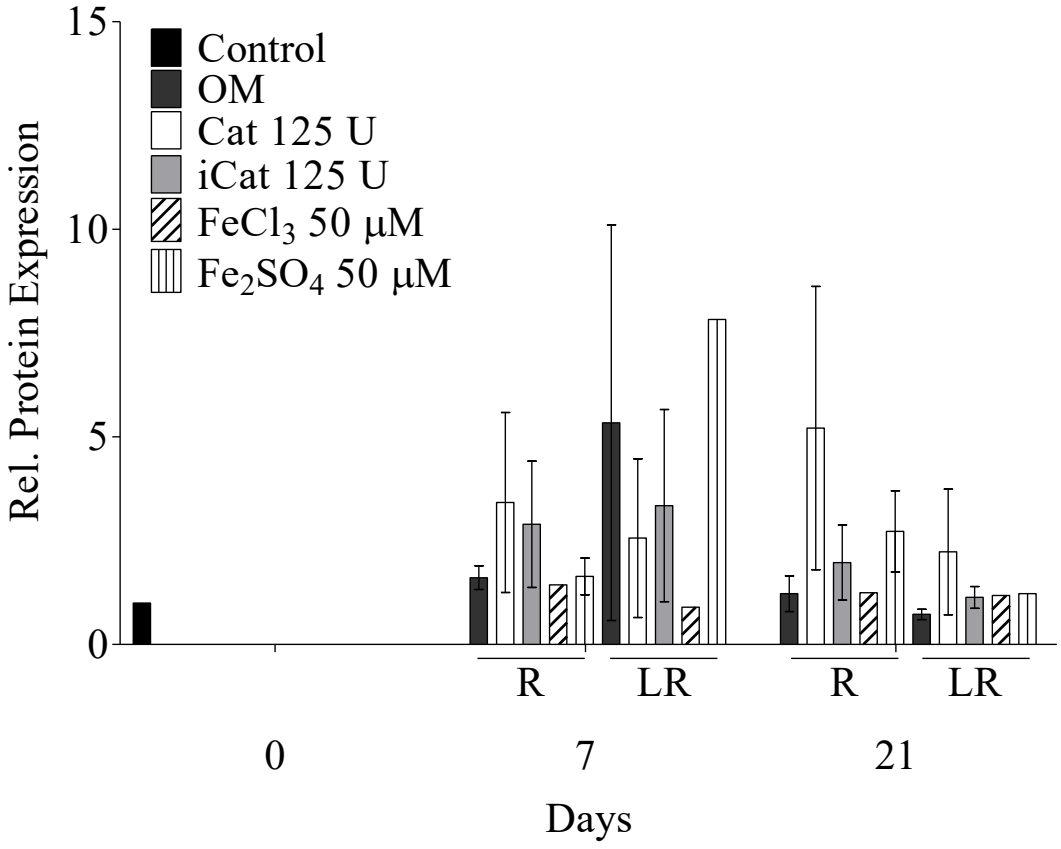

Figure 103: Protein expression of aconitase 2. Cell cultures of responder (n = 4) and low responder (n = 2) donors were treated with unsupplemented, catalase supplemented, heat inactivated catalase supplemented iron chloride supplemented or iron sulfate supplemented osteogenic differentiation medium for a total of 21 days. At day zero, seven and 21, proteins were extracted and the protein expressions were analyzed (OM = osteogenic differentiation, Cat = catalase, iCat = heat inactivated catalase).

Figure 104 shows the expression patterns of IRP-1 and aconitase 2 on the gels of a responder and a low responder donors at day zero (control), seven and 21. In *figure 103* and *figure 104*, the expressions of aconitase 2 of low responder cells at day 21 are slightly lower in comparison to the expressions of responder donors.

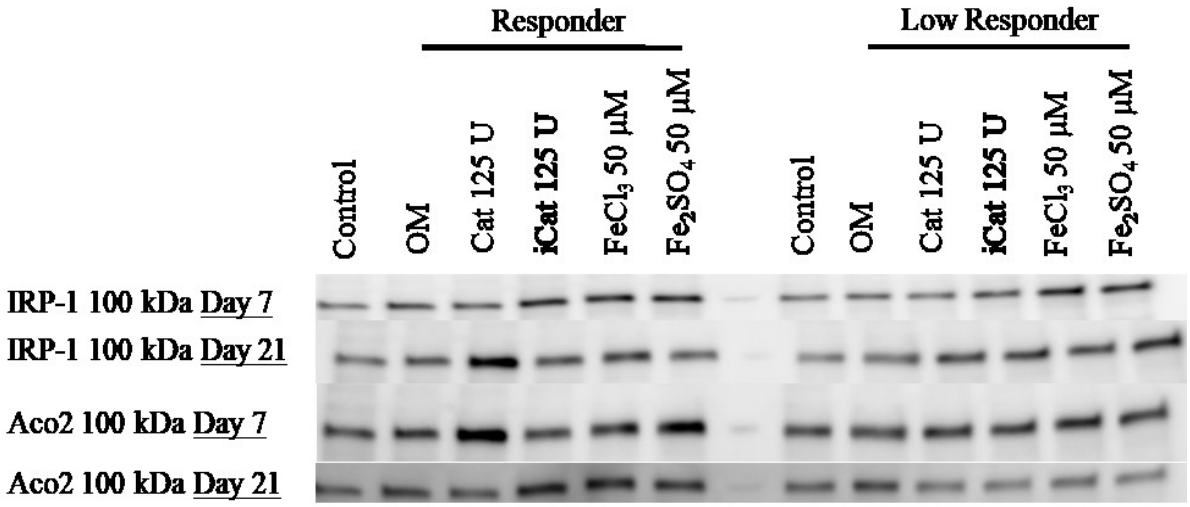

Figure 104: Detail of the IRP-1 and Aco2 expression of a gel a responder and a low responder donor at day zero (control), seven and 21 (OM = osteogenic differentiation, Cat = catalase, iCat = heat inactivated catalase)**.**

5.2.1.15 Determination of Osterix and the Matrix Proteins SPARC and Collagen Type 1

Due to the inclusion of the proteins SPARC and collagen type 1 in the calcified matrix, the proteins could not be determined by Western blot analysis. Therefore, the protein expressions were assessed by immunofluorescence staining and PCR analysis. Since the transcription factor osterix is known to be a critical regulator of the osteoblast differentiation [5], in particular of the SPARC and collagen type 1 [184, 185], the expression of osterix was also evaluated by immunofluorescence staining and PCR. The outcomes of the immunofluorescence staining are presented in *figure 105* and *figure 106*. The images of A in *figure 105* show low responder cells which were cultured for 21 days in unsupplemented osteogenic differentiation medium. The intact cell nuclei are colored blue and can be seen clearly. The weak intensity of the green colored osterix and the pink colored collagen type 1 are also visible. On the contrary, the images of B show cells which were cultured in catalase supplemented osteogenic differentiation medium for 21 days. After staining the hBMSCs at day 21 with immunofluorescence dyes, these cells exhibited a significant higher intensity of osterix and collagen type 1. Additionally, the cell nuclei were damaged. Both conspicuities were reliable indications of a formed calcified matrix.

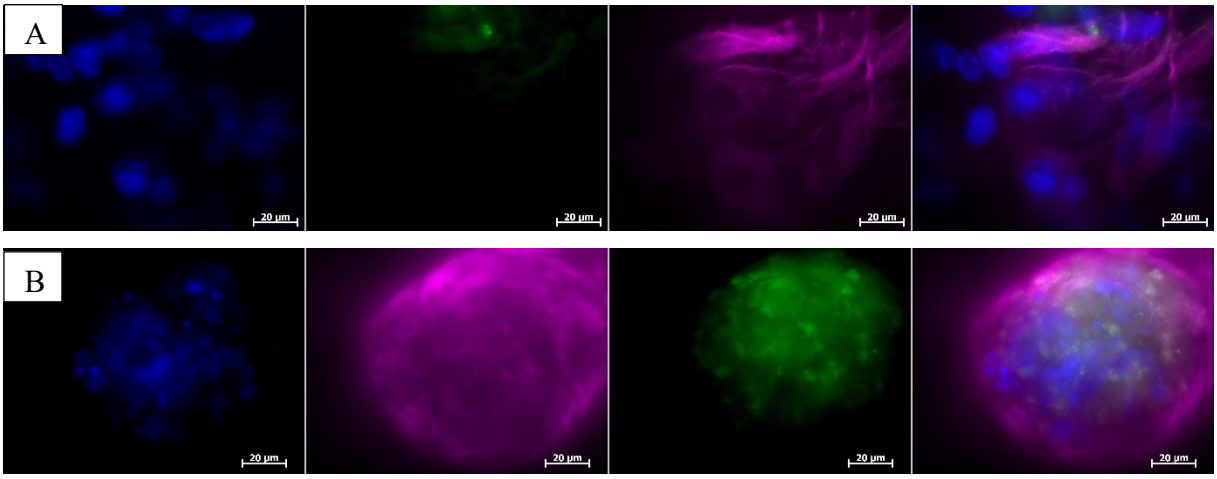

Figure 105: Immunofluorescence staining of osterix and collagen type 1 of low responder hBMSCs. The cell cultures were cultured in unsupplemented and catalase supplemented osteogenic differentiation medium. At day 21, the cell cultures were stained with immunofluorescence dyes. Image A: cells cultured in unsupplemented osteogenic differentiation medium; Image B: cells cultured in catalase supplemented osteogenic differentiation medium; Blue: cell nuclei; Green: osterix; Pink: collagen type 1

In *figure 106*, the expression of SPARC is highlighted. In images of A, cells are shown which were cultured in unsupplemented osteogenic differentiation medium for 21 days. The cell cultures were stained at day 21. The intact cell nuclei and the weak intensity of SPARC can be identified. In Images of B, cells are shown which were cultured in catalase supplemented osteogenic differentiation medium. The cell nuclei were damaged and the fluorescence intensity of the matrix protein SPARC is significantly heightened which was also a reliable sign for a formation of matrix calcification.

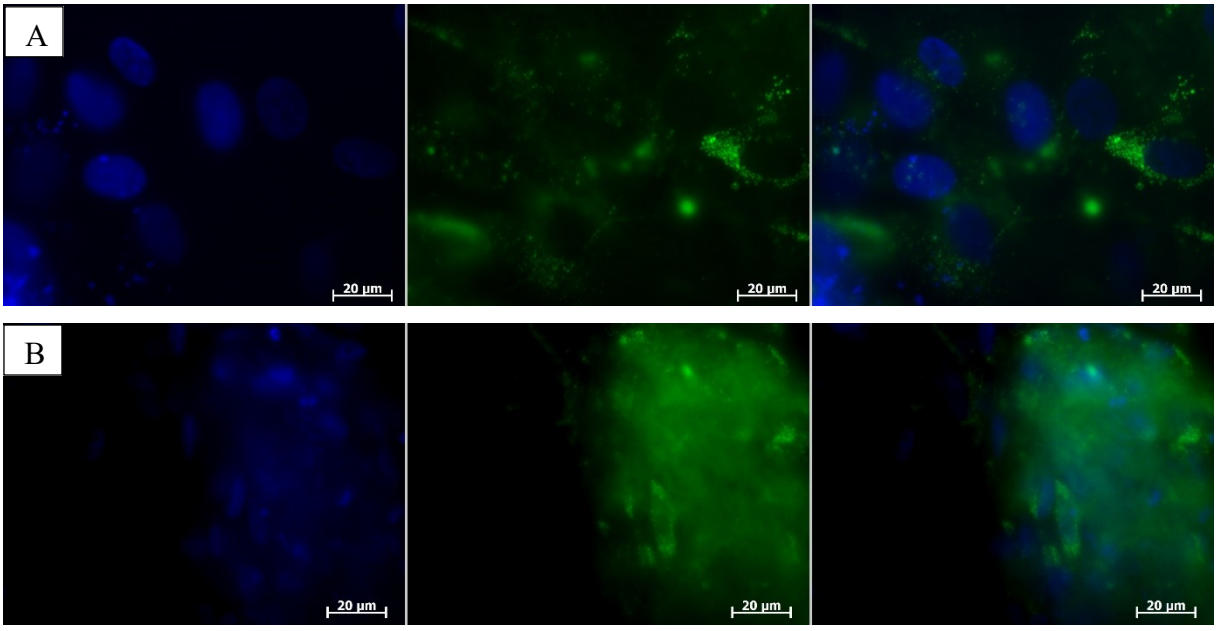

Figure 106: Immunofluorescence staining of SPARC of low responder hBMSCs. The cell cultures were cultured in unsupplemented and catalase supplemented osteogenic differentiation medium. At day 21, the cell cultures were stained with

immunofluorescence dyes. Image A: cells cultured in unsupplemented osteogenic differentiation medium; Image B: cells cultured in catalase supplemented osteogenic differentiation medium; Blue: cell nuclei; Green: SPARC

Furthermore, to confirm the results of the immunofluorescence staining, the gene expression of SPARC and collagen type 1 were determined by performing a Real-Time PCR (RT-PCR). During the same approach of the immunofluorescence staining, mRNA of the samples was isolated at day seven and 21 and was used to perform the RT-PCR. *Figure 107* presents the relative mRNA expression of collagen type 1 at day seven and 21 of cells which were cultured in unsupplemented, catalase supplemented or heat inactivated catalase supplemented osteogenic differentiation medium. In general, the expression rate was slightly increased in cells which were treated with catalase. The increase was more distinct at day 21. Interestingly, the treatment with heat inactivated catalase leads to a decreased expression at day seven and 21.

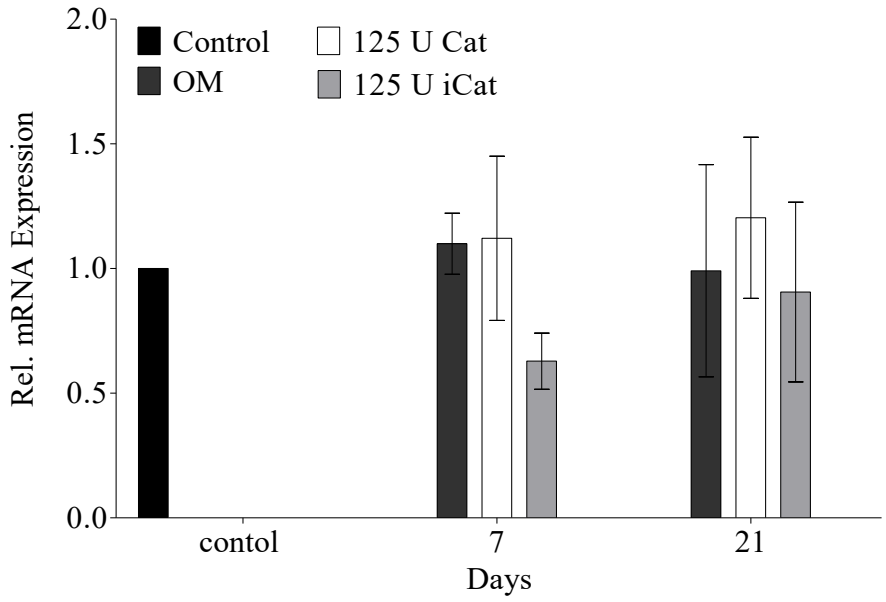

Figure 107: Expression of the collagen type 1 mRNA. The low responder cell cultures were cultured in unsupplemented and catalase supplemented and heat inactivated catalase supplemented osteogenic differentiation medium for a total of 21 days. At day zero, seven and 21, the mRNA was isolated of the cell cultures and the expression of the mRNA of collagen type 1 was determined by performing a PCR (OM = osteogenic differentiation, Cat = catalase, iCat = heat inactivated catalase; n = 5).

The expression rate of SPARC was clearly elevated by the addition of catalase or heat inactivated catalase at day seven and day 21 which can be seen in *figure 108*. Remarkably, the results after the treatment with heat inactivated catalase were more increased compared to the outcomes after a catalase treatment. Additionally, the gene expression was higher at day seven compared to day 21.

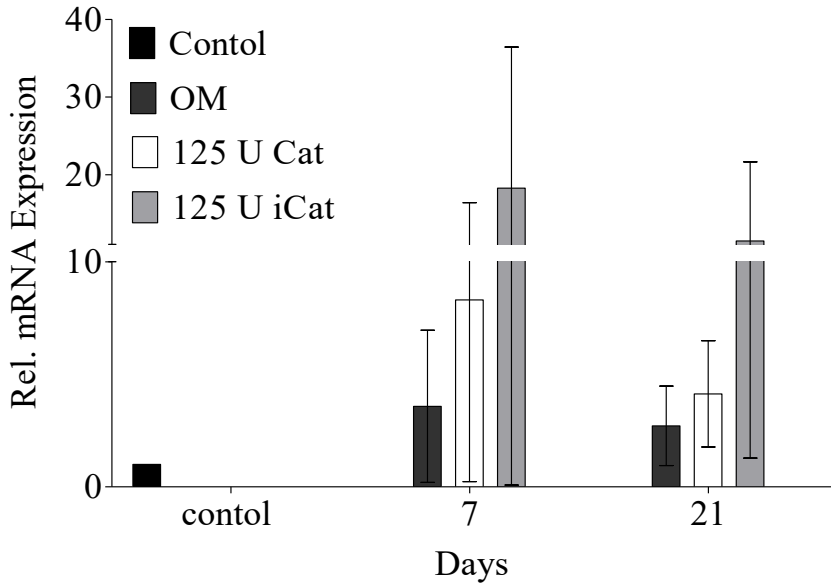

Figure 108: Expression of the SPARC mRNA. The low responder cell cultures were cultured in unsupplemented and catalase supplemented and heat inactivated catalase supplemented osteogenic differentiation medium for a total of 21 days. At day zero, seven and 21, the mRNA was isolated of the cell cultures and the expression of the mRNA of SPARC was determined by performing a PCR (OM = osteogenic differentiation, Cat = catalase, iCat = heat inactivated catalase; n = 4).

5.3 Immunohistological Visualization of Fat Cells and Neutral Fat by an Oil Red Staining

Due to the indications of adipogenic differentiation processes, for example in *figure 43,* and *figure 49*, an oil red staining of low responder hBMSCs was performed. Furthermore, reactive oxygen species facilitated adipogenic differentiation processes on the one hand and thus inhibited osteogenic differentiation processes on the other hand which is explained in section *6.1*[186, 187]. After reaching confluence in proliferation medium, the cells were cultured in unsupplemented, catalase supplemented, MnTBAP supplemented and EUK134 supplemented osteogenic differentiation medium. At day 21, the cell cultures were stained with oil red and images of the immunohistochemically staining were taken. *Figure 109* shows the results of the oil red staining. Interestingly, indications of an adipogenic differentiation can be seen in all images (A – D). The cultivation in EUK134 supplemented medium shows an equal extent of fat cells (images D) as well as cells which were cultured in unsupplemented osteogenic differentiation medium. In this case, it is important to note that the amount of ROS was significantly reduced by the mechanism of action of EUK134. EUK134 is a mimetic of MnSOD and catalase and therefore can degrade superoxide anions and hydrogen peroxide which in turn results in a reduced amount of ROS [159]. Even though catalase also reduces the amount of ROS by a degradation of hydrogen peroxide (see: chapter *1.4.2.1*), the

treatment with catalase also led to a weak adipogenic differentiation. Image A demonstrates that the adipogenic differentiation is the most pronounced in low responder cell cultures which were cultured in unsupplemented osteogenic differentiation medium. The addition of MnTBAP shows only a weak adipogenic differentiation (image C).

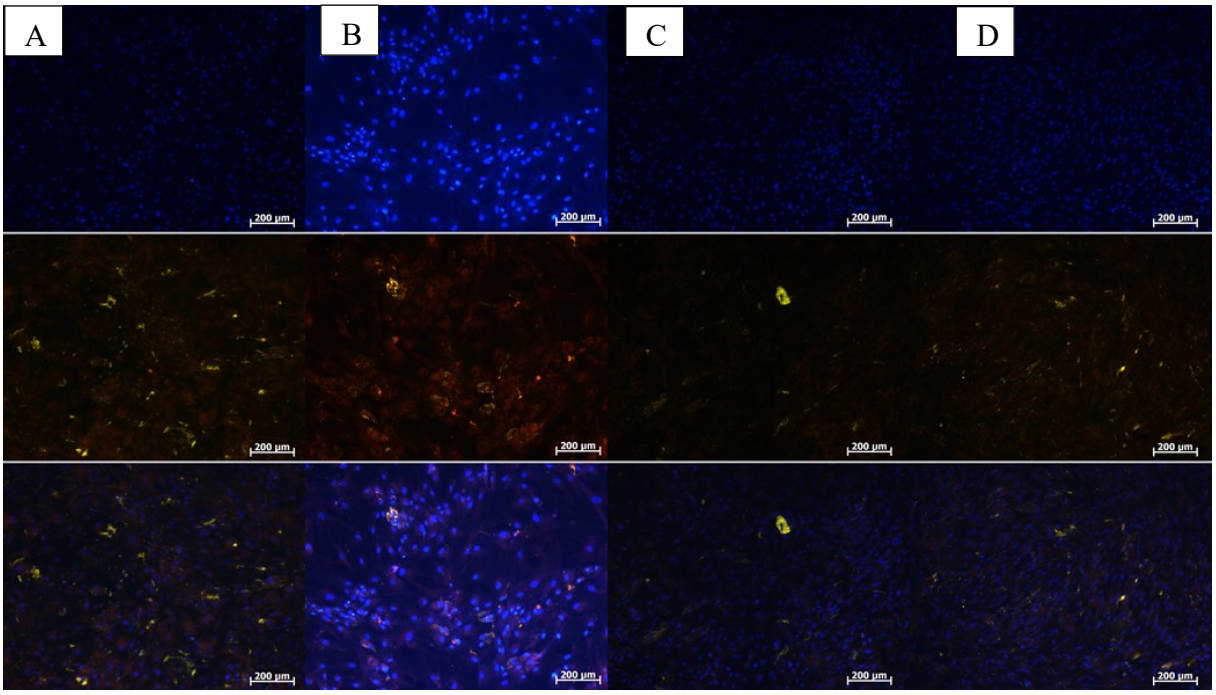

Figure 109: Oil red staining of fat cells. After reaching confluence in proliferation medium, low responder hBMSCs were cultured in differently supplemented osteogenic differentiation medium for a total time of 21 days. At day 21, the cultures were stained with oil red to evaluate the adipogenic differentiation potential during osteogenic differentiation conditions. The images were taken by the microscopic camera Zeiss Axiovert 40 with a 10-fold magnification. A: cells treated with unsupplemented osteogenic differentiation medium; B: cells treated with catalase supplemented osteogenic differentiation medium; C: cells treated with MnTBAP supplemented osteogenic differentiation medium; D: cells treated with EUK134 supplemented osteogenic differentiation medium

5.4 Evaluation of the Cell Viability of Responder and Low Responder Cells under Diverse Conditions

By analyzing the cell viability by the CellTiter Blue Assay, conclusion could be drawn from the proliferation rate of the cell cultures. To assess general differences of low responder and responder hBMSCs, the cell viability of the different donor types was analyzed. Furthermore, the investigation of the cell viability was required to evaluate many of the other results representatively.

5.4.1 FGF-2 Addition during the Proliferation

A defined number of cells of two cell cultures of responder donors and two cell cultures of low responder donors were cultured in proliferation medium with or without FGF-2 to find

differences between responder and low responder donors already during the proliferation processes. The differently treated cell cultures were analyzed by a CellTiter blue assay to assess the cell viability of the two types of donors which might result in an explanation for the controversy behavior during the osteogenic differentiation. Due to the known submitting and simultaneously inhibiting characteristics of FGF-2 during the osteogenic differentiation [174, 175, 188], the impact was tested within this project. Interestingly, no clear trend could be identified. *Figure 110, figure 111* and *figure 112* present three examples of the investigated cell cultures and it is apparent that the addition of FGF-2 led to different outcomes. In case of one of the responders which is presented in *figure 110*, the addition of catalase resulted in an impaired proliferation rate whereas the absence of FGF-2 led to a higher proliferation rate.

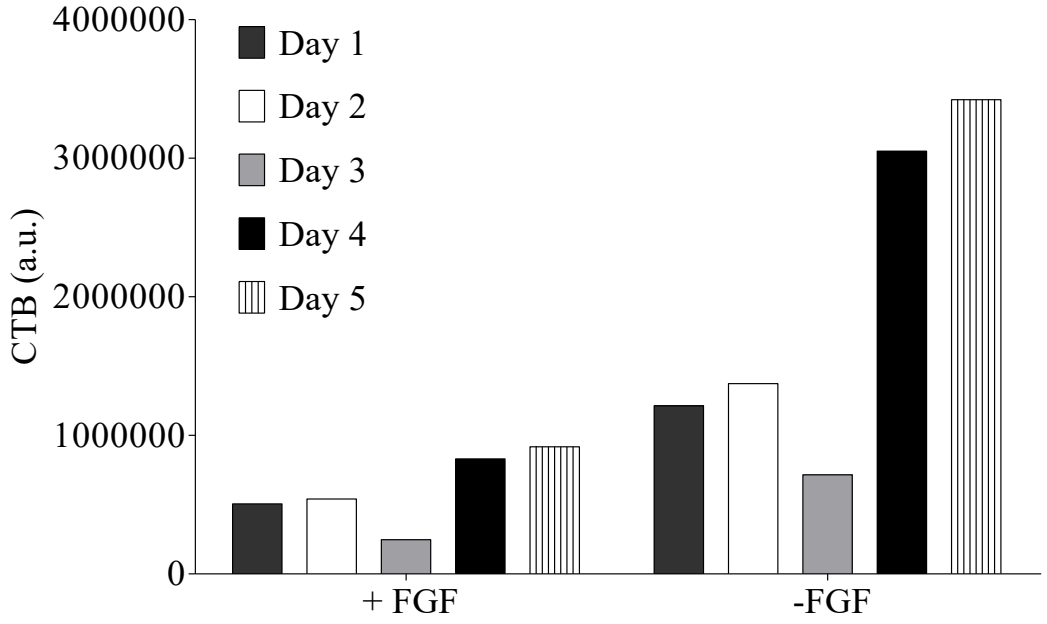

Figure 110: Evaluation of the cell viability after culturing in proliferation medium with rather or without FGF-2. Potential differences in cases of the cell viability of responder cells were analyzed by the CellTiter Blue Assay at day one, two, three, four and five. The results of one responder donor are shown in this figure.

A contrary pattern can be observed in *figure 111* which presents the results of a low responder culture. However, the second cell culture of a responder and a low responder showed comparable results regarding the cell viability.

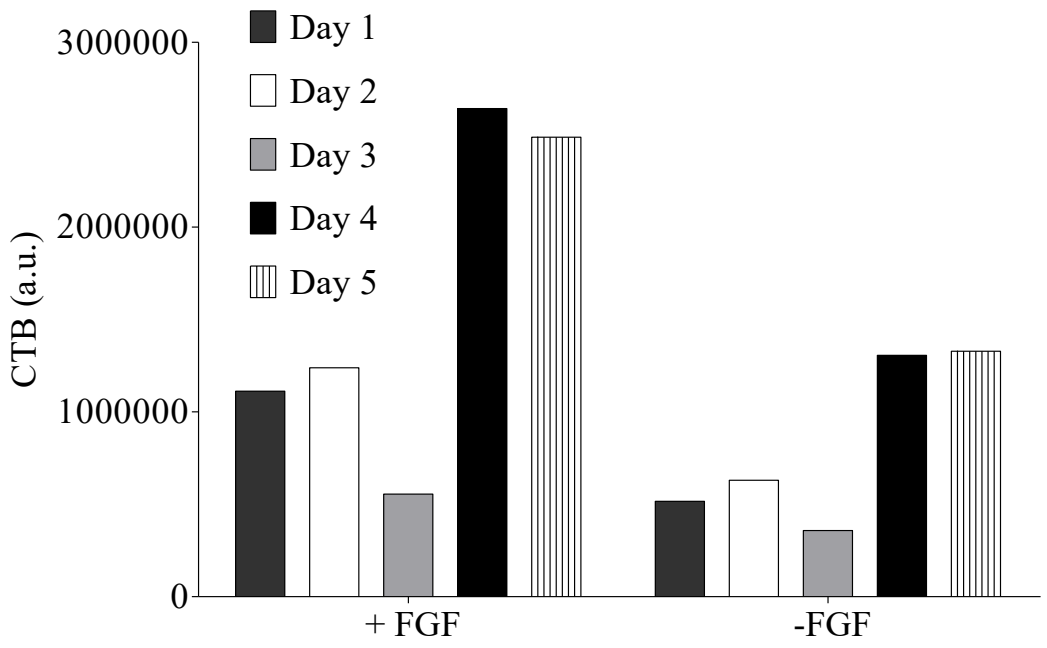

Figure 111: Evaluation of the cell viability after culturing in proliferation medium with or without FGF-2. Potential differences in cases of the cell viability of low responder cells were analyzed by the CellTiter Blue Assay at day one, two, three, four and five. The results of one low responder donor are shown in this figure.

Figure 112 constitutes a representative graph of the two other cell cultures. The graph describes that the addition and the absence of FGF-2 did not lead to a difference according the cell viability.

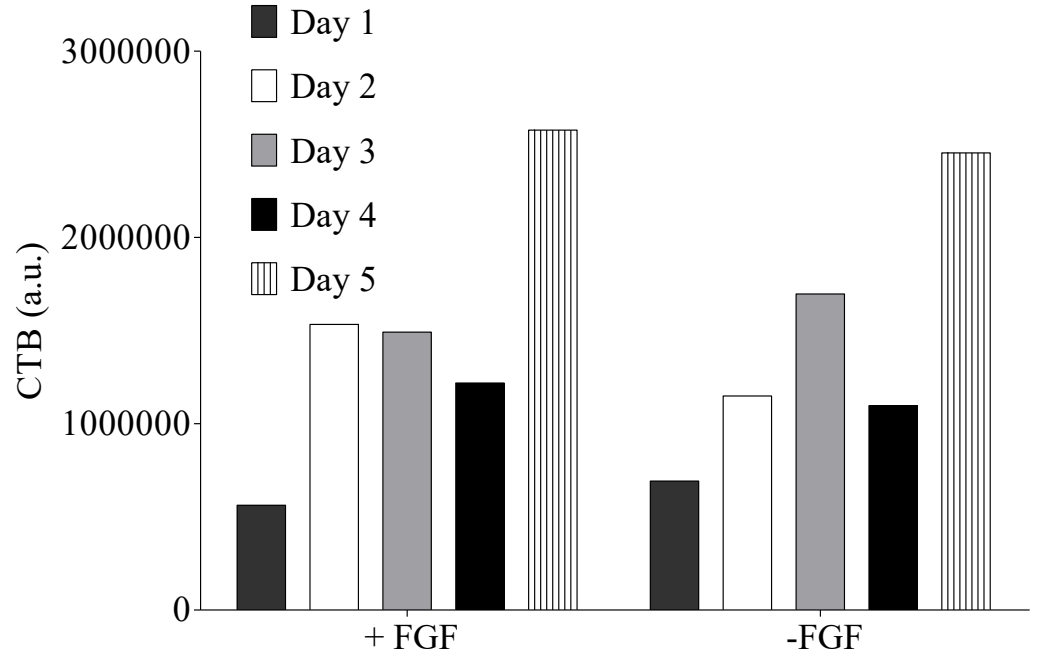

Figure 112: Evaluation of the cell viability after culturing in proliferation medium with or without FGF-2. Potential differences in cases of the cell viability of responder and low responder cells were analyzed by the CellTiter Blue Assay at day one, three, four and five. The results of another different behaving low responder donor are shown in this figure.

5.4.2 Effects of the Addition of Hydrogen Peroxide on the Cell Viability of HMBSCs

The addition of hydrogen peroxide resulted in an alteration of the osteogenic differentiation potential. For that reason, the effect of hydrogen peroxide on the cell viability had to be analyzed to draw a conclusion relating the effect of hydrogen peroxide addition on hBMSCs and the osteogenic differentiation process. *Figure 113* shows that the addition of hydrogen peroxide did significantly affect the cell viability of hBMSCs. Compared to the cell viability results after a catalase treatment, the cell viability was affected by every concentration of hydrogen peroxide. In this figure, the cytotoxic effect of concentrations of 20 mM, 2 mM and 200 µM is clearly presented.

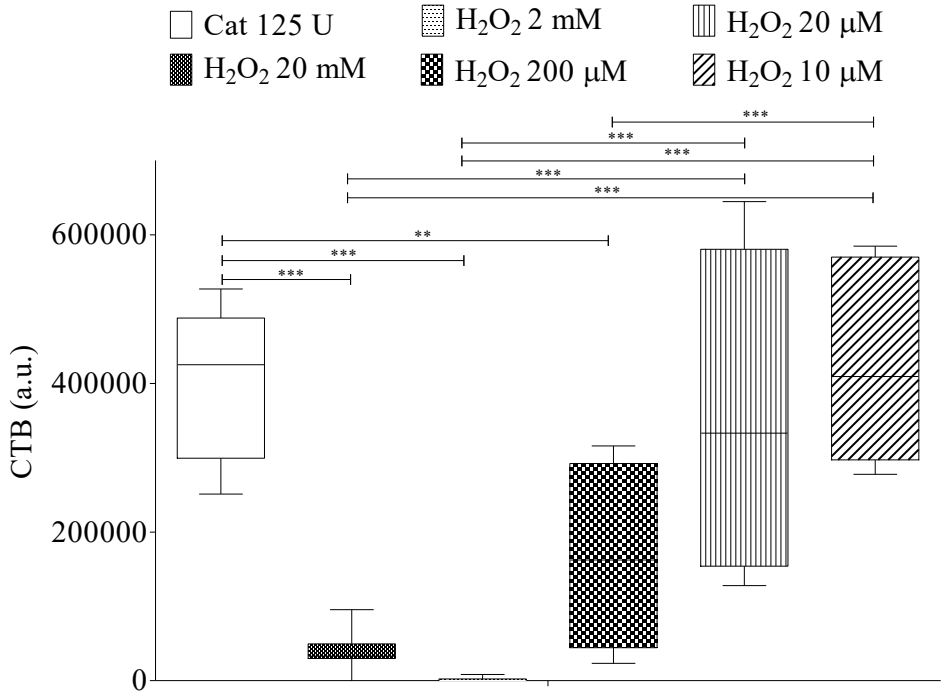

Figure 113: Evaluation of the cell viability after culturing in osteogenic differentiation medium supplemented with diverse concentrations of hydrogen peroxide. Low responder cell cultures were treated for three days with osteogenic differentiation medium which was supplemented with diverse concentrations of hydrogen peroxide. At day three, the CellTiter Blue Assay was performed (Cat = catalase; ** = significant [$p < 0.033$]; *** = significant [$p < 0.001$]; n = 2).

5.4.3 Differences Regarding Cell Viability of Cell Cultures Cultured in Differently Supplemented Proliferation or Osteogenic Differentiation Media

Since no meaningful differences were observed between responder and low responder donors, which was shown by the low standard deviation, the condensed results were interpreted. Except for the results after the treatment with EUK134, the outcomes just showed slight trends. No clear statement could be made of the results which are demonstrated in *figure 114*. EUK134 diminished the cell viability significantly in proliferation medium.

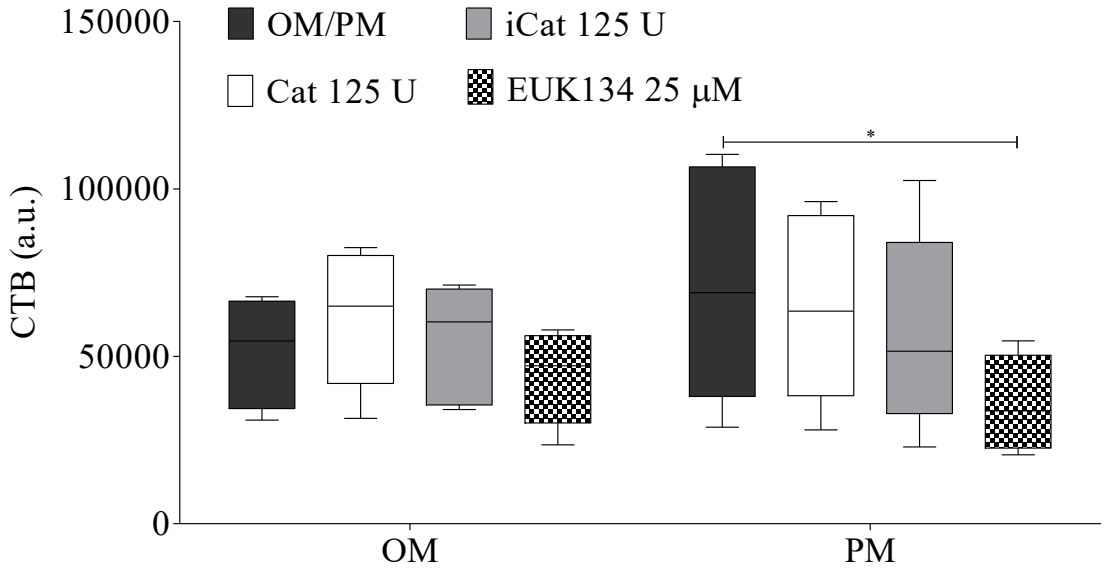

Figure 114: Comparison of the effects of culturing in proliferation and osteogenic differentiation medium supplemented with catalase, heat inactivated catalase or EUK134 on hBMSCs. Responder and low responder cell cultures were treated for three days with proliferation and osteogenic differentiation medium which was supplemented with different additives. At day three, the CellTiter Blue Assay was performed (OM = osteogenic differentiation, PM = proliferation medium, Cat = catalase, iCat = heat inactivated catalase; * = significant [$p < 0.05$]; n = 6).

5.4.4 Impact of Catalase on the Cell Viability

Since responder and low responder reacted differently during the cell viability investigations over seven days, the results of these two donor types were evaluated separately. In *figure 115*, the results of the CellTiter Blue Assay are presented. The proliferation rate of responder hBMSCs was slightly increased by the addition of catalase. Additionally, the cell viability and therefore the proliferation rate rose continuously from day zero to day seven. The control demonstrated the proliferation rate of cells cultured in proliferation medium until they got adherent to the well bottom (24 hours). Even though the dexamethasone in the osteogenic differentiation medium should initiate differentiation processes [189], the proliferation rate increased during the test period. To summarize, the addition of catalase did not also result in an improved osteogenic differentiation potential of responder hBMSCs but nonetheless led to a slight elevation of the cell viability.

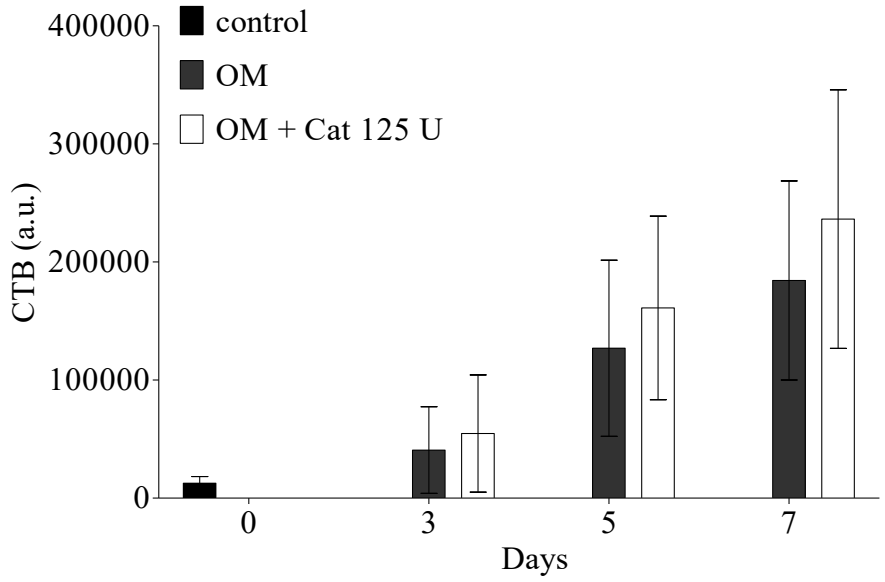

Figure 115: CellTiter Blue Assay of responder hBMSCs. The cells were treated for seven days with unsupplemented or with catalase supplemented osteogenic differentiation medium. The addition of catalase leads to no significant increase of the proliferation rate (OM = osteogenic differentiation, Cat = catalase, iCat = heat inactivated catalase; n = 4).

Figure 116 presents the effects of culturing low responder hBMSCs for a time duration of seven days in osteogenic differentiation medium with and without catalase. The results differed significantly from the proliferation rate of responder hBMSCs. The cell viability decreased during the test duration instead of stagnating or increasing like responder cells. Moreover, the addition of catalase did not lead to an increase of the proliferation rate which was another contradictory behavior of the two donor types. At day 3, the catalase addition even decreased the proliferation rate. Remarkably, the addition of catalase resulted in a significantly restored osteogenic differentiation potential which did not correlate with the cell viability results of *figure 116*. To conclude, the outcomes of the cell proliferation test did not correlate with the results of the calcified matrix formation for responder as well as low responder hBMSC cultures. Furthermore, a clear difference of the responder and low responder cells could be observed.

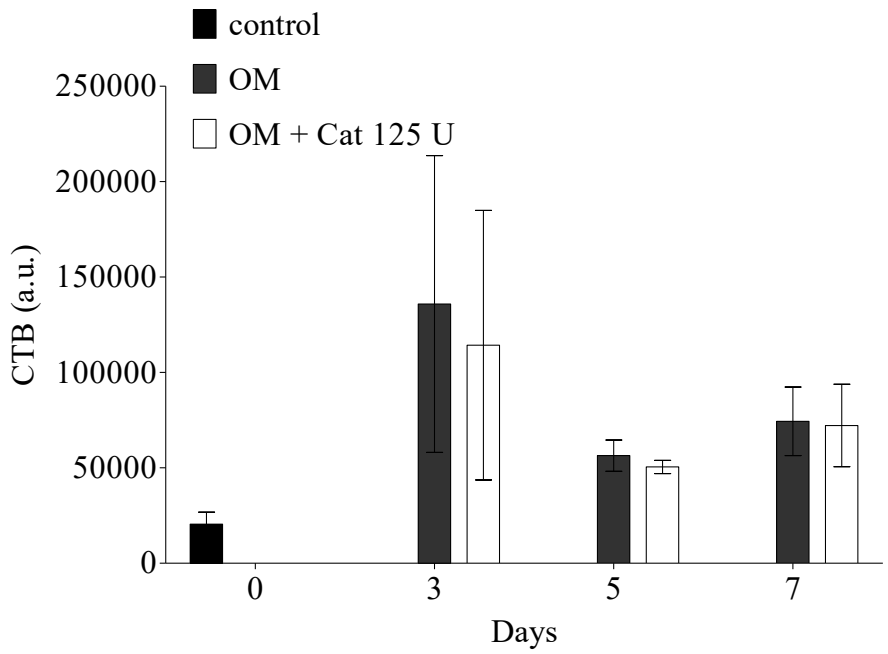

Figure 116: CellTiter Blue Assay of low responder hBMSCs. The cells were treated for seven days with unsupplemented or with catalase supplemented osteogenic differentiation medium. The addition of catalase leads to no significant increase of the proliferation rate (OM = osteogenic differentiation, Cat = catalase, iCat = heat inactivated catalase; n = 3).

5.4.5 Evaluation of the Cell Proliferation by a Cell Proliferation ELISA with Bromdesoxyuridine

As elaborated in paragraph *4.4,* the CellTiter Blue Assay affected the respiratory chain which in turn may have affected other energy metabolism processes of the cells. This again probably had negative effects on the results. To proof the reliability of the CellTiter Blue Assay, other cell viability tests were performed.

5.4.5.1 Cell Proliferation ELISA with Bromdesoxyuridine

Responder and low responder hBMSCs were tested by a Cell Proliferation ELISA with bromdesoxyuridine to demonstrate the reliability of the results of the CellTiter Blue Assay. This test was performed simultaneously to the test described in paragraph *5.4.3*. *Figure 117* shows the proliferation rate of six donors. Relating to *figure 114,* only the addition of EUK134 led to a decrease of the proliferation rate. Thus, EUK134 impaired the proliferation and differentiation progress.

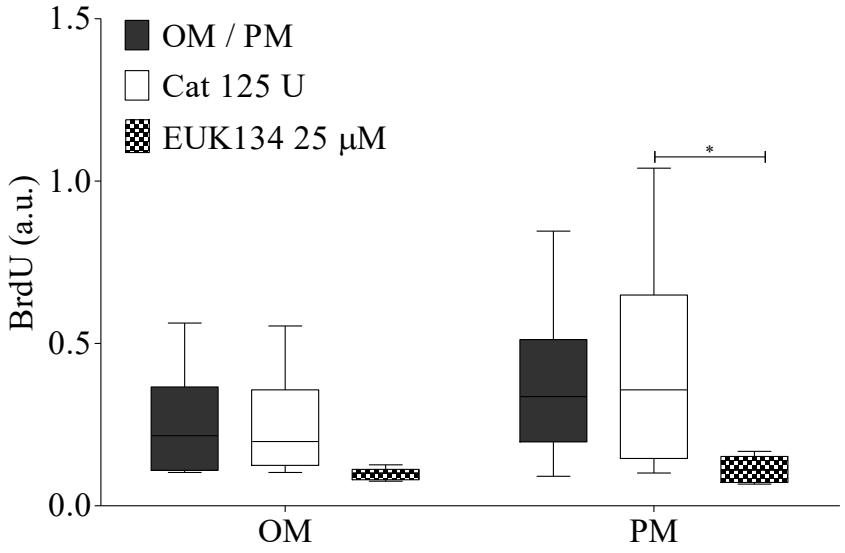

Figure 117: Performance of the Cell Proliferation ELISA with bromdesoxyuridine of responder and low responder hBMSCs. The cells were treated for three days with unsupplemented osteogenic differentiation medium or rather proliferation medium, with catalase supplemented media or with EUK134 supplemented media. (PM = proliferation medium, OM = osteogenic differentiation, Cat = catalase; * = significant [$p < 0.05$]; n = 6).

5.4.6 Evaluation of the Cell Viability by a Neutral Red Staining in Comparison to the CellTiter blue Assay

Because the different cell viability tests interacted with the energy metabolism in several ways, overall three different tests were performed to prove the reliability of the CellTiter Blue Assay.

5.4.6.1 Cell Viability Assessed by Neutral Red Staining

Seven donors were stained with neutral red and the dye was dissolved afterwards. The optical density of the solution of the dissolved dye was measured. The method is described in paragraph *4.4.3*. The cells were cultured in proliferation medium, unsupplemented osteogenic differentiation medium and catalase supplemented osteogenic differentiation medium for three, seven and 14 days. Since no differences between responder and low responder cells were detected, the results were condensed and assessed. Simultaneously to the neutral red test, a CellTiter Blue Assay was also performed to compare both outcomes regarding the cell viability of the same donors in the same passage and under equal conditions. *Figure 118* shows clearly that especially at day seven and 14, the cell viability was decreased significantly by unsupplemented osteogenic differentiation medium and osteogenic differentiation medium supplemented with catalase. At day 14, the cell viability decreased significantly low after a treatment with catalase.

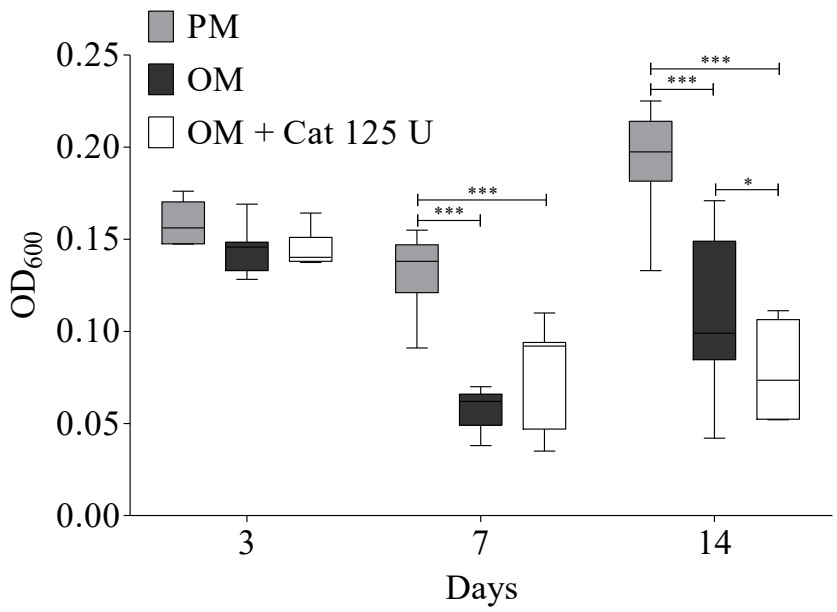

Figure 118: Performance of the neutral red staining of hBMSCs. The cells were treated for three, seven and 14 days with unsupplemented osteogenic differentiation medium or rather proliferation medium and osteogenic differentiation medium supplemented with catalase. The optical density of the obtained solution was determined at 600 nm. The optical density is proportional to the amount of calcified matrix (* = significant [$p < 0.05$]; *** = significant [$p < 0.001$]; n = 6).

Figure 119 demonstrates that the results regarding the cell viability, which were obtained by the neutral red test, confirm the outcomes of the CellTiter Blue Assay. The significant decrease at day 14 after the treatment with catalase was even more distinct which is presented in *figure 119*.

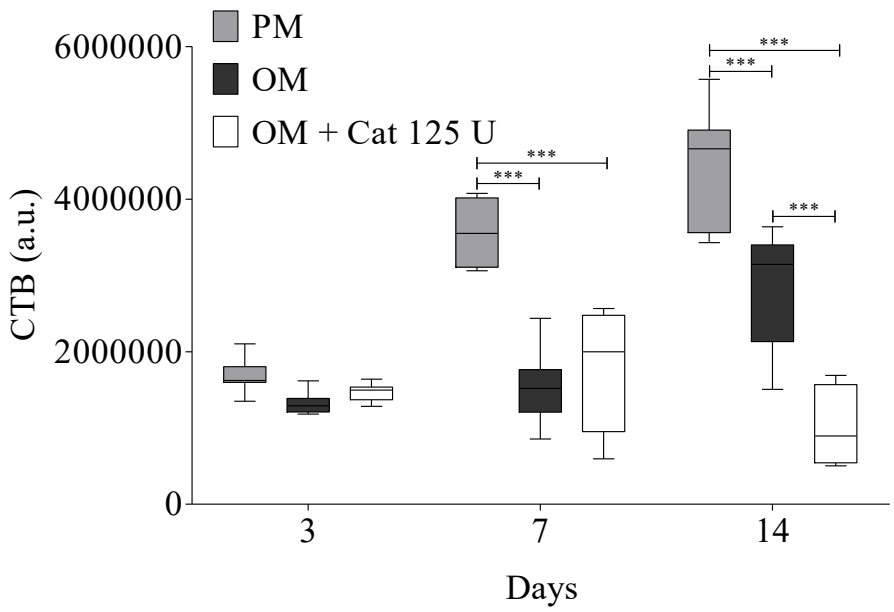

Figure 119: Performance of CellTiter Blue Assay of hBMSC cultures. The cells were treated with unsupplemented osteogenic differentiation medium or rather proliferation medium and osteogenic differentiation medium supplemented with catalase. The test was run at day three, seven and 14 (OM = osteogenic differentiation, PM = proliferation medium, Cat = catalase; *** = significant [$p < 0.001$]; n = 6).

Remarkably, not all seven donors showed the same reactions towards the different treatments. Nonetheless, the different outcomes did not correlate with the appearance of a responder or low responder donor. The two images in *figure 120* represent the neutral red results of two different donors. It can be observed that the results differ from each other even though the donors are both responder donors. Furthermore, the microscopic evaluation is highlighted in *figure 121*.

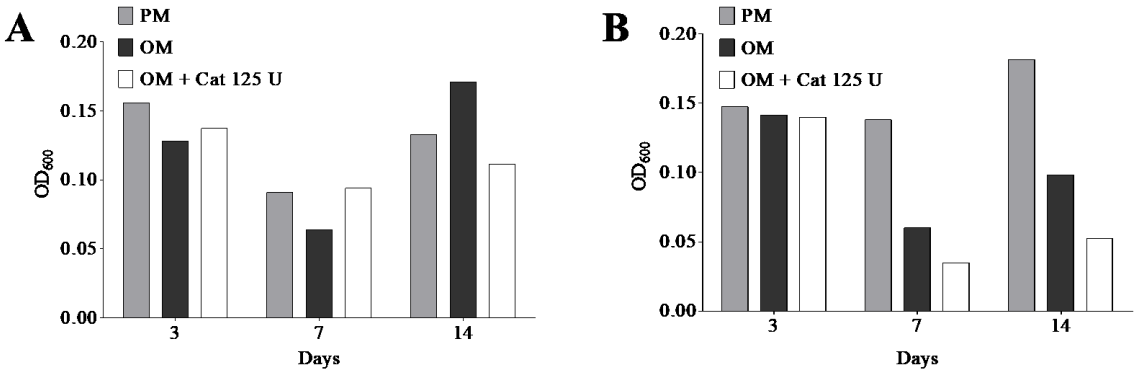

Figure 120: Performance of the neutral red staining of two different hBMSC donors. The cells were treated for three, seven and 14 days with unsupplemented osteogenic differentiation medium or rather proliferation medium and osteogenic differentiation medium supplemented with catalase. The optical density of the obtained solution was determined at 600 nm.

The optical density is proportional to the amount of calcified matrix (OM = osteogenic differentiation, PM = proliferation medium, Cat = catalase; A: donor 1; B: donor 2)

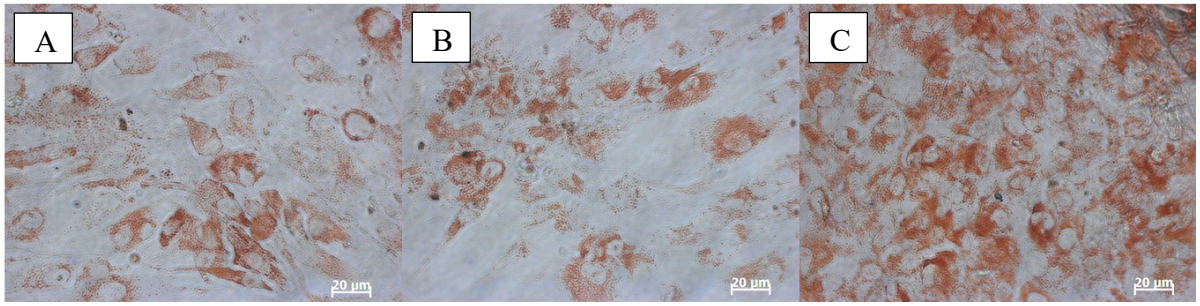

Figure 121: Neutral red staining of hBMSCs. The images show the red stained lysosomes of donor 1 at day seven. The images were taken with the microscope Zeiss Axiovert 40 with a 63x magnification. A: Cells cultured in proliferation medium; B: cells cultured in osteogenic differentiation medium; C: cells cultured in catalase supplemented osteogenic differentiation medium

5.5 Performance of the Glucose-Glo™ Assay

The amount of glucose in the supernatant of responder and low responder hBMSCs was analyzed to get indications to a potentially malfunction of the energy metabolism of low responder cells which explained the impaired osteogenic differentiation potential which could be restored by the addition of catalase. The glucose amount was tested at day zero, three and seven after treating the cells with unsupplemented proliferation and osteogenic differentiation medium or media supplemented with catalase or mannitol. *Figure 122* and *figure 123* illustrate the evaluation of the amount of glucose at day three and seven. The low responder hBMSC cultures, which were cultured in unsupplemented proliferation medium or in proliferation medium supplemented with catalase or mannitol, showed increased amounts of glucose in the supernatant at day three. These increased amounts could also be seen at day seven whereby the extent was less distinct, especially in case of the catalase supplemented proliferation medium. Interestingly, the cultivation in unsupplemented and in catalase supplemented osteogenic differentiation medium led to a substantially reduced amount of glucose at day seven of low responder hBMSCs which is shown in *figure 123*. The cultivation in the differently composed media showed no effect on responder hBMSCs at day three and seven. The amount of glucose remained constant. Nonetheless, the diverse cultivation conditions affected low responder donors.

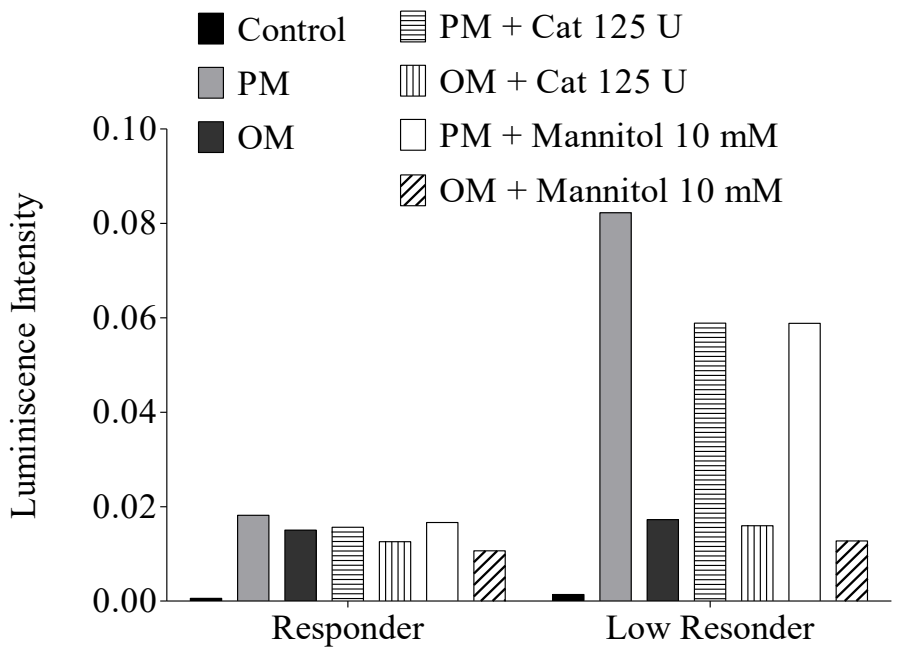

Figure 122: Determination of the amount of glucose by a Glucose-Glo™ Assay. Responder and low responder cells were cultured in proliferation and osteogenic differentiation medium which were used without any further additives or were supplemented with catalase or mannitol. The test was performed at day zero (control), three and seven. One responder and one low responder were tested and the results were compared. The results of this graph were acquired at day three (OM = osteogenic differentiation, PM = proliferation medium, Cat = catalase).

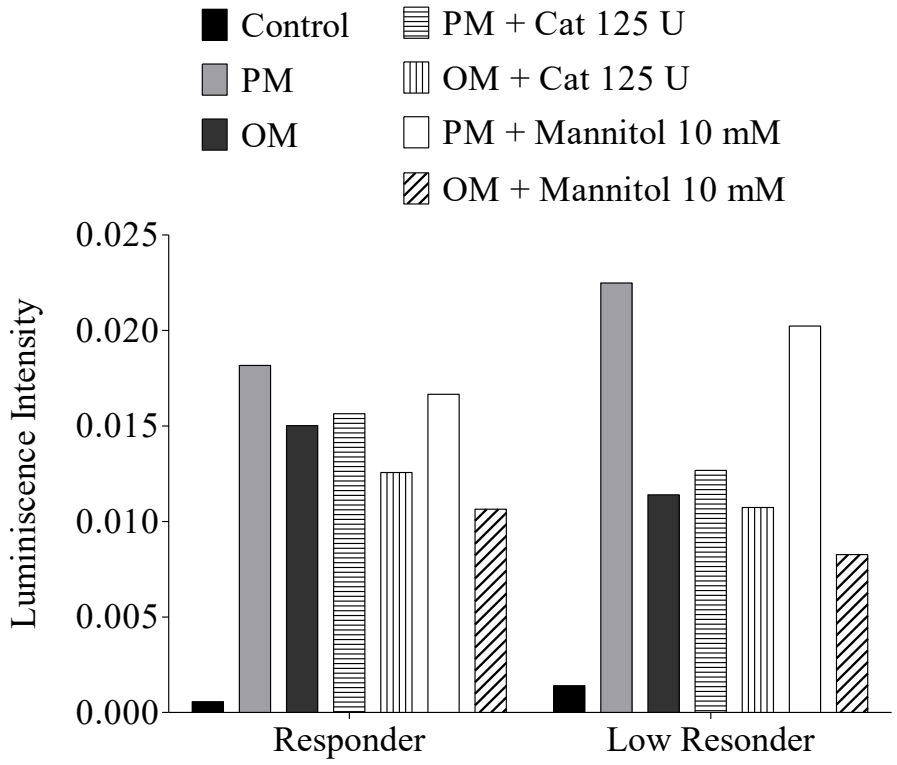

Figure 123: Determination of the amount of glucose by a Glucose-Glo™ Assay. Responder and low responder cells were cultured in proliferation and osteogenic differentiation medium which were used without any further additives or were supplemented with catalase or mannitol. The test was performed at day zero (control), three and seven. One responder and

one low responder were tested and the results were compared. The results of this graph were acquired at day seven (OM = osteogenic differentiation, PM = proliferation medium, Cat = catalase).

5.6 Determination of the Amount of ATP

The amount of ATP was determined to get further indications if modifications of the energy metabolism were the reason for the low osteogenic differentiation potential of low responder donors. First, the amount of ATP was measured of hBMSCs which were cultured in proliferation or osteogenic differentiation medium for three, seven and 14 days. *Figure 124* shows the evaluation of the amount of ATP at day three. Remarkably, the cultivation in osteogenic differentiation medium for three days resulted in a significant increase of the ATP amount.

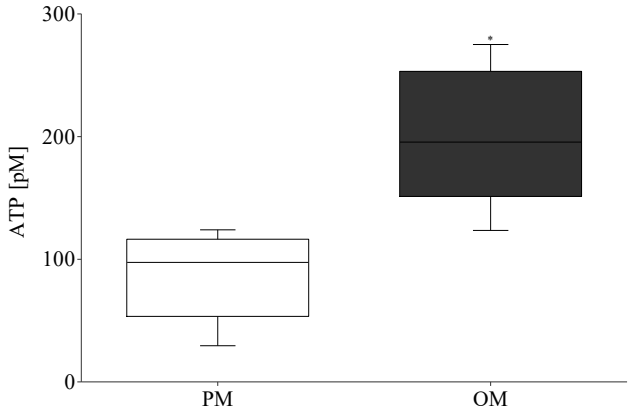

Figure 124: Determination of the amount of ATP at day three. Responder hBMSCs were cultured in proliferation or osteogenic differentiation medium for three days and the amount of ATP was determined by a kit system. (OM = osteogenic differentiation, PM = proliferation medium; * = significant to PM [$p < 0.05$]; n = 5).

Figure 125 demonstrates the ATP amount under equal conditions after seven days. In general, the ATP amount showed a distinct increase after cultivation in osteogenic differentiation medium for a total of seven days. The amount of ATP in proliferation medium cultured cells did not change.

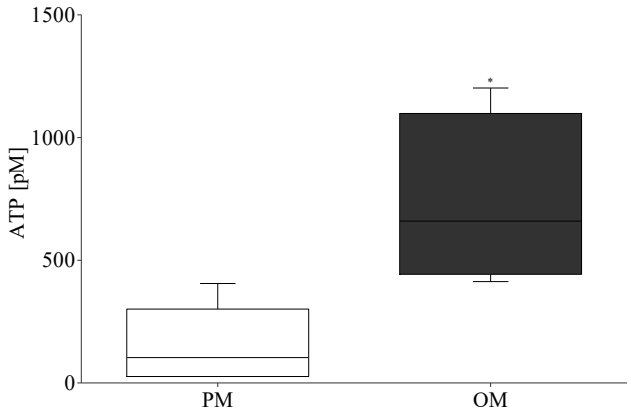

Figure 125: Determination of the amount of ATP at day seven. Responder hBMSCs were cultured in proliferation or osteogenic differentiation medium for seven days and the amount of ATP was determined by a kit system. (* = significant to PM [$p < 0.05$]; n = 4 - 6).

Interestingly, the ATP amount of responder cells was significantly decreased after culturing hBMSCs for 14 days in osteogenic differentiation medium compared to cells which were cultured in proliferation medium. *Figure 126* presents the results of the cells which were cultured for 14 days.

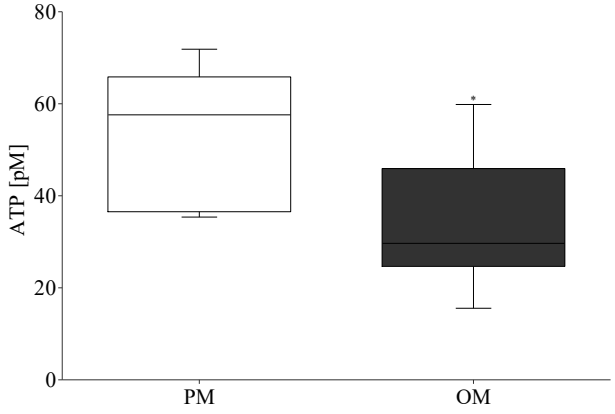

Figure 126: Determination of the amount of ATP at day 14. Responder hBMSCs were cultured in proliferation or osteogenic differentiation medium for 14 days and the amount of ATP was determined by a kit system. (OM = osteogenic differentiation, PM = proliferation medium: * = significant to PM [$p < 0.05$]; n = 6 - 7).

Figure 124, *figure 125* and *figure 126* show that the ATP amount varies during the test duration, in particular of cells which were treated in osteogenic differentiation medium. The cultivation in proliferation medium leads to very weak alterations.

In a second test series, responder and low responder cells were treated differently for 21 days. The low responder hBMSCs were cultured in osteogenic differentiation medium which was unsupplemented or supplemented with catalase, heat inactivated catalase, iron chloride or iron sulfate. The ATP amount was determined at day zero (control), seven and 21. The treatment

with catalase, heat inactivated catalase and the two iron bonds resulted in an increase of the ATP amount. Nonetheless, the elevation of the ATP amount was low and therefore the alterations were not significant. The results of three investigated low responder donors are shown in *figure 127*.

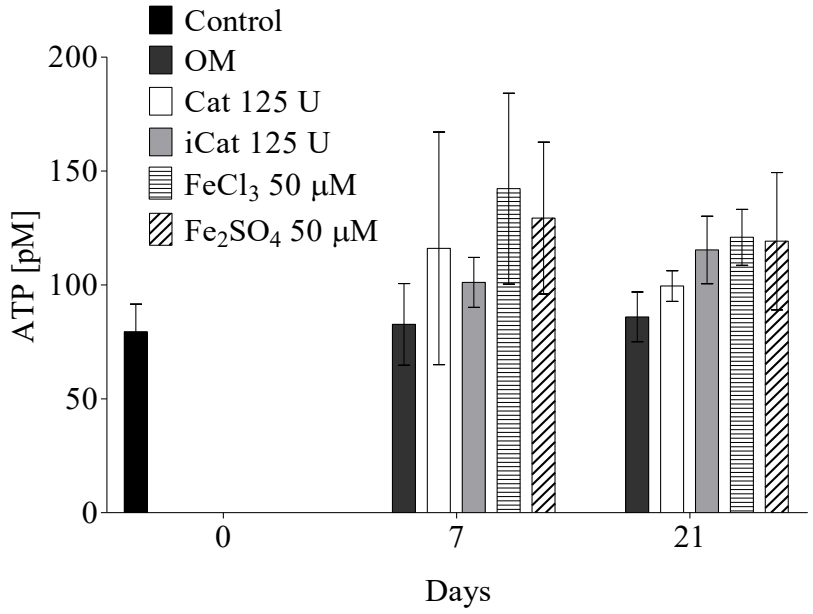

Figure 127: Analyzation of the amount of ATP at day zero, seven and 21. Low responder hBMSCs were cultured in proliferation medium until reaching confluence which is represented by day zero. For the following seven or rather 21 days, the cells were cultured in osteogenic differentiation medium which was supplemented differently (OM = osteogenic differentiation, PM = proliferation medium, Cat = catalase; iCat = heat inactivated catalase; n = 3).

Additionally, the ATP amount of one responder donor was also evaluated. *figure 128* demonstrates that the ATP amount reaches a maximum after cultivation in unsupplemented osteogenic differentiation medium. All additives led to a distinct decrease compared to the results of cells which were cultured in unsupplemented osteogenic differentiation medium for 21 days.

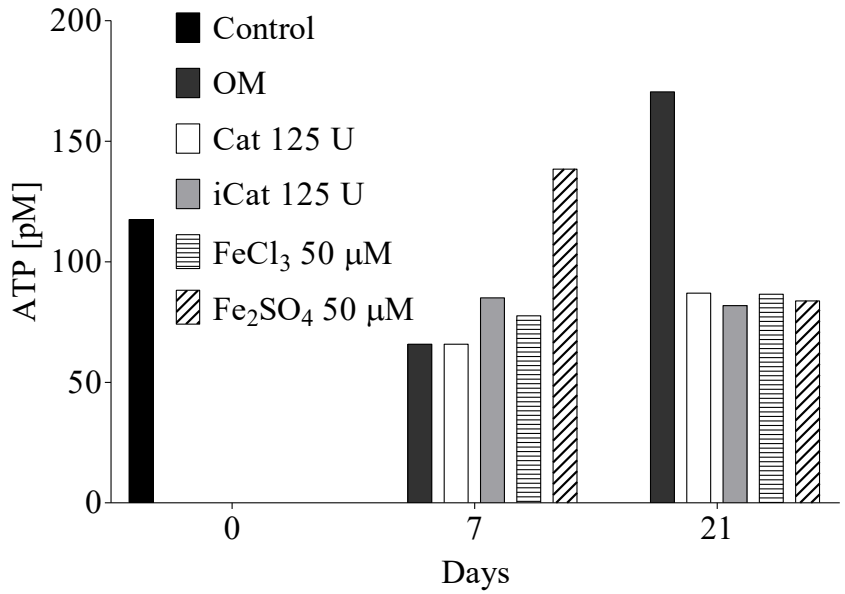

Figure 128: Analyzation of the amount of ATP at day zero, seven and 21. Responder hBMSCs were cultured in proliferation medium until reaching confluence which is represented by day zero. For the following seven or rather 21 days, the cells were cultured in osteogenic differentiation medium which was supplemented differently (OM = osteogenic differentiation, PM = proliferation medium, Cat = catalase iCat = heat inactivated catalase; n = 1).

5.7 Evaluation of the Amount of FGF-2

Because of the relevance of FGF-2 for proliferation and differentiation processes (see also: paragraph *5.4.1*), the alterations of FGF-2 amount depending on the different treatments were determined and assessed according to the impaired osteogenic differentiation potential of low responder cells. The cells were cultured in unsupplemented and catalase supplemented osteogenic differentiation medium for 14 days. The test was performed at day three, seven and 14. Since no differences of responder and low responder cultures were detectable, the results are presented condensed in *figure 129*. The figure presents that the catalase treatment resulted in a distinct increase of the FGF-2 amount. The high standard deviation indicates strong alterations of the individual donors.

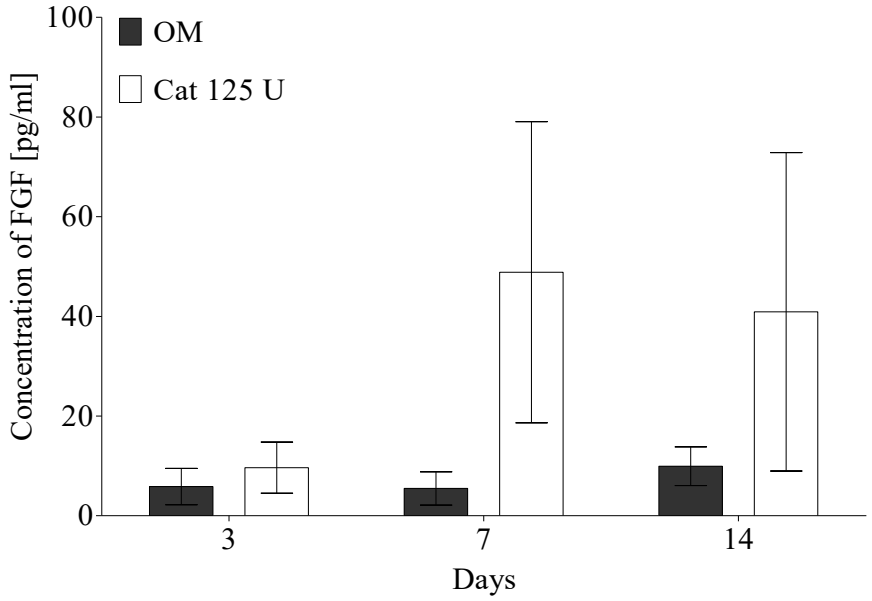

Figure 129: Measurement of the amount of FGF-2 of responder and low responder hBMSCs. At day three, seven and 14, the FGF-2 amount was determined by the FGF basic kit system. The cells were cultured in unsupplemented and catalase supplemented osteogenic differentiation medium (OM = osteogenic differentiation medium; Cat = catalase; n=6).

As shown in *figure 130*, the individual donors showed diverse reactions on the various treatments. A distinct consistency was not discernable during the test period.

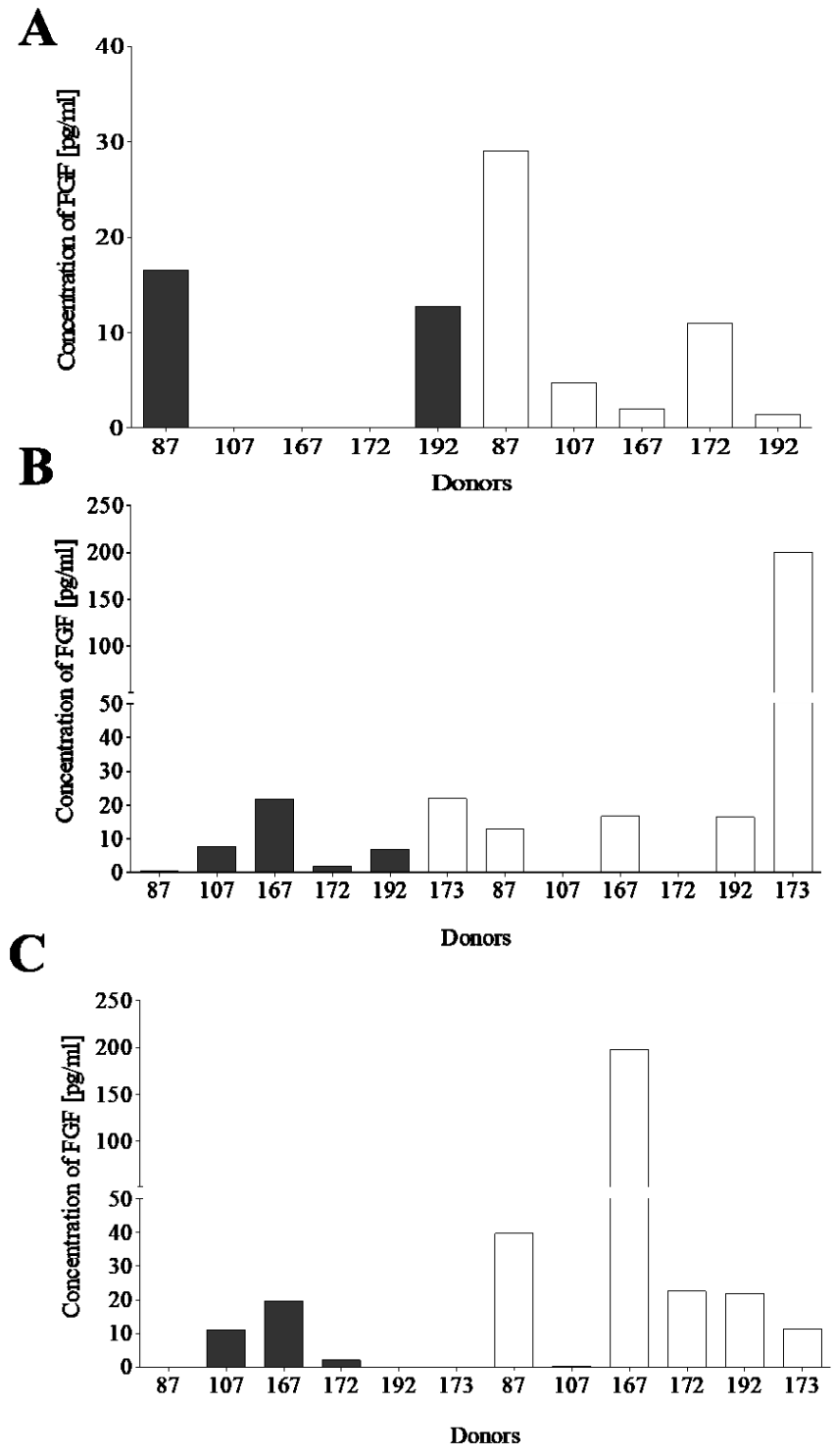

Figure 130: Individual measurements of the amount of FGF-2 of responder and low responder hBMSCs. At day three, seven and 21, the FGF-2 amount was determined by the FGF basic kit system. The cells were cultured in unsupplemented and catalase supplemented osteogenic differentiation medium for 14 days. A: results after three days of cultivation; B: results after seven days of cultivation; C: results after 14 days of cultivation (OM = osteogenic differentiation medium; iCat = heat inactivated catalase).

5.8 Determination of the Apoptosis Rate of Responder and Low Responder Cells

Since differences of responder and low responder donors regarding the extent of calcified matrix formation and the decreasing cell viability during culturing were observed, the apoptosis rate was investigated to find further indications for the reason of the impaired osteogenic differentiation potential of low responder cells. In *figure 131*, the apoptosis rate of three low responder donors is shown after culturing for four, seven and 14 days in osteogenic differentiation medium which was either unsupplemented or supplemented with catalase, heat inactivated catalase or EUK134. Since first signs of matrix calcification were seen at day 14, a heightened rate of apoptosis was expected in this test. The expected increase of the apoptosis rate can be seen in the figure. At day seven, the addition of catalase led to a decreased rate compared to cells which were treated in unsupplemented osteogenic differentiation medium. Remarkably, the addition of EUK134 resulted in a similar apoptosis rate at day 14. At day seven, this addition led to a distinct decrease whereas the supplementation of heat inactivated catalase resulted in a continuously increase of the apoptosis rate.

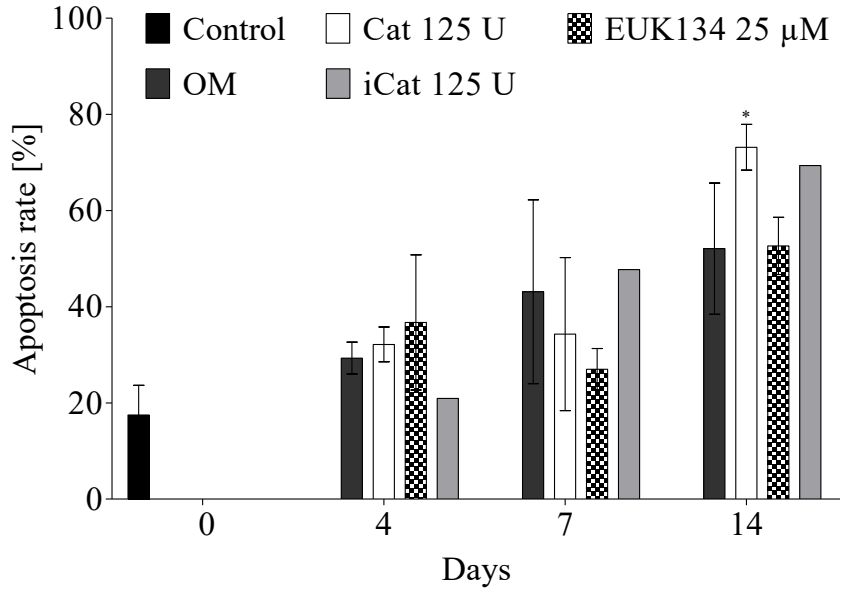

Figure 131: Apoptosis rate of low responder hBMSCs. After reaching confluence in proliferation medium (control), the low responder cells were cultured in differently supplemented osteogenic differentiation media (catalase, heat inactivated catalase, EUK134). The test was performed at day zero, four, seven and 14 (OM = osteogenic differentiation medium, Cat = catalase, iCat = heat inactivated catalase; * = significant to control [$p < 0.05$]; n = 1 - 3).

Figure 132 shows the results of the apoptosis determination of responder hBMSCs. The catalase treatment neither resulted in an increase nor in a distinct decrease of apoptosis. The addition of heat inactivated catalase led to a distinct decrease of the apoptosis rate. It is

important to point out that the test with heat inactivated catalase was run with only one donor. Only one donor was also treated with MnTBAP. Due to this fact, the results just provide indications and may not be representative. The apoptosis rate of responder and low responder cells were generally very similar. To conclude, a clear difference between responder and low responder hBMSCs was not detectable regarding apoptosis.

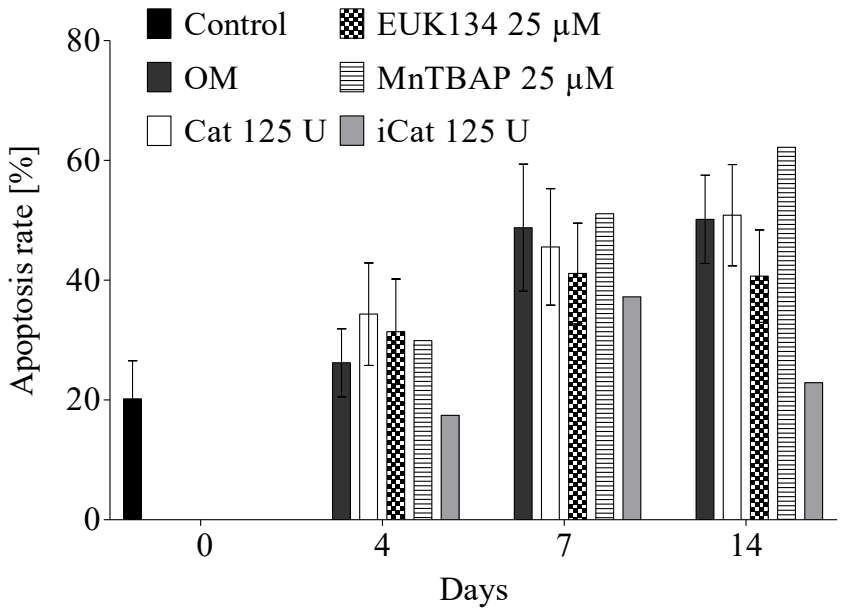

Figure 132: Apoptosis rate of responder hBMSCs. After reaching confluence in proliferation medium (control), the responder cells were cultured in differently supplemented osteogenic differentiation media (catalase, heat inactivated catalase, EUK134, MnTBAP). The test was performed at day zero, four, seven and 14 (OM = osteogenic differentiation medium; Cat = catalase, iCat = heat inactivated catalase n = 1 - 5).

5.9 Determination of the Amount of Hydroxyl Radicals

Paragraph *4.13.1* describes the procedure of the measurement of hydroxyl radicals. Since the hydroxyl radical generation theory discusses that catalase can also generate hydroxyl [105] radicals, the generated amount of hydroxyl radicals of low responder hBMSCs was determined. After a defined number of cells was cultured in proliferation medium until getting adherent, they were incubated with differently supplemented osteogenic differentiation media for 1.5 or 3.5 hours. In general, the incubation of 3.5 hours compared to an incubation of 1.5 hours resulted in a higher generated amount of hydroxyl radicals. Furthermore, it is important to note that the addition of catalase, heat inactivated catalase, hydrogen peroxide and the combination of catalase/heat inactivated catalase with hydrogen peroxide led to a higher amount of hydroxyl radicals. Interestingly, the incubations with catalase and with hydrogen

peroxide showed the most pronounced hydroxyl radical generation rate. The incubation of inactive catalase led to weak generation rate which is presented in *figure 133*.

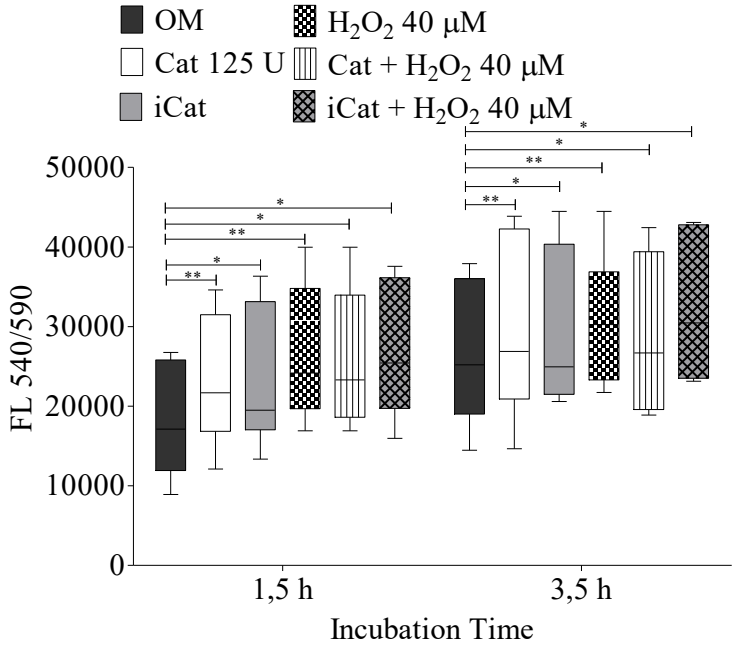

Figure 133: Evaluation of the amount of hydroxyl radicals. Low Responder and responder cells were incubated with unsupplemented or supplemented (catalase, heat inactivated catalase, hydrogen peroxide, combination of catalase / heat inactivated catalase with hydrogen peroxide) osteogenic differentiation medium for 1.5 or 3.5 hours. The amount of hydroxyl radicals is determined by a fluorescence reaction (OM = osteogenic differentiation medium, Cat = catalase, iCat= heat inactivated catalase; * = significant [$p < 0.05$]; (** = significant to control [$p < 0.033$]; n = 6).

5.10 Effects of the Degradation of Hydroxyl Radicals by Mannitol

The combination of 1 M mannitol and 125 U/ml catalase was added to osteogenic differentiation medium to assess the effect of hydroxyl radicals on the osteogenic differentiation of responder and low responder cell cultures. Mannitol is known as a hydroxyl radical scavenger [190]. To prove that the positive effect of catalase on the osteogenic differentiation was caused by the rise of the amount of hydroxyl radicals, the cells were treated with osteogenic differentiation medium which was supplemented with catalase and mannitol. In general, the catalase treatment resulted in a restored osteogenic differentiation potential of low responder cells. This effect was prevented by the further addition of mannitol. *Figure 134* demonstrates low responder cells which showed no indications of matrix formation. Analogously, responder cells, which are presented in *figure 135*, showed no matrix calcification. Remarkably, the cells of both donors showed stressed cell conditions.

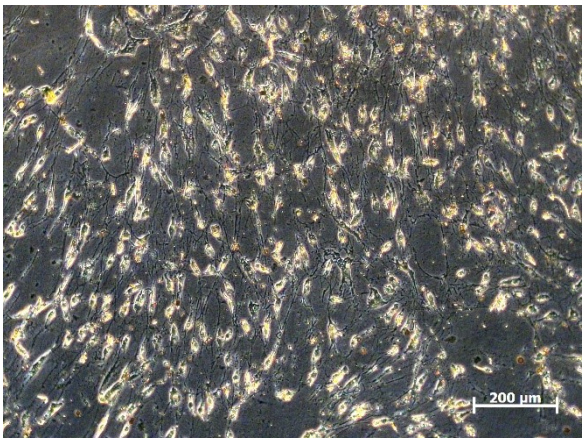

Figure 134: Low responder cells after a simultaneous treatment with a catalase and mannitol for 21 days. The cell cultures were stained with alizarin red to indicate calcified matrix.

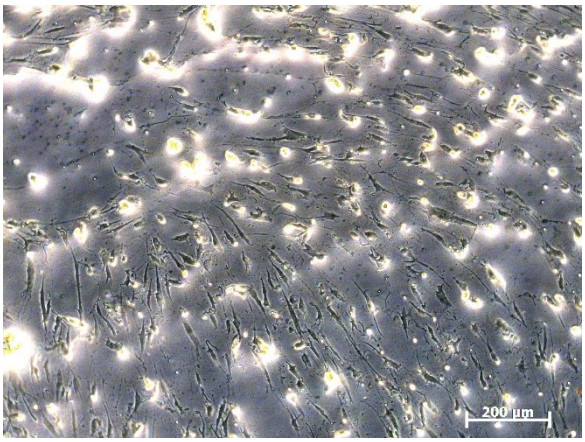

Figure 135: Responder cells after a simultaneous treatment with a catalase and mannitol for 21 days.

6 Discussion

To conclude, osteogenic differentiation of hBMSCs was characterized by a distinct formation of calcified matrix after culturing in an osteogenic differentiation medium. In case of an undisturbed osteogenic differentiation process, small calcified nodules were formed at least at day 14. At day 21, a pronounced calcified matrix covered the cell layer. To assess the dimension of osteogenic differentiation, the extent of matrix calcification and the elevation of the activity of alkaline phosphatase were determined. Interestingly, although treated equally, regular as well as osteogenically dysfunctional donors were observed. Regular donors are called responder donors and osteogenically dysfunctional donors are called low responder donors. Low responder donors are characterized by a significantly impaired osteogenic differentiation potential which is demonstrated by the loss of function to form a calcified matrix. During the cultivation of both donor types, no differences of the cell morphology were observed which would have indicated a reason for the disturbed osteogenic differentiation process.

The osteogenic differentiation potential of low responder hBMSCs could be restored by addition of 125 U/ml catalase to the osteogenic differentiation medium for a duration of 21 days. Whereas the catalase treatment did not influence the osteogenic differentiation potential of responder donors, the catalase treatment could restore the impaired osteogenic differentiation potential of low responder donors. Since catalase is known for the potential of degrading hydrogen peroxide, which is a harmful reactive oxygen species and therefore adversely affects cell proliferation and differentiation processes [76, 91, 191-193], impacts of other antioxidative substances on the osteogenic differentiation were also tested to assess the potentially positive effect of the antioxidative mechanism of catalase. The treatment with MnSOD, MnTBAP, trolox, mannitol, hemoglobin, thymol and EDTA, which is a chelator, affected the osteogenic differentiation potential of low responder cells slightly positive. Nevertheless, none of these additives could restore the osteogenic differentiation of low responder cells to the same extent as catalase did. Remarkably, the addition of EUK134 resulted in an impaired osteogenic differentiation of responder hBMSCs. The degradation of the superoxide anions as well as hydrogen peroxide by EUK134 supported the statement that a balanced amount of ROS was necessary for an undisturbed process of proliferation and differentiation [76]. Due to these outcomes, the impacts of an addition of hydrogen peroxide on the osteogenic differentiation of responder and low responder donors were also analyzed. The treatment neither promotes nor inhibited the osteogenic differentiation potential of responder and low responder cells up to a hydrogen peroxide concentration of 40 µM. The

treatment neither promotes nor inhibited the osteogenic differentiation potential of responder and low responder cells up to a hydrogen peroxide concentration of 40 µM.

In a next step, inactivated catalase was added to the hBMSCs during the cultivation in osteogenic differentiation medium. Since inactive catalase also restored osteogenic differentiation potential of low responder donors, the antioxidative mechanism of catalase seemed not to be the relevant mechanism to restore the impaired osteogenic differentiation potential of low responder donors. During the investigations of osteogenic differentiation, three diverse types of donors were observed. These donors included responder cells with a regular osteogenic differentiation potential, low responder cells with an impaired osteogenic differentiation potential which can be restored by the addition of catalase (so called: catalase responder cells) and low responder cells which showed before and after a treatment with catalase an impaired osteogenic differentiation potential (so called: catalase low responder cells).

As indicated that the antioxidative mechanism of catalase was not the only reason for an improvement of the osteogenic differentiation, further compounds of catalase such as iron of the active center of this enzyme [194] were tested. Therefore, hBMSCs were treated with iron chloride or iron sulfate. Both chemical bonds resulted in a restoration of the osteogenic differentiation potential of low responder donors. Simultaneously, the osteogenic differentiation of responder hBMSCs was impaired by a treatment with iron sulfate.

The treatments with catalase, heat inactivated catalase and iron compositions also influenced the protein expression of NOX4, catalase, FOXO1, Nrf2, GPX, AKT, p53, SOD1/2, aconitase1/2, SPARC, type 1collagen and osterix positively or adversely. In case of NOX4, catalase, FOXO1, Nrf2, p53, SOD1/2, aconitase1 and 2, no significant differences between the expression rates of responder or low responder were observed. SPARC, type 1 collagen and osterix are important matrix proteins [8] and were only demonstrated in responder or catalase responder hBMSCs.

Since no distinct differences of responder and low responder cells could be determined which would explain the two different osteogenic differentiation potentials, cell viability or rather proliferation rates of differently treated responder and low responder cell cultures were analyzed. The addition of catalase to proliferation medium did not enhance the cell viability of hBMSCs. The addition of catalase to osteogenic differentiation medium reduced the cell viability significantly compared to a treatment with unsupplemented proliferation and osteogenic differentiation medium. This was demonstrated by to different tests (see: *5.4.5.1*

and *5.4.6.1*) to exclude the idea that this effect was caused by a disturbed respiratory chain (see: chapter *4.4*).

Additionally, aspects of the energy metabolism, such as the amount of glucose and ATP, were determined to refer the results to the impaired osteogenic differentiation of low responder hBMSCs. The ATP amount of low responder cells was enhanced by catalase and the other additives at day seven and 21, whereas the cultivation of responder cells in unsupplemented osteogenic differentiation medium resulted in a significant enhanced amount of ATP at day three and seven and at day 14 in a reduced amount of ATP in comparison to responder cells which were cultured in proliferation medium.

Additionally, FGF-2 is known for being a regulator of the osteogenic differentiation [175, 188] and therefore was also evaluated according to the catalase treatment. Low responder and responder hBMSCs showed an enhanced FGF-2 amount caused by a catalase treatment. Nonetheless, the different donor types showed no differences among each other.

Since the formation of calcified matrix correlates with cell death (trapped osteocytes show within the balance of bone formation and resorption apoptosis [195]), the apoptosis rate of responder and low responder cells according to the different treatments was analyzed. At day 14, catalase treated low responder cells showed an elevated apoptosis rate compared to cells which were cultured in unsupplemented osteogenic differentiation medium. The heightened rate of apoptosis after a catalase treatment correlated with a formation of initial calcified nodules. In case of responder cells, the catalase treatment did not result in an elevated apoptosis rate compared to the outcome of untreated cells.

Interestingly, a hydroxyl radical generation theory is discussed in several scientific works which describes catalase as a hydroxyl radical generating substance [105, 196]. To test this theory, low responder and responder cell cultures were incubated with catalase, heat inactivated catalase, hydrogen peroxide and the combination of hydrogen peroxide with catalase or heat inactivated catalase which resulted in an elevated amount of hydrogen peroxide radicals compared to the amount which was measured in the unsupplemented osteogenic differentiation medium. To lastly investigate the effect of the hydroxyl radical degradation on the osteogenic differentiation potential, responder and low responder hBMSCs were cultured in osteogenic differentiation medium which was supplemented with a combination of mannitol and catalase. The osteogenic differentiation of responder cells was prevented by this treatment and the catalase-caused restoration of the impaired osteogenic differentiation potential was impeded.

6.1 Restoration of an Impaired Osteogenic Differentiation Potential

As illustrated in *Figure 34*, not all hBMSC cultures showed a pronounced osteogenic differentiation after cultivation in osteogenic differentiation medium. Since the osteogenic differentiation of MSCs is regulated by a series of molecular pathways, the causes for this serious phenomenon can be various [31, 57, 197]. Within this work, we concentrated on the adverse effects of oxidative stress [91, 198, 199]. Furthermore, the addition of catalase during the osteogenic differentiation process of adipogenic stromal cells showed promising effects. Low responder donors of adipogenic stromal cells with a weak or a non-existing osteogenic differentiation were treated with catalase. The treated cells showed a restored osteogenic differentiation potential. For that reason, hBMSCs were also treated with catalase to investigate the restoration potential of catalase also for this type of cells. Interestingly, low responder hBMSCs showed a distinct restoration of the osteogenic differentiation potential. Consequently, catalase influenced osteogenic differentiation regulatory pathways. In particular, catalase is known for its distinct antioxidative effect by the degradation of the harmful ROS hydrogen peroxide [98, 200, 201]. For that reason, it was assumed that the antioxidative reaction by degrading hydrogen peroxide to water and oxygen was the key mechanism to optimize osteogenic differentiation of low responder cells which might have had, according to the outcomes so far, an elevated amount of ROS which in turn would have had adversely affected the osteogenic differentiation potential. An elevated level of ROS inhibits osteogenesis and promotes adipogenesis, whereas low ROS concentrations show opposite effects [91, 202]. It is important to point out that in general, cells are cultured in normoxic conditions (21 % O_2) even though the oxygen level *in vitro* is significantly lower [203]. For example, in vascularized tissue, the oxygen level is about 10 – 15% [204]. In case of hypoxic conditions, chondrogenic differentiation is promoted and simultaneously osteogenic differentiation is inhibited [205-208]. However, it must be noted that the already heightened oxygen concentration [203] was further increased by the degradation reaction of hydrogen peroxide which potentially inhibited a pronounced *in vitro* osteogenic differentiation. Sheehy *et al.* proofed that BMSCs show an improved osteogenic differentiation potential if cultured at oxygen concentrations of 5 % [209]. Therefore, the *in vitro* investigation approach was not performed under realistic physiological conditions. The transferability of *in vitro* results to in vivo processes might not be fulfilled.

Continuously, to proof that the elevated concentration of ROS of low responder hBMSCs was the sole reason for the distinct impaired osteogenic differentiation processes, further antioxidative substances were individually added to the cell cultures during the osteogenic

differentiation process for 21 days. Since not one additive could restore the impaired osteogenic differentiation potential of low responder like catalase did, it was demonstrated that the antioxidative effects were not the only reason for the optimization of the impaired osteogenic differentiation potential. Nonetheless, it is important to note that all used additives showed different antioxidative reactions which is explained in paragraph *4.3*. Thus, the cellular hydrogen peroxide amount was only reduced by catalase. Moreover, the used MnSOD and catalase mimetic EUK134 could also degrade hydrogen peroxide but additionally degraded superoxide anions. The fact that the treatment with EUK134 resulted in visibly stressed cells and in a significant inhibition of osteogenic differentiation of even responder hBMSCs proved that a total reduction of ROS also affected the osteogenic differentiation potential adversely. Consequently, a balanced amount of ROS was obligatory to achieve an optimal osteogenic differentiation which is indicated by several publications [91, 210, 211]. *Figure 43* demonstrates that the treatment with trolox [212], a water-soluble analog of vitamin E, resulted in an enhanced adipogenic differentiation. It is important to note that adipogenic and osteogenic differentiation are balanced processes. *Inter alia*, transcription factors can promote adipogenic differentiation and simultaneously prevent osteogenic differentiation [213, 214] which is highlighted in *figure 8*.

Even though trolox showed antioxidative effects and consequently should have promoted osteogenic differentiation instead of adipogenic differentiation, the results were contrary. Authors such as Alcala *et al.* demonstrated that the treatment with vitamin E leads to degradation of ROS [215, 216]. The loss of ROS as a second messenger within the adipogenic regulation inhibits C/EBPα-dependent adipocyte differentiation. Furthermore, the expansion of rpWAT (retroperitoneal white adipose tissue) is blocked and the accumulation of lipids within the liver is forced [217, 218]. Since the accumulation of lipids was observed in every trolox treated donor, the function of trolox during the adipogenic differentiation process remains to be investigated more detailed. As a balance of an amount of ROS is obligatory for optimal osteogenic processes [217, 218], the effects of a treatment with hydrogen peroxide on the osteogenic differentiation were evaluated. The osteogenic differentiation of responder and low responder cells was not affected by the addition of hydrogen peroxide which proved that concentrations up to 40 µM did not adversely affect the osteogenic differentiation of hBMSCs, even though Bai and coworkers showed significant influences on differentiation processes [217, 218]. Additionally, Lee *et al.* showed that also the cell viability and the activity of alkaline phosphatase are clearly affected by a hydrogen peroxide treatment [192]. In this case, it is important to note that the investigated cells were not hBMSCs and the test

durations and hydrogen peroxide concentrations varied from our setting. Bais test duration was set to a maximum of 15 days and the lowest tested concentration of hydrogen peroxide was 100 µM [217, 218]. Our investigations of hBMSCs highlighted that a hydrogen peroxide concentration of 100 µM led to pronounced cell death. HBMSCs demonstrably exhibited a more sensible behavior to reactive oxygen species compared to other cell types. Furthermore, they showed a reduced alkaline phosphatase activity which resulted in an impaired osteogenic differentiation.

The osteogenic differentiation potential was assessed by determining the extent of formed calcified matrix and the activity of alkaline phosphatase [219]. Since the activity of alkaline phosphatase of low responder cell cultures during the osteogenic differentiation showed no abnormalities compared to responder cells, even though the activity was further increased by the treatment with substances which positively regulate the osteogenic differentiation such as catalase, also the protein expression of alkaline phosphatase of responder and low responder hBMSCs was determined to prove that the disturbance of the osteogenic differentiation of low responder donors was not related to the alkaline phosphatase expression or activity. Due to no differences of responder and low responder donors regarding the expression of alkaline phosphatase, the disturbed pathway, which could be corrected *inter alia* by catalase, is a pathway of the downstream osteogenic processes. For that reason, the investigation of upstream pathways or transcription factors was not reasonable and the transcription factor Runx2, which regulates the induction of alkaline phosphatase [220], was not further tested. Furthermore, a detection of Runx2 by Western blot, caused by a weak expression pattern, was not precisely possible. To safely exclude any influences by Runx2, further investigations of this protein are required [220].

6.1.1 Regulation of Osteogenic Differentiation by Catalase, Inactivated Catalase and Iron Compounds

Because of prooxidative and antioxidative mechanisms, 125 U/ml catalase was heat inactivated and used equally as active catalase to prove that the antioxidative effect was not or at least not the only reason for the ability of osteogenic differentiation restoration. Analogous to Gil and coworkers [98], we assessed the success of the inactivation by a performance of a catalase activity assay. The heat-treated catalase showed no activity and therefore lost the antioxidative effects. Due to multiple performances of this assay, the loss of activity was ensured. The addition of heat or aminotriazole inactivated catalase also restored the impaired osteogenic differentiation potential of low responder cells as significant as active catalase did

and therefore, the impairment of the osteogenic differentiation was not caused by oxidative stress of hydrogen peroxide. Consequently to these results, the structure of catalase was considered. The active center of catalase contains a protoporphyrin ring with iron (see: chapter *1.4.2.1*) and therefore, the treatment of hBMSCs during the osteogenic differentiation with various concentrations of iron chloride and sulfate was investigated. Since iron sulfate could achieve an equal restoration potential of impaired osteogenic differentiations of low responder cells, the restoration by only catalase was debunked. However, Fe^{2+} and Fe^{3+} ions are also able to degrade hydrogen peroxide [221]. Haber and coworkers established the chemical reaction of the hydrogen peroxidase degradation by Fe^{2+} ions and called this type of reaction Haber-Weiss-reaction. Nonetheless, this hydrogen peroxide degradation reaction is not a catalase mimetic reaction. In this case, a free radical mechanism, which describes the degradation of hydrogen peroxide by uncomplexed free iron ions, was performed [221-224]. It is important to note that Melnyk and coworkers found out that a pH range smaller than two is obligatory for a successful reaction [225]. Higher pH values demonstrably prevent the degradation of hydrogen peroxide nearly completely [226]. Since the investigated cell culture showed a physiological pH range for the entire test period (monitored by the phenol red indicator of the medium), it could be assumed that the hydroxyl peroxide degradation and the related reduction of reactive oxygen species were not the reason for an optimized osteogenic differentiation of low responder hBMSCs. Nonetheless, hydroxyl radicals were generated by the Haber-Weiss reaction and Fe^{3+} ions were reduced by the Fenton reaction [227] which in turn led to hydroxyl radical generation. Haber-Weiss reaction and Fenton reaction are the relevant reactions of the free radical mechanism which is shown in *figure 136*.

$$Fe^{3+} + H_2O_2 \rightarrow Fe^{2+} + H^+ + HO_2^{\cdot}$$

$$Fe^{3+} + H_2O_2 \rightarrow Fe^{2+} + 2H^+ + O_2^{\cdot -}$$

$$Fe^{2+} + H_2O_2 \rightarrow Fe^{3+} + OH^- + OH^{\cdot}$$

$$Fe^{2+} + H_2O_2 \rightarrow FeO^{2+} + H_2O$$

$$FeO^{2+} + H_2O \rightarrow Fe^{3+} + O_2^{\cdot -}$$

$$FeO^{2+} + RH \rightarrow Fe^{3+} + OH^- + R^{\cdot}$$

$$OH^{\cdot} + RH \rightarrow H_2O + R^{\cdot}$$

$$Fe^{3+} + O_2^{\cdot -} \rightarrow Fe^{2+} + O_2$$

$$OH^{\cdot} + H_2O_2 \rightarrow H_2O + HO_2^{\cdot}$$

$$OH^{\cdot} + H_2O_2 \rightarrow H_2O + H^+ + O_2^{\cdot -}$$

$$Fe^{2+} + OH^{\cdot} \rightarrow Fe^{3+} + OH^-$$

$$Fe^{3+} + HO_2^{\cdot} \rightarrow Fe^{2+} + O_2 + H^+$$

$$Fe^{2+} + HO_2^{\cdot} \rightarrow Fe^{3+} + HO_2^-$$

$$R^{\cdot} + O_2 \rightarrow RO_2^{\cdot}$$

$$Fe^{2+} + RO_2^{\cdot} \rightarrow Fe^{3+} + RO_2^- \qquad \text{R = substrate}$$

Figure 136: Hydrogen peroxide degradation by the free radical mechanism with hydrated Fe2+ und Fe3+ ions. Reaction 1 and 2 show the Haber-Weiss and Fenton reaction in detail. Own representation based on [226].

Figure 137 shows the physiological generation of reactive oxygen species by the NADPH oxidases. The importance of NADPH, superoxide dismutase, catalase and glutathione peroxidase as the most relevant enzymes during the reactive oxygen generation is highlighted. The enzymes form a reactivity series where all enzymes are interdependent. This schematic representation also emphasizes the relevance of Fe^{3+} ions within the hydroxyl radical generation.

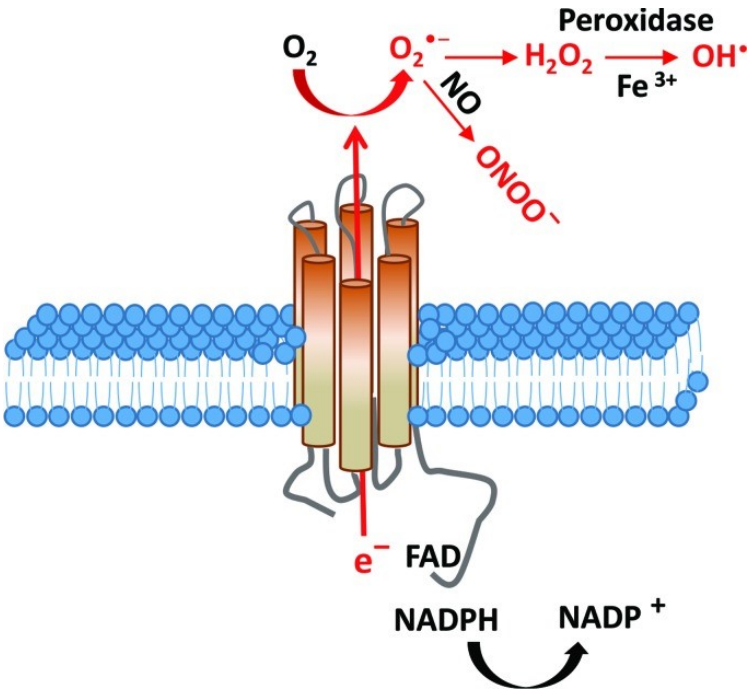

Figure 137: Generation of reactive oxygen species by NADPH oxidases. Oxygen is reduced to superoxide anions by NOX enzymes. Pyridine nucleotide NADPH as an electron donor and molecular oxygen as an electron acceptor are used. Superoxide anions can react with nitric oxide to form a harmful peroxynitrite. Superoxide anions can also be dismutated to hydrogen peroxide by the superoxide dismutase. Hydrogen peroxide can induce cell signaling cascades or react with catalase, glutathione peroxidase or Fe^{3+} to form hydroxyl radicals [91].

Within the hydroxyl radical generation theory, also catalase is discussed as a hydroxyl radical generating substance. The hydroxyl radical generation is performed at lower concentrations of hydrogen peroxide [105, 196]. In case of the reaction of catalase, the iron (III) protoporphyrin is the relevant component to generate hydroxyl radicals (see: chapter *1.4.2.1*). Furthermore, the heat inactivation presumable did not destroy the structure of iron (III) protoporphyrin. The iron (III) protoporphyrin structure could perform the catalytic reaction, even though it was not bound to rest of the protein, whereas the iron (III) protoporphyrin missing protein structure neither could degrade hydrogen peroxide nor generate hydroxyl radicals. In this case, it is important to note that catalase, which was irreversibly inhibited by aminotriazole, might be able to generate hydroxyl radicals because aminotriazole stabilizes the compound I structure which is formed during the chemical reaction of catalase. Due to the balance of the structures compound I, compound II and ferricatalase, the degradation is enabled. Compound I is relevant during the first steps of the chemical reaction and therefore is relevant for the hydroxyl radical generation [228].

Since hydroxyl radicals are highly active radicals, impacts on cell signaling, aging and apoptosis processes are hypothesized [229]. Assuming that hydroxyl radicals can restore the osteogenic differentiation potential of low responder cells, they were, despite their harmful

effects, promising substances in case of impaired bone healing. This hypothesis would have also explained why not one of the other tested antioxidatives resulted in a restoration of an impaired osteogenic differentiation potential. Due to this assumption, hydroxyl radicals were determined of the cell cultures which were incubated with catalase, inactivated catalase, hydrogen peroxide and the combination of hydrogen peroxide with catalase or inactivated catalase by a fluorescence assay. Since all additions resulted in an increase of the hydroxyl radical amount, catalase and heat inactivated catalase could generate hydroxyl radicals as hydrogen peroxide did. These results confirm the hydroxyl radical generation theory. As the half-life period of hydroxyl radicals in biological systems is approximately 1 ns, it is a highly reactive radical [230]. Therefore, it is reasonable that the radical is unselective according to the coreactants and this in turn results in various molecular changes. In consideration of the high reactivity of these radicals, a reliable determination was difficult. We evaluated the hydroxyl radical amount after incubation times of 1.5 and 3.5 hours. It was observed that the incubation period for 3.5 hours resulted in a higher fluorescence intensity and apparently in an increase of the amount of hydroxyl radicals of all tested samples which led to less significant differences among the samples. As the hydroxyl radicals fastly reacted with other coreactants, this increase appeared not to be reasonable. Nonetheless, the differences of the hydroxyl radical amounts after an incubation period of 1.5 hours were significant. Therefore, these results appeared to be reliable. Additionally, the number of tested donors emphasized this reliability. Moreover, the citations of other working groups also confirmed the credibility of this test procedure. Considering these facts, the total amount of ROS was not reduced which might have been the reason for observing few indications of adipogenesis. Adipogenesis was assessed under equal conditions as the osteogenic differentiation processes were analyzed. Oil red staining highlighted the formation of lipid accumulations. Interestingly, catalase did not inhibit adipogenic differentiation. For all osteogenic specific tests, osteogenic differentiation medium was used which in general prevents adipogenic processes. In this case, the addition of catalase led to a distinct restoration of osteogenic differentiation and additionally to a slight increase of the adipogenic differentiation. The fact that catalase aided adipogenic processes is an additional argument for the hydroxyl radical generation theory. Remarkably, catalase treated responder hBMSCs neither showed a further improvement nor an impairment of the osteogenic differentiation potential, whereas responder cells, which were treated with iron sulfate, showed a significant impairment of the osteogenic differentiation. If catalase as well as Fe^{2+} ions both had generated hydroxyl radicals and if in turn these had constituted the reason for a positive impact on an impaired osteogenic differentiation potential, it would have

been reasonable that the catalase addition and the addition of Fe^{2+} ions resulted in an impairment of osteogenic differentiation of responder cells. Since this was not the case, it needs to be further investigated if hydroxyl radicals can restore weakened osteogenic differentiation potentials. Furthermore, the cytotoxic effects of elevated iron concentrations might have also been the reason for the impairment of the osteogenic differentiation potential of responder donors. Nonetheless, it remains to be ascertained which osteogenesis relevant pathway eventually is affected by hydroxyl radicals or rather which pathway of osteogenically dysfunctional hBMSCs is disturbed and can be restored by an increase of hydroxyl radicals. Additionally, adversely effects of these highly reactive and harmful reactive oxygen species must be carefully considered. It also might have been the case that catalase and iron compounds affected the osteogenesis by different pathways. Even though the outcome – a significantly restored osteogenic differentiation – was obviously identical, the pathways, which led to the equal outcome, might have been different. Furthermore, the potential of catalase to react as an antioxidant by degrading hydrogen peroxide and thus to decrease the total amount of reactive oxygen species, which is a crucial factor to improve the osteogenesis and impair the adipogenesis, and the potential ability to form hydroxyl radicals and act as an oxidant might be conceivable reasons for the improvement of the impaired osteogenic differentiation of low responder cells.

Since NADPH oxidases are the most important physiological sources of reactive oxygen species [91, 231, 232], the protein expressions of linked enzymes were determined according to the different treatments during the osteogenic differentiation investigations. The added catalase led to a decrease of the NOX4 expression. If the degradation of hydrogen peroxide and the connected decrease of the amount of ROS had been performed, an opposite result would have been expected. Reactive oxygen species were generated by NOX4 (see: section *1.4.1*) and in case of a decrease of reactive oxygen species, a higher activity would have been reasonable to balance the physiological amount of reactive oxygen species, which, as previously explained, is obligatory for cell signaling processes in healthy conditions. Interestingly, the addition of inactivated catalase and the combination of Fe^{3+} and catalase showed similar outcomes which indicated that the mechanisms of action were potentially equal. As previously hypothesized, the used additives might have been capable of generating hydroxyl radicals which in turn might have been the reason for the decrease of the expression of NOX4 because the total amount would have been elevated instead of reduced and therefore, the generation of reactive oxygen species by NOX4 would not have been necessary. Since no significant differences between responder and low responder donors regarding the

NOX4 expression were observed, it could be assumed that the effect on the NOX4 expression was not the key factor according to the restoration of osteogenic differentiation of low responder hBMSCs.

Catalase protein expression showed a similar expression pattern compared to the NOX4 expression. Therefore, the additives also led to a decrease of the catalase expression at day 21, whereas the expression at day seven was non-significantly changed. Interestingly, the combination of Fe^{3+} and catalase resulted in the highest expression rate at day seven and at day 21 in the lowest rate. This outcome indicated that the regulation of the osteogenic differentiation by catalase might have been different to the impacts of the combination of Fe^{3+} and catalase. Nonetheless, the trend of the expressions resembled one another which indicated a similar regulation of the osteogenic differentiation. It is important to note that in general, the expression of catalase protein was increased as an effect of a higher amount of reactive oxygen species, in particular of hydrogen peroxide, to reduce the harmful high amount of reactive oxygen species. The expression of glutathione peroxidase was equal to the expression pattern of catalase protein which corroborated the hypothesis that the used additives led to an elevated amount of reactive oxygen species and consequently to an upregulated expression of antioxidative enzymes. The results confirmed that catalase, inactivated catalase and the combination of Fe^{3+} and catalase might have generated hydroxyl radicals which in turn resulted in a heightened oxidative stress. This oxidative stress regulated an upregulation of antioxidative pathways. The decrease of the expressions at day 21 might have been reasoned by an enhanced matrix calcification and the related increased cell death. Analogous to the expression of NOX4, no differences between responder and low responder donors were apparent which led to the assumptions that these results did not describe the key factor of the improved osteogenic differentiation potential. Due to the degradation potential of hydrogen peroxide by catalase, also the expression of SOD1 and SOD2 were analyzed. The expression rate of SOD2 increased significantly. In this case, it is important to note that, by degrading superoxide anions, the superoxide dismutase generated hydrogen peroxide which was degraded by catalase. Therefore, the reaction balance of the superoxide dismutase was changed because of the reduced hydrogen peroxide so that more superoxide anions could be degraded and thus, the expression rate of superoxide dismutase was elevated. In case of the assumption that hydrogen peroxide had been decreased by catalase and the other additives and therefore the balance of the reaction of superoxide dismutase had been disturbed, it would have been reasonable to result in a heightened expression so that more superoxide anions could be reduced. However, the addition of catalase and inactivated catalase showed the same

outcomes, even though the inactivated catalase could not degrade hydrogen peroxide. This in turn counteracted with the previous statement. The reason for an enhanced expression rate was not clarified. Nonetheless, distinct differences between responder and low responder donors were not apparent. Therefore, it could be assumed that also these results did not describe the key factor of the improved osteogenic differentiation potential. Additionally, to be sure that the cytosolic expression of the superoxide dismutase was equal to the expression of mitochondrial superoxide dismutase, the expression of SOD1 (cytosolic superoxide dismutase) was determined. The expression patterns were similar but not completely matching which might have been reasoned by the difficult determination caused by the weak expression pattern.

Since nuclear factor erythroid 2-related factor 2 (Nrf2) is known for influencing the osteoblastogenesis and the osteoclastogenesis [233, 234], the expression rate according to the different treatments was evaluated. Nrf2 mediates the redox dependent cellular adaptation [233, 234]. As shown in *figure 138*, oxidative stress led to an inhibition of Kelchc-like ECH-associated protein 1 (Keap 1, binding domain for Nrf2) and thus, Nrf2 was released and could migrate into the cell nucleus where it stimulated the expression of antioxidative enzymes. As previously explained, a diminished level of reactive oxygen species supports the osteogenic differentiation [235].

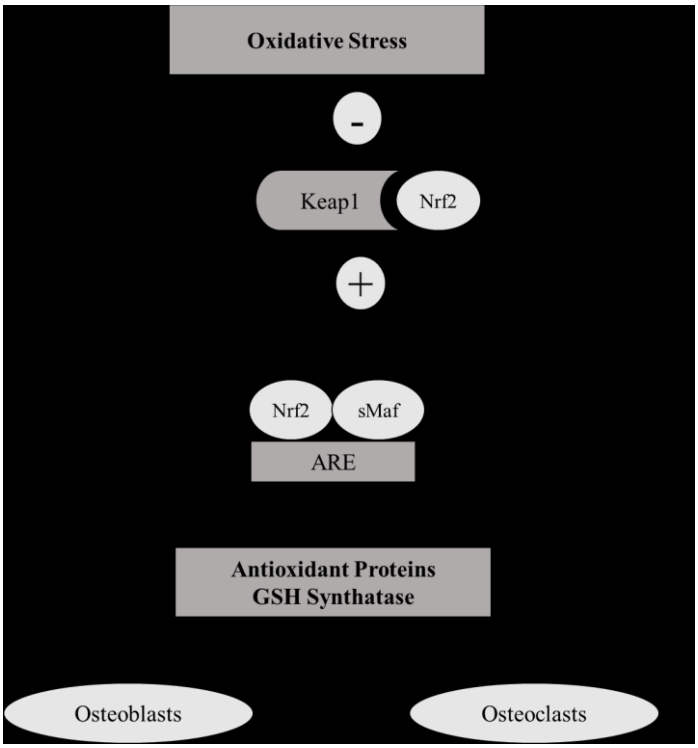

Figure 138: Nrf2 regulation in osteoblasts and osteoclasts. Inhibition of Keap1 by oxidative stress causes the release of Nrf2. In the following, Nrf2 activates antioxidant genes in the cell nucleus. Antioxidant proteins positively affect osteoblast differentiation and simultaneously adversely affect osteoclasts osteoclastogenesis. Own representation based on [202].

Additionally, Nrf2 deficiency supports osteoclastogenesis which in turn leads to a lower bone mass and diminished bone strength [236, 237]. Thus, Nrf2 is important for the regulation of the balance between bone formation and resorption. Furthermore, intracellular levels of reactive oxygen species in osteoclasts are elevated caused by a deletion of Nrf2. This in turn results in subsequent increasing osteoclast numbers and a higher osteoclast activity [236]. The relationship between osteoclast and osteoblast differentiation processes and Nrf2 or ROS appears to be complex since the deletion of Nrf2 promotes osteoclastogenesis and the related bone resorption and an overexpression of Nrf2 adversely affects osteoblast differentiation. Overexpression of Nrf2 results in an inhibition of Runx2 whose upregulation is obligatory for further osteogenic differentiation processes [238, 239]. These results highlight that Nrf2 only shows positives effects on the osteogenic differentiation within an ideal range [235]. Interestingly, the Nrf2 expression rate was decreased at day 7 and 21 by the addition of catalase, inactivated catalase and the combination of catalase and Fe^{3+}, even though it was hypothesized that these additives might have generated hydroxyl radicals which may have led to an elevated generation of antioxidative proteins and therefore to a support of osteoblastogenesis. Since the osteogenesis at day 21 was at its optimum, it was reasonable that the bone resorption by osteoclasts was inhibited. Referring to the outcomes of the NRf2

expression, it might have been the case that elevated levels of reactive oxygen species prevented a further Nrf2 expression which might have resulted in an overexpression. The overexpression could be the reason for an enhanced osteoclastogenesis and an impaired osteoblastogenesis. These results and the hypotheses matched the observations of Hinoi and coworkers that an ideal range of Nrf2 is necessary for an optimal osteogenic differentiation [239]. To clarify this problem, the Nrf2 expression of responder donors under the same conditions is required to be evaluated. Furthermore, determinations of Keap1 and indications of osteoclastogenesis also need to be analyzed to draw a representative conclusion.

FOXO1 is an important regulator of the osteogenic differentiation by influencing diverse osteogenic transcription factors [240]. Wang and coworkers showed that hydrogen peroxide activates the receptor activator of NF-κB ligand (RANKL) which results in a downregulation of FOXO1 by the activation of extracellular signal-regulated kinases (ERK) and Akt (protein kinase B) [218, 241, 242]. The downregulation of FOXO1 leads to a decrease of the expression of Runx2 and osterix and thus in an attenuation of bone formation [243]. The FOXO1 regulation also causes a downregulation of the catalase expression which is the reason for an elevation of hydrogen peroxide levels and a heightened stimulation of bone resorption [244]. Thus, a deletion of FOXO1 leads to a reduced bone mass and an activation of FOXO1 decreases the osteoclastogenesis and the related bone resorption [245]. Consequently, FOXO1 is a relevant transcription factor of the osteogenesis and needed to be investigated. Interestingly, just the addition of catalase changed the expression pattern of FOXO1. The expression rate was increased significantly at day seven as well as at day 21. The increased expression and correlated activity of FOXO1 resulted in an upregulation of catalase protein expression referring to the previously described scientific insights in the osteogenic differentiation. On the contrary, the expression of catalase was decreased by the catalase treatment. Since the other additives showed no visible influence on the FOXO1 expression, it might have been a catalase-specific effect which could have been attributed to the fact that catalase generates hydroxyl radicals but also can degrade hydrogen peroxide. It has been investigated that just hydrogen peroxide and not one of the other reactive oxygen species can adversely influence the FOXO1 regulation [245]. Nonetheless, the effects of FOXO1 need to be evaluated more detailed and the FOXO1 expression rates of responder donors are required to be determined.

6.1.2 The Matrix Proteins SPARC and Collagen Type 1 highlight the Impairment of the Osteogenic Differentiation of Low Responder Donors

By PCR and immunofluorescence staining, the matrix proteins SPARC and collagen type 1 were detected to show that low responder donors lost the ability to express matrix proteins and show insights of matrix calcification. Both analyses confirmed the hypothesis that low responder cells did not express matrix proteins such as SPARC or COL1A1 or the downstream regulator osterix. The restoration of the impaired osteogenic differentiation potential was enabled by the addition of catalase. As previously described, the addition of catalase elevated the formation of calcified matrix which was also confirmed with these investigations. Furthermore, the catalase treatment for different time durations highlighted that a short-term incubation of the cell cultures with catalase did not result in a restoration of the impaired osteogenic differentiation of low responder cells. Additionally, the protein expression and the activity of alkaline phosphatase, which is an initial regulator of the osteogenesis (see: paragraph *1.2.3.1*) did not vary between responder and low responder hBMSCs. Due to these facts, it could be assumed that in case of the impaired osteogenic differentiation potential of low responder cells, the regulation of the matrix formation including the expression of the matrix proteins was disturbed. For that reason, it was relevant to assess the expression of the matrix proteins.

6.2 Investigation of Apoptosis and Cell Viability of Responder and Low Responder Cells

Since the pathway, which caused the loss of the osteogenic differentiation potential, was not clearly enlightened, the apoptosis rate and cell viability were investigated under different conditions to reveal potential differences of the responder and low responder donors which might have explained the impaired osteogenic differentiation of low responder cells. An increased apoptosis rate, a decreased rate of the cell viability or rather proliferation rate would have been a sensible reason for the loss of the osteogenic differentiation potential and thus a disturbance of pro- and anti-apoptotic pathways could have caused the outcomes.

6.2.1 The Apoptosis Rate of Low Responder Cells Show no Conspicuous Features

The relevant additives such as catalase and inactivated catalase showed no significant impact on the apoptosis of hBMSCs during the osteogenic differentiation process. Although the catalase treatment resulted in a slightly elevated apoptosis rate which might have been caused by the beginning matrix calcification and the related simultaneous start of cell death, no significant differences between the diversely treated cells were observed. Additionally, no clear differences between responder and low responder were observed which would have

indicated that apoptosis related pathways of low responder hBMSCs show any disturbance. Nonetheless, Akt and p53 as one of the most important pro- and anti-apoptotic regulators were investigated to certainly exclude a disturbance of the apoptosis pathways [246-248].

p53 promotes many cellular processes such as cell senescence cell cycle arrest and programmed cell death [249]. In case of increased levels of active p53 reduced proliferation rates, a decreased expression of Runx2 and an impaired osteogenic differentiation are observed. On the contrary, a p53 deficiency in osteoprogenitor cells exhibits increased proliferation rates, an enhanced expression of Runx2 and an improved osteoblast maturation [250]. Akt (also known as Phosphatidylinositol-3-kinase) is also characterized by a diversity of functions regarding the cell viability [251, 252]. As shown in *figure 139*, the pro-apoptotic regulator p53 counteracted with the anti-apoptotic regulator Akt. The crosstalk was linked via Mdm2. Due to this interaction of these two important regulators of cell death or cell survival, the expression patterns according to the diverse treatments during the osteogenic differentiation process were determined and assessed. Interestingly, the expression of p53 of low responder cells was enhanced by the addition of catalase at day seven and 21. The increase was more distinct at day 21. In particular at day 21, the individual additions of catalase, heat inactivated catalase and the combination of catalase and iron chloride showed a distinct upward trend. Since the matrix formation is associated with cell death (see: paragraph *1.2.3.1*), an increasing expression of p53 was reasonable because the used additives demonstrably led to an improved matrix formation. However, the slight increase of the p53 expression at day seven was not reasonable considering that at these early stages, the cells just started the osteogenic differentiation processes and no calcified matrix was already formed at this time. On the contrary, the expression of p53 of responder hBMSCs was decreased at day seven by the treatments. Due to the weak expression patterns of p53, these results might have been biased. Since an increase was not visible which would have been associated with an increased apoptosis at day seven, the results of the responder cells were reasonable. Furthermore, an elevation of the apoptosis rate by catalase was not detectable at day 7, neither for responder nor for low responder hBMSCs. However, an increase of the apoptosis rate caused by a catalase treatment was observed at day 21which matched the results of the p53 expression and the fact that a peak of matrix calcification was reached at day 21.

Due to the counteracting crosstalk between p53 and Akt, the expression of Akt was also determined. Akt is crucial for the regulation of several cell signaling processes. Contrary to p53, Akt is a relevant regulator of cellular survival processes [253]. Even though the Akt

expression was investigated of only two donors, the trend was reasonable referred to the known facts. At day seven, the different treatments resulted in an increase of the expression compared to the untreated samples, whereas at day 21, the expression was decreased by the additives. At day seven, the cells were not finally differentiated and no calcified matrix was formed at that time and therefore it was reasonable that the survival of the cells was supported by Akt. However, at day 21, the maximum of matrix formation was reached and thus the cells exhibited cell death which made a downregulation of the Akt expression and the simultaneous p53 expression reasonable. Thus, the expression patterns of responder and low responder were not significantly different and the addition of catalase during the osteogenic differentiation influenced survival and cell death processes by the Akt-p53-pathway. Nonetheless, it could be assumed that the effects on the Akt-p53-pathway by catalase were not the crucial factors to lead to a restoration of the impaired osteogenic differentiation potential. The changed expression patterns of Akt and p53 could be attributed to the linked cellular process of the osteogenic differentiation such as a higher rate of survival to form a heightened amount of osteogenic progenitor cells and the increased apoptosis rate caused by the matrix formation. The effect of increased and decreased apoptosis rates was reasoned by the bone homeostasis which is explained in paragraph *1.2.3.1.1*.

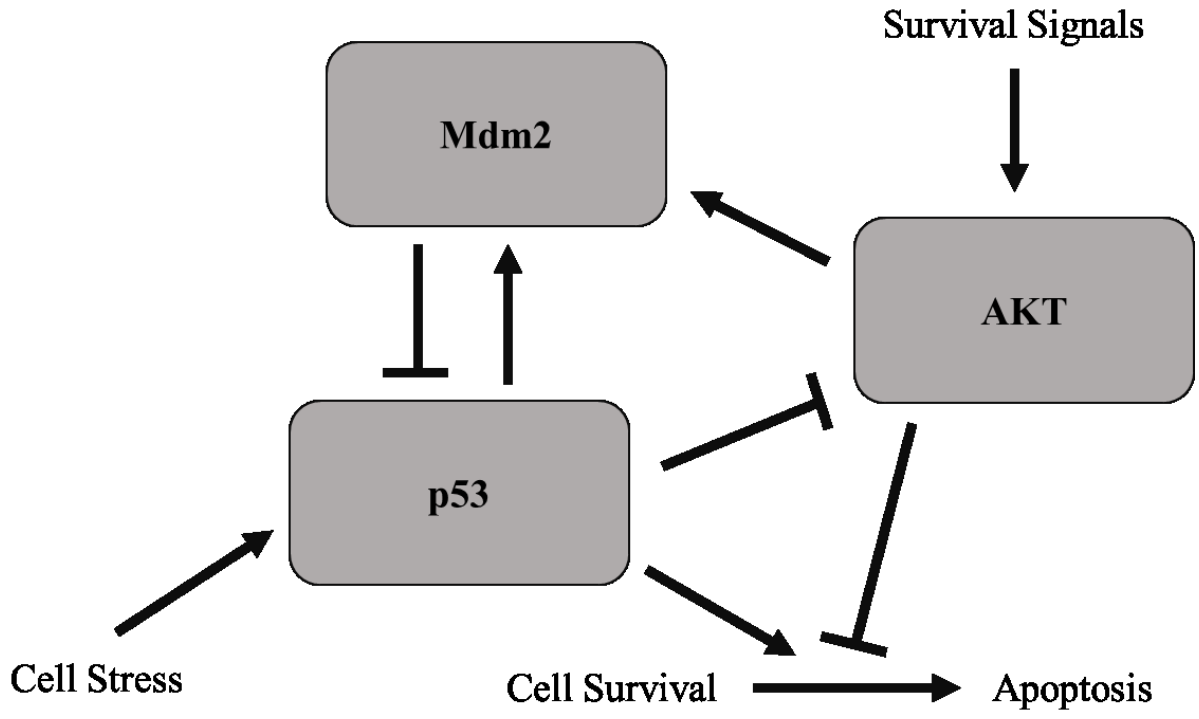

Figure 139: Cross-talk of Akt and the p53. Stress activates p53 which may inhibit AKT and consequently the correlated cell survival. On the contrary, Akt is activated by survival signals and consequently the activated Akt activates Mdm2 which inhibits p53 and in consequence leads to apoptosis. Own representation based on p53 [254].

6.3 The Impaired Osteogenic Differentiation Potential of Low Responder Cells Might be Attributed to a Modified Energy Metabolism

An unmodified energy metabolism is obligatory for all living cells to obtain regular cell signaling processes. ATP is the most important universal energy source and additionally a signal molecule within many cell signaling processes [255, 256]. Furthermore, a local phosphate source (Pi) is obligatory to form the main component of the extracellular matrix hydroxyapatite which consists of Ca^{2+} and phosphate ions. Nakano and coworkers proved that ATP as a Pi source is necessary to achieve an optimal osteogenic differentiation [257]. For that reason, the amount of ATP and glucose was determined during the processes of the osteogenic differentiation. The influences of the diverse treatments were also thoroughly assessed. The ATP amount of responder donors was significantly elevated after culturing in osteogenic differentiation medium for three and seven days compared to the amount after cultivation in proliferation medium. Interestingly, the amount of ATP at day 14 after cultivation in osteogenic differentiation was significantly decreased. These results indicated on one hand that the initial phases of osteogenic differentiation required an elevated energy amount and on the other that the late phases, which were attributed with matrix calcification, did not have a high energy requirement. The ATP amount of responder and low responder cells did not significantly change during the time of osteogenic differentiation. The treatments with catalase, heat inactivated catalase and iron compounds of low responder cells resulted in a slight increase of the ATP amount at day 21, whereas the ATP amount of responder hBMSCs was increased by the equal treatments. Due to the small number of cases, the outcomes of the investigated responder donor might not be representative. As it is highlighted by the investigations of the required energy of responder hBMSCs, the increase of the ATP amount during the final osteogenic differentiation processes seemed not to be obligatory for a successful process of matrix calcification. This hypothesis was further emphasized by the investigations of the glucose concentration during the osteogenesis. As no significant and relevant alterations of the glucose ratio could be observed, it could be assumed that the energy metabolism of low responder was not adversely modified which would have explained the impairment of the osteogenic differentiation potential and the correlated restoration by the addition of exemplary catalase. Also, the hypothesis that ATP is needed as a relevant Pi source seemed not be confirmed in case of hBMSCs. To make a more reliable and detailed statement, investigations of ATP treated low responder hBMSCs during the osteogenic differentiation are required.

Since it became obvious that iron compounds were also able to restore the impaired osteogenic differentiation potential of low responder hBMSCs, the effects of iron ions were analyzed. As previously highlighted, iron ions might have been capable to generate hydroxyl radicals which in turn affected several cell signaling processes caused by the enormous reactivity. A further plausible scenario was the interference of iron ions with the iron responsive protein, aconitase 2 and consequently with the citric acid cycle. The iron responsive protein, which is a protein of the aconitase family, and aconitase 2 are important regulator proteins of the iron hemostasis [258-260]. In iron deficient cells, the iron responsive proteins bind iron responsive elements such as ferritin. These formed complexes reduce the expression of ferritin and simultaneously promote the expression of transferrin or the transferrin receptor. Therefore, this regulation induces the compensation of the iron deficiency. Transferrin can bind iron and elevate the iron concentration of cells by the corresponding transferrin receptor. Ferritin is an iron-storage protein which inhibits the transfer of iron ions into the cells. In general, the iron responsive protein and aconitase 2 are balanced. Whereas the iron responsive element regulates the compensation of an iron deficiency in the cytoplasm, the aconitase 2 represents the mitochondrial active form which mainly catalyzes the chemical reaction of citrate to isocitrate within the citric acid cycle. Thus, the aconitase 2 directly influences the energy metabolism [261-264]. Furthermore, Pantopoulos *et al.* observed an activation of the iron responsive protein by hydrogen peroxide or rather oxidative stress which is an interesting aspect regarding the restoration potential of catalase and the hypothesized generation of hydroxyl radicals [265].

To analyze if the addition of catalase inactivated catalase or iron compounds result in a downregulation of the iron responsive protein 1 and simultaneously an upregulation of the aconitase 2 and therefore an elevated activity of the citric acid cycle, the expression of these proteins was evaluated. In case of an elevation of this activity, the citrate concentration would have been reduced and the ATP amount would have been increased [266]. Since the regulation of the restoration potential seemed to be unlikely caused by an alteration of the ATP amount, it was assumed that the expression of aconitase 2 was not elevated, whereas the expression of the iron responsive element 1 was upregulated to compensate a potential iron deficiency and an increase of the citrate concentration. The citrate concentration was increased which was caused by the diminished catalytic reaction of aconitase 2. Remarkably, the expression of the iron responsive protein was significantly increased by the addition of catalase at day 21 and the expression of aconitase 2 was not significantly altered. In this case, it is important to note that the different treatments also changed the expression patterns of

responder hBMSCs. Furthermore, the iron responsive element and aconitase 2 expressions at day zero, seven and 21 of untreated responder donors exhibited no distinct changes. On top of that, the expression patterns after treatments with catalase, inactivated catalase or iron compounds showed distinct differences which indicated that the iron elements of catalase were not the reason for the impacts on the expression regulation of the iron responsive proteins and aconitase 2. Since the treatments with catalase and iron compounds led to similar outcomes regarding the restoration of the osteogenic differentiation of low responder cells but simultaneously showed diverse effects on the up- and downregulation of regulatory proteins of the iron homeostasis, it was unlikely that the restoration was regulated by the reactions of the iron responsive protein or aconitase 2.

Nonetheless, citrate degradation to isocitrate was prevented by a reduced aconitase 2 expression and consequently the concentration of citrate was elevated. An increased concentration of citrate demonstrably promotes formation of calcified matrix. Davies and coworkers proved that citrate anions can bridge between calcium phosphate mineral layers [267]. Additionally, citrate is known for stabilizing apatite nanocrystals in bones [268]. Franklin and coworkers found out that osteoblasts are specialized cells which can inhibit the mitochondrial citrate oxidation. Thus, the isocitrate generation is prevented and the surplus amount of citrate is transferred into the extracellular environment where it stabilizes the bone matrix [269]. Interestingly, the osteoblastic citrate production is mediated by diverse mechanisms such as the iron homeostasis but also via an *in vitro* BMP2 stimulation which hints at further investigation models [270]. Since the analyses of the expression pattern of aconitase 2 did not indicate that the citrate production of low responder cells was modified, which would have explained the impaired matrix calcification of low responder cells, it could be assumed that the used additives did not influence the citrate production via interfering with the citric acid cycle. To ensure this statement, further investigations regarding the citrate involvement during the osteogenic differentiation are required.

6.4 Cultivation of HBMSCs under Diverse Conditions Alters the Cell Viability

To preclude the possibility that the impaired matrix calcification was caused by a modification of the proliferation process which interfered with the cell viability, proliferations rates of hBMSCs during diverse conditions previous to the initiation of the osteogenic differentiation and while osteogenic differentiation were investigated. For instance, the addition of hydrogen peroxide effects the osteogenic differentiation in two diverse ways. On one hand, the addition increases the amount of ROS which promotes the contrary adipogenic

differentiation (see: paragraph *6.1*) and on the other hand, it also stresses the cells and results in an impaired cell viability and consequently reduced proliferation rate and increased apoptosis [271]. This phenomenon was observed in osteogenic differentiation and proliferation medium. Interestingly, our investigation emphasized that the cultivation in osteogenic differentiation medium supplemented with catalase showed the lowest cell viability. In this case, it is important to note that the used osteogenic differentiation medium contained dexamethasone which was added to initiate the differentiation [272, 273]. For that reason, it was reasonable that cells, which were cultured in osteogenic differentiation medium, showed a lower proliferation rate and cell viability as cells which were cultured in regular proliferation medium. Furthermore, the cultivation of hBMSCs in catalase supplemented osteogenic differentiation medium led to an even stronger reduction of the cell viability at day 14. Because catalase treated low responder cells showed the first indication of matrix calcification at day 14, which implicated the loss of proliferation and beginning cell death, the results were reasonable. To prove the reliability of the cell viability investigations, three assays with different mechanisms were performed. The credibility is demonstrated by the similar outcomes of all procedures.

6.5 Osteogenic Differentiation: Stimulation by FGF-2

Byun and coworkers demonstrated in their work that FGF-2 increases the expression of TAZ (transcriptional coactivator with PDZ-binding motif) which is known as a relevant regulator of the mesenchymal stem cell differentiation. The reduction of FGF-2 impairs the differentiation potential of mesenchymal stem cells by diminishing the TAZ expression [175]. Furthermore, it was published that an intramuscular injection of FGF-2 can elevate ERK and Runx2 which initiate further osteogenic differentiation processes [188]. Additionally, Nakayama and coworkers proved that FGF-2 induces expressions of relevant osteogenic genes [176]. On the contrary, the upregulation of the bone morphogenetic protein 2 (BMP-2) is prevented by FGF-2 which in turn indicates inhibitory effects on the osteogenic differentiation processes of hBMSCs [174]. Due to these results, the amount of FGF-2 during the osteogenic differentiation processes of responder and low responder was determined. As no distinct differences between responder and low responder donors were observed, the results were interpreted condensed. The addition of catalase at day three, seven and 14 resulted in an increase of the FGF-2 amount. As both donor types showed the same outcomes regarding the FGF-2 amount after an addition of catalase, it seemed obvious that a disturbed FGF-2 regulated pathway was not the reason for the impaired osteogenic differentiation

potential of low responder cells. To emphasize this statement, transcription factors such as TAZ and BMP-2 (bone morphogenetic protein 2) should be investigated in relation with FGF-2.

7 Conclusion

In conclusion, responder hBMSCs can differentiate into osteoblasts and form a calcified matrix but osteogenically dysfunctional low responder cells have lost the ability of osteogenic differentiation. Interestingly, the impaired osteogenic differentiation potential can be restored by the addition of 125 U/ml catalase for 21 days to the osteogenic differentiation medium. Nonetheless, the known antioxidative effects of catalase of degrading hydrogen peroxide seem not to be the reason for the restoration potential. The treatments with heat inactivated catalase as well as catalase which was inactivated with ATA and iron compounds (iron chloride and iron sulfate) showed similar positive effects on the impaired osteogenic differentiation potential of low responder hBMSCs. Since investigations of the *inter alia* apoptosis rate, energy metabolism regulations, FGF-2 influences or cell viability showed no distinct differences between responder and low responder cells, we tested the hydroxyl radical generation theory of catalase. Catalase has an iron ion in the active center which we assume is not destroyed by the inactivation processes and consequently can form hydroxyl radicals via the Haber-Weiss and Fenton reactions. Thus, all tested substances can generate hydroxyl radicals which might be, due to their high reactivity, interacting with osteogenically relevant cell signaling pathways. Since this crosstalk is yet not fully understood, further investigations are required to confirm this theory.

Literature

1. Felsenberg, D., *Struktur und funktion des knochens: stützwerk aus kollagen und hydroxylapatit.* Pharmazie in unserer Zeit, 2001. **30**(6): p. 488-494.
2. Hu, Y., et al., *[Progress in the regulation of bone remodeling at the cellular level].* Sheng Wu Yi Xue Gong Cheng Xue Za Zhi, 2017. **34**(3): p. 471-479.
3. Atkins, G.J., et al., *Vitamin K promotes mineralization, osteoblast-to-osteocyte transition, and an anticatabolic phenotype by {gamma}-carboxylation-dependent and -independent mechanisms.* Am J Physiol Cell Physiol, 2009. **297**(6): p. C1358-67.
4. Sasano, Y., et al., *Expression of major bone extracellular matrix proteins during embryonic osteogenesis in rat mandibles.* Anat Embryol (Berl), 2000. **202**(1): p. 31-7.
5. Fu, X., et al., *Runx2/Osterix and Zinc Uptake Synergize to Orchestrate Osteogenic Differentiation and Citrate Containing Bone Apatite Formation.* Advanced Science, 2018: p. 1700755.
6. Melouane, A., et al., *Implication of SPARC in the modulation of the extracellular matrix and mitochondrial function in muscle cells.* PloS one, 2018. **13**(2): p. e0192714.
7. Bradshaw, A.D., *The role of SPARC in extracellular matrix assembly.* J Cell Commun Signal, 2009. **3**(3-4): p. 239-46.
8. Brekken, R.A. and E.H. Sage, *SPARC, a matricellular protein: at the crossroads of cell-matrix.* Matrix Biol, 2000. **19**(7): p. 569-80.
9. Betts, J.G.D., P.; Johnson, E.; Johnson J. E.; Korol, O.; Kruse, D.; Poe, B.; Wise, J. A.; Womble, M.; Zoung, K. A. *Bone Classification* 2013 [cited 2018 04/14/2018]; Available from: https://cnx.org/contents/FPtK1zmh@6.27:8x7YlLHu@4/Bone-Classification.
10. Gilbert, S., *Osteogenesis: the development of bones.* Developmental biology, 2000. **6**.
11. Mackie, E., et al., *Endochondral ossification: how cartilage is converted into bone in the developing skeleton.* The international journal of biochemistry & cell biology, 2008. **40**(1): p. 46-62.
12. Cserjesi, P., et al., *Scleraxis: a basic helix-loop-helix protein that prefigures skeletal formation during mouse embryogenesis.* Development, 1995. **121**(4): p. 1099-110.
13. Sosic, D., et al., *Regulation of paraxis expression and somite formation by ectoderm- and neural tube-derived signals.* Dev Biol, 1997. **185**(2): p. 229-43.
14. Oberlender, S.A. and R.S. Tuan, *Expression and functional involvement of N-cadherin in embryonic limb chondrogenesis.* Development, 1994. **120**(1): p. 177-87.
15. Bruder, S.P. and A.I. Caplan, *Cellular and molecular events during embryonic bone development.* Connect Tissue Res, 1989. **20**(1-4): p. 65-71.
16. Hatori, M., et al., *End labeling studies of fragmented DNA in the avian growth plate: evidence of apoptosis in terminally differentiated chondrocytes.* J Bone Miner Res, 1995. **10**(12): p. 1960-8.
17. Rajpurohit, R., et al., *Chondrocyte death is linked to development of a mitochondrial membrane permeability transition in the growth plate.* J Cell Physiol, 1999. **179**(3): p. 287-96.
18. Dalle Carbonare, L., G. Innamorati, and M.T. Valenti, *Transcription factor Runx2 and its application to bone tissue engineering.* Stem Cell Rev, 2012. **8**(3): p. 891-7.
19. Cao, X. and D. Chen, *The BMP signaling and in vivo bone formation.* Gene, 2005. **357**(1): p. 1-8.
20. Day, T.F., et al., *Wnt/beta-catenin signaling in mesenchymal progenitors controls osteoblast and chondrocyte differentiation during vertebrate skeletogenesis.* Dev Cell, 2005. **8**(5): p. 739-50.

21. Xu, J., et al., *Potential mechanisms underlying the Runx2 induced osteogenesis of bone marrow mesenchymal stem cells.* Am J Transl Res, 2015. **7**(12): p. 2527-35.
22. Valenti, M.T., et al., *Runx2 expression: A mesenchymal stem marker for cancer.* Oncol Lett, 2016. **12**(5): p. 4167-4172.
23. Whyte, J.L., A.A. Smith, and J.A. Helms, *Wnt signaling and injury repair.* Cold Spring Harbor perspectives in biology, 2012. **4**(8): p. a008078.
24. Chambers, T.J., et al., *Wnt signalling in pituitary development and tumorigenesis.* Endocr Relat Cancer, 2013. **20**(3): p. R101-11.
25. Boras-Granic, K. and J.J. Wysolmerski, *Wnt signaling in breast organogenesis.* Organogenesis, 2008. **4**(2): p. 116-122.
26. Williams, B.O. and K.L. Insogna, *Where Wnts went: the exploding field of Lrp5 and Lrp6 signaling in bone.* J Bone Miner Res, 2009. **24**(2): p. 171-8.
27. Honma, M., et al., *Regulatory mechanisms of RANKL presentation to osteoclast precursors.* Curr Osteoporos Rep, 2014. **12**(1): p. 115-20.
28. Liu, H.Y., et al., *The balance between adipogenesis and osteogenesis in bone regeneration by platelet-rich plasma for age-related osteoporosis.* Biomaterials, 2011. **32**(28): p. 6773-80.
29. Chen, Q., et al., *Fate decision of mesenchymal stem cells: adipocytes or osteoblasts?* Cell death and differentiation, 2016. **23**(7): p. 1128.
30. Berendsen, A.D. and B.R. Olsen, *Regulation of adipogenesis and osteogenesis in mesenchymal stem cells by vascular endothelial growth factor A.* J Intern Med, 2015. **277**(6): p. 674-80.
31. Valenti, M.T., L. Dalle Carbonare, and M. Mottes, *Osteogenic differentiation in healthy and pathological conditions.* International journal of molecular sciences, 2016. **18**(1): p. 41.
32. Javed, A., et al., *Groucho/TLE/R-esp proteins associate with the nuclear matrix and repress RUNX (CBF(alpha)/AML/PEBP2(alpha)) dependent activation of tissue-specific gene transcription.* J Cell Sci, 2000. **113 (Pt 12)**: p. 2221-31.
33. Komori, T., *Regulation of osteoblast differentiation by transcription factors.* Journal of cellular biochemistry, 2006. **99**(5): p. 1233-1239.
34. Jing, D., et al., *The role of microRNAs in bone remodeling.* Int J Oral Sci, 2015. **7**(3): p. 131-43.
35. Zernik, J., K. Twarog, and W.B. Upholt, *Regulation of alkaline phosphatase and alpha2 (I) procollagen synthesis during early intramembranous bone formation in the rat mandible.* Differentiation, 1990. **44**(3): p. 207-215.
36. Wopenka, B. and J.D. Pasteris, *A mineralogical perspective on the apatite in bone.* Materials Science and Engineering: C, 2005. **25**(2): p. 131-143.
37. McKee, M.D. and A. Nanci, *Osteopontin at mineralized tissue interfaces in bone, teeth, and osseointegrated implants: ultrastructural distribution and implications for mineralized tissue formation, turnover, and repair.* Microsc Res Tech, 1996. **33**(2): p. 141-64.
38. Reinholt, F.P., et al., *Osteopontin--a possible anchor of osteoclasts to bone.* Proc Natl Acad Sci U S A, 1990. **87**(12): p. 4473-5.
39. Nomura, S., et al., *Developmental expression of 2ar (osteopontin) and SPARC (osteonectin) RNA as revealed by in situ hybridization.* J Cell Biol, 1988. **106**(2): p. 441-50.
40. Kersten-Thiele, P.V., *Osteogene Differenzierung von humanen Nabelschnurblutstammzellen (USSC) in der adhärenten Zellkultur sowie auf boviner, kollagener Knochenmatrix.* 2011.
41. Liu, Y., et al., *Therapeutic application of mesenchymal stem cells in bone and joint diseases.* Clin Exp Med, 2014. **14**(1): p. 13-24.

42. Awad, H.A., et al., *Autologous mesenchymal stem cell-mediated repair of tendon.* Tissue Eng, 1999. **5**(3): p. 267-77.
43. Ferrari, G., et al., *Muscle regeneration by bone marrow-derived myogenic progenitors.* Science, 1998. **279**(5356): p. 1528-30.
44. Armstrong, L., et al., *mTert expression correlates with telomerase activity during the differentiation of murine embryonic stem cells.* Mech Dev, 2000. **97**(1-2): p. 109-16.
45. Li, Y., et al., *Nicotinamide phosphoribosyltransferase (Nampt) affects the lineage fate determination of mesenchymal stem cells: a possible cause for reduced osteogenesis and increased adipogenesis in older individuals.* J Bone Miner Res, 2011. **26**(11): p. 2656-64.
46. Monroe, D.G., et al., *Update on Wnt signaling in bone cell biology and bone disease.* Gene, 2012. **492**(1): p. 1-18.
47. Huang, J., et al., *MicroRNA-204 regulates Runx2 protein expression and mesenchymal progenitor cell differentiation.* Stem Cells, 2010. **28**(2): p. 357-64.
48. Greer, E.L. and A. Brunet, *FOXO transcription factors at the interface between longevity and tumor suppression.* Oncogene, 2005. **24**(50): p. 7410-25.
49. Atadja, P., et al., *Increased activity of p53 in senescing fibroblasts*. Proc Natl Acad Sci U S A, 1995. **92**(18): p. 8348-52.
50. Campisi, J., *From cells to organisms: can we learn about aging from cells in culture?* Exp Gerontol, 2001. **36**(4-6): p. 607-18.
51. Odorico, J.S., D.S. Kaufman, and J.A. Thomson, *Multilineage differentiation from human embryonic stem cell lines.* Stem Cells, 2001. **19**(3): p. 193-204.
52. Labat, M.L., *Stem cells and the promise of eternal youth: embryonic versus adult stem cells.* Biomed Pharmacother, 2001. **55**(4): p. 179-85.
53. Wexler, S.A., et al., *Adult bone marrow is a rich source of human mesenchymal 'stem'cells but umbilical cord and mobilized adult blood are not.* British journal of haematology, 2003. **121**(2): p. 368-374.
54. Zvaifler, N.J., et al., *Mesenchymal precursor cells in the blood of normal individuals.* Arthritis Res, 2000. **2**(6): p. 477-88.
55. Kuznetsov, S.A., A.J. Friedenstein, and P.G. Robey, *Factors required for bone marrow stromal fibroblast colony formation in vitro.* Br J Haematol, 1997. **97**(3): p. 561-70.
56. Krebsbach, P.H., et al., *Bone marrow stromal cells: characterization and clinical application.* Crit Rev Oral Biol Med, 1999. **10**(2): p. 165-81.
57. Pittenger, M.F., et al., *Multilineage potential of adult human mesenchymal stem cells.* Science, 1999. **284**(5411): p. 143-7.
58. Majumdar, M.K., et al., *Isolation, characterization, and chondrogenic potential of human bone marrow-derived multipotential stromal cells.* J Cell Physiol, 2000. **185**(1): p. 98-106.
59. Liechty, K.W., et al., *Human mesenchymal stem cells engraft and demonstrate site-specific differentiation after in utero transplantation in sheep.* Nat Med, 2000. **6**(11): p. 1282-6.
60. Mackay, A.M., et al., *Chondrogenic differentiation of cultured human mesenchymal stem cells from marrow.* Tissue Eng, 1998. **4**(4): p. 415-28.
61. Haynesworth, S.E., et al., *Characterization of cells with osteogenic potential from human marrow.* Bone, 1992. **13**(1): p. 81-8.
62. Pelled, G., et al., *Mesenchymal stem cells for bone gene therapy and tissue engineering.* Curr Pharm Des, 2002. **8**(21): p. 1917-28.
63. Marsh, J.C., et al., *In vitro assessment of marrow 'stem cell' and stromal cell function in aplastic anaemia.* Br J Haematol, 1991. **78**(2): p. 258-67.

64. Marsh, J.C., et al., *The hematopoietic defect in aplastic anemia assessed by long-term marrow culture.* Blood, 1990. **76**(9): p. 1748-57.
65. Schipani, E. and H.M. Kronenberg, *Adult mesenchymal stem cells.* 2009.
66. Bianco, P., P.G. Robey, and P.J. Simmons, *Mesenchymal stem cells: revisiting history, concepts, and assays.* Cell stem cell, 2008. **2**(4): p. 313-319.
67. Takagi, M., et al., *In vitro proliferation of human bone marrow mesenchymal stem cells employing donor serum and basic fibroblast growth factor.* Cytotechnology, 2003. **43**(1): p. 89-96.
68. Deans, R.J. and A.B. Moseley, *Mesenchymal stem cells: biology and potential clinical uses.* Exp Hematol, 2000. **28**(8): p. 875-84.
69. Mackenzie, T.C. and A.W. Flake, *Human mesenchymal stem cells persist, demonstrate site-specific multipotential differentiation, and are present in sites of wound healing and tissue regeneration after transplantation into fetal sheep.* Blood Cells, Molecules, and Diseases, 2001. **27**(3): p. 601-604.
70. Witt, R.G., et al., *Systemic multilineage engraftment in mice after in utero transplantation with human hematopoietic stem cells.* Blood advances, 2018. **2**(1): p. 69-74.
71. Henrotin, Y.E., P. Bruckner, and J.P. Pujol, *The role of reactive oxygen species in homeostasis and degradation of cartilage.* Osteoarthritis Cartilage, 2003. **11**(10): p. 747-55.
72. Zhang, Y., et al., *Redox control of the survival of healthy and diseased cells.* Antioxid Redox Signal, 2011. **15**(11): p. 2867-908.
73. Fleury, C., B. Mignotte, and J.L. Vayssiere, *Mitochondrial reactive oxygen species in cell death signaling.* Biochimie, 2002. **84**(2-3): p. 131-41.
74. Schieber, M. and N.S. Chandel, *ROS function in redox signaling and oxidative stress.* Current biology, 2014. **24**(10): p. R453-R462.
75. Zhang, J., et al., *ROS and ROS-mediated cellular signaling.* Oxidative medicine and cellular longevity, 2016. **2016**.
76. Ye, Z.-W., et al., *Oxidative stress, redox regulation and diseases of cellular differentiation.* Biochimica et Biophysica Acta (BBA)-General Subjects, 2015. **1850**(8): p. 1607-1621.
77. Nordberg, J. and E.S. Arner, *Reactive oxygen species, antioxidants, and the mammalian thioredoxin system.* Free Radic Biol Med, 2001. **31**(11): p. 1287-312.
78. Balazy, M. and S. Nigam, *Aging, lipid modifications and phospholipases--new concepts.* Ageing Res Rev, 2003. **2**(2): p. 191-209.
79. Halliwell, B., *Free radicals and metal ions in health and disease.* Proc Nutr Soc, 1987. **46**(1): p. 13-26.
80. Murphy, M.P., *How mitochondria produce reactive oxygen species.* Biochemical Journal, 2009. **417**(1): p. 1-13.
81. Andreyev, A.Y., Y.E. Kushnareva, and A.A. Starkov, *Mitochondrial metabolism of reactive oxygen species.* Biochemistry (Mosc), 2005. **70**(2): p. 200-14.
82. Bedard, K. and K.H. Krause, *The NOX family of ROS-generating NADPH oxidases: physiology and pathophysiology.* Physiol Rev, 2007. **87**(1): p. 245-313.
83. Meitzler, J.L., et al., *NADPH oxidases: a perspective on reactive oxygen species production in tumor biology.* Antioxidants & redox signaling, 2014. **20**(17): p. 2873-2889.
84. Coso, S., et al., *NADPH oxidases as regulators of tumor angiogenesis: current and emerging concepts.* Antioxid Redox Signal, 2012. **16**(11): p. 1229-47.
85. Cave, A., et al., *NADPH oxidase-derived reactive oxygen species in cardiac pathophysiology.* Philosophical Transactions of the Royal Society B: Biological Sciences, 2005. **360**(1464): p. 2327-2334.

86. Gamaley, I.A. and I.V. Klyubin, *Roles of reactive oxygen species: signaling and regulation of cellular functions.* Int Rev Cytol, 1999. **188**: p. 203-55.
87. Frey, R.S., M. Ushio-Fukai, and A.B. Malik, *NADPH oxidase-dependent signaling in endothelial cells: role in physiology and pathophysiology.* Antioxid Redox Signal, 2009. **11**(4): p. 791-810.
88. Pendyala, S., et al., *Regulation of NADPH oxidase in vascular endothelium: the role of phospholipases, protein kinases, and cytoskeletal proteins.* Antioxid Redox Signal, 2009. **11**(4): p. 841-60.
89. Guida, M., et al., *Nuclear Nox4-derived reactive oxygen species in myelodysplastic syndromes.* BioMed research international, 2014. **2014**.
90. Valdivia, A., C. Duran, and A. San Martin, *The role of Nox-mediated oxidation in the regulation of cytoskeletal dynamics.* Current pharmaceutical design, 2015. **21**(41): p. 6009-6022.
91. Atashi, F., A. Modarressi, and M.S. Pepper, *The role of reactive oxygen species in mesenchymal stem cell adipogenic and osteogenic differentiation: a review.* Stem cells and development, 2015. **24**(10): p. 1150-1163.
92. Tan, J., et al., *Decreased osteogenesis of adult mesenchymal stem cells by reactive oxygen species under cyclic stretch: a possible mechanism of age related osteoporosis.* Bone research, 2015. **3**: p. 15003.
93. Wang, W., et al., *Mitochondrial reactive oxygen species regulate adipocyte differentiation of mesenchymal stem cells in hematopoietic stress induced by arabinosylcytosine.* PloS one, 2015. **10**(3): p. e0120629.
94. Chaiswing, L. and T.D. Oberley, *Extracellular/microenvironmental redox state.* Antioxid Redox Signal, 2010. **13**(4): p. 449-65.
95. Trachootham, D., et al., *Redox regulation of cell survival.* Antioxid Redox Signal, 2008. **10**(8): p. 1343-74.
96. Ighodaro, O. and O. Akinloye, *First line defence antioxidants-superoxide dismutase (SOD), catalase (CAT) and glutathione peroxidase (GPX): Their fundamental role in the entire antioxidant defence grid.* Alexandria Journal of Medicine, 2017.
97. Zámocký, M. and F. Koller, *Understanding the structure and function of catalases: clues from molecular evolution and in vitro mutagenesis.* Progress in biophysics and molecular biology, 1999. **72**(1): p. 19-66.
98. Gil, D., et al., *Antioxidant Activity of SOD and Catalase Conjugated with Nanocrystalline Ceria.* Bioengineering, 2017. **4**(1): p. 18.
99. Schriner, S.E., et al., *Extension of murine life span by overexpression of catalase targeted to mitochondria.* Science, 2005. **308**(5730): p. 1909-11.
100. Dai, D.F., et al., *Overexpression of catalase targeted to mitochondria attenuates murine cardiac aging.* Circulation, 2009. **119**(21): p. 2789-97.
101. Liao, A.C., et al., *Mitochondrial-targeted human catalase affords neuroprotection from proton irradiation.* Radiat Res, 2013. **180**(1): p. 1-6.
102. Brown, G. and V. Borutaite, *Interactions between nitric oxide, oxygen, reactive oxygen species and reactive nitrogen species*. 2006, Portland Press Limited.
103. Loew, O., *A NEW ENZYME OF GENERAL OCCURRENCE IN ORGANISMIS.* Science, 1900. **11**(279): p. 701-2.
104. Kettler-Thiel, T., *Eisen (III)-Komplexe und Untersuchung ihrer Eigenschaften als Enzymmimetika für Katalasen und Peroxidasen*. 2007, Universität Duisburg-Essen, Fakultät für Chemie» Organische Chemie.
105. Goyal, M.M. and A. Basak, *Hydroxyl radical generation theory: a possible explanation of unexplained actions of mammalian catalase.* Int J Biochem Mol Biol, 2012. **3**(3): p. 282-9.

106. Cederbaum, A.I. and A. Qureshi, *Role of catalase and hydroxyl radicals in the oxidation of methanol by rat liver microsomes.* Biochem Pharmacol, 1982. **31**(3): p. 329-35.
107. Gutteridge, J.M., *Lipid peroxidation initiated by superoxide-dependent hydroxyl radicals using complexed iron and hydrogen peroxide.* FEBS Lett, 1984. **172**(2): p. 245-9.
108. Chen, C.S., et al., *Hydroxyl radical-induced decline in motility and increase in lipid peroxidation and DNA modification in human sperm.* IUBMB Life, 1997. **43**(2): p. 291-303.
109. Chen, T.L., *Inhibition of growth and differentiation of osteoprogenitors in mouse bone marrow stromal cell cultures by increased donor age and glucocorticoid treatment.* Bone, 2004. **35**(1): p. 83-95.
110. Shigeno, Y. and B.A. Ashton, *Human bone-cell proliferation in vitro decreases with human donor age.* J Bone Joint Surg Br, 1995. **77**(1): p. 139-42.
111. Stolzing, A., et al., *Age-related changes in human bone marrow-derived mesenchymal stem cells: consequences for cell therapies.* Mech Ageing Dev, 2008. **129**(3): p. 163-73.
112. Muschler, G.F., et al., *Age- and gender-related changes in the cellularity of human bone marrow and the prevalence of osteoblastic progenitors.* J Orthop Res, 2001. **19**(1): p. 117-25.
113. Baxter, M.A., et al., *Study of telomere length reveals rapid aging of human marrow stromal cells following in vitro expansion.* Stem Cells, 2004. **22**(5): p. 675-82.
114. Zhou, S., et al., *Age-related intrinsic changes in human bone-marrow-derived mesenchymal stem cells and their differentiation to osteoblasts.* Aging Cell, 2008. **7**(3): p. 335-43.
115. Campisi, J., *Senescent cells, tumor suppression, and organismal aging: good citizens, bad neighbors.* Cell, 2005. **120**(4): p. 513-22.
116. D'Ippolito, G., et al., *Age-related osteogenic potential of mesenchymal stromal stem cells from human vertebral bone marrow.* J Bone Miner Res, 1999. **14**(7): p. 1115-22.
117. Gibon, E., L. Lu, and S.B. Goodman, *Aging, inflammation, stem cells, and bone healing.* Stem cell research & therapy, 2016. **7**(1): p. 44.
118. Marler, J.J., et al., *Transplantation of cells in matrices for tissue regeneration.* Adv Drug Deliv Rev, 1998. **33**(1-2): p. 165-182.
119. Langer, R.S. and J.P. Vacanti, *Tissue engineering: the challenges ahead.* Sci Am, 1999. **280**(4): p. 86-9.
120. Griffith, L.G. and G. Naughton, *Tissue engineering--current challenges and expanding opportunities.* science, 2002. **295**(5557): p. 1009-1014.
121. Ellis, W. *Iron Man, Extremis, and Tissue Engineering*. 2013 04/20/2018]; Available from: http://www.warrenellis.com/?p=14814.
122. Rueger, J.M., *[Bone substitution materials. Current status and prospects].* Orthopade, 1998. **27**(2): p. 72-9.
123. Reichert, J.C. and D.W. Hutmacher, *Bone tissue engineering*, in *Tissue Engineering*. 2011, Springer. p. 431-456.
124. Blokhuis, T.J. and J.J. Arts, *Bioactive and osteoinductive bone graft substitutes: definitions, facts and myths.* Injury, 2011. **42 Suppl 2**: p. S26-9.
125. Barradas, A.M., et al., *Osteoinductive biomaterials: current knowledge of properties, experimental models and biological mechanisms.* Eur Cell Mater, 2011. **21**: p. 407-29; discussion 429.
126. Habibovic, P. and K. de Groot, *Osteoinductive biomaterials--properties and relevance in bone repair.* J Tissue Eng Regen Med, 2007. **1**(1): p. 25-32.

127. LeGeros, R.Z., *Properties of osteoconductive biomaterials: calcium phosphates.* Clin Orthop Relat Res, 2002(395): p. 81-98.
128. Yuan, N., K.S. Rezzadeh, and J.C. Lee, *Biomimetic scaffolds for osteogenesis.* Receptors & clinical investigation, 2015. **2**(3).
129. Caballero, M., et al., *(*) Tissue Engineering Strategies to Improve Osteogenesis in the Juvenile Swine Alveolar Cleft Model.* Tissue Eng Part C Methods, 2017. **23**(12): p. 889-899.
130. Bose, S., M. Roy, and A. Bandyopadhyay, *Recent advances in bone tissue engineering scaffolds.* Trends in biotechnology, 2012. **30**(10): p. 546-554.
131. Roseti, L., et al., *Scaffolds for Bone Tissue Engineering: State of the art and new perspectives.* Mater Sci Eng C Mater Biol Appl, 2017. **78**: p. 1246-1262.
132. Black, C.R., et al., *Bone tissue engineering.* Current molecular biology reports, 2015. **1**(3): p. 132-140.
133. Amini, A.R., C.T. Laurencin, and S.P. Nukavarapu, *Bone tissue engineering: recent advances and challenges.* Critical Reviews™ in Biomedical Engineering, 2012. **40**(5).
134. Henkel, J., et al., *Bone Regeneration Based on Tissue Engineering Conceptions - A 21st Century Perspective.* Bone Res, 2013. **1**(3): p. 216-48.
135. Bouet, G., et al., *In vitro three-dimensional bone tissue models: from cells to controlled and dynamic environment.* Tissue Eng Part B Rev, 2015. **21**(1): p. 133-56.
136. Kumbar, S., C. Laurencin, and M. Deng, *Natural and synthetic biomedical polymers*. 2014: Newnes.
137. Zhu, N. and X. Chen, *Biofabrication of tissue scaffolds*, in *Advances in biomaterials science and biomedical applications*. 2013, InTech.
138. Matassi, F., et al., *New biomaterials for bone regeneration.* Clinical cases in mineral and bone metabolism, 2011. **8**(1): p. 21.
139. Gasperini, L., J.F. Mano, and R.L. Reis, *Natural polymers for the microencapsulation of cells.* J R Soc Interface, 2014. **11**(100): p. 20140817.
140. Dhandayuthapani, B., et al., *Polymeric scaffolds in tissue engineering application: a review.* International journal of polymer science, 2011. **2011**.
141. Thavornyutikarn, B., et al., *Bone tissue engineering scaffolding: computer-aided scaffolding techniques.* Prog Biomater, 2014. **3**: p. 61-102.
142. Ventola, C.L., *Medical applications for 3D printing: current and projected uses.* Pharmacy and Therapeutics, 2014. **39**(10): p. 704.
143. Chia, H.N. and B.M. Wu, *Recent advances in 3D printing of biomaterials.* Journal of biological engineering, 2015. **9**(1): p. 4.
144. Groll, J., et al., *Biofabrication: reappraising the definition of an evolving field.* Biofabrication, 2016. **8**(1): p. 013001.
145. Jeong, C.G. and A. Atala, *3D Printing and Biofabrication for Load Bearing Tissue Engineering.* Adv Exp Med Biol, 2015. **881**: p. 3-14.
146. Portal, H.I., *Performing Cell Counts with a Hemacytometer.*
147. Hong, C., et al., *Porous silicon nanoparticles for cancer photothermotherapy.* Nanoscale research letters, 2011. **6**(1): p. 321.
148. Scientific™, T. *Mr. Frosty™ Gefrierbehälter*. 04012018]; Available from: http://www.thermofisher.com/order/catalog/product/5100-0001.
149. Kohli, R., et al., *Mitochondrial reactive oxygen species signal hepatocyte steatosis by regulating the phosphatidylinositol 3-kinase cell survival pathway.* Journal of Biological Chemistry, 2007. **282**(29): p. 21327-21336.
150. Decraene, D., et al., *A synthetic superoxide dismutase/catalase mimetic (EUK-134) inhibits membrane-damage-induced activation of mitogen-activated protein kinase pathways and reduces p53 accumulation in ultraviolet B-exposed primary human keratinocytes.* Journal of investigative dermatology, 2004. **122**(2): p. 484-491.

151. George, S., et al., *Comparison of the response of human embryonic stem cells and their differentiated progenies to oxidative stress.* Photomed Laser Surg, 2009. **27**(4): p. 669-74.
152. Dolashka-angelova, P., et al., *Isolation and characterization of a novel superoxide dismutase from fungal strain Humicola lutea 110.* Chemical Biology & Drug Design, 1999. **54**(4): p. 279-289.
153. Macrides, T.A., et al., *A comparison of the hydroxyl radical scavenging properties of the shark bile steroid 5β-scymnol and plant pycnogenols.* IUBMB Life, 1997. **42**(6): p. 1249-1260.
154. Lee, J.-H., et al., *Trolox prevents osteoclastogenesis by suppressing RANKL expression and signaling.* Journal of Biological Chemistry, 2009. **284**(20): p. 13725-13734.
155. Sigma-Aldrich. *Ethylenediaminetetraacetic acid disodium salt dihydrate*. 04052018]; Available from: https://www.sigmaaldrich.com/content/dam/sigma-aldrich/docs/Sigma/Product_Information_Sheet/e5134pis.pdf.
156. Zhu, X., et al., *Dectin-1 signaling inhibits osteoclastogenesis via IL-33-induced inhibition of NFATc1.* Oncotarget, 2017. **8**(32): p. 53366.
157. Davies, M.J., L.G. Forni, and R.L. Willson, *Vitamin E analogue Trolox CEsr and pulse-radiolysis studies of free-radical reactions.* Biochemical Journal, 1988. **255**(2): p. 513.
158. Goldstein, S. and G. Czapski, *Mannitol as an OH· scavenger in aqueous solutions and in biological systems.* International Journal of Radiation Biology and Related Studies in Physics, Chemistry and Medicine, 1984. **46**(6): p. 725-729.
159. Rong, Y., et al., *EUK-134, a synthetic superoxide dismutase and catalase mimetic, prevents oxidative stress and attenuates kainate-induced neuropathology.* Proceedings of the National Academy of Sciences, 1999. **96**(17): p. 9897-9902.
160. Malassagne, B., et al., *The superoxide dismutase mimetic MnTBAP prevents Fas-induced acute liver failure in the mouse.* Gastroenterology, 2001. **121**(6): p. 1451-1459.
161. Szabó, C., B.J. Day, and A.L. Salzman, *Evaluation of the relative contribution of nitric oxide and peroxynitrite to the suppression of mitochondrial respiration in immunostimulated macrophages using a manganese mesoporphyrin superoxide dismutase mimetic and peroxynitrite scavenger.* FEBS letters, 1996. **381**(1-2): p. 82-86.
162. Grinstein, M., M.D. Kamen, and C.V. Moore, *The utilization of glycine in the biosynthesis of hemoglobin.* J. biol. Chem, 1949. **179**: p. 359.
163. Corporation, P. *CellTiter-Blue®*

Cell Viability Assay. 04/06/2018]; Available from: https://www.promega.de/-/media/files/resources/protocols/technical-bulletins/101/celltiter-blue-cell-viability-assay-protocol.pdf.
164. Scientific, T.F. *Pierce™ BCA Protein Assay Kit*. 04/06/2018]; Available from: https://assets.thermofisher.com/TFS-Assets/LSG/manuals/MAN0011430_Pierce_BCA_Protein_Asy_UG.pdf.
165. Garfin, D., E. *Gel Electrophoresis of Proteins*. 2003 04/08/2018]; Available from: http://www.aesociety.org/areas/pdfs/Garfin_1DE_WebArticle9-07.pdf.
166. Yadav, G.L., N., *Trends in Protein Separation and Analysis — the Advance of Stain-Free Technology*. 2014, BioRad.
167. BioRad, *Western Blotting Membranes and Filter Paper*. BioRad.
168. Shi, S., M. Kirk, and A.J. Kahn, *The role of type I collagen in the regulation of the osteoblast phenotype.* J Bone Miner Res, 1996. **11**(8): p. 1139-45.

169. Bottagisio, M., et al., *Osteogenic Differentiation of Human and Ovine Bone Marrow Stromal Cells in response to beta-Glycerophosphate and Monosodium Phosphate.* Cell Reprogram, 2015. **17**(4): p. 235-42.
170. Chomczynski, P. and N. Sacchi, *Single-step method of RNA isolation by acid guanidinium thiocyanate-phenol-chloroform extraction.* Anal Biochem, 1987. **162**(1): p. 156-9.
171. Biocompare, *Qiagen AllPrep DNA/RNA Extraction Kit for FFPE*. 2013, Biocompare.
172. Kim, Y.-J., et al., *The bone-related Zn finger transcription factor Osterix promotes proliferation of mesenchymal cells.* Gene, 2006. **366**(1): p. 145-151.
173. Promega. *Glucose-Glo™ Assay*. 04/09/2018]; Available from: https://www.promega.de/-/media/files/resources/protocols/technical-manuals/101/glucose-glo-assay.pdf?la=de-de.
174. Biver, E., et al., *Fibroblast growth factor 2 inhibits up-regulation of bone morphogenic proteins and their receptors during osteoblastic differentiation of human mesenchymal stem cells.* Biochem Biophys Res Commun, 2012. **427**(4): p. 737-42.
175. Byun, M.R., et al., *FGF2 stimulates osteogenic differentiation through ERK induced TAZ expression.* Bone, 2014. **58**: p. 72-80.
176. Nakayama, Y., et al., *Fibroblast growth factor 2 and forskolin induce mineralization-associated genes in two kinds of osteoblast-like cells.* J Oral Sci, 2012. **54**(3): p. 251-9.
177. Riccardi, C. and I. Nicoletti, *Analysis of apoptosis by propidium iodide staining and flow cytometry.* Nature protocols, 2006. **1**(3): p. 1458.
178. Dojindo Molecular Technologies, I., *Assay system to determine viable cells and dead cells*. Dojindo Molecular Technologies, Inc.
179. Siffert, R.S., *The role of alkaline phosphatase in osteogenesis.* Journal of Experimental Medicine, 1951. **93**(5): p. 415-426.
180. Golub, E.E. and K. Boesze-Battaglia, *The role of alkaline phosphatase in mineralization.* Current Opinion in Orthopaedics, 2007. **18**(5): p. 444-448.
181. Kiyomiya, H., et al., *IL-33 inhibits RANKL-induced osteoclast formation through the regulation of Blimp-1 and IRF-8 expression.* Biochem Biophys Res Commun, 2015. **460**(2): p. 320-6.
182. Ambrogini, E., et al., *FoxO-mediated defense against oxidative stress in osteoblasts is indispensable for skeletal homeostasis in mice.* Cell metabolism, 2010. **11**(2): p. 136-146.
183. Yap, T.A., et al., *Targeting the PI3K–AKT–mTOR pathway: progress, pitfalls, and promises.* Current opinion in pharmacology, 2008. **8**(4): p. 393-412.
184. Felber, K., et al., *Expression of osterix is regulated by FGF and Wnt/β-catenin signalling during osteoblast differentiation.* PloS one, 2015. **10**(12): p. e0144982.
185. Renn, J. and C. Winkler, *Osterix/Sp7 regulates biomineralization of otoliths and bone in medaka (Oryzias latipes).* Matrix Biology, 2014. **34**: p. 193-204.
186. Lee, H., et al., *Reactive oxygen species facilitate adipocyte differentiation by accelerating mitotic clonal expansion.* Journal of Biological Chemistry, 2009. **284**(16): p. 10601-10609.
187. Ho, P.-J., et al., *H2O2 accumulation mediates differentiation capacity alteration, but not proliferative decline, in senescent human fetal mesenchymal stem cells.* Antioxidants & redox signaling, 2013. **18**(15): p. 1895-1905.
188. Qian, X., et al., *Effects of BMP-2 and FGF2 on the osteogenesis of bone marrow-derived mesenchymal stem cells in hindlimb-unloaded rats.* Cell Biochem Biophys, 2014. **70**(2): p. 1127-36.
189. McCulloch, C. and H. Tenenbaum, *Dexamethasone induces proliferation and terminal differentiation of osteogenic cells in tissue culture.* The Anatomical Record, 1986. **215**(4): p. 397-402.

190. Shen, B., R.G. Jensen, and H.J. Bohnert, *Mannitol protects against oxidation by hydroxyl radicals.* Plant physiology, 1997. **115**(2): p. 527-532.
191. Li, Q., et al., *The role of mitochondria in osteogenic, adipogenic and chondrogenic differentiation of mesenchymal stem cells.* Protein Cell, 2017. **8**(6): p. 439-445.
192. Lee, D.H., et al., *Effects of hydrogen peroxide (H2O2) on alkaline phosphatase activity and matrix mineralization of odontoblast and osteoblast cell lines.* Cell Biol Toxicol, 2006. **22**(1): p. 39-46.
193. Chen, M., S. Chen, and D. Lin, *Carvedilol protects bone marrow stem cells against hydrogen peroxide-induced cell death via PI3K-AKT pathway.* Biomed Pharmacother, 2016. **78**: p. 257-263.
194. Putnam, C.D., et al., *Active and inhibited human catalase structures: ligand and NADPH binding and catalytic mechanism1.* Journal of molecular biology, 2000. **296**(1): p. 295-309.
195. Cardoso, L., et al., *Osteocyte apoptosis controls activation of intracortical resorption in response to bone fatigue.* Journal of bone and mineral research, 2009. **24**(4): p. 597-605.
196. Kirkman, H.N. and G.F. Gaetani, *Mammalian catalase: a venerable enzyme with new mysteries.* Trends Biochem Sci, 2007. **32**(1): p. 44-50.
197. Van Vlasselaer, P., et al., *Characterization and purification of osteogenic cells from murine bone marrow by two-color cell sorting using anti-Sca-1 monoclonal antibody and wheat germ agglutinin.* Blood, 1994. **84**(3): p. 753-63.
198. Denu, R.A. and P. Hematti, *Effects of oxidative stress on mesenchymal stem cell biology.* Oxidative medicine and cellular longevity, 2016. **2016**.
199. Yang, S.-R., J.-R. Park, and K.-S. Kang, *Reactive oxygen species in mesenchymal stem cell aging: implication to lung diseases.* Oxidative Medicine and Cellular Longevity, 2015. **2015**.
200. Glorieux, C. and P.B. Calderon, *Catalase, a remarkable enzyme: targeting the oldest antioxidant enzyme to find a new cancer treatment approach.* Biological chemistry, 2017. **398**(10): p. 1095-1108.
201. Matés, J.M., C. Pérez-Gómez, and I.N. De Castro, *Antioxidant enzymes and human diseases.* Clinical biochemistry, 1999. **32**(8): p. 595-603.
202. Kanda, Y., et al., *Reactive oxygen species mediate adipocyte differentiation in mesenchymal stem cells.* Life sciences, 2011. **89**(7-8): p. 250-258.
203. Shao, J., W. Zhang, and T. Yang, *Using mesenchymal stem cells as a therapy for bone regeneration and repairing.* Biological research, 2015. **48**(1): p. 62.
204. Bizzarri, A., et al., *Continuous oxygen monitoring in subcutaneous adipose tissue using microdialysis.* Anal Chim Acta, 2006. **573-574**: p. 48-56.
205. Hirao, M., et al., *Oxygen tension regulates chondrocyte differentiation and function during endochondral ossification.* J Biol Chem, 2006. **281**(41): p. 31079-92.
206. Scherer, K., et al., *The influence of oxygen and hydrostatic pressure on articular chondrocytes and adherent bone marrow cells in vitro.* Biorheology, 2004. **41**(3-4): p. 323-33.
207. Krinner, A., et al., *Impact of oxygen environment on mesenchymal stem cell expansion and chondrogenic differentiation.* Cell Prolif, 2009. **42**(4): p. 471-84.
208. Robins, J.C., et al., *Hypoxia induces chondrocyte-specific gene expression in mesenchymal cells in association with transcriptional activation of Sox9.* Bone, 2005. **37**(3): p. 313-22.
209. Sheehy, E.J., C.T. Buckley, and D.J. Kelly, *Oxygen tension regulates the osteogenic, chondrogenic and endochondral phenotype of bone marrow derived mesenchymal stem cells.* Biochem Biophys Res Commun, 2012. **417**(1): p. 305-10.

210. Kobayashi, C.I. and T. Suda, *Regulation of reactive oxygen species in stem cells and cancer stem cells.* J Cell Physiol, 2012. **227**(2): p. 421-30.
211. D'Autreaux, B. and M.B. Toledano, *ROS as signalling molecules: mechanisms that generate specificity in ROS homeostasis.* Nat Rev Mol Cell Biol, 2007. **8**(10): p. 813-24.
212. Sagach, V.F., et al., *The water-soluble vitamin E analogue Trolox protects against ischaemia/reperfusion damage in vitro and ex vivo. A comparison with vitamin E.* Pharmacol Res, 2002. **45**(6): p. 435-9.
213. Rosen, C.J. and M.L. Bouxsein, *Mechanisms of disease: is osteoporosis the obesity of bone?* Nat Clin Pract Rheumatol, 2006. **2**(1): p. 35-43.
214. Greco, E.A., A. Lenzi, and S. Migliaccio, *The obesity of bone.* Therapeutic advances in endocrinology and metabolism, 2015. **6**(6): p. 273-286.
215. Alcala, M., et al., *Short-term vitamin E treatment impairs reactive oxygen species signaling required for adipose tissue expansion, resulting in fatty liver and insulin resistance in obese mice.* PLoS One, 2017. **12**(10): p. e0186579.
216. Hamad, I., et al., *Intracellular scavenging activity of Trolox (6-hydroxy-2, 5, 7, 8-tetramethylchromane-2-carboxylic acid) in the fission yeast, Schizosaccharomyces pombe.* Journal of natural science, biology, and medicine, 2010. **1**(1): p. 16.
217. Bai, X.C., et al., *Oxidative stress inhibits osteoblastic differentiation of bone cells by ERK and NF-kappaB.* Biochem Biophys Res Commun, 2004. **314**(1): p. 197-207.
218. Bai, X.C., et al., *Reactive oxygen species stimulates receptor activator of NF-kappaB ligand expression in osteoblast.* J Biol Chem, 2005. **280**(17): p. 17497-506.
219. Zajdel, A., et al., *Osteogenic differentiation of human mesenchymal stem cells from adipose tissue and Wharton's jelly of the umbilical cord.* Acta Biochimica Polonica, 2017. **64**(2).
220. Teplyuk, N.M., et al., *The osteogenic transcription factor Runx2 regulates components of the fibroblast growth factor/proteoglycan signaling axis in osteoblasts.* Journal of cellular biochemistry, 2009. **107**(1): p. 144-154.
221. Barb, W., et al., *Reactions of ferrous and ferric ions with hydrogen peroxide. Part II.—The ferric ion reaction.* Transactions of the Faraday Society, 1951. **47**: p. 591-616.
222. Harber, F. and J. Weiss, *The catalytic decomposition of hydrogen peroxide by iron salts.* Proc. R. Soc. Lond. A, 1934. **147**(861): p. 332-351.
223. Gozzo, F., *Radical and non-radical chemistry of the Fenton-like systems in the presence of organic substrates.* Journal of Molecular Catalysis A: Chemical, 2001. **171**(1-2): p. 1-22.
224. Ensing, B., et al., *Chemical Involvement of Solvent Water Molecules in Elementary Steps of the Fenton Oxidation Reaction We gratefully acknowledge the helpful discussions with Michiel Gribnau (Unilever-Vlaardingen) and we thank the Netherlands Organization for Scientific Research (NWO) for support through the PPM-CMS program and the NCF for providing computer time.* Angew Chem Int Ed Engl, 2001. **40**(15): p. 2893-2895.
225. Melnyk, A.C., et al., *Catalysis of the decomposition of hydrogen peroxide by a complex of iron (III) with a synthetic macrocyclic ligand.* Journal of the American Chemical Society, 1979. **101**(12): p. 3232-3240.
226. Busch, D. and R. Eldik, *Catalytic action of the iron (II) complexes of 8-methyl-1, 4-bis (2-pyridylmethyl)-1, 4, 8-triazacycloundecane and 1-methyl-5, 9-bis (2-pyridylmethyl)-1, 5, 9-triazacyclododecane.* Journal of the Chemical Society, Dalton Transactions, 1999(16): p. 2751-2758.
227. Fenton, H.J.H., *LXXIII.—Oxidation of tartaric acid in presence of iron.* Journal of the Chemical Society, Transactions, 1894. **65**: p. 899-910.

228. Nicholls, P., *The reaction between aminotriazole and catalase.* Biochimica et biophysica acta, 1962. **59**(2): p. 414-420.
229. Sies, H., *Oxidative stress: oxidants and antioxidants.* Experimental physiology, 1997. **82**(2): p. 291-295.
230. Jonah, C., et al., *Yield and decay of the hydrated electron from 100 ps to 3 ns.* The Journal of Physical Chemistry, 1976. **80**(12): p. 1267-1270.
231. Borchi, E., et al., *Enhanced ROS production by NADPH oxidase is correlated to changes in antioxidant enzyme activity in human heart failure.* Biochimica et Biophysica Acta (BBA)-Molecular Basis of Disease, 2010. **1802**(3): p. 331-338.
232. Sumimoto, H., K. Miyano, and R. Takeya, *Molecular composition and regulation of the Nox family NAD(P)H oxidases.* Biochem Biophys Res Commun, 2005. **338**(1): p. 677-86.
233. Yuan, Z., et al., *NRF2 overexpression in mesenchymal stem cells induces stem-cell marker expression and enhances osteoblastic differentiation.* Biochemical and biophysical research communications, 2017. **491**(1): p. 228-235.
234. Tao, J., et al., *Downregulation of Nrf2 promotes autophagy-dependent osteoblastic differentiation of adipose-derived mesenchymal stem cells.* Experimental cell research, 2016. **349**(2): p. 221-229.
235. Sun, Y.-X., et al., *Role of Nrf2 in bone metabolism.* Journal of biomedical science, 2015. **22**(1): p. 101.
236. Hyeon, S., et al., *Nrf2 deficiency induces oxidative stress and promotes RANKL-induced osteoclast differentiation.* Free Radical Biology and Medicine, 2013. **65**: p. 789-799.
237. Kanzaki, H., et al., *The Keap1/Nrf2 protein axis plays a role in osteoclast differentiation by regulating intracellular reactive oxygen species signaling.* Journal of Biological Chemistry, 2013. **288**(32): p. 23009-23020.
238. Park, C.K., et al., *Nrf2 is a novel regulator of bone acquisition.* Bone, 2014. **63**: p. 36-46.
239. Hinoi, E., et al., *Nrf2 negatively regulates osteoblast differentiation via interfering with Runx2-dependent transcriptional activation.* J Biol Chem, 2006. **281**(26): p. 18015-24.
240. Teixeira, C.C., et al., *Foxo1, a novel regulator of osteoblast differentiation and skeletogenesis.* Journal of biological chemistry, 2010. **285**(40): p. 31055-31065.
241. Wang, Y.Y., S.M. Chen, and H. Li, *Hydrogen peroxide stress stimulates phosphorylation of FoxO1 in rat aortic endothelial cells.* Acta Pharmacol Sin, 2010. **31**(2): p. 160-4.
242. Schmidt, K.N., et al., *The roles of hydrogen peroxide and superoxide as messengers in the activation of transcription factor NF-κB.* Chemistry & biology, 1995. **2**(1): p. 13-22.
243. Iyer, S., et al., *FOXOs attenuate bone formation by suppressing Wnt signaling.* The Journal of clinical investigation, 2013. **123**(8): p. 3409-3419.
244. Greer, E.L., M.R. Banko, and A. Brunet, *AMP-activated Protein Kinase and FoxO Transcription Factors in Dietary Restriction–induced Longevity.* Annals of the New York Academy of Sciences, 2009. **1170**(1): p. 688-692.
245. Bartell, S.M., et al., *FoxO proteins restrain osteoclastogenesis and bone resorption by attenuating H2O2 accumulation.* Nat Commun, 2014. **5**: p. 3773.
246. Gottlieb, T.M., et al., *Cross-talk between Akt, p53 and Mdm2: possible implications for the regulation of apoptosis.* Oncogene, 2002. **21**(8): p. 1299-303.
247. Yamaguchi, A., et al., *Akt activation protects hippocampal neurons from apoptosis by inhibiting transcriptional activity of p53.* Journal of Biological Chemistry, 2001. **276**(7): p. 5256-5264.

248. Fraser, M., et al., *p53 is a determinant of X-linked inhibitor of apoptosis protein/Akt-mediated chemoresistance in human ovarian cancer cells.* Cancer research, 2003. **63**(21): p. 7081-7088.
249. Ko, L.J. and C. Prives, *p53: puzzle and paradigm.* Genes & development, 1996. **10**(9): p. 1054-1072.
250. Lengner, C.J., et al., *Osteoblast differentiation and skeletal development are regulated by Mdm2–p53 signaling.* J Cell Biol, 2006. **172**(6): p. 909-921.
251. Skurk, C., et al., *The Akt-regulated forkhead transcription factor FOXO3a controls endothelial cell viability through modulation of the caspase-8 inhibitor FLIP.* Journal of Biological Chemistry, 2004. **279**(2): p. 1513-1525.
252. Alvarez-Tejado, M., et al., *Hypoxia induces the activation of the phosphatidylinositol 3-Kinase/Akt cell survival pathway in PC12 cells protective role in apoptosis.* Journal of Biological Chemistry, 2001. **276**(25): p. 22368-22374.
253. Osaki, M., M. Oshimura, and H. Ito, *PI3K-Akt pathway: its functions and alterations in human cancer.* Apoptosis, 2004. **9**(6): p. 667-76.
254. Momand, J., H.H. Wu, and G. Dasgupta, *MDM2--master regulator of the p53 tumor suppressor protein.* Gene, 2000. **242**(1-2): p. 15-29.
255. Knowles, J.R., *Enzyme-catalyzed phosphoryl transfer reactions.* Annu Rev Biochem, 1980. **49**: p. 877-919.
256. Mishra, N.S., R. Tuteja, and N. Tuteja, *Signaling through MAP kinase networks in plants.* Arch Biochem Biophys, 2006. **452**(1): p. 55-68.
257. Nakano, Y., W.N. Addison, and M.T. Kaartinen, *ATP-mediated mineralization of MC3T3-E1 osteoblast cultures.* Bone, 2007. **41**(4): p. 549-61.
258. Yarian, C.S., D. Toroser, and R.S. Sohal, *Aconitase is the main functional target of aging in the citric acid cycle of kidney mitochondria from mice.* Mechanisms of ageing and development, 2006. **127**(1): p. 79-84.
259. Oexle, H., E. Gnaiger, and G. Weiss, *Iron-dependent changes in cellular energy metabolism: influence on citric acid cycle and oxidative phosphorylation.* Biochimica et Biophysica Acta (BBA)-Bioenergetics, 1999. **1413**(3): p. 99-107.
260. Ross, K.L. and R.S. Eisenstein, *Iron deficiency decreases mitochondrial aconitase abundance and citrate concentration without affecting tricarboxylic acid cycle capacity in rat liver.* The Journal of nutrition, 2002. **132**(4): p. 643-651.
261. Cairo, G. and A. Pietrangelo, *Iron regulatory proteins in pathobiology.* Biochemical Journal, 2000. **352**(Pt 2): p. 241.
262. Walden, W.E., et al., *Structure of dual function iron regulatory protein 1 complexed with ferritin IRE-RNA.* Science, 2006. **314**(5807): p. 1903-1908.
263. Rouault, T.A., *The role of iron regulatory proteins in mammalian iron homeostasis and disease.* Nature chemical biology, 2006. **2**(8): p. 406.
264. Gourley, B.L., et al., *Cytosolic aconitase and ferritin are regulated by iron in Caenorhabditis elegans.* J Biol Chem, 2003. **278**(5): p. 3227-34.
265. Pantopoulos, K., et al., *Differences in the regulation of iron regulatory protein-1 (IRP-1) by extra-and intracellular oxidative stress.* Journal of Biological Chemistry, 1997. **272**(15): p. 9802-9808.
266. Krebs, H.A., *The citric acid cycle.* Science, Technology and Management, 1937. **5**.
267. Davies, E., et al., *Citrate bridges between mineral platelets in bone.* Proc Natl Acad Sci U S A, 2014. **111**(14): p. E1354-63.
268. Hu, Y.Y., A. Rawal, and K. Schmidt-Rohr, *Strongly bound citrate stabilizes the apatite nanocrystals in bone.* Proc Natl Acad Sci U S A, 2010. **107**(52): p. 22425-9.
269. Franklin, R.B., et al., *Evidence that Osteoblasts are Specialized Citrate-producing Cells that Provide the Citrate for Incorporation into the Structure of Bone.* Open Bone J, 2014. **6**: p. 1-7.

270. Costello, L.C., et al., *In vitro BMP2 stimulation of osteoblast citrate production in concert with mineralized bone nodule formation.* J Regen Med Tissue Eng, 2015. **4**.
271. Liu, X.R., et al., *Oxidative stress inhibits growth and induces apoptotic cell death in human U251 glioma cells via the caspase-3-dependent pathway.* Eur Rev Med Pharmacol Sci, 2015. **19**(21): p. 4068-75.
272. Langenbach, F. and J. Handschel, *Effects of dexamethasone, ascorbic acid and β-glycerophosphate on the osteogenic differentiation of stem cells in vitro.* Stem cell research & therapy, 2013. **4**(5): p. 117.
273. Jaiswal, N., et al., *Osteogenic differentiation of purified, culture-expanded human mesenchymal stem cells in vitro.* Journal of cellular biochemistry, 1997. **64**(2): p. 295-312.

Acknowledgment

First, I want to thank Prof. Dr. Christoph V. Suschek and Prof. Dr. Joachim Windolf for giving me the opportunity to prepare my dissertation project within the research laboratory of the trauma and hand surgery. Furthermore, I would like to thank Prof. Dr. Heise and Prof. Dr. Beller for co-advising my project.

Christoph, during my project in your laboratory, you taught me so much. You always supported every step of my work and you were *always* there for me. You are an absolutely wonderful person. I cannot explain with words how much I thank you.

The team of the laboratory is not just my team, they became family. You supported me during my work in the lab and always helped emotionally. You all mean a lot to me. I thank every single one for the rest of my life. I want to emphasize that Samira Seghrouchni, Jutta Schneider and Christa Wilkens are the heart of the whole team. You are such great people. Christoph, Christa, Samira, Jutta – I truly owe you my successes within this project. I really thank you!

"Mama and Papa", I thank you for every support – emotionally and financially. I would not have advanced this far without you. I thank you so much.

Furthermore, I thank all my friends – in particular Mi, Anne, Marcella, Lauren, Katharina – for understanding me, supporting me with so much love, just being always there for me. Mi, very special thanks to you. You not just always had a sympathetic ear for me – you saved June. I cannot thank you enough for that. What we have is magical.

Very super special thanks to Tobi; I thank you so incredibly much. You believed in me when I again lost the faith in me – you *always* believed in me. This means the world to me.

Scientific Contributions

Talks

Deutscher Kongress der Orthopädie und Unfallchirurgie (DKOU) 2018

"The lack of osteogenic differentiation potential of osteogenically dysfunctional human mesenchymal bone marrow stem cells can be significantly restored by addition of catalase"

Dana Strangmann[1], Christoph V. Suschek[1], Joachim Windolf[1]

135. Kongress der Deutschen Gesellschaft für Chirurgie 2018

"Investigations of the osteogenic differentiation potential of regular — as well as osteogenically dysfunctional — human bone marrow mesenchymal stem cells (hBMSCs) influenced by pro- and antioxidative approaches"

Dana Strangmann[1], Christoph V. Suschek[1], Joachim Windolf[1]

Deutscher Kongress der Orthopädie und Unfallchirurgie (DKOU) 2017

"NADPH- oxidase 4 might represents a pivotal molecular target in improving the osteogenic differentiation potential of regular as well as osteogenically dysfunctional human bone marrow mesenchymal stem cells"

Dana Strangmann[1], Christoph V. Suschek[1], Joachim Windolf[1]

Poster Presentations

9th International Meeting of Kompetenznetzwerk Stammzellforschung NRW

"Effects of an antioxidative treatment with catalase on the osteogenic differentiation of human mesenchymal bone marrow-derived stem cells"

Dana Strangmann[1], Christoph V. Suschek[1], Joachim Windolf[1]

Declaration of Authorship

I declare with my signature that I have completed the present thesis independently, without making use of other than the specified literature and aids and under consent of "Good Scientific Practice" of Heinrich-Heine University Düsseldorf. Sentences or parts of sentences quoted literally are marked as quotations; identification of other references with regard to the statement and scope of the work is quoted. The thesis in this form or in any other form has not been submitted to an examination body and has not been published.

_____

Signature

_____

City, date

Appendix

Example of the achieved medical history questionnaire.

Certificate of Analysis

Product:	human mesenchymal stem cells
Isolation on:	12.01.2016
Donor ID:	*20160112124*
Cellnumber:	500.000
Passage (Freezing):	1
Storage:	Cryoconservation

Characterization

Information:	Unit:	Result:
Age	years	62
Sex		M
BMI		28
ASA Score		2
Reason for hospital stay	ICD	S72.40; S82.0
Comorbidities	ICD	E03.9; N40
HIV test		negative
HBV test		negative
HCV test		negative
Smoker		no
Allergies		no
Alcohol consumption		weekly
Sports		yes
Nutrition		normal diet
Leukocytes	Tsd/µl	6,6
Erythrocytes	Mio/µl	3,07
Hemoglobin	g/dl	9,3
Hematokrit	%	28,2
MCV	fl	91,9
MCH	pg	30,3
MCHC	g/dl	33,0
RDW	%	14,1
Thrombocytes	Tsd/µl	384
Thrombocytevolume	fl	8,8
Quicktest	%	n.a.
INR	Ratio	n.a.
APTT	sec	n.a.
CFU Passage 1	%	1,3
CFU Passage 3	%	n.a.

Information:	Unit:	
Adipogenic differentiation		 positive
Osteogenic differentiation		 positive
Chondrogenic differentiation		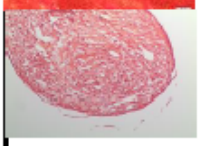 negative
Surface antibodies:		
CD11B	%	negative
CD11C	%	negative
CD13	%	65
CD14	%	negative
CD15	%	negative
CD19	%	negative
CD29	%	100
CD31	%	negative
CD34	%	13
CD44	%	82
CD45	%	negative
CD73	%	89
CD90	%	94
CD105	%	100
CD166	%	98
HLA DR	%	87
SSEA5	%	negative
STRO1	%	negative